AN INVESTIGATION INTO THE PATHOPHYSIOLOGY OF A NEW MODEL OF TRANSIENT FOCAL CEREBRAL ISCHAEMIA IN THE RAT.

DEBORAH A. DAWSON, B.Sc. (Hons.)

A thesis submitted for the Degree of Doctor of Philosophy
to the Faculty of Medicine, University of Glasgow

Wellcome Surgical Institute & Hugh Fraser Neuroscience Laboratories,
University of Glasgow
Garscube Estate, Bearsden Road, Glasgow
and
University Dept. of Medicine & Therapeutics, Western Infirmary, Glasgow

ProQuest LLC.
789 East Eisenhower Parkway
P.O. Box 1346
Ann Arbor, MI 48106 – 1346

TABLE OF CONTENTS PAGE NOS.

PART I: INTRODUCTION

PAGE NOS.

PART II: MATERIALS AND METHODS

PART III: RESULTS AND DISCUSSION PAGE NOS.

PAGE NOS.

LIST OF FIGURES

PAGE NOS.

LIST OF TABLES

PAGE NOS.

ACKNOWLEDGEMENTS

I would like to thank all the staff at the Wellcome Surgical Institute (academic, technical and secretarial) whose cheerful nature and helpful attitude have enabled me to survive the last 3 years and made much of it highly enjoyable.

I am most indebted to my supervisor Dr Mhairi Macrae for her continued support and guidance (and frequent lifts home) over the last 3 years. In particular I am grateful for her unswerving faith in my scientific ability, which frequently was greater than my own, and without which I would never have mastered the art of MCA occlusion or published in the European Journal of Pharmacology. I must also thank Prof James McCulloch whose knowledge and enthusiasm for all things neuroscientific has been a constant source of inspiration and aspiration for me. Thanks also to Sue Browne, Dr Debbie Dewar, Dr Karen Horsburgh, Elaine Irving, Kenny Mackay, Dr Moira McAuley, Ailsa MacGregor and Tosh Patel for their help and assistance during my time at the Wellcome. Special thanks are extended to Gail Gartshore with whom I collaborated on the double-label autoradiography study and who spent many days chained to the densitometer and BBC computer completing the data analysis.

The technical expertise of the technicians at the Wellcome is gratefully acknowledged. Without the expert assistance of Hayley-Jane Dingwall, Lyndsay Dover, Michael Dunne, Gordon Littlejohn, Margaret Roberts, Marion Steele, Joan Stewart and Margaret Stewart none of the experiments included in this thesis could have been completed. Thanks also to Dr Joyce Ferguson, Christine Stirton, Morag Findlay and all the animal nurses for their assistance with completion of the survival studies and for their expert care of the animals. I am also grateful to Prof David Graham and his staff at the Dept. of Neuropathology, Southern General Hospital for processing brains for histopathology and quantification of ischaemic damage. In addition I thank Prof Graham, Prof Murray Harper and Prof John Reid for their continued support and interest in my present and future career.

Finally thanks to Dennis '& Co.' for tea and sympathy, and Wendy and Andrew for long-distance pep talks. If I can finish this thesis, then the Robins can win a game!

SUMMARY

This study aimed to investigate the consequences of a transient focal ischaemic insult using a novel model of transient focal cerebral ischaemia that utilises the vasoconstrictor peptide endothelin-1 to induce temporary occlusion of the left middle cerebral artery (MCA) in the rat. Quantitative histopathology and *in vivo* autoradiographical techniques were used to assess this model and compare it to the standard model of permanent MCA occlusion originally developed in these laboratories (Tamura *et al.* 1981a). *In vivo* double-label autoradiography using the blood flow tracers [^{14}C]iodoantipyrine (IAP) and [^{99m}Tc]hexamethylpropylamine oxime (HMPAO) revealed that application of endothelin-1 (2.5 nmol in 25 μl) to the MCA in the halothane-anaesthetised rat resulted in profound reductions in local cerebral blood flow throughout the territory of the MCA 5 min post-endothelin-1 application (measured by [^{99m}Tc]HMPAO). In the same animals reperfusion (measured by [^{14}C]IAP) was apparent 2 h post-endothelin-1 application in both the cerebral cortex and caudate nucleus. Thus in this model endothelin-1 induces a period of profound ischaemia followed by gradual, spontaneous reperfusion.

In a separate study the same dose of endothelin-1 was found to induce a reproducible lesion (assessed by quantitative histopathology) located in the cortex and caudate nucleus 4 h post-endothelin-1 application in the anaesthetised rat. Neurones within the lesion exhibited the classic morphology characteristic of ischaemic cell change. Withdrawal of anaesthetics following transient MCA occlusion was found to reduce the volume of ischaemic damage measured at the 4 h time point when compared with maintained anaesthesia. This was probably due to the increase in blood pressure in conscious compared with anaesthetised rats. In contrast withdrawal of anaesthetics did not affect outcome 4 h following permanent MCA occlusion.

The volume of ischaemic damage was found to increase from 4 to 24 h post-transient MCA occlusion (23 ± 14 and 87 ± 14 mm^3 (mean ± S.D.) respectively), while there was no significant difference in the volumes of ischaemic damage for permanent MCA occlusion at the same time points (131 ± 37 and 126 ± 29 mm^3 for 4 and 24 h post-MCA occlusion respectively). Thus it was concluded that the volume of ischaemic damage continues to increase after the onset of reperfusion in the endothelin-1 model of transient ischaemia. This result suggests that reperfusion injury (as yet undefined) may contribute to outcome in this model. Factors associated with both the ischaemic (*e.g.* severity of constriction induced by endothelin-1) and reperfusion (*e.g.* blood pressure 1 h post-MCA occlusion) phases were found to impact directly on lesion size assessed 24 or 72 h post-transient MCA occlusion.

Pre-treatment with the NMDA receptor antagonist MK-801 (0.12 mg/kg i.v. bolus followed by continuous i.v. infusion of 108 μg/kg/h at 0.6 ml/h) was found to significantly and dramatically reduce the volume of ischaemic damage (by more than 70%) in both the whole hemisphere and caudate nucleus following transient MCA occlusion, but only when the treatment was initiated 2.5 h pre-MCA occlusion. This result is in contrast to previous studies of permanent MCA occlusion in which the caudate nucleus was reported to be resistant to MK-801 or other neuroprotective agents. Thus the restoration of blood flow following a transient ischaemic insult renders the caudate nucleus potentially amenable to pharmacological intervention. When MK-801 treatment was started 1 h pre-MCA occlusion the transient hypotension induced by the drug was still present at the time of occlusion and no significant neuroprotection was observed.

Nitric oxide (NO) is an important mediator of vascular tone both centrally and in the periphery and has also been implicated in excitotoxicity *in vitro*. In an *in vivo* model of glutamate toxicity in the anaesthetised rat, pre-treatment with the NO synthase inhibitor L-NAME (10 mg/kg) signficantly reduced the volume of tissue damage measured 4 h post-onset of glutamate infusion into the parietal cortex, and was found to be of equal effectiveness as MK-801 (0.5 mg/kg) demonstrating the importance of NO as a mediator of excitotoxic damage. In contrast, in models of both permanent and transient MCA occlusion (using the 4 h paradigm in the anaesthetised rat) the protection achieved with L-NAME (3-30 mg/kg) was more modest that that observed for MK-801. The higher dose of L-NAME (tested only in the permanent MCA occlusion model) did not significantly alter the volume of ischaemic damage, while the lower dose (3 mg/kg) reduced the total volume of ischaemic damage by 16% (statistically significant) and 29% (not statistically significant) for permanent and transient MCA occlusion respectively.

In a series of parallel studies L-NAME (0.3-30 mg/kg) was found to significantly increase blood pressure and reduce cerebral blood flow in a dose-dependent fashion in the conscious, non-ischaemic rat with a prolonged (>3 h) duration of action. The reductions in cerebral blood flow (for 30 mg/kg L-NAME) were rather homogenous throughout the brain - reducing flow by approximately 25% when compared with saline controls. In the halothane-anaesthetised rat the pressor response to L-NAME (30 mg/kg) was attenuated but significant cerebral hypoperfusion was still present. Thus it is likely that the observed reductions in cerebral blood flow induced by L-NAME detracted from its inherent anti-excitotoxic properties and accounted in part for its weak efficacy against focal ischaemic damage *in vivo*.

PREFACE AND DECLARATION

Stroke is the third most common cause of death in the Western world after heart disease and cancer (McCulloch *et al.*1991). There is therefore a great need for investigation into the pathophysiology of cerebrovascular disease to improve the management of stroke patients and lead to the discovery of effective pharmacological treatments. In the past decade one of the most pertinent and useful animal models of cerebral ischaemia has proven to be permanent focal ischaemia (induced by middle cerebral artery (MCA) occlusion) in the rat. This model has yielded important insights into the pathogenesis of cerebral ischaemic damage and has been extensively used to assess the efficacy of putative anti-ischaemic drugs. However the utility of this approach is limited by the very fact that the ischaemic insult is permanent and consequently the potential beneficial or detrimental effects of restoring blood flow to the compromised tissue can not be investigated.

Continued vascular occlusion leads inevitably to tissue death due to depletion of oxygen and energy supplies. Therefore in the clinical situation some treatment strategies have been directed towards restoring blood flow to the ischaemic tissue in the belief that reperfusion is vital for long term survival. However there is evidence to suggest that reperfusion, instigated several hours following onset of ischaemia, may itself be associated with further pathological events that can potentially worsen outcome following stroke. The restoration of flow to an ischaemic region can promote vascular damage that may result in oedema formation and haemorrhagic transformation, factors which in turn are associated with increased mortality rates. In man spontaneous recanalisation of the occluded vessel occurs in approximately 20% of all stroke cases (Wardlaw & Warlow 1992). For embolic stroke, spontaneous reperfusion plus the increased use of thrombolytic and anti-thrombotic therapy designed to dissolve emboli, mean recanalisation rates can approach 90% of all patients. Thus potential reperfusion injury is a problem of increasing importance in the field of clinical stroke. To address this problem current experimental research is expanding to include models of transient as well as permanent focal cerebral ischaemia, since the transient ischaemia models allow the contribution of reperfusion to cerebral injury to be assessed.

The primary aim of the current thesis is to further characterise a novel model of transient focal cerebral ischaemia, developed at the Wellcome Surgical Institute, that utilises endothelin-1 to induce temporary vascular occlusion of the MCA. The volume of ischaemic damage induced by this model will be assessed at different time intervals (4, 24 and 72 h) following the onset of ischaemia. Our main hypothesis is that the volume of damage will continue to increase after the onset of reperfusion due to the contribution of 'reperfusion injury' to the maturation of the lesion.

Secondly, the relative efficacy of different treatment strategies in permanent and transient focal ischaemia will be determined with the aim of improving our understanding of the processes underlying ischaemic/reperfusion injury in the endothelin-1 model. Finally, the physiological/ pathophysiological roles of nitric oxide, a novel mediator of cerebrovascular regulation and neurotoxicity, will be investigated in non-ischaemic and ischaemic animals.

This thesis comprises my own original work and has not been presented previously as a thesis in any form. Some of the experiments reported in this thesis were carried out in collaboration with other researchers: the double label autoradiography study was conducted jointly with Ms G Gartshore; the glutamate toxicity study was conducted with Dr H Fujisawa, Mr K Mackay and Ms S Browne; while Dr K Kasumoto performed permanent MCA occlusions for the first L-NAME drug study.

1.1. CEREBROVASCULAR DISEASE IN MAN

'Stroke' is a generic term referring to cerebrovascular accidents where blood flow through a cerebral artery is interrupted resulting in damage in a discrete, focal area of the brain. The focal nature of stroke distinguishes it from the global ischaemic damage that occurs with complete interruption of the cerebrovascular supply *e.g.* following cardiac arrest. Stroke can be either ischaemic or haemorrhagic in origin. Ischaemic stroke, caused by occlusion of a vessel by emboli (*e.g.* blood clots carried in the bloodstream until they lodge in a vessel) or thrombosis (where the vessel slowly becomes blocked by debris and the onset of symptoms may be more gradual) account for approximately 84% of stroke cases while the remaining 16% are haemorrhagic in nature (Graham 1988). The incidence of occlusive stroke can be further subdivided into embolic (31%) and thrombotic (53%), while haemorrhagic stroke can be subdivided into spontaneous intracerebral haemorrhage (10%) and subarachnoid haemorrhage (6%).

Thrombosis is the major cause of stroke affecting the carotid and basilar arteries while embolism is more common for intra-cerebral arteries (Mohr *et al.* 1986). Most embolic strokes occur in the territory of the MCA (since this vessel is the main continuation of the internal carotid artery) and account for approximately one third of all stroke cases (Mohr *et al.* 1986). In man MCA occlusion results in contralateral hemiparesis and aphasia if the speech centre is affected. The degree of hemiparesis and the size of infarct are dependent on whether the obstruction is localised in the main trunk or a branch of the MCA (Olsen 1991). MCA occlusions resulting in large infarcts with severe neurological symptoms are associated with the poorest outcome (Olsen 1991).

The majority of embolic MCA occlusions undergo spontaneous recanalisation: 25% by 24 h post-onset of clinical symptoms, 65-90% within 1 week (Mohr *et al.* 1986; Dalal *et al.* 1965). However, because the occurence of embolic stroke in the Western world is much less frequent than thrombotic stroke and the spontaneous reperfusion rate for thrombotic occlusion is much lower, overall approximately 20% of stroke patients will show recanalisation after 24 h (Wardlaw and Warlow 1992). The use of thrombolytic (*e.g.* tissue plasminogen activator) and/or antithrombotic (*e.g.* aspirin, heparin) therapy will however increase this figure. Recanalisation, if it occurs early enough (*e.g.* within 8 h), is associated with reduced infarct size and improved clinical outcome (Olsen 1986; Ringelstein *et al.* 1992). In contrast later reperfusion may not be beneficial (Ringelstein *et al.* 1992) and can be associated with much higher mortality rates than permanent occlusion (Irino *et al.* 1977), suggesting that reperfusion itself causes further injury to ischaemically-damaged tissue. Animal models of focal ischaemia are beginning to uncover potential contributors to reperfusion injury and these will be introduced in later sections.

1.2. CEREBROVASCULAR ANATOMY OF HUMAN AND RAT

The major anatomical features of the cerebrovascular system in humans and normotensive rats are strikingly similar (Yamori *et al.* 1976). The brain in both species is supplied by the paired internal carotid and vertebral arteries that anastomose on the inferior brain surface to form the circle of Willis (see Figure 1). The internal carotid artery divides into 2 branches - the smaller branch forms the anterior cerebral artery (ACA), the larger branch and main continuation of the internal carotid artery becomes the middle cerebral artery (MCA). In man the cortical supply from the ACA is to the inferior frontal lobe and medial surfaces of the frontal and parietal lobes. Small penetrating branches such as the medial striate artery supply subcortical structures including the head of the caudate nucleus. The MCA supplies cortical rami to most of the dorsolateral surface of the cerebral hemispheres (except for border regions supplied by the ACA and posterior cerebral artery (PCA)). This includes the motor and sensory areas (controlling trunk, hand and face), and speech and language areas. Penetrating branches including the lenticulostriates supply the putamen and body of the caudate nucleus. The vertebral arteries join at the junction of the pons and medulla to form the basilar artery which bifurcates into the posterior cerebral arteries. The PCA supplies the inferior temporal and medial occipital lobes of the cerebrum.

In the rat the cortical territories of the 3 major cerebral arteries are essentially similar to man (Yamori *et al.* 1976; see Figure 2). The medial anterior portion of the caudate nucleus is supplied by branches from the ACA, while the lateral anterior and posterior portions are supplied by lenticulostriate branches from the MCA (Rieke *et al.* 1981; Yamori *et al.* 1976).

In both species the cerebral arteries are interconnected at the circle of Willis by the small anterior and posterior communicating arteries that act as potential alternative flow routes if one of the major supply vessels becomes occluded. Additionally both the rat and human possess numerous anastomoses between distal branches of the MCA and ACA or PCA resulting in cortical boundary zones where the tissue can receive blood supply derived from 2 major vessels. In the rat ACA-MCA anastomoses are located dorsally at the cortical interface of the 2 vessels along the frontal-occipital axis. Connections between the PCA and MCA are located in the occipital region and run parallel to the transverse fissure separating the cerebrum from the cerebellum (Coyle & Jokelainen 1982). The collateral circulation is more extensive in the rat than man with 4-5 times the number of anastomoses between the ACA and MCA, however individual collateral diameter is less in the rat (Coyle & Jokelainen 1982). In both species the presence of an efficient collateral circulation can reduce the volume of infarcted tissue following an ischaemic insult (Yamori *et al.* 1976; Saito *et al.* 1987).

Figure 1 Diagram of arteries at the base of the brain showing the interconnections that form the circle of Willis

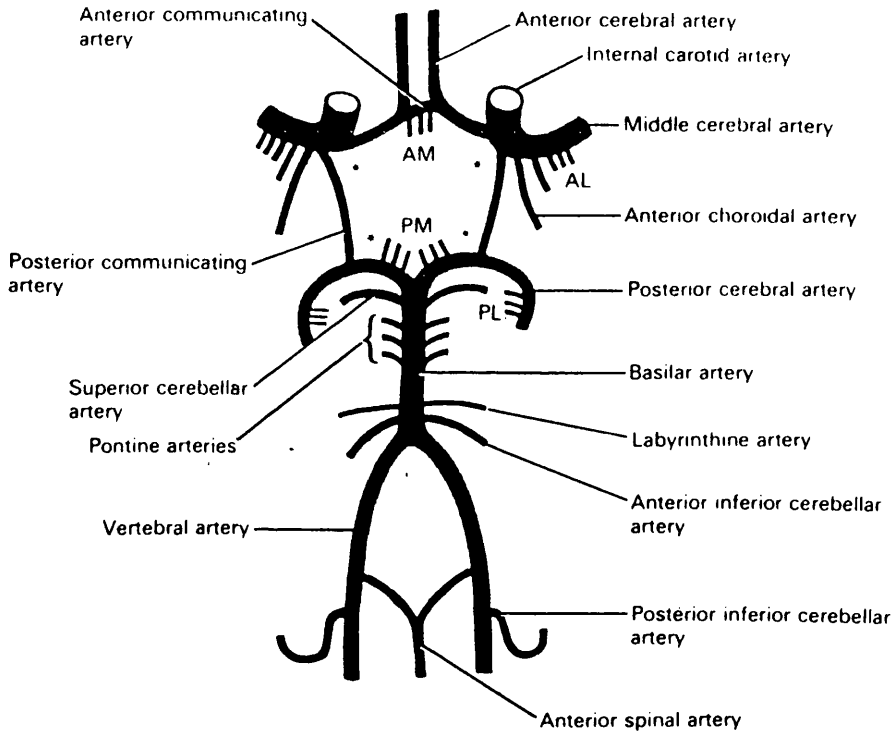

The blood supply to the brain is derived from the vertebral and internal carotid arteries which anastomose in the circle of Willis. The 3 major intracerebral arteries - the paired anterior, middle and posterior cerebral arteries - branch off from the circle of Willis and are interconnected by the anterior and posterior communicating arteries. The groups of central branches are anteromedial (AM), anterolateral (AL), posteromedial (PM) and posterolateral (PL). Adapted from Wilkinson 1986.

Figure 2 Diagram of cortical blood supply in rats and humans

a) Dorsal view of the distribution of arterial territories in the cerebral cortex of the rat

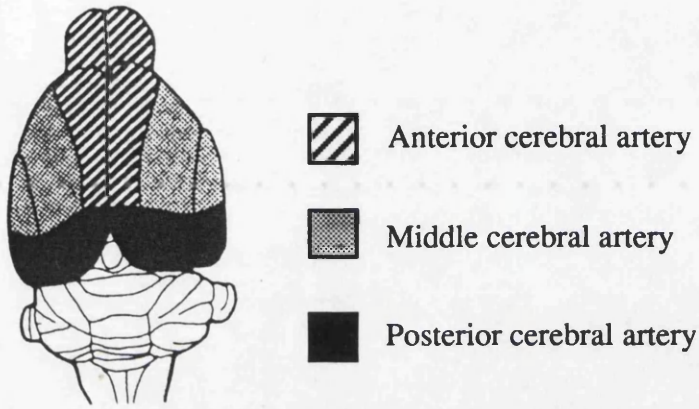

b) Lateral view of the distribution of arterial territories of the left cerebral hemisphere in man

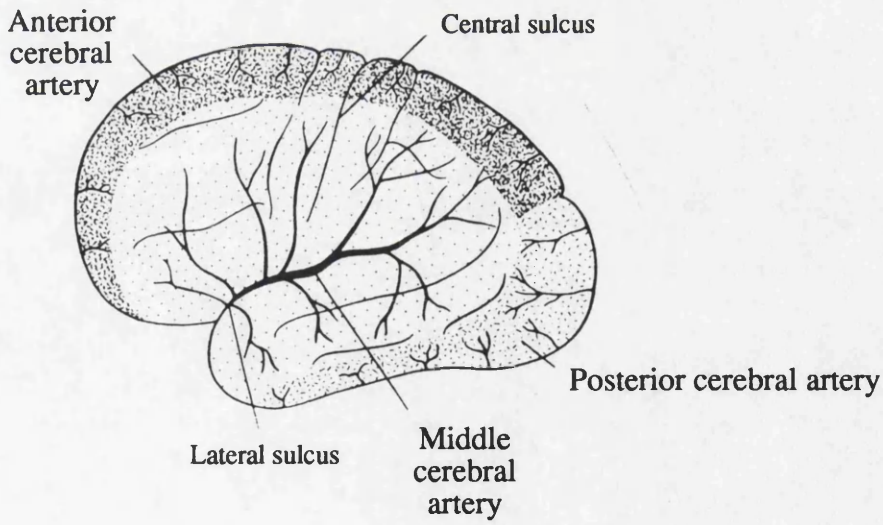

Adapted from Yamori *et al.* 1976 and Wilkinson 1986.

1.3. ANIMAL MODELS OF CEREBRAL ISCHAEMIA

Many species (*e.g.* primates, cats, dogs, rodents) have been used in experimental models of cerebral ischaemia. However rodent models, and particularly the rat, are by far the most popular. The rat is particularly suited for this role for several reasons: 1) the cerebrovascular anatomy of the rat more closely resembles that of man (Yamori *et al.* 1976, see Section 1.2) than other species such as the cat or gerbil 2) the normal functioning of the rat central nervous system, particularly with regards to cerebrovascular regulation, is well documented 3) there are practical advantages associated with using a small, low cost animal that is more ethically acceptable than 'higher' species.

In this section I shall describe the most commonly used models of cerebral ischaemia in the rat. These models can be divided into 2 main groups 1) global or forebrain ischaemia - where the blood supply to the entire brain or cerebral hemispheres is reduced or eliminated completely and 2) focal ischaemia - where only blood supply to a localised brain region is affected.

1.3.1. **Rat models of global ischaemia**

Although originally developed as models of stroke, these models more closely mimic clinical conditions such as cardiac arrest and severe hypotension where blood supply to the entire brain is disrupted.

Complete global ischaemia

a) Decapitation ischaemia. Decapitation induces irreversible global ischaemia that can be maintained for any desired time period by keeping the whole head at 37°C. Alternatively the head can be subjected to controlled cooling to mimic post-mortem changes. The main advantage of this model is its obvious simplicity. It is particularly well suited to investigating changes in biochemical parameters or receptor function.

b) Neck Tourniquet. The vessels in the neck are compressed by inflation of a pressure cuff (Levine & Marvin, 1960). This method interrupts blood supply to the brain stem and therefore causes major disruption of cardiovascular and respiratory control that results in a high mortality rate. The relevance of this model to any clinical condition (apart from strangulation) is also debatable.

Incomplete global ischaemia

Incomplete or forebrain ischaemia models maintain blood supply to the brain stem and hence preserve normal cardiovascular control. These models involve extracranial occlusion of blood vessels which prevents complicating factors such as mechanical damage to the blood-brain barrier and brain parenchyma, and interactions with intracranial pressure, from influencing outcome. One advantage of these models over models of focal cerebral ischaemia is their comparative surgical simplicity which means they are widely used to study cerebral ischaemia despite their questionable relevance to stroke.

a) Bilateral occlusion of the common carotid arteries. In this model originally described by Eklof & Siesjo (1972) the common carotid arteries are exposed and occluded by ligation either permanently, or more usually, transiently for periods from 10-60 minutes. This technique is usually combined with systemic hypotension induced by controlled haemorrhage (Kagstrom *et al.* 1983) that is necessary to reduce cerebral blood flow sufficiently to obtain reproducible ischaemic damage.

b) Four Vessel Occlusion. This model involves permanent bilateral occlusion of the vertebral arteries by electrocoagulation under anaesthesia followed by transient bilateral occlusion of the carotid arteries which may be carried out in conscious rats (Pulsinelli & Brierley, 1979).

Both these models of transient global ischaemia induce selective neuronal necrosis in selectively vulnerable areas of the brain such as the CA1 region of the hippocampus (Pulsinelli *et al.* 1982, Smith *et al.* 1984). Both 2 vessel occlusion and 4 vessel occlusion produce variable results between laboratories (reviewed in Ginsberg & Busto 1989). This variability may be attributable to several factors including: 1) variations in the collateral vascular supply both between and within strains (Ginsberg & Busto 1989) and 2) the failure to monitor and/or maintain brain temperature. Following global ischaemia brain temperature falls rapidly, independently of core body temperature, due to interruption of the entire blood supply to the cerebral hemispheres. Moderate hypothermia (34°C) has a marked neuroprotective effect in these models (Busto *et al.* 1987) so that failure to control brain temperature introduces unacceptable variability.

1.3.2. Rat models of focal ischaemia

The majority of intracerebral strokes involve occlusion of the middle cerebral artery (Mohr *et al.* 1986). Consequently animal models of focal cerebral ischaemia are predominantly models of MCA occlusion. This technique was originally described in large species such as primates (Hudgins & Garcia 1970; Symon 1970) and cats (O'Brien & Waltz 1973) using a transorbital surgical approach to expose the MCA. A reproducible infarct in these models could only be achieved with strict control of physiological parameters. This problem of variability (Morawetz *et al.* 1978; Garcia 1984), and the advantages associated with using the rat as an experimental species (see above), led to the development of rat models of MCA occlusion.

1.3.2.1. Models of **permanent** focal cerebral ischaemia

a) Permanent MCA occlusion. Unilateral MCA occlusion in the rat was first reported by Robinson *et al.* in 1975. They employed a large frontoparietal craniectomy to expose a portion of the MCA distal to its origin from the circle of Willis. Ligation of the distal MCA resulted in a lesion of variable size restricted to the cerebral cortex, with apparent differences in the consequences of left and right MCA occlusion (Robinson & Coyle 1980). Later studies described a subtemporal approach that enabled the artery to be occluded closer to its origin (Albanese *et al.* 1980; Tamura *et al.* 1981a). The method reported by Tamura *et al.* has become the standard model of MCA occlusion in the rat although the artery is more frequently occluded by electrocoagulation rather than by a miniclip as described in the original articles (Tamura *et al.* 1981b). Proximal occlusion of the MCA results in a reproducible lesion incorporating a large proportion of the frontoparietal cortices and the dorsolateral caudate nucleus. The most consistent lesion is produced by electrocoagulation of the MCA from where it crosses the inferior cerebral vein distally to below the olfactory tract proximal to the lenticulostriate end-arteries that supply the caudate nucleus (Bederson *et al.* 1986).

The variability in lesion size produced by distal MCA occlusion can be reduced by combining the MCA occlusion with temporary contralateral and/or permanent ipsilateral common carotid artery occlusion (Chen *et al.* 1986; Brint *et al.* 1988) to reduce collateral perfusion of the MCA territory. However this still produces a lesion that is restricted predominantly to cerebral cortex with little sub-cortical necrosis. An alternative strategy to improve reproducibility of lesion size for either proximal (Duverger & Mackenzie 1988) or distal (Brint *et al.* 1988) MCA occlusion is to use spontaneously hypertensive rats (SHR) rather than a normotensive strain. MCA occlusion in SHR results in a large consistent lesion due to the absence of a well defined collateral circulation in this strain. However the

greater severity of the ischaemic insult also makes the SHR more resistant to treatment strategies that are effective in normotensive strains (Roussel *et al.* 1992a). Thus the differences in cerebrovascular anatomy between SHR and normotensive rats should be borne in mind in the interpretation of studies conducted solely in SHR.

b) Photochemically induced focal cerebral ischaemia. This method, introduced by Watson *et al.* 1985, induces a thrombotic cortical infarct by directing a light beam through the skull onto an intravascular photosensitive dye such as rose Bengal. The light initiates a photochemical reaction that induces platelet aggregation and thrombus formation. By adjusting the position and intensity of the light beam a thrombus can be produced in any cortical location.

Permanent MCA occlusion in the rat has become the most commonly used model in both mechanistic and pharmacological studies of focal cerebral ischaemia. The variability in infarct volume lies within acceptable limits (Duverger & Mackenzie 1988) so that relatively small numbers of animals are required to show statistically significant neuroprotection in drug testing. In particular, the repeated demonstration of the efficacy of glutamate receptor antagonists in these models has led to the current emphasis on excitotoxic mechanisms as the main mediator of cerebral ischaemic damage. The main disadvantage of the Tamura model of MCA occlusion is that electrocoagulation of the vessel results in permanent ischaemia with no possibility of reperfusion through the MCA. The increasing frequency of recirculation following stroke in humans has therefore necessitated the development of animal models of transient ischaemia to investigate the potential beneficial and/or detrimental effects of reperfusion on infarct size. Investigation of the underlying pathophysiology in these models may reveal secondary mechanisms occuring within the reperfusion phase that play an equal, or even greater, role than glutamate in determining final outcome.

1.3.2.2. Models of **transient** focal cerebral ischaemia

As for permanent MCA occlusion, models of transient focal ischaemia were first developed in large species such as the monkey (Crowell *et al.* 1970) and cat (Kamijyo *et al.* 1977) before being adapted for the rat. Several of the strategies used to induce permanent MCA occlusion can be modified to induce transient occlusion:

a) Extravascular MCA occlusion. Where an aneurysm clip or ligature has been used to occlude the MCA, simple removal of the occluder may initiate reperfusion (Shigeno *et al.* 1985). Because of the practical difficulty involved in placement of the clip or ligature below the olfactory tract most of these models involve distal MCA occlusion and hence induce a purely cortical infarct. These methods may produce unsatisfactory results for 2 reasons. Firstly, as discussed above, a single point occlusion of the MCA produces a more variable region of ischaemia than electrocoagulation of a longer portion of the artery due to the presence of collateral supply. Therefore the initial ischaemic insult in these models is more variable than that achieved by electrocoagulation of the MCA. Variability in blood flow during the ischaemic phase may in turn influence the degree of reflow during the reperfusion phase (Tamura *et al.* 1980). However as for permanent distal MCA occlusion, initial variability can be reduced by using carotid artery occlusion in tandem with MCA occlusion and/or by the use of SHR (Kaplan *et al.* 1991; Buchan *et al.* 1992b). Secondly, placement and removal of the occluder may result in mechanical damage to the vessel (Shigeno *et al.* 1985) which may prevent adequate reperfusion from occuring.

b) Thrombolysis of photochemically induced occlusion. By administration of thrombolytic drugs to resolve the clot the photo-thrombotic model can be converted to a model of transient occlusion (Watson *et al.* 1987) that is particularly suited to studying the efficacy of such treatment strategies.

c) Intravascular MCA occlusion. In these models, introduced by Koizumi *et al.* 1986 and Zea Longa *et al.* 1989, a surgical thread or filament is inserted into the common carotid artery and gradually advanced via the internal carotid artery to occlude the origin of the MCA in the circle of Willis. By leaving the thread in this position permanent MCA occlusion can be achieved. More frequently, reperfusion is initiated by withdrawal of the thread back into the internal carotid artery to allow blood to reach the MCA via the circle of Willis. While placement of the thread is performed under anaesthesia, restoration of blood flow can subsequently be induced in the conscious rat. The 2 models differ in the type of thread used to induce the intraluminal occlusion - either heat-blunted (Zea Longa *et al.* 1989) or silicone-coated (Koizumi *et al.* 1986). When used by researchers outwith the original laboratories the Koizumi method has proven more reliable (Laing *et al.* 1993) due

to the larger diameter of the silicone coated thread that results in a more consistent reduction in cerebral blood flow and therefore a more reproducible lesion.

The noninvasive nature of this approach means surgical damage to the brain parenchyma is avoided and intracranial pressure changes due to oedema formation are not ameliorated by craniectomy. However vascular (particularly endothelial) damage caused by insertion and removal of the intraluminal filament may contribute to the gross oedema and high mortality rates observed in these models (Hara *et al.* 1990; Koizumi *et al.* 1989; Zea Longa *et al.* 1989).

d) Endothelin-1 Induced MCA Occlusion

Preliminary studies conducted at these laboratories have established the validity of this approach. Firstly application of endothelin-1 (10^{-5} M) to the MCA, surgically exposed as for permanent MCA occlusion, was demonstrated to cause severe reductions in local cerebral blood flow of approximately 75% in core MCA territory 10 min post-application of the peptide (Robinson *et al.* 1990). In a second series of experiments the dose-dependency and time course of this ischaemia were investigated (Macrae *et al.* 1993). Endothelin-1 (10^{-7} M-10^{-4} M in 25 µl) induced a rapid reduction in blood flow in the caudate nucleus that was maximal at 10 min, followed by progressive return of flow (Figure 3). The initial ischaemia and the duration of action (expressed as the time taken for flow to return to 50% of control) were dose-dependent (Figure 4). Finally histopathological studies revealed endothelin-1 induced dose-dependent ischaemic damage 4 h post-application of the peptide (Macrae *et al.* 1993). The location of the lesion (frontal and parietal cortices and dorsolateral caudate nucleus) and volume of damage at the highest dose (25 µl x 10^{-4} M) were comparable to that achieved with permanent proximal MCA occlusion. Further characterisation of this model, including extension of survival time beyond 4 h, will form the basis of my thesis.

Figure 3 Time course for alterations in blood flow in the ipsilateral caudate nucleus following application of endothelin-1 to the middle cerebral artery in anaesthetised rats

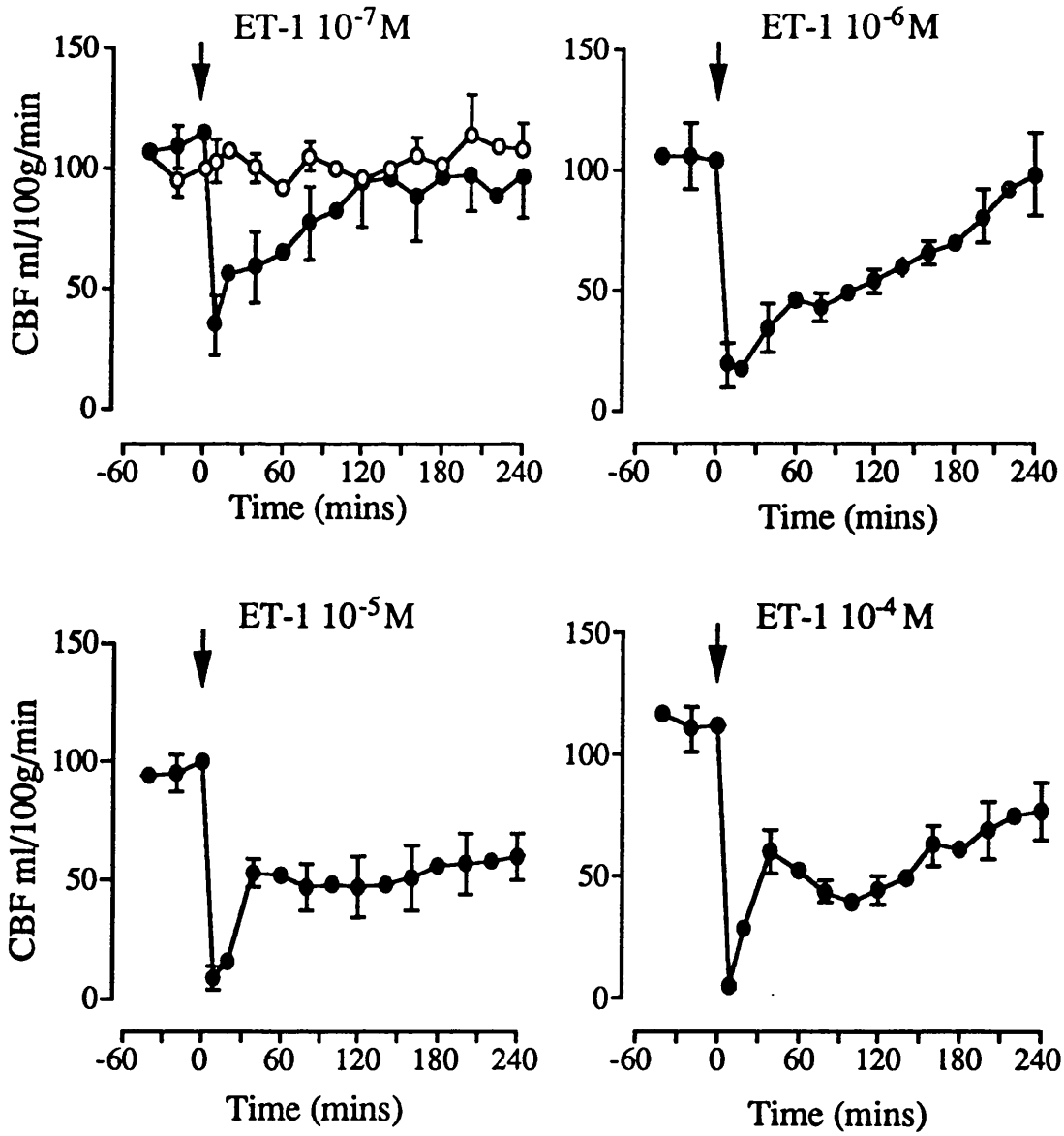

Blood flow was measured using the hydrogen clearance technique. Endothelin-1 (filled symbols) induced a rapid, marked reduction in striatal blood flow compared to the saline control (open symbols). The ischaemia was maximal at approximately 10 min post-endothelin-1 application to the MCA and was followed by progressive restoration of blood flow. From Macrae *et al.* 1993.

Figure 4 Dose-dependency of the severity and duration of striatal ischaemia induced by endothelin-1

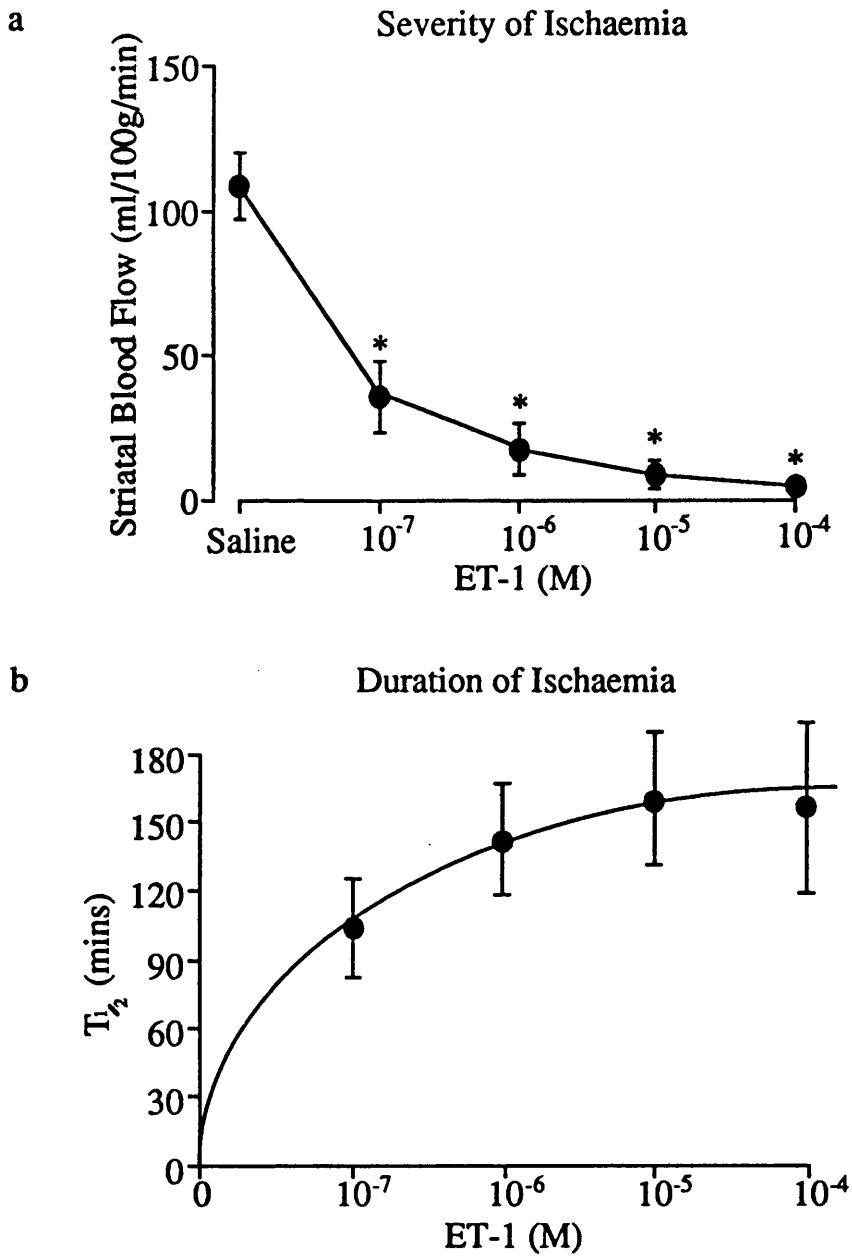

The magnitude of a) the initial marked ischaemia induced by endothelin-1 and b) the duration of action (expressed as time taken for flow to return to 50% of original value) of the peptide are dose-dependent. Data derived from Figure 3. * $p < 0.05$ comparison with saline control. From Macrae *et al.* 1993.

A superficially similar model has recently been described using intracortical, perivascular injection of endothelin-1 (120 pmol in 3 μl) to induce vasoconstriction of the MCA in conscious rats (Sharkey *et al.* 1993). This approach remains to be extensively characterised but, unlike our model, does not appear to induce reperfusion within 3 h of endothelin-1 application (Sharkey *et al.* 1993).

1.3.3. Histopathological Features of Ischaemic Damage

The type and extent of cell damage following experimental cerebral ischaemia depends both on the model used (focal or global) and the duration of the ischaemic insult. Transient global ischaemia results in delayed neurodegeneration that becomes apparent 1-3 days after induction of ischaemia (Kirino 1982; Pulsinelli *et al.* 1982). In these models neurones are selectively affected while other cellular elements within the brain remain morphologically normal. The neuronal necrosis is also selective in that it affects particular vulnerable populations of neurones such as pyramidal cells in the CA1 region of the hippocampus. As discussed previously models of global ischaemia do not mimic human stroke and the morphological changes observed are more similar to those found in the brains of patients who have suffered brief cardiac arrest which show evidence of selective neuronal necrosis in certain areas of the cortex, hippocampus and cerebellum at post-mortem (Graham 1977). Animal models of focal ischaemia result in cellular damage within the vascular territory of the occluded artery. The damage is initially restricted to neurones, but if the ischaemic insult is of sufficient duration then other cellular elements (oligodendrocytes, astrocytes, microglia and blood vessels) become recruited to the lesion to form a cerebral infarct which, by definition, must include all cell types within the affected tissue.

Following all types of hypoxia, neurones undergo a series of well defined morphological changes termed the ischaemic cell process. Ischaemic cell change was first described by Spielmeyer in 1922 (quoted in Brown 1977) and has subsequently been further characterised by others (Brown 1977). The ischaemic cell process proceeds via 4 stages from subtle changes in the cytoplasm to eventual complete cell loss as follows:

1) Microvacuolation: under the light microscope microvacuoles may be visible as small circular or oval spaces in the cytoplasm. Ultrastructural analysis has shown that microvacuoles are swollen mitochondria and endoplasmic reticulum. In this early stage the nucleus and cell body appear normal.

2) Ischaemic Cell Change: in the transition from microvacuolation to ischaemic cell change the cell body and nucleus become shrunken and triangular in shape, and the nucleolus

disappears. The cytoplasm is eosinophilic and the nucleus is also densely stained.

3) Ischaemic Cell Change with Incrustations: in this stage further shrinkage of the cytoplasm and nucleus occurs. Small densely stained spherical bodies - incrustations - appear close to the cell surface. The incrustations are caused by indentation and compression of the cytoplasm by adjacent swollen astrocytic processes.

4) Homogenizing Cell Change: finally the cell undergoes progressive degeneration. The incrustations are lost and the cytoplasm becomes progressively paler and homogenous. Eventually this process leads to the formation of 'ghost cells' and ultimately cell loss.

The ischaemic cell process is a vital process requiring a minimal supply of energy to initiate it. Thus ischaemic cell change is most easily identifiable towards the edge of a lesion at the boundary between ischaemic and normal tissue where some degree of flow is maintained by the collateral circulation. Neurones within the core of an ischaemic region (*e.g.* dorsolateral caudate nucleus following permanent MCA occlusion) may appear morphologically normal due to the complete absence of cerebral blood flow. Such neurones are assumed to be within the infarcted region if they are totally surrounded by neurones demonstrating the characteristic morphology of ischaemic cell change.

The ischaemic cell process described above occurs only in neurones. Thus, strictly speaking, tissue exhibiting ischaemic cell change should not be referred to as an area of infarct but as 'an area exhibiting changes associated with early evidence of infarction'. The unstated assumption being that with continued ischaemia the selective neuronal necrosis will progress to infarction incorporating neurones, glia and blood vessels. At 4 h post-permanent MCA occlusion (the time point used for acute histopathological studies in this thesis) only the neuronal cell bodies and neuropil show evidence of necrosis. Neurones that have undergone ischaemic cell change appear triangulated and intensely stained with pyknotic nuclei (incrustations may also be present) while the surrounding neuropil is spongiform in appearance. By 24 h other cellular elements have been recruited to the lesion and a true infarct is formed.

In fixed tissue prepared for histology there are 3 types of artefact (dark cell change, hydropic cell change and perineuronal and perivascular spaces) that may be misinterpreted as evidence of hypoxic damage (Brown 1977). These artefacts arise from inadequate fixation or perfusion of the fixative at too low or too high a perfusion pressure, and thus can be minimised by careful monitoring of the fixation procedure. In general artefacts can be distinguished from true ischaemic cell change by their distribution outwith the territory supplied by the occluded vessel.

1.4. MEDIATORS OF ISCHAEMIC/REPERFUSION INJURY

1.4.1. Energy failure and acidosis

The brain is unique in its reliance on the aerobic oxidation of glucose for its energy supply (Sokoloff 1981). Despite this dependence on glucose the carbohydrate stores in the brain are sufficient to maintain energy production for only 5 min (Pulsinelli 1985). Therefore depletion of oxygen and glucose following the onset of cerebral ischaemia has an immediate and potentially lethal effect upon cerebral energy metabolism. ATP and phosphocreatine levels fall to undetectable levels within 2 min of global ischaemia (Siesjo *et al.* 1990) at which point all energy-dependent processes will cease to function. In this respect failure of the Na^+/K^+/ATPase membrane pump resulting in rapid loss of ionic homeostasis may be of critical importance (Lees 1991). Failure of normal homeostatic mechanisms leads to an efflux of K^+ from cells that is countered by entry of Na^+, Cl^- and water resulting in cytotoxic oedema formation (Yang *et al.* 1992). In addition loss of the Na^+ gradient that normally drives glutamate re-uptake (Lees 1991) will lead to accumulation of this potentially cytotoxic neurotransmitter (see Section 1.4.3.).

In an attempt to maintain ATP levels during ischaemia any residual glucose will be metabolised anaerobically to lactic acid and CO_2. Accumulation of lactate and CO_2 results in severe tissue acidosis during ischaemia (Kobatake *et al.* 1984; Mabe *et al.* 1983). Acidosis can damage cells by inactivation or denaturation of enzymes and other proteins, alteration of neurotransmitter reuptake, disruption of mitochondrial function and promotion of free radical formation through the release of free Fe^{2+} (Siesjo *et al.* 1989; Welch & Barkley 1986). Lactic acid formation is dependent on the amount of glucose present (Gardiner *et al.* 1982), therefore tissue damage is more severe in hyperglycaemic animals (Duverger & MacKenzie 1988) particularly in regions of incomplete ischaemia, where a minimal glucose supply is maintained (Prado *et al.* 1988).

If complete energy failure is prolonged then cells will ultimately die, but mitochondrial function (assessed by restoration of normal ATP and phosphocreatine levels) can be recovered if reperfusion occurs within 1 h following global ischaemia (Pulsinelli & Duffy 1983). However despite this recovery, cell damage may continue due to induction of a biochemical cascade of pathological events triggered by an increase in intracellular $[Ca^{2+}]$ during the ischaemic phase (see below). Similarly in the focal ischaemic penumbra (a border zone between the central ischaemic core and normal viable tissue where collateral perfusion is sufficient to maintain minimal ATP levels), alterations in Ca^{2+} homeostasis may be the critical factor in determining whether damage becomes irreversible.

1.4.2. Calcium

Ca^{2+} plays an important role in many cell processes including the control of cell metabolism, enzyme function, intercellular signalling and growth and differentiation (Cheung *et al.* 1986). The precise regulation of intracellular Ca^{2+} levels is therefore critical for normal cell functioning. Under resting conditions, the free intracellular Ca^{2+} concentration ($[Ca^{2+}]_i$) of neurones is 10^{-7}M while extracellular Ca^{2+} concentration is 10^{-3}M (Vibulsreth et al. 1987). This steep concentration gradient is normally maintained by 2 Ca^{2+}-extruding pumps (a Ca^{2+}-ATPase and an electrogenic Na^+/ Ca^{2+} exchanger energised by the Na^+/K^+-ATPase pump) and by active sequestration of Ca^{2+} into intracellular organelles such as endoplasmic reticulum and mitochondria (Siesjo & Bengttson 1989). Loss of normal Ca^{2+} homeostasis was first postulated as the mechanism of cerebral ischaemic injury in 1981. The Ca^{2+} hypothesis, as originally formulated, proposed that energy failure during ischaemia leads to elevated $[Ca^{2+}]_i$ that activates a biochemical cascade of Ca^{2+}-dependent processes resulting ultimately in cell death (Siesjo 1981).

Since the formulation of the Ca^{2+} hypothesis it has been repeatedly demonstrated that $[Ca^{2+}]_i$ (measured directly or indirectly) increases during an ischaemic insult (Benveniste *et al.* 1988; Rappaport *et al.* 1987; Uematsu *et al.* 1989). This was originally thought to be due to Ca^{2+} entry through voltage-sensitive Ca^{2+} channels (VSCC) activated by membrane depolarisation as a result of ATP depletion (Harris *et al.* 1981). More recently the role of glutamate in causing Ca^{2+} influx (particularly via the NMDA receptor gated ion channel) has been recognised (Benveniste *et al.* 1988, see Section 1.4.3.). In addition to Ca^{2+} accumulation during focal ischaemia, further accumulation may occur after the onset of reperfusion following a period of transient focal ischaemia (Greenberg *et al.* 1991; Hara *et al.* 1990). This is probably due in part to free radical-induced inactivation of the Ca^{2+}-extrusion pumps (Araki *et al.* 1992; Hirosumi *et al.* 1988) since $[Ca^{2+}]_i$ does decline during the reperfusion phase following pre-treatment with the free radical scavenger superoxide dismutase (Araki *et al.* 1992). Thus Ca^{2+} accumulation may contribute to neuronal injury during both focal ischaemia and reperfusion.

Ca^{2+} has many potentially cytotoxic effects. Firstly Ca^{2+} can disrupt mitochondrial function by uncoupling oxidative phosphorylation that will lead ultimately to cellular dysfunction and death (Siesjo & Bengttson 1989). Secondly Ca^{2+} can activate several deleterious enzymatic pathways in the neurone that are detailed below. Ca^{2+} activates phospholipase A_2, an enzyme that cleaves membrane phospholipids to release fatty acids including arachidonic acid. Once liberated arachidonic acid is rapidly converted, in the

presence of oxygen, into prostaglandins, thromboxanes and leukotrienes via the cyclooxygenase and lipoxygenase pathways. These compounds can induce vasoconstriction, platelet aggregation and oedema formation which may exacerbate the original ischaemic insult (Kiwak *et al.* 1986). Moreover free radicals, produced as byproducts of arachidonic acid metabolism, can promote oxidative damage to membrane lipids, DNA and proteins (see Section 1.4.4.1.). Another source of free radical production is xanthine oxidase. This enzyme is produced from its normal form (xanthine dehydrogenase) by a Ca^{2+}-activated protease. Free radicals are released when xanthine oxidase catalyses the conversion of hypoxanthine to uric acid (see Section 1.4.4.2.).

Ca^{2+} can also directly activate phospholipase C independent of a receptor coupled G protein (Verity 1992). Phospholipase C hydrolyses membrane phosphatidylinositides releasing 2 intracellular messengers inositol trisphosphate (IP_3) and diacyl glycerol (DAG). IP_3 promotes the release of further Ca^{2+} from intracellular stores, while DAG and Ca^{2+} activate protein kinase C. Protein kinase C regulates neuronal excitability by phosphorylation of membrane ion channels and can promote further Ca^{2+} influx via VSCC (Kaczmarek 1987).

The calpains are another family of Ca^{2+}-activated proteases. The calpains can degrade cytoskeletal and membrane proteins (including receptors) and several enzymes (Melloni & Pontremoli 1989). Their capacity for causing severe cell damage is therefore considerable and calpain inhibitors can give significant protection against ischaemic damage (Rami & Krieglstein 1993).

By binding to the regulatory protein calmodulin (CaM) Ca^{2+} can activate a further series of enzymes including phospholipases, proteases and kinases that can cause further structural degradation (Grotta *et al.* 1990). Ca^{2+}-CaM also stimulates nitric oxide production by activation of nitric oxide synthase. Nitric oxide is a free radical and may be an important mediator of excitotoxic and ischaemic damage (see Section 1.6.).

Due to the Ca^{2+} hypothesis of ischaemic cell injury VSCC antagonists have been investigated for potential neuroprotective efficacy in experimental ischaemia. The most commonly used Ca^{2+} antagonists are dihydropyridines *e.g.* nimodipine and nicardipine, and diphenylalkylamines *e.g.* flunarizine which bind to separate sites on the L-type Ca^{2+} channel (Wong *et al.* 1990). The results of studies utilising Ca^{2+} antagonists have been varied and contradictory. For example nicardipine and nimodipine have been reported to reduce Ca^{2+} accumulation during permanent focal ischaemia (Hadani *et al.* 1988) and in the reperfusion phase following transient focal ischaemia (Greenberg *et al.* 1991; Hara *et*

al. 1990) while flunarizine did not prevent Ca^{2+} accumulation following global ischaemia (Hossmann *et al.* 1983). Similarly for histopathological studies, Ca^{2+} channel antagonists reduce ischaemic damage in some reports (Hara *et al.* 1990; Sauter & Rudin 1986) but not others (Hossmann *et al.* 1983; Vibulsreth *et al.* 1987, and see Hossmann 1989 for comprehensive review). Overall it appears that Ca^{2+} channel antagonists are more effective when administered prior to the onset of ischaemia (Mohammed *et al.* 1985) rather than following it (Gotoh *et al.* 1986). This beneficial effect may be mediated by increased cerebral blood flow rather than prevention of neuronal Ca^{2+} influx (Gotoh *et al.* 1986).

The failure of VSCC antagonists to reliably reduce ischaemic damage probably reflects the multiple routes of Ca^{2+} influx and release that converge to increase $[Ca^{2+}]_i$ following ischaemia. The more recent development of N-type Ca^{2+} channel antagonists *e.g.* CNS1145 that inhibit glutamate release from presynaptic terminals may prove more effective as anti-ischaemic agents, by interrupting the ischaemic cascade upstream from the rise in $[Ca^{2+}]_i$ (McBurney *et al.* 1992).

1.4.3. **Glutamate**

The dicarboxylic amino acids glutamate and aspartate are the main excitatory neurotransmitters in the brain (Monaghan *et al.* 1989). While activation of excitatory amino acid (EAA) receptors is essential for normal neuronal functioning, prolonged exposure to EAA can be neurotoxic. This was first demonstrated by Lucas and Newhouse (1957) who found that high concentrations of glutamate induced degeneration of mouse retinal neurones. The neurotoxicity of glutamate was confirmed by Olney and coworkers who showed that exogenous glutamate caused neuronal lesions within the brain (Olney *et al.* 1971; Olney 1978). The close correspondence between the excitatory and neurotoxic properties of a range of glutamate analogs led Olney to formulate the excitotoxic hypothesis in which he postulated that overactivation of EAA receptors was responsible for glutamate-induced neuronal death (Olney *et al.* 1971).

Before further reviewing the evidence that implicates glutamate in both excitotoxic and ischaemia-induced cell death it is necessary to introduce the basic physiology and pharmacology of glutamatergic neurotransmission. Glutamate and its related EAA agonists act at 5 different receptor subtypes, each with distinct pharmacological and physiological properties, which may be colocalised within a single synaptic unit. The EAA receptor subtypes, named according to their most selective agonists, are: N-methyl-

D-aspartate (NMDA); kainate; amino-3-hydroxy-5-methyl-isoxazole-4-propionate (AMPA, previously known as the quisqualate receptor); *trans*-1-amino-cyclopentyl-1,3-dicarboxylate (*trans*-ACPD, also called the metabotropic receptor) and 2-amino-4-phosphonobutyrate (AP4), (Monaghan *et al.* 1989). The NMDA, kainate and AMPA receptors are ionotropic *i.e.* coupled to an ion channel whereas signal transduction at the *trans*-ACPD receptor is mediated via phosphoinositide hydrolysis (Monaghan *et al.* 1989). The AP4 receptor may also be linked to a second messenger system involving cGMP hydrolysis and suppression of pre-synaptic glutamate release (Gasic & Hollmann 1992). Glutamatergic transmission via these receptor subtypes is discussed below and summarised in Figure 5.

Fast excitatory synaptic transmission is mediated by AMPA and kainate receptors whose ion channels are selectively permeable to Na^+ and K^+ (although certain isoforms also permeable to Ca^{2+} have been identified (Iino *et al.* 1990)). AMPA receptors are selectively antagonised by 2,3-dihydroxy-6-nitro-7-sulfamoxylbenzo(F)quinoxaline (NBQX), whereas other related compounds *e.g.* 6-cyano-7-nitro-quinoxaline-2,3-dione (CNQX) show limited selectivity between AMPA and kainate receptors (Monaghan *et al.* 1989). The NMDA receptor-gated ion channel, permeable to Ca^{2+} as well as Na^+ and K^+, does not contribute to normal synaptic transmission due to the presence of a voltage-dependent blockade of the ion channel by Mg^{2+} (MacDermott & Dale 1987). Removal of this Mg^{2+} block occurs during prolonged depolarisation which subsequently allows Ca^{2+} influx into the post-synaptic neurone (MacDermott & Dale 1987).

Figure 5 Schematic representation of a glutamatergic synapse

Glutamate released from the pre-synaptic terminal mediates fast synaptic transmission via the AMPA and kainate receptors which are permeable to Na^+ and K^+. Subsequent membrane depolarisation removes the Mg^{2+}-blockade of the NMDA receptor-gated ion channel allowing Ca^{2+} influx into the post-synaptic neurone. Intracellular Ca^{2+} can also be increased via the *trans*-ACPD receptor that stimulates mobilisation of Ca^{2+} from intracellular stores. At certain synapses glutamate interacts with the presynaptic AP4 receptor to inhibit further glutamate release. Overactivation of post-synaptic glutamate receptors is also prevented by a high affinity, Na^+-dependent glutamate uptake mechanism, present in both neurones and glia, that removes glutamate from the extracellular space.

Abbreviations: NMDA: N-methyl-D-aspartate; AMPA: amino-3-hydroxy-5-methyl-isoxazole-4-propionate; *trans*-ACPD: *trans*-1-amino-cyclopentyl- 1,3-dicarboxylate and AP4: 2-amino-4-phosphonobutyrate.

Figure 5 Schematic representation of a glutamatergic synapse

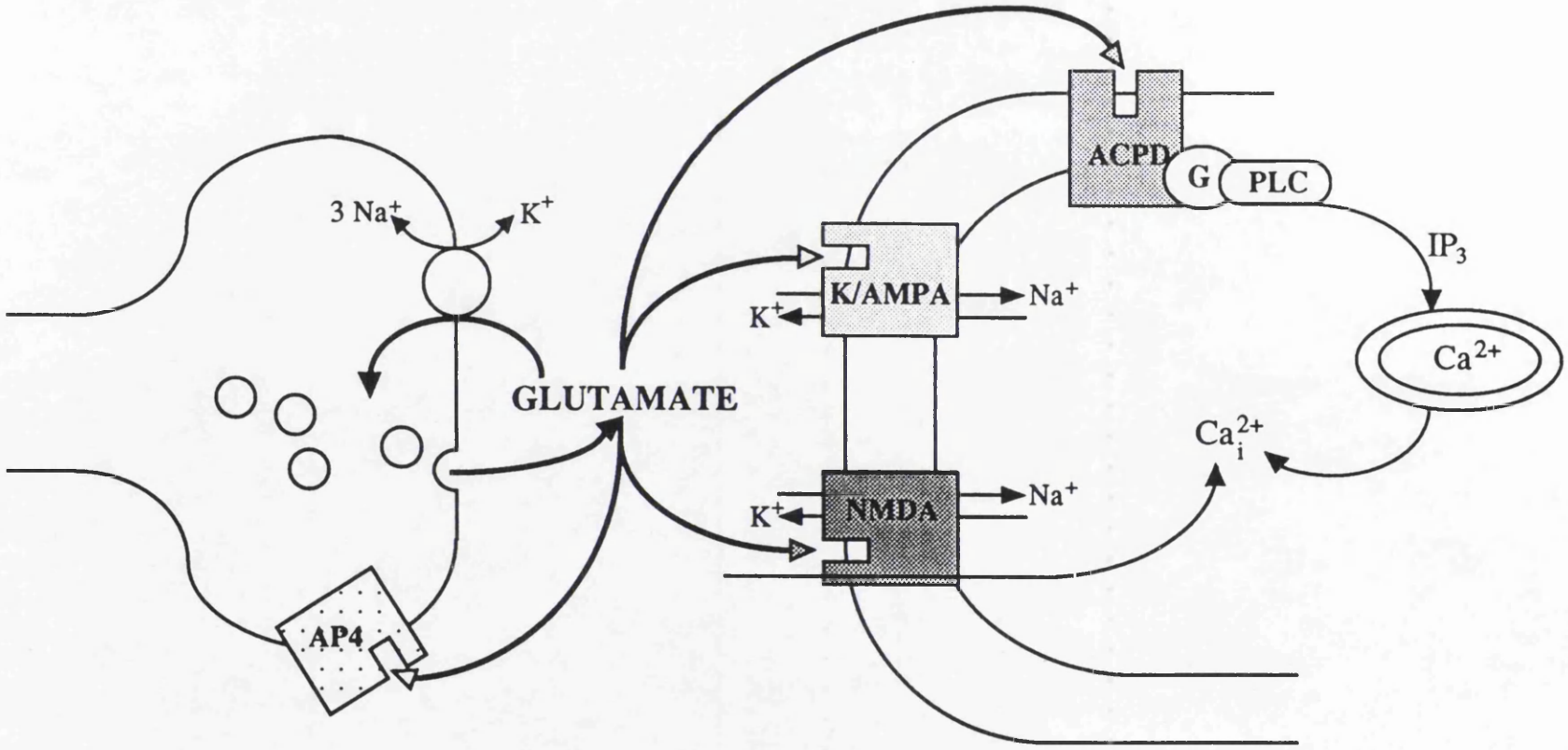

The activity of the NMDA receptor-ion channel complex can be modulated at several distinct pharmacological sites located both on the receptor and within the ion channel (Monaghan *et al.* 1989). Glutamate and NMDA binding to the *transmitter recognition site* can be inhibited by competitive antagonists including 2-amino-5-phosphonovalerate (AP5) and 3-(2-carboxypiperazin-4-yl)propyl-1-phosphate (CPP). Glycine acts as a positive allosteric modulator at the strychnine-insensitive *glycine binding site*, and is necessary for agonist-activation of the receptor. Analogues of the non-selective excitatory amino acid antagonist kynurenate *e.g.* 7-chlorokynurenate act as selective antagonists at this site. Ifenprodil and related compounds act as antagonists at another allosteric modulatory site - the *polyamine site* (Carter *et al.* 1989). Within the ion channel, the *divalent cations* Mg^{2+} and Zn^{2+} can bind at separate sites to inhibit transmembrane ion flux. Finally, another class of antagonists including the dissociative anaesthetics ketamine and phencyclidine (PCP) bind at the *phencyclidine site* within the open channel. These noncompetitive antagonists are use-dependent in that an agonist must bind to the receptor and open the ion channel before the antagonist in turn can bind to its site. Dibenzocycloheptenеimine (MK-801), which is structurally related to PCP, is a more selective and potent antagonist at this site.

The *trans*-ACPD receptor, of which several subtypes have been proposed (Schoepp et al. 1990), is linked via a G protein to phospholipase C which hydrolyses phosphoinositide to release inositol-tris phosphate (IP_3) and diacyl glycerol. IP_3 stimulates the release of Ca^{2+} from intracellular stores. This receptor is also activated by quisqualate but is insensitive to AMPA. 2-amino-3-phosphonoproprionate (AP3) is a relatively selective antagonist at the *trans*-ACPD receptor (more accurately a weak partial agonist, Schoepp *et al.* 1990).

In vitro experiments have established that excess glutamate is toxic to neurones and that the excitotoxic process involves 2 distinct components: 1) acute neuronal swelling due to depolarisation-mediated influx of Na^+, Cl^- and water and 2) delayed neuronal degeneration due to excessive Ca^{2+} influx mainly through the NMDA receptor gated ion channel (Choi 1987). Elevation of intracellular [Ca^{2+}] promotes injury by activation of the cascade of potentially toxic pathways described in Section 1.4.2., and the Ca^{2+} accumulation induced by glutamate has been found to closely correlate with the extent of neuronal damage (Hartley *et al.* 1993). Although the NMDA receptor complex represents the major receptor gated ion channel for Ca^{2+} entry, the role of other EAA receptors is also of importance (Courtney *et al.* 1990). Membrane depolarisation following activation of AMPA and kainate receptors removes the Mg^{2+} blockade of the NMDA receptor ion channel and also allows Ca^{2+} influx through voltage-dependent Ca^{2+} channels. Intracellular Ca^{2+} can also be increased by activation of the *trans*-ACPD receptor which promotes release of Ca^{2+} from intracelluar stores. The importance of interactions between EAA receptor subtypes in mediating the increase in intracellular Ca^{2+} is illustrated by the fact that both NMDA antagonists (Choi *et al.* 1988) and non-NMDA antagonists (Frandsen *et al.* 1989) are neuroprotective against glutamate toxicity *in vitro*.

EAA receptor antagonists were subsequently shown to inhibit hypoxic damage *in vitro* (Goldberg *et al.* 1987; Rothman 1984). This observation led to the extension of the excitotoxic hypothesis to propose that glutamate-induced neurotoxicity also underlies ischaemic neuronal damage. Under normal physiological conditions, the potential toxicity of glutamate is limited by a highly efficient, Na^+-dependent glutamate uptake carrier system present in the plasma membranes of both glia and presynaptic neurones (Nicholls & Atwell 1990). Due to this efficient uptake mechanism glutamate must be administered at high concentrations (100 μM-1 mM with up to 30 min exposure time) to induce neurotoxicity *in vitro* (see Meldrum & Garthwaite 1991 for review). If the normal Na^+ or K^+ gradients are lost, *e.g.* by failure of the Na^+/K^+/ATPase pump during ischaemia, then the resultant decrease in the thermodynamic driving force for glutamate uptake means the glutamate carrier will reverse its direction and release glutamate into the extracellular space (Szatkowski *et al.* 1990). Thus simulated ischaemic conditions *in vitro* both potentiates the toxicity of exogenous glutamate (Novelli *et al.* 1988) and leads to accumulation of endogenous glutamate in the extracellular space (Cazevieille *et al.* 1993; Pellegrini-Giampietro *et al.* 1990).

In vivo extracellular concentrations of glutamate and aspartate are dramatically elevated during global (Benveniste *et al.* 1984) and permanent focal ischaemia (Butcher *et al.* 1990), and there is a high correlation between the extent of ischaemic damage and the

extracellular EAA concentration (Butcher *et al.* 1990; Gemba *et al.* 1992). However the most convincing evidence for a pivotal role of glutamate in the mediation of ischaemic damage *in vivo* is the significant protection achieved with both NMDA and non-NMDA receptor antagonists in a range of animal models (see McCulloch *et al.* 1991 for review). The neuroprotective action of NMDA receptor antagonists was first demonstrated in models of transient global ischaemia (Simon *et al.* 1984; Swan & Meldrum 1990). However neuroprotection in these early studies has subsequently been attributed to the hypothermia induced by NMDA receptor antagonists and/or the anticonvulsant action of these drugs (Buchan & Pulsinelli 1990; Ginsberg & Busto 1989). When brain temperature is strictly controlled the neuroprotective action of NMDA antagonists against global ischaemic damage is less dramatic (Gill & Woodruff 1990) or completely abolished (Buchan *et al.* 1991). It may be that the severe acidosis that occurs during global ischaemia (which can reduce Ca^{2+} influx through NMDA receptor gated ion channels (Takadera *et al.* 1992)) acts to limit NMDA receptor-mediated toxicity and thereby increase the relative importance of non-NMDA receptor mechanisms of injury. Thus AMPA receptor antagonists such as NBQX are neuroprotective in models of global ischaemia (Nellgard & Wieloch 1992; Sheardown *et al.* 1990).

In permanent focal ischaemia both competitive (Bullock *et al.* 1990) and noncompetitive (Park *et al.* 1988) NMDA receptor antagonists provide significant neuroprotection. In addition the noncompetitive antagonist MK-801 is equally effective when administered either pre- or 30 min post-permanent MCA occlusion in the rat (Park *et al.* 1988). Pre- or post-treatment with AMPA receptor antagonists also significantly reduces the volume of ischaemic damage following permanent MCA occlusion, but in this model AMPA antagonists are less efficacious than NMDA receptor antagonists (Gill *et al.* 1992). In contrast to permanent focal ischaemia the efficacy of EAA receptor antagonists against transient focal ischaemic damage has received little attention in the published literature. Therefore in this thesis the neuroprotective efficacy of MK-801 will be assessed using the endothelin-1 model of transient focal ischaemia.

1.4.4. Free Radicals

A free radical is defined as any atom or molecule that contains one or more unpaired electrons (Halliwell 1989). Free radicals can be based on any atom but oxygen radicals are particularly implicated in ischaemic-reperfusion injury. Molecular oxygen can form radicals by sequential, univalent reductions that produce superoxide ($O_2\bullet^-$), hydrogen peroxide (H_2O_2) and hydroxyl radicals ($\bullet OH$) by the following reactions:

$$O_2 + 1e^- \text{ ---> } O_2\bullet^- \qquad (1)$$

$$2\,O_2\bullet^- + 2H^+ \text{ ---> } H_2O_2 + O_2 \qquad (2)$$

$$H_2O_2 + Fe^{2+} \text{ ---> } OH\bullet + OH^- + Fe^{3+} \text{ (Fenton Reaction)} \qquad (3)$$

H_2O_2 is not a free radical and is a comparatively weak oxidising agent. However because it is non-polar it can cross cell membranes and mediate local toxicity by generating highly reactive hydroxyl radicals. The Fe^{3+} formed in this reaction is then converted back to Fe^{2+} by reaction with superoxide:

$$Fe^{3+} + O_2\bullet^- \text{ ---> } Fe^{2+} + O_2 \qquad (4)$$

Combination of equations 3 and 4 gives the Haber-Weiss reaction:

$$O_2\bullet^- + H_2O_2 \xrightarrow{\text{Fe catalyst}} OH^- + \bullet OH + O_2$$

Because the hydroxyl radical is more reactive than either superoxide or hydrogen peroxide, much of the toxicity of these 2 radicals is thought to be mediated by their combination to form hydroxyl radicals via the Haber-Weiss reaction. This reaction is dependent on a free iron catalyst which *in vivo* is normally derived from the metalloproteins ferritin or haemoglobin (Halliwell 1989).

1.4.4.1. Mechanisms of free radical induced tissue damage

Most free radicals are highly reactive. The presence of an unpaired electron means that radicals can initiate and propagate chain reactions since when a radical reacts with a nonradical another free radical must be formed. *In vivo* oxygen radicals can react with and

damage proteins, DNA and membrane lipids.

Lipid Peroxidation. The structure of polyunsaturated fatty acids makes them highly susceptible to •OH damage. The reaction is initiated by •OH abstracting a hydrogen atom from a carbon in the fatty acid chain to produce a lipid radical. This molecule then rearranges to form a conjugated diene which subsequently reacts with molecular oxygen to form a peroxy radical. This radical can then propagate the chain reaction by abstracting another H atom from a neighbouring fatty acid.

Lipid peroxidation can be detected by measuring the specific ultraviolet absorbance of conjugated dienes or more indirectly by the TBARS (thiobarbituric acid reactive substance) test that detects a pink chromogen formed by the reaction of the peroxidation by-product malondialdehyde with thiobarbituric acid. However this test has been criticised for its nonspecificity and lack of correlation with other assays (Valenzuala 1991).

The brain membrane lipids are rich in polyunsaturated fatty acid side chains that make the brain particularly vulnerable to lipid peroxidative damage (Halliwell 1989). Lipid peroxidation initiates cross-linking between different membrane lipids and between lipids and membrane proteins that compromise the structural integrity of the membrane, decreasing its fluidity while increasing its permeability (Watson & Ginsberg 1989). Neuronal injury due to lipid peroxidation may be secondary to vascular injury in that free radical induced increases in the permeability of the cerebrovasculature may lead to the accumulation of vasogenic oedema (Kontos 1989).

In global ischaemia models, lipid peroxidation (estimated by the TBARS method) is negligible during ischaemia but increases on reperfusion to peak 30 min to several hours post-ischaemia depending on the severity of the original ischaemic insult (Bromont *et al.* 1989; Yoshida *et al.* 1980). Using the more specific conjugated diene method significant increases in whole rat cortex have been reported (Sakamoto *et al.* 1991; Vanella *et al.* 1992), while others have found only small localised changes (Watson *et al.* 1984). Following transient focal ischaemia increases in conjugated dienes are very limited (Ginsberg *et al.* 1988) leading these authors to suggest that lipid peroxidation is not an important mediator of free radical induced damage (Ginsberg *et al.* 1988).

Protein and DNA oxidation Oxidation of proteins by free radicals can cause enzyme inactivation, cytoskeletal disruption and affect the conformational integrity of proteins so that they are recognised as 'foreign' by the immune system (Siesjo *et al.* 1989). Oxidative damage to proteins (assessed by increased protein carbonyl content) increases during the reperfusion phase following transient global ischaemia (Oliver *et al.* 1990). Oxidative

inactivation of glutamine synthetase, the enzyme that degrades L-glutamate, may be of particular importance in relation to ischaemic/reperfusion injury since excess glutamate is neurotoxic. Glutamine synthetase is inactivated by oxygen free radicals *in vitro* (Schor 1988). Following transient global ischaemia whole cortex glutamine synthetase activity is decreased during the first 3 hours of reperfusion (Oliver *et al.* 1990), although with longer reperfusion periods enzyme activity recovers (Oliver *et al.* 1990) and may even increase (Petito *et al.* 1992) due to astrocytic proliferation.

Free radicals can also damage DNA by strand breakage and modification of the nucleic acid bases (Floyd & Carney 1992). Subsequent activation of poly(ADP-ribose) synthetase to repair the strand breaks may further deplete energy supplies already compromised by ischaemia.

It has been suggested that free radical induced damage to proteins and DNA is more important in the pathogenesis of ischaemic-reperfusion injury than lipid peroxidation (Watson & Ginsberg 1989). However in some models of global and transient focal ischaemia no protein or DNA damage is detectable (Folbergrova *et al.* 1993; Krause *et al.* 1992; White *et al.* 1992).

1.4.4.2. Sources of free radicals during ischaemia and reperfusion

Mitochondria The limited oxygen supply during ischaemia means that components of the electron transport chain (*e.g.* FAD) become reduced. With reperfusion the reduced molecules undergo autooxidation with generation of superoxide.

Xanthine Oxidase Production of free radicals via the xanthine oxidase pathway was first proposed by McCord from studies of intestinal ischaemia (McCord 1985). During ischaemia ATP can not be regenerated so that AMP levels increase. The AMP is catabolised via adenosine and inosine to hypoxanthine which accumulates during ischaemia (Hagberg *et al.* 1986; Hillered *et al.* 1989) Hypoxanthine is normally metabolised by xanthine dehydrogenase, but under ischaemic conditions this enzyme is converted to an oxidase by Ca^{2+}-dependent proteolysis. With the restoration of oxygen during reperfusion xanthine oxidase catalyses the conversion of hypoxanthine to uric acid with the formation of superoxide.

Infusion of xanthine oxidase into the caudate nucleus induces oedema formation and neuronal injury (Chan *et al.* 1984). However the importance of this pathway as a source of free radicals during cerebral ischaemia-reperfusion is still debatable. Significant conversion

of xanthine dehydrogenase to xanthine oxidase occurs following global ischaemia (Kinuta *et al.* 1989; Vanella *et al.* 1992), but only moderate (Lindsay *et al.* 1991) or no (Betz *et al.* 1991) increases have been reported following permanent focal ischaemia. Free radicals produced by this mechanism are more likely to be formed in the cerebrovasculature since xanthine oxidase activity is higher in brain endothelial cells than brain parenchyma (Betz 1985).

Arachidonic Acid Metabolism During ischaemia Ca^{2+} activation of phospholipases results in release of free arachidonic acid from membrane phospholipids (see Section 1.4.2.). With the restoration of oxygen supplies, metabolism of arachidonic acid by the cyclooxygenase and lipoxygenase pathways is initiated generating radical forms of prostaglandin H (PGH) synthase and the lipoxygenases. These enzyme radicals can abstract hydrogen atoms from NADH or NADPH to produce free radical forms (NAD• or NADP•) which in turn react rapidly with molecular oxygen to release superoxide (Kubreja *et al.* 1986; Chan *et al.* 1988). NMDA agonists have also been shown to generate superoxide by a Ca^{2+}- and arachidonic acid-dependent process *in vitro* (Lafon-Cazal *et al.* 1993).

Intracerebral injection of arachidonic acid induces brain oedema (Chan *et al.* 1983) by a mechanism involving superoxide (Chan & Fishman 1980). However arachidonic acid can also induce membrane permeability changes independent of free radical mediated mechanisms (Villacara *et al.* 1989).

Polymorphonuclear Leucocytes and Macrophages During reperfusion these blood-borne cells may accumulate within the brain (see Section 1.4.5.). Prostaglandins and leukotrienes can activate NADPH oxidase in these cells resulting in the generation of superoxide (Lunec 1990). Leukocytes in turn can synthesize further prostaglandins and leukotrienes and thereby release more radicals.

Acidosis The accumulation of lactic acid under ischaemic conditions promotes the dissociation of protein-bound iron (Bralet *et al.* 1992; Rehncrona *et al.* 1989). Superoxide formed by one or more of the pathways discussed above would then be able to react with the free iron and form hydroxyl radicals via the Haber-Weiss reaction. In support of this mechanism infusion of Fe^{2+} into the rat cortex has been demonstrated to induce lipid peroxidation and oedema formation (Willmore & Rubin 1982).

These potential pathways for free radical production are summarised in Figure 6. It can be seen that complete ischaemia 'primes' the brain for the generation of free radicals by inducing the formation of the necessary substrates. However free radical production in appreciable quantities is only initiated with the restoration of adequate oxygen supplies during reperfusion. In support of this theory increased oxygen levels during early reperfusion have been reported to exacerbate ischaemic damage (Halsey *et al.* 1991; Mickel *et al.* 1987) presumably by enhancement of free radical formation. The development of spin trapping techniques has enabled direct measurement of free radicals by electron spin resonance spectroscopy. These techniques show that low levels of free radicals are generated during global ischaemia (presumably because blood flow is not completely abolished) while at the onset of reperfusion a burst of free radical production occurs which then slowly decays back to the ischaemic level after 30-60 min reperfusion (Sakamoto *et al.* 1991; Zini *et al.* 1992). Thus most free radical induced damage is likely to occur when blood flow is restored to previously ischaemic tissue, and free radicals may therefore be a major contributor to reperfusion injury.

1.4.4.3. Pharmacological inhibition of free radical-associated cerebral injury

The most convincing, though indirect, evidence for the involvement of oxygen radicals in ischaemic brain injury is the reported neuroprotective action of several antioxidant and radical scavenging drugs. Pharmacological treatment strategies aimed at reducing free radical damage can be divided into 3 types:

1) Scavenging of free radicals by nonenzymatic antioxidants

The endogenous antioxidants alpha-tocopherol (Vitamin E), ascorbic acid (Vitamin C) and glutathione can scavenge oxygen radicals in the normal brain. However under ischaemic conditions the concentration of these antioxidants falls (Kinouchi *et al.* 1991; Lyrer *et al.* 1991; Uemura *et al.* 1991), due to reaction with free radicals (Hogg *et al.* 1993). This may compromise the ability of the brain to scavenge free radicals during reperfusion since it has been demonstrated that chemical depletion of glutathione prior to onset of ischaemia can exacerbate tissue damage (Mizui *et al.* 1992). To compensate for this effect, systemic adminstration of the lipophilic alpha-tocopherol prior to induction of global ischaemia reduces lipid peroxidation (Vanella *et al.* 1992) and improves neurological outcome (Yamamoto *et al.* 1983).

Figure 6 Schematic representation of the generation of free radicals following ischaemia and reperfusion

The acidosis, energy store depletion and increase in free intracellular Ca^{2+} that occur during an ischaemic insult (described in more detail in the text) prime the brain for generation of free radicals following the onset of reperfusion and concomitant restoration of oxygen supplies. In addition invasion of blood-borne leucocytes from the periphery during reperfusion introduces another potential source of free radicals. The radicals can then induce tissue damage by peroxidation of membrane lipids, oxidation of proteins and DNA.

Figure 6 Schematic representation of the generation of free radicals following ischaemia and reperfusion

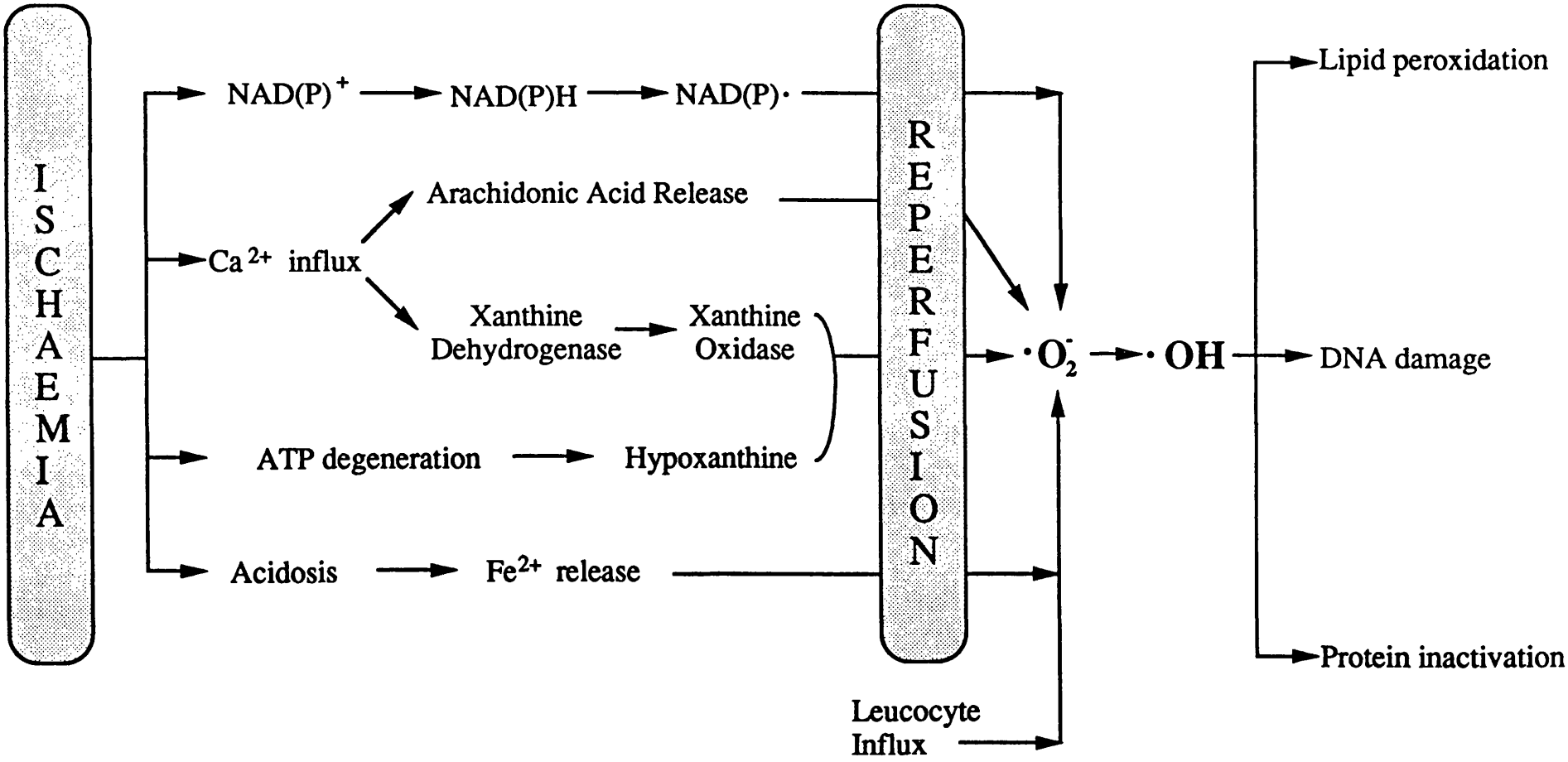

Spin-trapping agents such as phenyl-t-butyl-nitrone are essentially oxygen radical scavengers and can reduce ischaemic damage (Yue *et al.* 1992). Dimethylthiourea, a hydroxyl scavenger, can reduce ischaemic damage and oedema formation following permanent focal ischaemia (Martz *et al.* 1989) by a mechanism independent of changes in cerebral blood flow (Martz *et al.* 1990).

Tirilizad (U74006F) is one of a group of compounds, the 21-aminosteroids, that inhibit lipid peroxidation *in vitro* by a variety of mechanisms including free radical scavenging. The anti-ischaemic efficacy of tirilizad is controversial as it reduces ischaemic cell damage and oedema formation in some animal models but not others (reviewed in Hall 1993).

2) Scavenging by specific enzymes

Three enzymes - superoxide dismutase (SOD), catalase and glutathione peroxidase - exist specifically to 'detoxify' oxygen radicals (Freeman & Crapo 1982). SOD, which exists in 2 forms (Mn-SOD in mitochondria; CuZn-SOD in cytosol) catalyses the dismutation of superoxide to produce hydrogen peroxide:

$$2O_2^{\bullet-} + 2H^+ \xrightarrow{\text{SOD}} H_2O_2 + O_2$$

To prevent formation of hydroxyl radicals, catalase and glutathione peroxidase then convert the hydrogen peroxide to water by the following reactions:

$$2H_2O_2 \xrightarrow{\text{catalase}} 2H_2O + O_2$$

$$H_2O_2 + 2\ \text{glutathione} \xrightarrow{\text{glutathione peroxidase}} 2H_2O + \text{glutathione disulphide.}$$

Levels of these 3 enzymes are relatively low in the brain (Schmidley 1990). Glutathione peroxidase is relatively resistant to ischaemia, but SOD is depleted following permanent focal ischaemia (Michowiz *et al.* 1990; Imaizumi *et al.* 1989). Transgenic mice that overexpress CuZn-SOD (3.1-fold higher than control) show significantly less oedema and a reduced infarct size following permanent focal ischaemia than their nontransgenic controls (Kinouchi *et al.* 1991).

Pretreatment with SOD conjugated to polyethylene glycol (PEG) (in order to prolong the plasma half-life of SOD) either alone (He *et al.* 1993; Matsumiya *et al.* 1991) or in combination with PEG-catalase (Liu *et al.* 1989) reduces the volume of ischaemic damage

following transient focal ischaemia in cats and rats. The site of action of PEG-SOD is probably intravascular as PEG-SOD has a very slow uptake rate into the brain (Yoshida *et al.* 1992). Liposomal entrapped SOD (designed to facilitate access to the brain) also reduces ischaemic damage and oedema formation following permanent focal ischaemia in rats (Imaizumi *et al.* 1990). However post-ischaemic treatment with either PEG-SOD (Matsumiya *et al.* 1991) or liposome-entrapped SOD (Chan 1992) is ineffective.

3) Inhibition of Xanthine Oxidase

Pre-treatment with the xanthine oxidase inhibitors allopurinol and oxypurinol reduces neuronal damage and oedema following permanent focal ischaemia (Betz *et al.* 1991; Martz *et al.* 1989; Lindsay *et al.* 1991). Oxypurinol is also effective 1 h post-onset of ischaemia (Lin & Phillis 1991). However the neuroprotective doses of allopurinol are higher than those necessary to inhibit xanthine oxidase suggesting allopurinol may be acting by another mechanism - possibly as a hydroxyl radical scavenger (Moorhouse *et al.* 1987).

1.4.4.4. Interactions between glutamate neurotoxicity and free radical-induced cell damage

The exact relationship between these 2 mechanisms of cell injury remains undetermined, but increasing evidence suggests they form part of a common pathway. The glutamate-induced elevation in intracellular Ca^{2+} can stimulate free radical production via arachidonic acid metabolism, xanthine oxidase production and activation of nitric oxide synthase (see Section 1.4.2. and Lafon-Cazal *et al.* 1993). In addition glutamate may stimulate free radical production by a mechanism independent of the ionotropic and metabotropic receptors (Bondy & Lee 1993). Thus free radicals may be an important mediator of glutamate toxicity. In support of this a variety of free radical scavengers attenuate glutamate-induced neurotoxicity *in vitro* (Miyamoto *et al.* 1989; Monyer *et al.* 1990; Yue *et al.* 1992) and cultured neurones derived from transgenic mice overexpressing CuZn-SOD show increased resistance to glutamate-induced neuronal swelling and cell death (Chan *et al.* 1990). A bidirectional cooperativity may exist between glutamate and free radicals because free radicals can also promote further glutamate release (Gilman *et al.* 1992; Pellegrini-Giampetro *et al.* 1988) that can be attenuated by free radical scavengers (Cazevieille *et al.* 1993; Pellegrini-Giampetro *et al.* 1990). Combined treatment with the free radical scavenger dimethylthiourea and the NMDA receptor antagonist MK-801 has no additive effect on oedema formation following permanent focal ischaemia (Oh & Betz 1991) suggesting free radicals and glutamate promote oedema formation *in vivo* by a common mechanism.

1.4.5. Leucocytes and mediators of inflammation

Leucocytes, both polymorphs and monocytes/macrophages, have been implicated in the pathogenesis of cerebral ischaemic damage. Originally the delayed accumulation of leucocytes seen several days after the onset of stroke (Alcala *et al.* 1978) or permanent MCA occlusion (Garcia & Kamijyo 1974) led to the hypothesis that leucocytes were only involved in the phagocytic removal of dead tissue and scar formation (Kochanek & Hallenbeck 1992). However it has recently become apparent that leucocyte accumulation is much more pronounced following transient focal ischaemia. Leucocytes accumulate in brain microvessels within 1 h of reperfusion following MCA occlusion (del Zoppo *et al.* 1991) and begin to infiltrate brain parenchyma within the MCA territory by 3 h (Shiga *et al.* 1991), with marked infiltration at 24 h (Barone *et al.* 1992; Shiga *et al.* 1991). This early accumulation of leucocytes following transient focal ischaemia raises the possibility that leucocytes may be directly involved in ischaemic/reperfusion injury.

There are several possible mechanisms by which leucocytes could contribute to reperfusion-injury (Kochanek & Hallenbeck 1992). Firstly leucocytes may induce post-ischaemic hypoperfusion by physically occluding brain capillaries or by the release of vasoconstrictive prostaglandins and leukotrienes. Depletion of leucocytes prior to induction of ischaemia or reperfusion has been shown to reduce post-ischaemic hypoperfusion following transient global ischaemia in rats (Grogaard *et al.* 1989) and transient MCA occlusion in baboons (Mori *et al.* 1992). Secondly the release of a variety of potentially harmful mediators (Weismann *et al.* 1980) including glutamate (Piani *et al.* 1991), leukotrienes, free radicals, platelet activating factor, proteases and cytokines (see below) could induce direct cell damage, vasoconstriction and increased vascular permeability leading to oedema formation. Depletion of leucocytes reduces both the amount of oedema and volume of ischaemic damage assessed 24 h following transient MCA occlusion in rats (Chen *et al.* 1992; Shiga *et al.* 1991).

The cytokines are a family of peptides synthesized and released by macrophages, microglia and other cell types that mediate a diverse range of physiological functions related to the immune system, cell growth and repair. (Rothwell 1991). Within the CNS attention has focussed on interleukin-1 (IL-1) as a possible mediator of both beneficial and detrimental responses following brain injury. IL-1 is constitutively expressed at low levels in neurones and glia (Yao *et al.* 1992), but following brain injury or stimulation by lipopolysaccharide, activated microglia dramatically increase their production of IL-1 (Giulian *et al.* 1988; Yao *et al.* 1992). IL-1 has been proposed to mediate wound healing by inducing nerve growth factor (Rothwell 1991), and promoting astrogliosis and neovascularisation (Giulian *et al.* 1988). More recently induction of IL-1ß mRNA has been reported following permanent

MCA occlusion in SHR (Liu *et al.* 1993) and within 15 min of the onset of reperfusion following transient global ischaemia (Minami *et al.* 1992). The timing of the peak levels of IL-1ß mRNA in these studies (12 h and 4 h respectively) suggests the IL-1 could be derived from both intrinsic microglia and invading monocytes/macrophages from the periphery.

While IL-1 is postulated to play a beneficial role by promoting growth and repair following brain injury, some of its actions may be detrimental in the context of cerebral ischaemia. IL-1 is pyrogenic (Rothwell 1991), and hyperthermia is known to exacerbate ischaemic damage (Morikawa *et al.* 1992a; Xue *et al.* 1992a). In addition IL-1 can stimulate arachidonic acid metabolism and induce NO synthase (Rothwell 1991), both of which may promote free-radical damage and increase oedema formation. In support of this zinc protoporphyrin, a selective IL-1 antagonist, decreases oedema 24 h following 1 h transient MCA occlusion in the rat, while intracerebral administration of IL-1 exacerbates oedema formation in the same model (Yamasaki *et al.* 1989). Intraventricular administration of an IL-1 receptor antagonist (IL-1ra) has also been reported to reduce the volume of ischaemic damage (assessed from TTC stained sections) 24 h post-permanent MCA occlusion (Relton & Rothwell 1992). IL-1 may also be directly implicated in excitotoxicity since pre-infusion of IL-1ra reduces the volume of striatal damage induced by the selective NMDA agonist cis-2,4-methanoglutamate (Relton & Rothwell 1992). In contrast interleukin-6, the synthesis of which is induced by IL-1 (Rothwell 1991), co-infused with NMDA selectively protects striatal cholinergic neurones *in vivo* against excitotoxic damage (Toulmond *et al.* 1992). This effect may be mediated by induction of nerve growth factor (Toulmond *et al.* 1992).

1.5. ENDOTHELIN-1

Within this thesis endothelin-1 is utilised purely as a tool to induce transient focal ischaemia in the rat. However a brief review of the structure and physiology of endothelin-1 is presented herein to give insight into the mechanism of action of this novel vasoconstrictor peptide.

1.5.1. Structure and synthesis of endothelin-1

Endothelin-1 (ET-1) is a potent vasoconstrictor peptide synthesized and released by endothelial cells. The first 'endothelium derived contracting factor' to be identified, it was isolated from porcine aorta endothelial cells by Yanagisawa *et al.* in 1988. DNA sequencing revealed that ET-1, originally called porcine endothelin, was a 21 amino acid peptide. The compound was renamed endothelin-1 with the subsequent discovery of 2 further isoforms endothelin-2 (ET-2) and endothelin-3 (ET-3) (Inoue *et al.* 1989). The endothelins show close homology - all are 21 amino acid peptides with 2 disulphide bonds between the cysteine residues, but ET-2 and ET-3 differ from ET-1 in 2 and 6 of their amino acid positions respectively (Figure 7a). Each of the peptides derives from a separate gene that synthesizes a preproprotein precursor that is cleaved in 2 stages to yield the active endothelin peptide (Yanagisawa *et al.* 1988). The processing path for the formation of ET-1 from preproET-1 is shown in Figure 7b. The synthesis of ET-1 is thought to be regulated predominantly at the level of mRNA transcription (Yanagisawa *et al.* 1988) and several stimuli *e.g.*thrombin, interleukin-1, phorbol esters and mechanical shear stress can increase the production rate of all 3 endothelins by induction of the appropriate preproendothelin mRNA (Rubanyi & Botehlo 1991).

Vascular endothelium only expresses the gene for ET-1 synthesis. However the 3 endothelins are also expressed in a wide range of tissues (including heart, brain, intestine, kidney and adrenal glands) with differing distribution patterns e.g. ET-2 is predominantly located in the intestine and kidney (Shigeno & Mima 1990). Within the brain ET-1 and ET-3 have been located in neurones (Shinmi *et al.* 1989) and glia (MacCumber *et al.* 1990) as well as the cerebrovasculature (Yoshimoto *et al.* 1990).

Figure 7 Structure and synthesis of the endothelin family of peptides.

a) The amino acid sequences (for rat and human) of the 21 amino-acid peptides endothelin-1 (ET-1), endothelin-2 (ET-2) and endothelin-3 (ET-3). Filled symbols represent differences in the amino-acid sequence of ET-2 and ET-3 compared to ET-1. Solid lines represent disulphide bonds between the cysteine residues.

b) Schematic representation of the biosynthesis of endothelin-1. The preproET-1 (203 amino acids) undergoes proteolytic cleavage to form big ET-1 (39 amino acids), which in turn is cleaved by an endothelin converting enzyme to form ET-1 (21 amino acids). ET-2 and ET-3 are formed by similar processing of separate precursor forms.
Adapted from Rubanyi & Parker Botelho 1991.

Figure 7 Structure and synthesis of the endothelin family of peptides

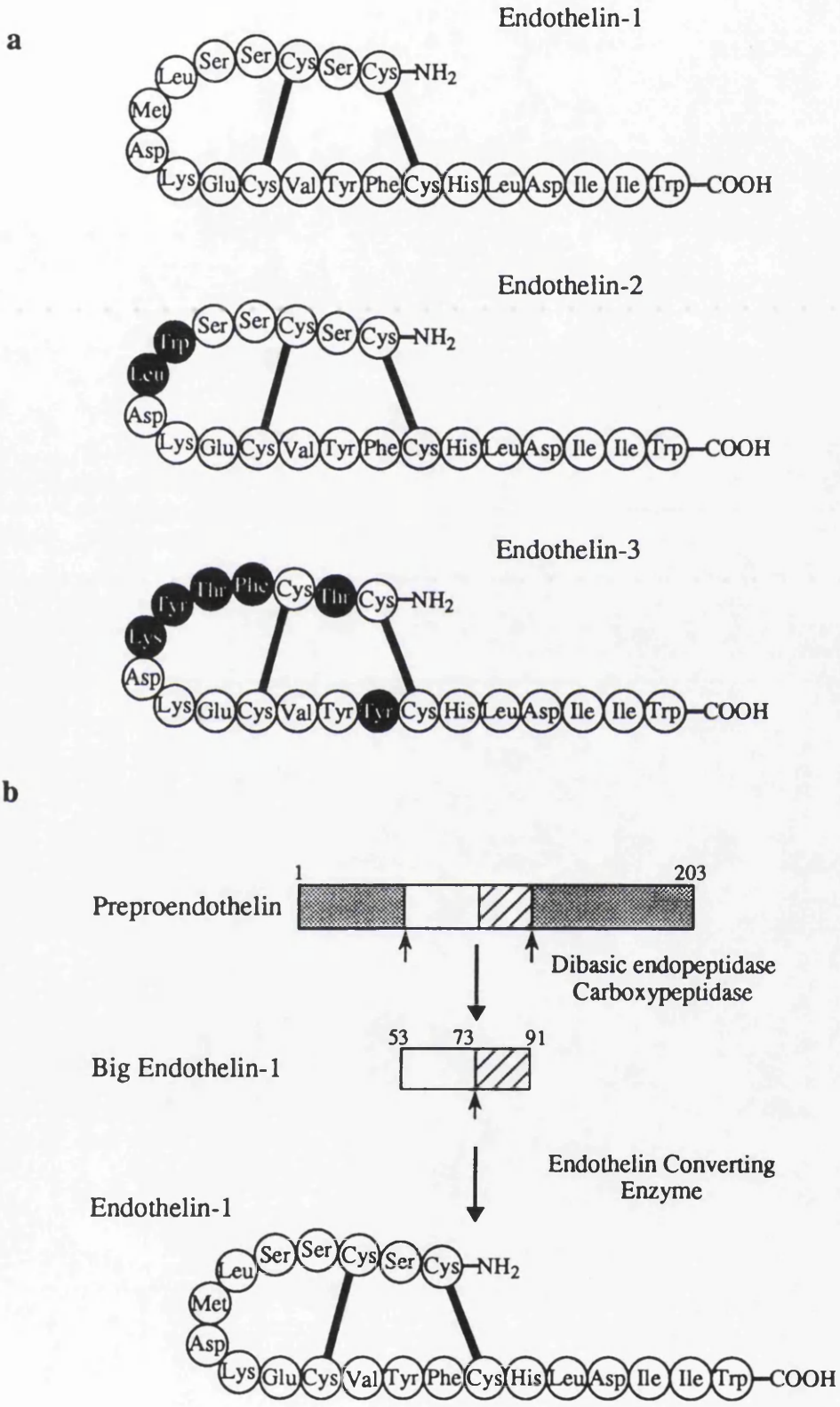

1.5.2. Receptors and signal transduction

Two structurally and functionally distinct endothelin receptors, classified as ET_A and ET_B have been cloned and sequenced (Sakurai *et al.* 1992). ET_A is predominantly located in vascular smooth muscle and has higher affinity for ET-1 than ET-3, while ET_B is found in the endothelium and has equal affinity for the 3 isoforms. Both receptors contain 7 transmembrane domains that are the characteristic feature of the G protein-coupled family of receptors. Further subtypes of receptor have been proposed (Sokolovsky *et al.* 1992; Kloog *et al.* 1989; Samson *et al.* 1990) but the cDNA for these receptors has not yet been isolated. In the brain endothelin receptors have been located in all tissue elements including endothelium (Frelin *et al.* 1991), neurones (Jones *et al.* 1989; Niwa *et al.* 1991) and glia (Hosli & Hosli 1991). Binding sites for ^{125}I-labelled ET-1, ET-2, ET-3 are located throughout the brain including cortex, striatum and hippocampus with the highest density of receptors in the cerebellum (Davenport & Morton 1991). The overall density of ET-1 binding sites is higher than for ET-3 (Davenport & Morton 1991; Fuxe *et al.* 1989a). More recently *in situ* hybridisation has revealed ET_A receptors on cerebral blood vessels and ET_B receptors in glia (Hori *et al.* 1992).

ET-1 induces vasoconstriction by increasing the concentration of free Ca^{2+} within vascular smooth muscle cells via 2 pathways - intracellular Ca^{2+} mobilization and Ca^{2+} influx (See Figure 8). The relative contribution of these 2 pathways depends on the particular vascular bed being studied (see Luscher *et al.* 1992 for review). Initially ET-1 binds to the ET_A receptor and activates phospholipase C via a G protein leading to formation of inositol trisphosphate and diacyl glycerol, and the subsequent release of Ca^{2+} from intracellular stores. ET-1 then indirectly activates voltage-dependent Ca^{2+} channels to allow Ca^{2+} influx into the cell. The ET_B receptor is also coupled to phospholipase C by a G protein and can induce elevations in intracellular Ca^{2+} in endothelial cells by the same pathways. This increase in intracellular Ca^{2+} activates nitric oxide synthase and cyclooxygenase to stimulate production of nitric oxide (NO) and prostacyclin respectively (Emori *et al.* 1991; Hirata *et al.* 1993). ET-1 induces sustained increases in intracellular Ca^{2+} within neurones and glia by the same mechanisms (Chuang *et al.* 1991; Goldman *et al.* 1991; Greenberg *et al.* 1992) and can also increase NO production (Reiser 1990). However the action of ET-1 on neuronal voltage-dependent Ca^{2+} channels has been disputed (Hamilton *et al.* 1989). In addition to phospholipase C endothelin receptors can couple to adenylate cyclase in vascular smooth muscle and endothelium via different G proteins (Ladoux & Frelin 1991; Eguchi *et al.* 1993).

Figure 8 Endothelin-1 induced alterations in intracellular Ca^{2+}

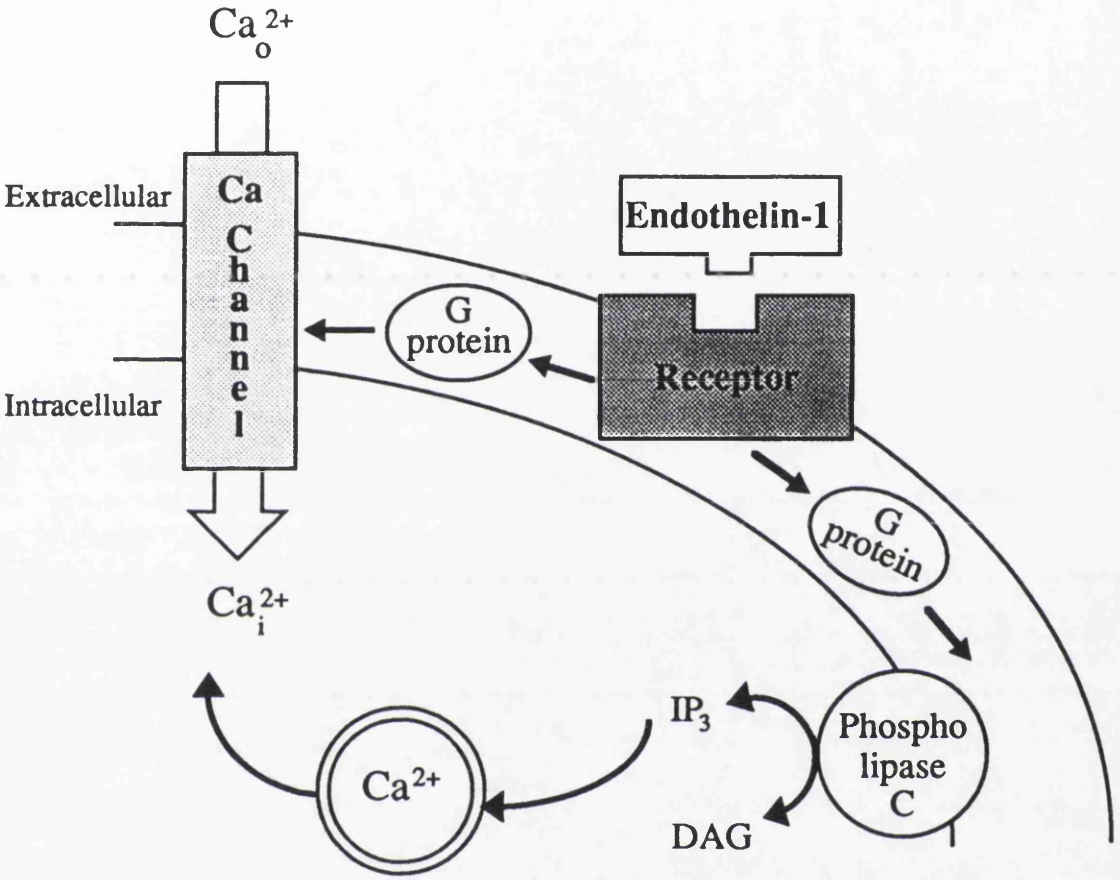

Endothelin receptors are coupled by G proteins to both phospholipase C and receptor-gated Ca^{2+} channels. ET-1 can increase intracellular Ca^{2+} by 2 mechanisms. Following activation of the endothelin receptor, the early transient increase in Ca^{2+} is mediated by activation of phospholipase C resulting in hydrolysis of membrane phospholipids and release of the second messengers diacyl glycerol (DAG) and inositol 1,4,5-trisphosphate (IP_3). IP_3 subsequently stimulates release of Ca^{2+} from intracellular stores. The delayed increase in intracellular Ca^{2+} is mediated by activation of Ca^{2+} channels and influx of Ca^{2+} into the cell.

Adapted from Shigeno & Mima 1990, and Greenberg *et al.* 1992.

1.5.3. Vascular actions of endothelin-1

ET-1 is a potent vasoconstrictor both *in vitro* and *in vivo*. It induces contraction in a wide range of vessels, both arteries and veins, obtained from different species (Yanagisawa *et al.* 1988). The vasoconstriction induced by ET-1 is of prolonged duration and difficult to wash out due to the tight binding of the peptide to its receptor (Yanagisawa *et al.* 1988). *In vivo* systemic administration of ET-1 or ET-3 induces a biphasic blood pressure response: a transient decrease in blood pressure followed by a sustained increase in pressure (Inoue *et al.* 1989). The hypertensive response is mediated by direct vasoconstriction induced via the ET_A receptor, while the initial depression is initated indirectly via the ET_B receptor which stimulates release of the vasodilators NO and prostacyclin from the endothelium (Sudjarwo *et al.* 1992).

As well as local control of vascular tone ET-1 has been postulated to have other important roles in the cardiovascular system including modulation of central cardiovascular control centres, direct effects on cardiac output and growth and proliferation of blood vessels (see Rubanyi & Botehlo 1991 for review).

ET-1 is also a potent constrictor of cerebral vessels of various sizes from different species (Jansen *et al.* 1989; Martin de Aguilera *et al.* 1990; Ogura *et al.* 1991; Yanagisawa *et al.* 1988; Vila *et al.* 1989) with a long duration of action due to the slow dissociation rate from its receptor (Saito *et al.* 1989). In the rat topical application of ET-1 *in situ* to pial arterioles induces slight vasodilation (5% change in diameter) at low doses (10^{-10} M) and dose-dependent constriction at higher doses (*e.g.* 22% decrease in diameter with 10^{-7} M, Faraci 1989). There appear to be regional differences in the response to ET-1 since in the same study when ET-1 was applied to the basilar artery, the low dose did not induce vasodilation, while the constrictor response to the highest dose was significantly greater (Faraci 1989). In the cat ET-1 induces dose-dependent and prolonged constriction of both pial arterioles and veins (Robinson & McCulloch 1990). In peripheral vessels *in vitro* ET-1 was more potent, by an order of magnitude than other vasoconstrictors such as vasopressin (Yanagisawa *et al.* 1988). This is not the case for cerebral vessels in situ where ET-1 is approximately equipotent with other vasoconstrictors (Faraci 1989; Robinson & McCulloch 1990; McCulloch & Edvinsson 1984). *In vivo* it is likely that NO and prostacyclin released from the intact endothelium via stimulation of the ET_B receptor may directly antagonise the vasoconstriction induced by ET-1 stimulation of the ET_A receptor, thereby apparently reducing its potency. While ET-1 is therefore equipotent with other vasoconstrictors its unique characteristic is its very prolonged duration of action which markedly exceeds that of other vasoactive compounds (Edvinsson 1984; McCulloch *et al.* 1986).

Due to the presence of the blood-brain barrier intraluminal ET-1 is less effective in inducing cerebrovasoconstriction than ET-1 applied to the adventitial side of the vessel (Ogura *et al.* 1991). Thus systemic administration of ET-1 does not decrease cerebral blood flow (Mima *et al.* 1989; Kadel & Heistad 1990) unless administered at high concentrations (Willette *et al.* 1990). These findings are consistent with the fact that cerebral microvessel endothelial cells secrete ET-1 mainly to the adventitial side (Yoshimoto *et al.* 1991b) and suggest a predominantly local role for ET-1 in the control of cerebrovascular tone. In contrast administration of ET-1 by routes that allow access to the abluminal side of cerebral vessels *e.g.* intrastriatal (Fuxe *et al.* 1992) or intracisternal (Macrae *et al.* 1991) injection cause profound reductions in local cerebral blood flow in structures in close proximity to the injection site.

1.5.4. **Endothelin-1-induced ischaemic cell damage**

The profound and prolonged vasoconstriction of cerebral vessels induced by ET-1 raised the possibility that local application of the peptide could cause a reduction in cerebral blood flow of sufficient severity and duration to induce ischaemic cell damage. Fuxe *et al.* (1989b) first reported that intrastriatal injection of ET-1 (1 μg/μl) in Sprague-Dawley rats resulted in a purely striatal lesion located around the injection site. Subsequently they demonstrated that striatal blood flow, measured by laser Doppler flowmetry, was reduced by 60% immediately following administration of ET-1 (0.43 nmol/0.5 μl) and was still significantly reduced (by 40%) 3 hours later (Fuxe *et al.* 1992). They concluded the small striatal lesion (6 mm^3) induced by ET-1 was due to this local ischaemia as the vasodilator dihydralazine coinjected with ET-1 attenuated the ET-1 induced reduction in blood flow and reduced the area of striatal damage.

Similar topical application of ET-1 to the proximal MCA results in severe reductions in local cerebral blood flow throughout the territory of the MCA (Robinson *et al.* 1990). This is associated with dose-dependent ischaemic neuronal damage 4 h post-application of the peptide in the anaesthetised Sprague-Dawley rat (Macrae *et al.* 1993). These observations form the basis of our ET-1 model of transient focal cerebral ischaemia introduced in Section 1.3.2.2. and more fully characterised in this thesis.

1.5.5. Endothelin-1-induced cytotoxicity

We have assumed that the neuronal lesions produced by ET-1 in our model of transient focal ischaemia, and also Fuxe's model of intrastriatal injection, are a direct result of the profound ischaemia induced by ET-1 and that mechanisms of excitotoxic cell death are initiated secondary to this ischaemic insult. However it is also possible that the excitotoxic process contributes directly to the lesion induced by ET-1. ET-1 can induce sustained increases in neuronal intracellular Ca^{2+} (see Section 1.5.2.) and the role of elevated intracellular Ca^{2+} in excitotoxicity is well documented (see Section 1.4.2.). In addition ET-1 can stimulate production of neuronal NO (Reiser 1990) which may be a mediator of glutamate-induced excitotoxicity (Dawson *et al.* 1991). However ET-1 is not likely to have a direct neurotoxic action since, unlike glutamate, it is not neurotoxic in cortical or cerebral culture (Lustig *et al.* 1992b; Nikolov *et al.* 1993). However under ischaemic conditions ET-1 can potentiate cell damage *in vitro* (Kataoka *et al.* 1989; Stawski *et al.* 1991). *In vivo* ET-1 can stimulate the release of excitatory amino acids (Lin *et al.* 1990) and increase the rate of cerebral glucose metabolism (Gross *et al.* 1992) factors that may potentiate the effect of an ischaemic insult. For example excitotoxic mechanisms may be contributing to ET-1 induced damage in Fuxe's intrastriatal model since the vasodilator dihydralzine, which completely prevents the ischaemia induced by ET-1, can not completely antagonise the neuronal loss.

1.5.6. Possible pathological role of endothelin-1 in ischaemic injury

It is possible that endogenous endothelin-1 contributes to the pathogenesis of ischaemic injury since severe hypoxia is known to stimulate *de novo* synthesis of endothelin-1 in the periphery (Hieda & GomezSanchez 1990; Horio *et al.* 1991) and plasma endothelin-1 levels are elevated in patients with nonhaemorrhagic stroke (Ziv *et al.* 1992). Vasoconstriction induced by endothelin-1 could reduce collateral blood supply and exacerbate an ischaemic insult. Indeed pre-treatment with exogenous endothelin-1 (5 or 10 pmol intracisternally) has been found to increase ischaemic damage assessed 48 h post-permanent MCA occlusion (electrocoagulation) in the mouse (Nikolov *et al.* 1993). However cerebral endothelial cells do not increase their production of endothelin-1 under hypoxic conditions (Yoshimoto *et al.* 1991a), and increased plasma levels of endothelin-1 are not likely to induce cerebrovasoconstriction if the blood-brain barrier is intact. In addition the increases in endothelin-immunoreactivity observed following transient global ischaemia in rats and gerbils (Giuffrida *et al.* 1992; Willette *et al.* 1992; Yamashita *et al.* 1993) are coincident with the appearance of delayed neuronal degeneration in these models and do not precede morphological evidence of ischaemic damage. Similarly for transient

and permanent focal cerebral ischaemia significant elevations in endothelin-like immunoreactivity are not seen until 24 h post-ischaemia and are most marked at 72 h (Duverger *et al.* 1992). Thus endothelin-1 is not likely to play a causative role in the pathogenesis of cerebral ischaemic injury. Instead it is possible that vasoconstriction induced by this late production of endothelin-1 acts to 'seal off' an area of irreversibly damaged tissue to prevent transfer of potentially toxic species from the infarct to neighbouring viable tissue.

1.6. NITRIC OXIDE

1.6.1. Biosynthesis of nitric oxide

Research into the biological role of nitric oxide (NO) has expanded rapidly over the last few years. It has become apparent that this simple gas is implicated in important physiological functions including vasodilation, platelet aggregation, neural transmission and macrophage-induced cytotoxicity (see Moncada *et al.* 1991 for review). Nitric oxide synthase (NOS), the enzyme that catalyses the production of NO in biological systems, exists as 2 major types. These are a constitutive form (cNOS) present predominantly in endothelial cells and neurones and an inducible form (iNOS) whose expression is induced in cells such as macrophages and glia in response to cytokines and other inductants. cNOS is Ca^{2+}/calmodulin-dependent and releases NO rapidly and transiently in response to agonists that increase intracellular Ca^{2+} (Bredt & Snyder 1990; Mayer *et al.* 1990). In contrast iNOS is Ca^{2+}-independent, and once expressed can continue to produce NO for days (Xie *et al.* 1992). iNOS was originally thought to be independent of calmodulin but is now known to contain calmodulin as a tightly bound subunit that makes it independent of Ca^{2+} transients (Cho *et al.* 1992). The DNA sequences for NOS derived from brain (rat cerebellum, Bredt *et al.* 1991), endothelium (bovine aorta, Lamas *et al.* 1992) and macrophage (mouse, Xie *et al.* 1992) have been elucidated and shown to be encoded by 3 separate genes with 50-60% homology.

Both types of NOS (inducible and constitutive) release NO in the conversion of L-arginine to L-citrulline via an N-hydroxyl-L-arginine intermediate (see Figure 9). Molecular oxygen is required to donate one atom each to citrulline and NO, while NADPH donates 2 electrons for the formation of the intermediate and one electron for its further oxidation to citrulline. In addition both NOS forms require flavin adenine dinucleotide (FAD), flavin mononucleotide (FMN), tetrahydrobiopterin and heme as cofactors (Nathan 1992). cNOS also has distinct phosphorylation sites for several protein kinases (Bredt *et al.* 1992) including protein kinase C and Ca^{2+}/calmodulin- dependent protein kinase II (CaM kinase II). CaM kinase II down-regulates rat cNOS activity (Nakane *et al.* 1991) while protein kinase C has been reported to both up-regulate (Marin *et al.* 1992; Nakane *et al.* 1991) and down-regulate (Bredt *et al.* 1992) NOS activity. NO can also act as a negative feedback system to limit its own synthesis possibly by interaction with the heme subgroup of NOS (Rogers & Ignarro 1992). In the absence of L-arginine, NADPH-reduced NOS can act as a diaphorase to reduce nitroblue tetrazolium to a formazan precipitate. This 'NADPH-diaphorase activity' can be used to detect NOS histochemically (Hope *et al.* 1991).

Figure 9 The biosynthesis of nitric oxide from L-arginine

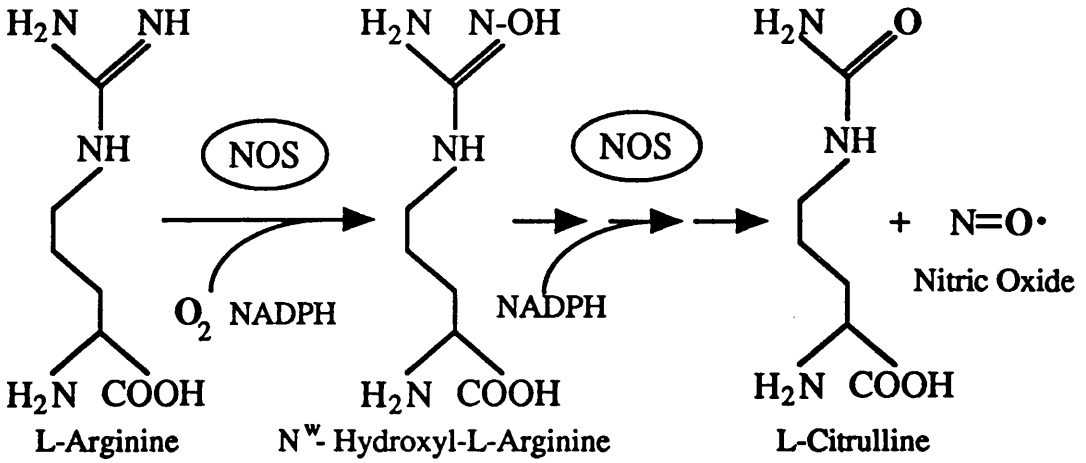

Schematic view of nitric oxide synthase showing interactions between cofactors

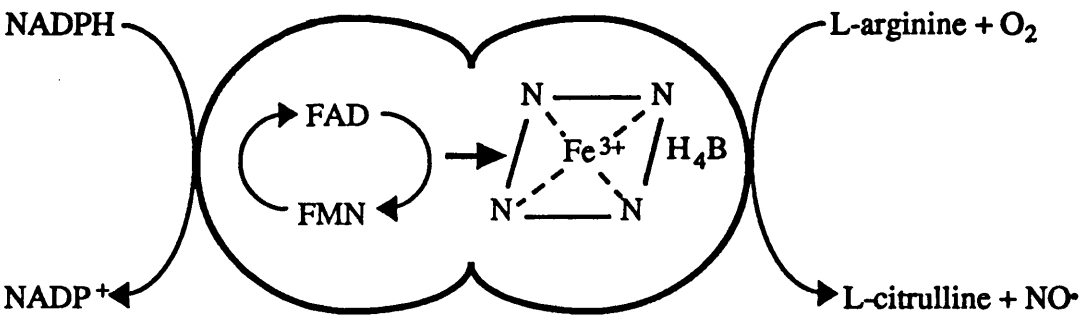

Nitric oxide synthase

The enzyme nitric oxide synthase (NOS) catalyses the reaction of L-arginine with molecular oxygen to form L-citrulline and nitric oxide (NO). The reaction proceeds via at least one intermediate species (Nw-hydroxyl-L-arginine). NADPH, flavin adenine dinucleotide (FAD), flavin mononucleotide (FMN), tetrahydrobiopterin (BH_4) and heme are required as cofactors for the donation and cycling of electrons.
Adapted from Nathan 1992.

1.6.2. Pharmacological inhibition of nitric oxide synthesis

NOS can be inhibited nonspecifically by compounds that prevent interaction with its various cofactors (Nathan 1992), while glucocorticoids *e.g.* hydrocortisone can inhibit the expression of iNOS but have no effect on cNOS (Radomski *et al.* 1990b). More specific inhibition is achieved with several structural analogues of L-arginine including N^G-monomethyl- L-arginine (L-NMMA) and N^G-nitro-L-arginine (L-NA). These NOS inhibitors act as competitive antagonists when co-administered with L-arginine, but can irreversibly inhibit NOS when administered alone (Dwyer *et al.* 1991; Feldman *et al.* 1993). Some NOS inhibitors also act as weak muscarinic antagonists (Buxton *et al.* 1993), while both L-NMMA and L-NA are low potency, non-stereospecific inhibitors of electron transfer in iron containing enzymes such as cytochrome C (Peterson *et al.* 1992).

1.6.3. Nitric oxide and endothelium-derived relaxing factor

Furchgott & Zawadzki (1980) first demonstrated that endothelial cells released a labile substance that mediated acetylcholine induced relaxation of vascular smooth muscle. This agent - termed endothelium derived relaxing factor (EDRF) - was subsequently found to mediate the response to other vasodilators including bradykinin, substance P and histamine (see Ignarro 1990a; Moncada *et al.* 1991 for reviews). In 1987 EDRF was identified as NO by Palmer and co-workers who showed that bradykinin caused release of NO from endothelial cells in sufficient quantity to account for the biological activity of EDRF. EDRF/NO released from endothelial cells diffuses into the underlying smooth muscle where it induces vasorelaxation by increasing cGMP production. NO binds with high affinity to the heme group of soluble guanylate cyclase causing a conformational change that increases the enzyme's activity and stimulates cGMP formation (Ignarro 1990b). cGMP alters the cascade involved in muscle contraction leading to relaxation. Inhibition of NO synthesis induces endothelium-dependent contraction of vascular rings *in vitro* and inhibition of acetylcholine dependent relaxation (Rees *et al.* 1990). Systemic adminstration of NOS inhibitors to conscious rats *in vivo* causes an immediate, sustained hypertensive response accompanied by bradycardia (Gardiner *et al.* 1990a; Rees *et al.* 1990). These results indicate there is a continual, basal release of NO that maintains the vasculature in a state of active vasodilation. The vascular effects of NO inhibition are found to varying degrees in all vascular beds and across species (see Ignarro 1990a; Moncada *et al.* 1991 for reviews). The vasodilation induced by NO is complemented by its ability to inhibit platelet aggregation and adhesion - effects that are also mediated by stimulating cGMP production (Radomski *et al.* 1987; Radomski *et al.* 1990a).

1.6.4. Localisation of nitric oxide synthase in the brain

NO can not be visualised directly because of its lability. The gross localisation of NO was first estimated using a guanylate cyclase bioassay system. Highest NO enzymatic activity was reported in the cerebellum, intermediate activity in the striatum and cortex and lowest in the medulla (Forstermann *et al.* 1990). Immunohistochemical localisation of NOS using antisera raised against cerebellar NOS confirmed this distribution - with densest staining in the cerebellum and olfactory bulbs (Bredt *et al.* 1990). Immunoreactivity was found in discrete neuronal populations and in the vascular endothelium of cerebral vessels which in some cases were surrounded by NOS-immunoreactive nerve terminals. No NOS was found in glia suggesting the cNOS activity reported in cerebral astrocytes (Murphy *et al.* 1990; Agullo & Garcia 1992) may be overshadowed by iNOS (Simmons & Murphy 1993) that is not recognised by the neuronal NOS antisera. Interestingly the distribution of the NO precursor L-arginine is the reverse of that for cNOS with most immunoreactive-arginine located in astrocytes (Aoki *et al.* 1991).

Within the cortex, striatum and hippocampus, NOS-immunoreactivity is found in scattered, isolated medium to large aspiny neurones that respresent only 0.5-2% of the total neuronal number (Bredt & Snyder 1992; Valtschanoff *et al.* 1993). However these neurones possess a large number of processes that form a diffuse network of NOS-positive fibres throughout each region (Vincent & Kimura 1992). The regional distribution of NOS does not correspond to that of NMDA receptors (Garthwaite 1991) or any neurotransmitter. However in some areas NOS does colocalise with particular neurotransmitters or neuropeptides *e.g.* in the striatum NOS colocalises with somatostatin and neuropeptide Y (Bredt & Snyder 1992), whereas in the cortex NOS neurones all contain gamma-aminobutyric acid (Valtschanoff *et al.* 1993). NOS neurones can also be visualised histochemically using NADPH diaphorase staining (Vincent & Kimura 1992) which correlates well with immunocytochemistry in fixed tissue (Bredt *et al.* 1991). However other enzymes can also produce NADPH diaphorase staining in non-fixed tissue so that not all stained neurones can be attributed to NOS (Matsumoto *et al.* 1993). This probably explains why citrulline, the co-product of NO synthase was found in only a proportion of NADPH diaphorase positive neurones (Pasqualotto *et al.* 1991).

NOS-containing nerve fibres (assessed by NADPH-diaphorase staining or NOS-immunoreactivity) form a dense perivascular plexus in the anterior portion of the circle of Willis and the proximal anterior and middle cerebral arteries. In the basilar artery and more distal middle cerebral artery the density of NOS neurones is lower (Iadecola *et al.* 1993; Nozaki *et al.* 1993). These fibres originate extracranially mainly from the sphenopalantine ganglia (Iadecola *et al.* 1993; Nozaki *et al.* 1993). Within the cortex a

precise spatial relationship between NOS neurones (NADPH diaphorase-positive) and arterioles descending from the pial surface exists (Regidor *et al.* 1993). The close association between NOS neurones and both large cerebral arteries and the microcirculation suggests neuronal NO may regulate global changes in cerebral blood flow (but see also Section 6.5.) and more localised blood flow changes in response to metabolic demand.

1.6.5. Nitric oxide and glutamatergic signal transduction

Over a decade ago endogenous NO was known to stimulate soluble guanylate cyclase in the brain (Miki *et al.* 1977), while L-arginine had been identified as an endogenous activator of the enzyme (Deguchi & Yoshioka 1982). However it was not until the discovery of the vascular L-arginine-NO-cGMP pathway that a possible role of L-arginine derived NO in CNS function was further investigated. NO was discovered to mediate NMDA-induced elevations in cGMP in cerebellar culture (Garthwaite *et al.* 1988), and subsequently in neonatal and adult cerebellum (Bredt & Snyder 1989), hippocampus (East & Garthwaite 1991) and striatum (Marin *et al.* 1992). The NMDA-induced NO production (measured by accumulation of cGMP or citrulline) could be antagonised by NOS inhibitors (L-NA being more potent than L-NMMA by an order of magnitude (East & Garthwaite 1991; Kiedrowski *et al.* 1992a) or mimicked by several NO donors (Southam & Garthwaite 1991). *In vivo* NOS inhibition was demonstrated to inhibit both basal and excitatory amino acid-stimulated guanylate cyclase activity in mouse cerebellum (Wood *et al.* 1990).

The glutamate-induced increase in NO production was proposed to be mediated by Ca^{2+} influx since characterisation of neuronal NOS revealed the enzyme was Ca^{2+}-dependent (Knowles *et al.* 1990) and activated by the same range of Ca^{2+} concentrations found on activation of NMDA receptors (Garthwaite 1990). Thus quisqualate, which only slightly increases intracellular Ca^{2+}, minimally activates neuronal NOS *in vitro* (Garthwaite *et al.* 1989). The route leading to increased Ca^{2+} may also be important for NOS activation since kainate, at concentrations that give equivalent Ca^{2+} influx to NMDA, is less effective than NMDA in stimulating NOS activity (Kiedrowski *et al.* 1992a). Thus neuronal NOS may be localised in the cytoplasm close to the NMDA receptor (Garthwaite 1990). *In vivo* both kainate and quisqualate can stimulate NO-induced cGMP production (Wood *et al.* 1990). It is likely that a substantial proportion of this *in vivo* response is mediated by non-NMDA receptors localised on astrocytes rather than neurones (Agullo & Garcia 1992).

From this data the following model of NO mediated signal transduction at the glutamatergic synapse has been proposed (Garthwaite 1991; Knowles *et al.* 1990; see Figure 10). Glutamate released from the presynaptic terminal induces Ca^{2+} influx predominantly through NMDA receptor-gated ion channels. The increase in intracellular Ca^{2+} promotes calmodulin binding to NOS and activates the enzyme to produce NO from the conversion of L-arginine to L-citrulline. NO can then freely diffuse into neighbouring cells (neurones, glia or vascular smooth muscle) or back into the presynaptic terminal to activate guanylate cyclase and increase cGMP production. The elevation of intracellular Ca^{2+} required to activate NOS prevents NO-induced cGMP accumulation in the NOS neurone itself byactivation of a calmodulin- dependent cGMP phosphodiesterase (Mayer *et al.* 1992).

It is becoming increasingly apparent that increases in cGMP induced by other neurotransmitters e.g. noradrenaline and acetylcholine are also mediated by NO (Castoldi *et al.* 1993; Agullo & Garcia 1991). The precise roles of cGMP in brain function remain to be established but involve cGMP-activated kinases, phosphodiesterases and ion channels (Goy 1991).

1.6.6. Proposed roles of nitric oxide within the nervous system

In the peripheral nervous system NO has been identified as the neurotransmitter of NANC (nonadrenergic-noncholinergic) nerves that mediate smooth muscle relaxation (Moncada *et al.* 1991). In the CNS NO may play a role in synaptic plasticity mediated by long term potentiation (LTP) and long term depression (LTD). The short-lived, highly diffusible nature of NO makes it an ideal candidate for the retrograde messenger necessary to transfer information back from the post-synaptic neurone to the pre-synaptic terminal to alter the strength of synaptic transmission (Gally *et al.* 1990). NOS inhibitors block both LTP and LTD, while NO donors can promote both forms of synaptic plasticity (Bohme *et al.* 1991; Shibuki & Okada 1991). However because little or no NOS has been demonstrated in CA1 pyramidal cells this proposed role for NO remains controversial (Morris & Collingridge 1993).

Specific NO donors can modulate glutamatergic neurotransmission by reducing NMDA induced Ca^{2+} influx (Manzoni *et al.* 1992; Lei *et al.* 1992). Thus NO may act as a negative feedback mechanism to prevent overactivation of NMDA receptors. It is now known that NO exists in distinct oxidation-reduction states: the reduced free radical form ($NO^{\bullet}$) and the oxidised nitrosonium ion (NO^{+}) form (Lipton *et al.* 1993), and it is NO^{+} that can interact with the thiol group of the redox modulatory site on the NMDA receptor to

Figure 10 Nitric oxide mediated signal transduction at the NMDA receptor

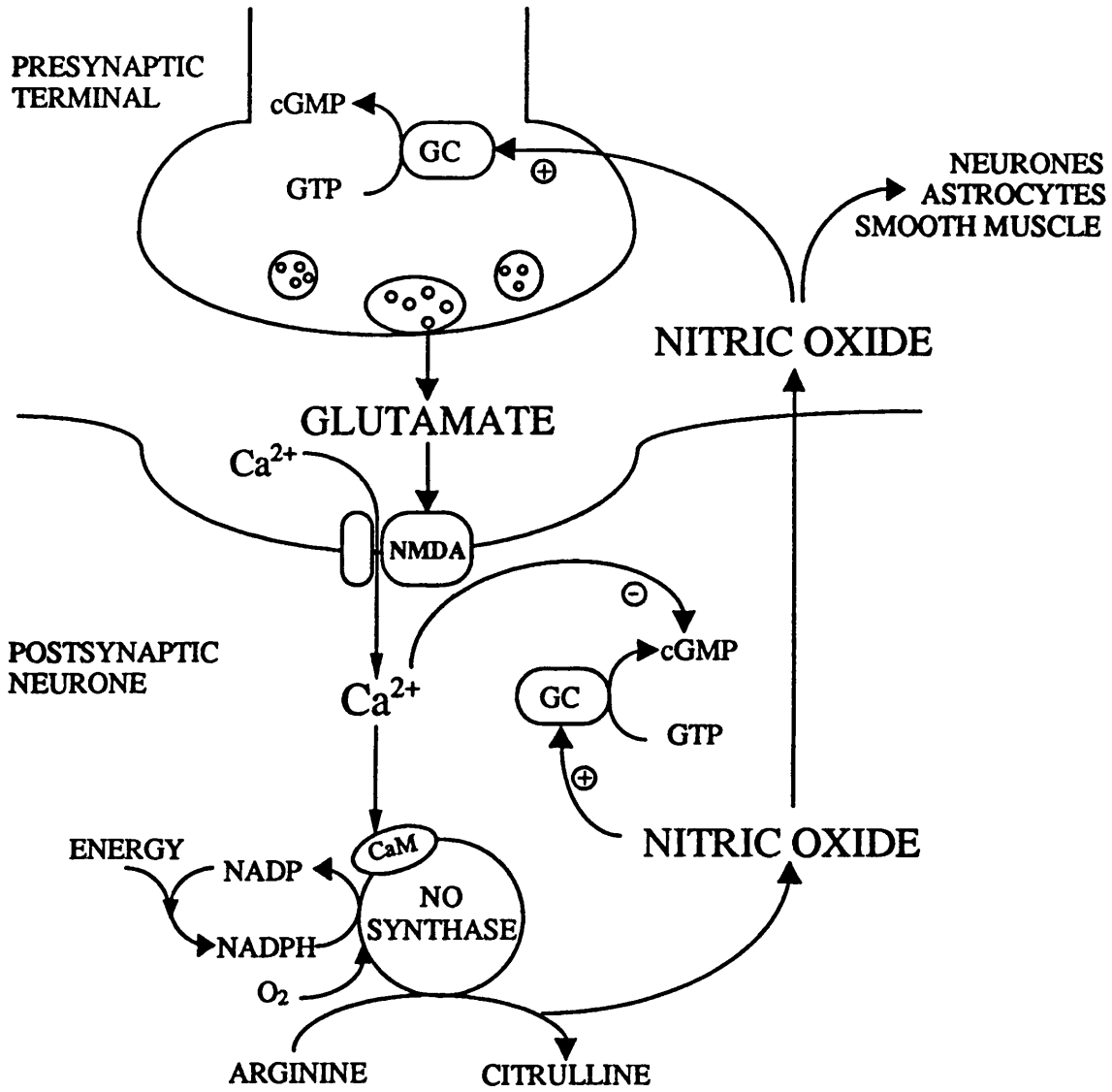

Glutamate released from the pre-synaptic terminal activates the NMDA receptor resulting in increased free intracellular Ca^{2+}, which in turn activates the calmodulin-dependent NO synthase to release NO from the conversion of L-arginine to L-citrulline. The freely diffusible NO can then pass into neighbouring target cells to activate guanylate cyclase (GC) and increase cGMP production. A calmodulin-dependent cGMP phosphodiesterase prevents cGMP accumulation in the NO-generator cell itself.

down-regulate NMDA evoked ion currents (Lei *et al.* 1992). However paradoxically NO can also stimulate further release of glutamate and aspartate (Dickie *et al.* 1992; Lawrence & Jarrott 1993) which may act to potentiate glutamatergic transmission.

The NO donor sodium nitroprusside (SNP) has been demonstrated to inhibit glutamate binding to NMDA receptors (Fujimori & Pan-Hou 1991) and prevent NMDA-induced depolarisation (East *et al.* 1991), but these effects are due to the ferrrocyanide portion of SNP and are independent of its NO-releasing ability (East *et al.* 1991; Kiedrowski *et al.* 1992b).

Within the CNS NO can mediate non-synaptic communication between neurones and nonneuronal elements such as astrocytes and blood vessels. For example NO produced by NMDA-stimulated cerebellar granule cells promotes cGMP accumulation in astrocytes which themselves lack NMDA receptors (Kiedrowski *et al.* 1992c). In addition the important role of neural NO in the control of cerebrovascular tone is becoming increasingly recognised. NOS inhibitors block neurally induced vasodilation in cerebral arteries (Toda & Okamura 1991) and pial arteriolar vasodilation induced by exogenous NMDA (Faraci & Breese 1993). An investigation of the role of NO in cerebrovascular regulation is included in this thesis and this subject will be addressed in more detail in the discussion.

1.6.7. Nitric oxide as a potential mediator of neurotoxicity

Dawson *et al.* 1991 originally proposed NO as a mediator of glutamate neurotoxicity in cortical cell culture. They demonstrated firstly that the NOS inhibitors L-NA and L-NMMA dose-dependently prevented NMDA-induced cell death with EC_{50} of 20 and 170 μM respectively (Dawson *et al.* 1991), and secondly that the NO donor SNP induced neurotoxicity with a concentration-response curve and time-course of action very similar to NMDA. Since this report was published the role of NO in mediating glutamate toxicity *in vitro* remains controversial. Some studies have reported that NOS inhibitors attenuate NMDA-induced toxicity (Corasaniti *et al.* 1992; Izumi *et al.* 1992; Kolleger *et al.* 1993), while others found no beneficial effect (Demerle-Pallardy *et al.* 1991; Regan *et al.* 1993). Similarly while some authors find NO donors to be neurotoxic (Chen *et al.* 1991; Boje & Skolnick 1992) others do not (Kiedrowski *et al.* 1991). The neurotoxic effects of SNP have also been attributed to a mechanism independent of NO release (Izumi *et al.* 1993). These discrepant results may be explained by the recent finding that NO can exist in 2 different redox states (see above) with distinct neuroprotective (NO^+) and neurotoxic ($NO^\bullet$) actions (Lipton *et al.* 1993). Enriching culture medium with the reducing agents

cysteine or ascorbate, which will promote the formation of NO•, increases the neurotoxicity of NO donors in culture (Lipton *et al.* 1993). Thus differences in the amino acid content of the culture media used in different laboratories may affect the redox state of NO and convert it from a neurotoxin to a neuroprotective agent or vice versa.

The sustained release of NO from glia due to activation of iNOS by lipopolysaccharide (LPS) and/or cytokines does appear to be consistently cytotoxic to neurones (Boje & Arora 1992; Chao *et al.* 1992). Commercially available culture medium is contaminated by endotoxin (containing LPS) in concentrations that can induce significant NO production from iNOS (Simmons & Murphy 1992). This unintended source of NO may also partly account for the contradictory results of NOS inhibition *in vitro* reported above.

1.6.8. Proposed mechanism of nitric oxide-induced toxicity

NO is a free radical and at high concentrations can directly induce cell damage *e.g.* DNA strand breakage (Nguyen *et al.* 1992). However *in vivo* the lower concentrations of NO and its short half-life (Gally *et al.* 1990) suggest that it can not mediate toxicity directly. Beckman and colleagues first postulated that NO may mediate excitotoxic or ischaemic injury through participation in the generation of hydroxyl radicals by the following reactions:

$$NO\bullet + O_2\bullet^- \text{ ---> } ONOO^-$$

$$ONOO^- + H^+ \text{ ---> } ONOOH$$

$$ONOOH \text{ ---> } HO\bullet + NO_2\bullet$$

NO was proposed to react with superoxide to form peroxynitrite ($ONOO^-$). Peroxynitrite rapidly decomposes at physiological pH (<7.5) and temperature (37°C) to form hydroxyl radical and nitrogen dioxide (Beckman *et al.* 1990). This hypothetical reaction sequence was confirmed by Hogg *et al.* 1992 who demonstrated the generation of hydroxyl radicals from superoxide and nitric oxide. Recent evidence suggests that peroxynitrite may actually undergo rearrangement to form a complex with $NO_2\bullet$ and HO• characteristics rather than decompose into 2 separate species (Lipton *et al.* 1993).

This pathway represents an alternative mechanism to the Haber-Weiss reaction for the generation of hydroxyl radicals. The NO pathway may be of equal or greater importance than the Haber-Weiss reaction *in vivo* because it is not dependent on an iron catalyst (Beckman *et al.* 1990). Moreover peroxynitrite, as well as hydroxyl radicals, can directly

induce tissue damage (Lipton *et al.* 1993; Radi *et al.* 1991). Although some authors view the scavenging of superoxide by nitric oxide as potentially cytoprotective (Kanner *et al.* 1992; Rubanyi *et al.* 1991), the general consensus is that the increased formation of hydroxyl radicals will be cytotoxic.

It is now known that NOS can generate superoxide radicals (Pou *et al.* 1992). Production of both NO and superoxide by NOS is likely to promote NO-superoxide interaction and increase the formation of peroxynitrite and hydroxyl radicals. The biological importance of this interaction is illustrated by the fact that removal of superoxide with SOD prolongs the half-life of endothelial EDRF/NO (Gryglewski *et al.* 1986). In addition SOD attenuates neurotoxicity induced by NO donors confirming that combination of NO with superoxide is necessary to produce maximal toxicity (Dawson *et al.* 1993; Lipton *et al.* 1993). The anti-ischaemic efficacy of SOD (see Section 1.4.4.3.) may therefore be dependent not only on its ability to prevent hydroxyl radical formation but also on the stabilisation of NO thereby promoting vasodilation and possibly improving cerebral blood flow.

The increase in cGMP levels induced by NO is not likely to contribute to its neurotoxic action because cGMP analogues are not neurotoxic in cortex or cerebellum *in vitro* (Garthwaite & Garthwaite 1988; Lustig *et al.* 1992a).

Following the observations that NO mediates glutamate toxicity *in vitro* (Dawson *et al.* 1991) and that NOS inhibitors protect neurones against hypoxia/reoxygenation injury *in vitro* (Cazevieille *et al.* 1993; Wallis *et al.* 1992) we wished to investigate the possibility that NO is also neurotoxic *in vivo*. Therefore we studied the effect of the NOS inhibitor L-NAME on cell damage invoked firstly in response to intracerebral administration of exogenous glutamate and secondly in response to ischaemia/reperfusion in the permanent and transient (endothelin-1) models of middle cerebral artery occlusion. The roles of glutamate, Ca^{2+} and free radicals in ischaemic/reperfusion injury are well documented (see Section 1.4.). The possibility that NO mediates ischaemic/reperfusion injury is therefore attractive because it allows the merging of these 3 hypothesis into one final common pathway of neuronal death.

2. MATERIALS AND METHODS

2.1. ANIMALS

Adult male Sprague-Dawley rats (approximately 300-350 g, Harlan Olac, U.K.) were used in all experiments. The rats received free access to food (labchow pellets) and water prior to experimentation. The experimental group sizes for each study are shown in the relevant results tables.

2.2. GENERAL SURGICAL PREPARATION

Anaesthesia Rats were weighed then placed in a clear perspex box for induction of anaesthesia. Anaesthesia was induced with 5% halothane in nitrous oxide: oxygen (70:30) and was subsequently maintained with 0.75-1% halothane (depending on individual animal's requirement for adequate anaesthesia). For rats maintained under anaesthesia throughout the experimental period the trachea was cannulated and the animal artificially ventilated via a small animal respirator pump. Rats intended to regain consciousness following surgery breathed spontaneously throughout and received anaesthetic gases via a small nose cone. Rectal temperature was monitored and maintained around 37°C by means of heating blankets and lamps.

Blood vessel cannulation The rat was placed on its back and small incisions made on either side of the groin to expose the femoral blood vessels. The femoral arteries and veins were cannulated using polyethylene catheters (outer diameter 0.96 mm, inner diameter 0.58 mm, length 15 cm) filled with heparinised saline (10 I.U. heparin/1 ml saline). The arterial catheters were used for continuous monitoring of blood pressure and for blood sampling to measure plasma glucose and blood gases. The venous catheters were used for administration of drug or vehicle and radioactive tracers where appropriate. The surgical sites were infiltrated with anaesthetic gel (survival animals only) and skin sutured. Blood samples were taken at regular intervals to monitor blood gases and, if necessary, the pump rate was altered to maintain gases within the following limits for anaesthetised rats: $PaCO_2$ 35-42 mmHg, PaO_2 >100 mmHg.

2.3. MODELS OF CEREBRAL ISCHAEMIA/EXCITOTOXICITY AND HISTOLOGICAL QUANTIFICATION OF ISCHAEMIC DAMAGE

2.3.1. Induction of focal cerebral ischaemia

Exposure of middle cerebral artery

The left middle cerebral artery (MCA) was exposed using a subtemporal approach based on the method originally described by Tamura *et al.* 1981a. The rat was laid on its right side and a vertical incision (2 cm) made midway between the left eye and ear. The skin was retracted and the temporal muscle divided into 2. The muscle was detached from the bone and 2 retractors inserted to hold back the muscle and obtain a clear view of the infero-temporal fossa. The zygomatic arch was left intact and 2 further retractors inserted to improve the view of the foramen ovale. The remainder of the procedure was carried out using an operating microscope. A small circular craniectomy (2 mm diameter) was made using a saline-cooled dental drill. The skull opening was positioned approximately 1mm dorsal to the foramen ovale. The underlying dura membrane was opened with a fine needle to reveal the MCA. The main trunk of the MCA was exposed from where it crossed the inferior cerebral vein to proximal to the lateral olfactory tract. The lenticulostriate branch(es) that originate below the olfactory tract were usually visible (see Figure 11). In some experiments a fine temperature probe was then inserted into the ipsilateral temporalis muscle to monitor temperature during surgery.

Permanent MCA occlusion

The main artery was occluded by temparature-controlled (maximum 84°C) bipolar electrocoagulation (Bipolator T50, Fischer, Germany) from where it crossed the inferior cerebral vein to proximal to the origin of the lenticulostriate branch. All visible side-branches, including the lenticulostriate, were also coagulated. The artery was then transected midway between the inferior cerebral vein and olfactory tract to ensure the completeness of the occlusion and to prevent recanalisation. The time of transection was taken as the exact time of MCA occlusion. The retractors and temperature probe were then removed and the temporal muscle and skin sutured.

Figure 11 Schematic representation of the middle cerebral artery

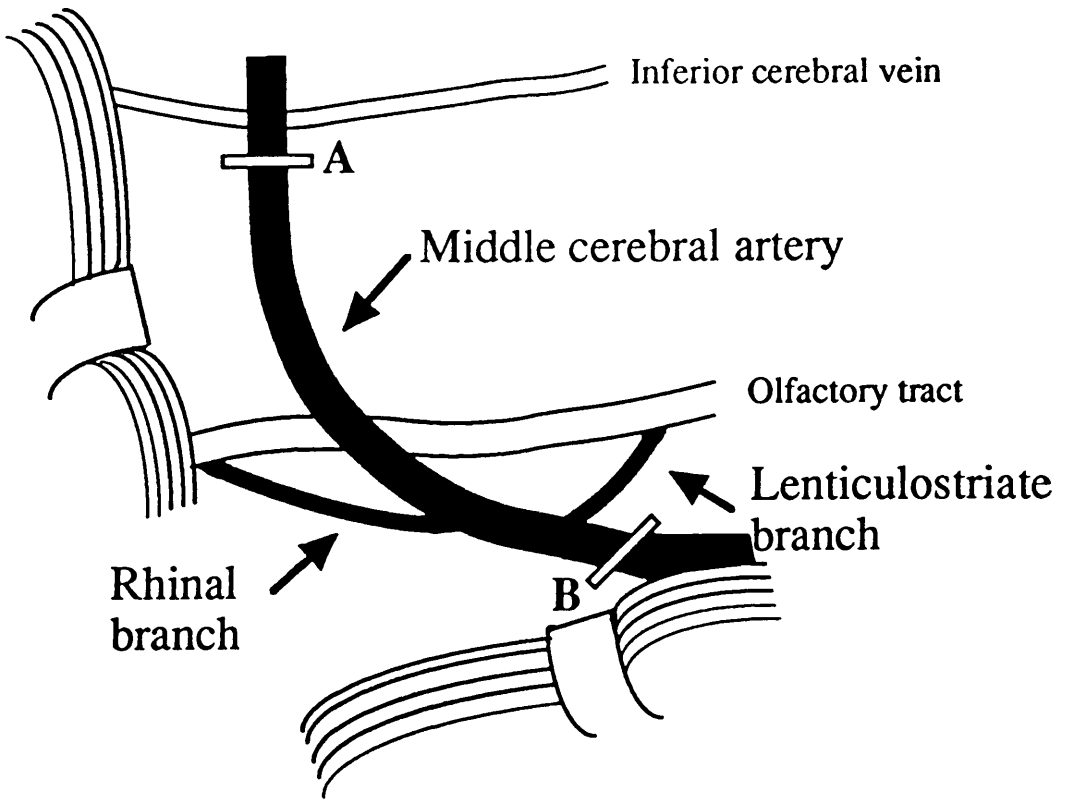

The left middle cerebral artery (MCA) was exposed using a sub-temporal approach. For permanent MCA occlusion the artery was then occluded by electrocoagulation from where it crossed the inferior cerebral vein (A) to proximal to the origin of the lenticulostriate branch (B). For transient MCA occlusion endothelin-1 was topically applied to the same region of the artery (A-B) to constrict both the main trunk and the lenticulostriate branch(es).

Transient MCA occlusion

Following removal of the dura, the arachnoid membrane was pierced 3-4 times down either side of the MCA to facilitate access of endothelin-1 to the artery. Endothelin-1 (2.5 nmol, 25 µl x 10^{-4} M; Peninsula Lab. Inc., USA) was applied using a microsyringe to the same portion of the artery that would be occluded for permanent MCA occlusion. Constriction of the main artery and lenticulostriate branch(es) was verified via the operating microscope. Only constrictions rated moderate (approximately 25% of the original diameter), severe (20% of the original diameter) or very severe ($\leqslant$20% of the original diameter) were included in the study. The degree of constriction was noted and the time of occlusion taken as when satisfactory constriction was achieved. The retractors were removed and the operation site closed as for permanent MCA occlusion.

Prior to application, the concentration of the endothelin-1 solution was verified by absorbance spectrophotometry at 280 nm using a molar extinction coefficient of 7250 for a 10 mm path length (Douglas *et al.* 1991).

Sham procedure

The MCA was exposed as for transient MCA occlusion and the arachnoid membrane pierced. Saline (25 µl) was applied to the artery using a microsyringe. The retractors were removed and the wound sutured as above.

Survival animals for ischaemia studies

Under sterile conditions the right femoral artery only was cannulated. The cannula was shunted under the skin and exteriorised at the back of the neck. Thus blood samples could be taken for physiological monitoring both during surgery and the post-operative period. Following removal of a blood sample a concentrated heparin solution (0.1 ml) in a viscous medium (10,000 units heparin, 25 g polyvinyl pyrollidine, 50 ml saline) was injected into the cannula to keep the line patent (care was taken not to allow the heparin to enter the rat's bloodstream). A permanent, transient or sham MCA occlusion was then performed as described above. All wounds were infiltrated with anaesthetic gel and sutured. A broad spectrum antibiotic (0.1 ml ampicillin s.c., to maintain patency of arterial cannula) and 2.5 ml saline s.c. (to prevent dehydration) were administered (24 h and 72 h survival animals only). Anaesthetics were withdrawn and the animal allowed to regain consciousness. For long term survival (24 h and 72 h) rats were transferred to a special post-operative recovery room where their overall condition was closely monitored throughout the survival period. Rats were housed individually and received a special soft diet to encourage feeding.

2.3.2. Tissue processing and histopathological quantification of ischaemic damage

Perfusion fixation

Rats from recovery experiments were reanaesthetised. For all animals the halothane concentration was increased to 3% immediately prior to perfusion fixation. The animal was placed on its back and the thorax opened via a midline incision. A blunt needle was inserted into the left ventricle and passed into the ascending aorta. The right atrium was cut. Heparinised saline was infused until the perfusate ran clear (approximately 50 ml) followed by FAM (40% formaldehyde, acetic acid and absolute methanol in ratio of 1:1:8; approximately 150 ml). Both heparinised saline and FAM were perfused at a pressure of approximately 120-130 mmHg. The rat was decapitated and the head stored in FAM for 24 h. The brain was then carefully removed and stored in 70% methanol prior to quantitative histopathology.

Tissue Processing

The cerebellum and olfactory bulbs were removed and the cerebrum cut into 4 equal coronal slices. These slices were embedded in paraffin wax blocks, then sections (10 μm) were cut and stained with haematoxylin and eosin or luxol fast blue and examined under a light microscope.

Quantification of ischaemic damage

Volumetric assessment was performed as described by Osborne *et al.* 1987. This method of quantification removes the confounding influence of oedema (brain swelling) from the measurement of volumes of ischaemic damage. Regions showing evidence of ischaemic cell change were transcribed onto scale drawings (*e.g.* see Figure 15) at 8 pre-selected stereotactic levels taken from the stereotactic atlas of Konig & Klippel 1963. The transcription of areas of ischaemic damage was performed blind by an experienced neuropathologist (Prof. D. Graham).

The areas of ischaemic damage in the whole hemisphere, cortex and caudate nucleus were measured at each level on the line drawings using an image analyser (Quantimet 970, Cambridge Instruments, U.K.). The areas of damage were then converted by integration to provide a total volume of ischaemic damage, normalised to the mean hemispheric volume of the adult male Sprague-Dawley rat (570 mm^3).

2.3.3. Induction of permanent global (decapitation) ischaemia

Conscious rats were killed by cervical dislocation and decapitated. The heads were placed in individual sealed plastic bags and maintained in a water bath at 37°C for 15 min to 4 h. The brains were then rapidly removed and processed for *in vitro* autoradiography. For the control group, brains were removed from the skull immediately following decapitation.

2.3.4. Glutamate toxicity *in vivo*

Surgical preparation and induction of excitotoxic damage

Rats were anaesthetised, tracheostomised and the femoral vessels cannulated as described in Section 2.2. The rat was placed prone in a Kopf stereotactic frame and, using an operating microscope, a small craniectomy was made through the right parietal skull. The dura and arachnoid membranes were pierced and a microdialysis probe (Carnegie Medicine, Sweden; membrane length 3 mm, outside diameter 0.5 mm), angled at 15° to the sagittal plane, was inserted 3.5 mm into the parietal cortex (stereotactic surgery was performed by Dr. H. Fujisawa). The stereotactic co-ordinates for probe placement were anterior 0.0 mm, lateral 4.0 mm relative to Bregma. The microdialysis probe was perfused with mock cerebrospinal fluid (135 mM NaCl, 1mM KCl, 2mM KH_2PO_4, 1.2 mM $CaCl_2$, 1mM $MgCl_2$, pH 7.4) followed by 0.5 M glutamate solution (0.5 M monosodium glutamate dissolved in mock CSF) at a flow rate of 1.5 µl/min for 90 min using a Carnegie Medicine CMA 100 infusion pump (Biotech Instruments, U.K.). Following the 90 min glutamate perfusion the probe was removed and the scalp wound sutured. The experiment was terminated by decapitation 4 h after the start of the infusion.

Quantification of damage

Immediately following decapitation the brains were removed and frozen in isopentane (-42°C). 20µm sections were cut on a cryostat using a cutting schedule in which 3 consecutive sections were collected onto a microscope slide at 200 µm intervals throughout the brain. The sections were then stained with haematoxylin and eosin. The cortical damage was clearly visible to the naked eye as a region of pallor on the stained sections. The area of damage was measured directly from each section using an image analyser and averaged for each group of 3 consecutive sections. The total volume of damage was then determined by integration. This novel model of excitotoxicity *in vivo* has been characterised in previous studies (Fujisawa *et al.* 1993; Landolt *et al.* 1993).

2.4. AUTORADIOGRAPHICAL TECHNIQUES

2.4.1. *In vitro* ligand binding

Theory

Quantitative binding assays utilising ligands labelled with radioisotopes such as ^{3}H or ^{125}I have been widely used to characterise receptor populations within the brain. In the context of cerebral ischaemia assays can be used to detect changes in receptor number and/or affinity following an ischaemic insult. Assays measure the amount of ligand bound to the receptors at various ligand concentrations and are based on simple equilibrium reaction kinetics.

The binding of a ligand to its receptor can be expressed as the following reversible reaction:

$$[R] + [L] \underset{k_{-1}}{\overset{k_{+1}}{<---->}} [RL] \qquad (1)$$

where [L] = concentration of ligand; [R] = concentration of receptor;
[RL] = concentration of receptor-ligand complex= [B] = amount bound;
k_{+1} = association rate constant; k_{-1} = dissociation rate constant.

At equilibrium: $$k_{+1}[R][L] = k_{-1}[B] \qquad (2)$$

and the equilibrium dissociation constant for the ligand is defined as:

$$K_d = \frac{k_{-1}}{k_{+1}} = \frac{[R][L]}{[B]} \qquad (3)$$

Let B_{max} represent the total number of receptors *i.e.*

$$B_{max} = [R] + [RL]$$

Substitution in equation 3 then gives:

$$K_d = \frac{(B_{max} - [B])\,[L]}{[B]} \qquad (4)$$

which can be rearranged to:

$$[B] = \frac{B_{max}\,[L]}{[L] + K_d} \qquad (5)$$

Equation 5 represent the concentration of ligand bound to the receptors as a function of concentration of ligand and is shown in Figure 12a. In practice the amount bound includes ligand bound to the specific receptor population and also nonspecific binding *i.e.* binding to other components of the assay system. Non-specific binding is non-saturable and proportional to the concentration of ligand present. In an assay non-specific binding is determined by the addition of a high concentration of an unlabelled 'displacer' ligand that is also a specific ligand for the receptor being studied. Subtraction of the amount of non-specific binding from total binding will give the amount of specific binding to the receptor.

Further rearrangement of equation 4 gives:

$$\frac{[B]}{[L]} = \frac{B_{max}}{K_d} - \frac{[B]}{K_d} \qquad (6)$$

$$(y = \quad m.x + \quad c)$$

This equation (6), known as the Scatchard equation describes a straight line with slope equal to the negative reciprocal of the dissociation constant ($-1/K_d$) and intercept on the x-axis equal to total concentration of receptors (B_{max}) (see Figure 12b). Thus if the concentrations of bound and free ligand at equilibrium are known, then K_d and B_{max} can be determined.

Figure 12 Analysis of saturation data for the binding of a radioligand to its receptor

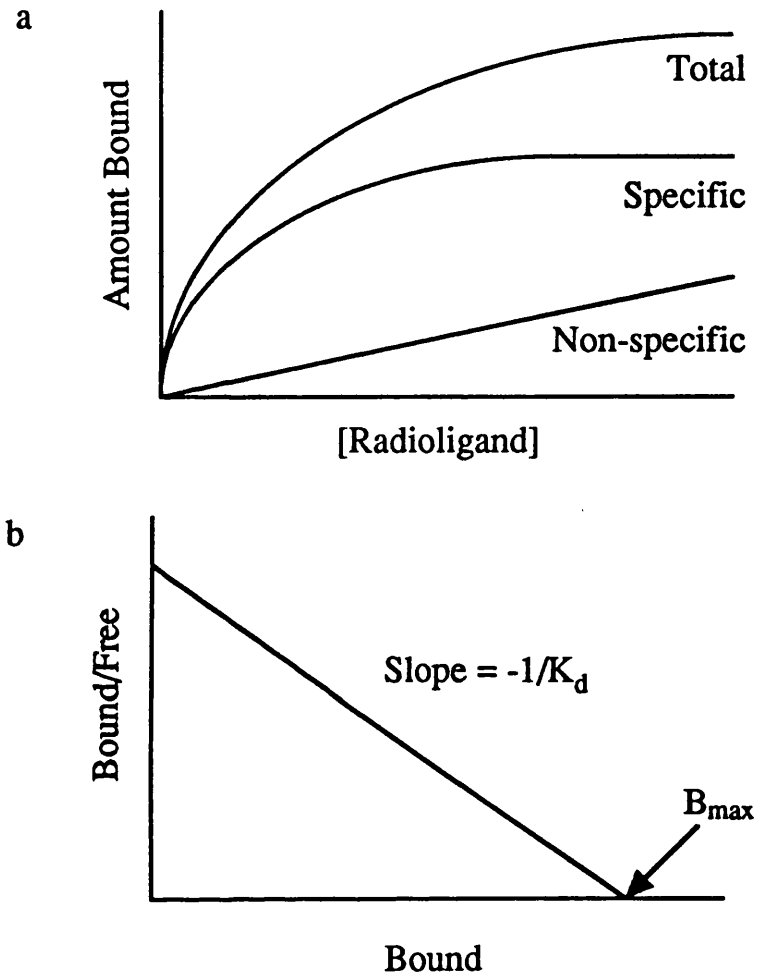

a) The total amount of bound radioligand is measured at increasing concentrations of radioligand until virtually all receptors are saturated. Non-specific binding is assessed in parallel by the addition of an excess amount of unlabelled ligand. Specific binding is then determined by subtracting the amount of non-specific binding from the total amount bound.
b) The data is then transformed using Scatchard analysis to describe the linear relationship between the ratio of bound to free ligand against the concentration of bound ligand. Extrapolation of this line to the X-axis gives an estimate of the total number of receptors (B_{max}), while the slope of the line is equivalent to the negative reciprocal of the equilibrium dissociation constant (K_d).
From McGonigle & Molinoff 1981.

In the present study *in vitro* autoradiography was used to assess the effects of focal and global cerebral ischaemia on the adenylate cyclase-cyclic AMP second messenger system. Adenylate cyclase, an important mediator of intracellular signalling, catalyses the conversion of ATP to cyclic AMP. Many neurotransmitter receptors are coupled to adenylate cyclase via guanine nucleotide binding proteins (G proteins, G_s and G_i) and either stimulate (D_1 dopamine, ß adrenergic, A_2 adenosine) or inhibit (D_2 dopamine, α_2 adrenergic, A_1 adenosine) its activity (Cooper 1986; Kebabian & Calne 1979). We chose to study the D_1 dopamine receptor because of the high density of D_1 dopamine receptor binding sites in the caudate nucleus (Savasta *et al.* 1986) - one of the main neuroanatomical regions affected by proximal MCA occlusion. The tritiated ligands SCH23390 (a selective D_1 antagonist (Kebabian & Calne 1979)) and forskolin were used to map D_1 receptors and adenylate cyclase respectively. Forskolin at high concentrations (µM) binds to a low affinity site on the catalytic subunit of adenylate cyclase and directly activates the enzyme (Seamon & Daly 1981). However at the concentrations used in the binding assay (nM), forskolin binds to a high affinity site located on the activated form of adenylate cyclase and provides a marker of the agonist-stimulated enzyme (Gehlert 1986).

Practice

At specified time intervals following induction of ischaemia (see individual experimental protocols, Section 5) the rat was decapitated and the brain rapidly dissected out. The whole brain was frozen in isopentane (-42°C) for 10 min. Coronal sections (20µm) were cut in a cryostat and thaw mounted onto gelatin-coated subbed slides. Three consecutive sections (2 for total binding on one slide, one for non-specific binding on another slide) were collected and allowed to dry at room temperature. Sections were stored in sealed plastic boxes at -20°C until required for binding assay.

Sections were removed from the storage freezer and dried rapidly in a stream of air at room temperature. For experiments combining *in vitro* autoradiography with [^{14}C]IAP assessment of cerebral blood flow the [^{14}C]IAP was first removed from the sections by 2 x 15 min washes in the appropriate buffer (see Table 1). The sections were then redried prior to start of the binding protocol.

The binding protocols for both forskolin and SCH23390 binding follow the same general procedure (see Table 1 for specific details). Tissue sections were incubated at room temperature in the appropriate buffer containing a known concentration of the specific [^{3}H]ligand. Non-specific binding was determined in parallel in adjacent sections by

addition of an unlabelled displacer to the incubation buffer. The sections were incubated for a specific time calculated to allow equilibrium to be achieved. Unbound radioligand was then removed by washing the sections in cold fresh buffer (4°C) followed by a dip in distilled water (4°C). The sections were then dried in a stream of air and mounted onto cardboard together with a set of precalibrated standards (1105 - 24,148 nCi/g, Amersham Int., U.K.). The cards were then apposed to ^{3}H-sensitive film (Hyperfilm-^{3}H, Amersham Int., U.K.) for 7 (SCH23390) or 14 days (forskolin). The films were then developed and the resultant autoradiograms analysed using computer-assisted densitometry (see Section 2.4.3.). The binding protocols for [^{3}H]forskolin and [^{3}H]SCH23390 were based on the methods of Gehlert *et al.* 1985 and Savasta *et al.* 1986 respectively.

Table 1 Protocols for [^{3}H]forskolin and [^{3}H]SCH23390 binding

Binding Site	Ligand (Specific activity)	Displacer	Incubation Time	Buffer	Washes
Forskolin	20nM [^{3}H]forskolin (20Ci/mmol)	20μM forskolin	20 minutes	50mM Tris HCl, 10mM $MgCl_2$, pH7.5	2 x 1 minute
D_1 Receptor	2nM [^{3}H]SCH23390 (73Ci/mmol)	10μM piflutixol	90 minutes	50mM Tris HCl, 10mM $MgCl_2$, 5mM KCl, 2mM $CaCl_2$, 120mM NaCl, 10μM sulpiride, pH7.4	2 x 10 minute

2.4.2. *In vivo* assessment of local cerebral blood flow

2.4.2.1. Local cerebral blood flow determination using [^{14}C]iodoantipyrine

Theory

The iodoantipyrine (IAP) method of measuring local cerebral blood flow (CBF) is one of a group of techniques, utilising different tracer compounds, which are based on measuring the cerebral uptake of a metabolically inert, freely diffusible tracer from the arterial blood. This basic method was first introduced by Kety & Schmidt (1945) who used the inert gas nitrous oxide to measure CBF in man. The mathematical theory underlying their work was in turn derived from the Fick principle which states that the quantity of tracer taken up by an organ in time t equals the blood flow through the organ multiplied by the difference in concentration between the arterial blood delivered to the organ and the venous blood draining it. This can be expressed as follows:

$$Q = F\,(Ca\text{-}Cv)$$

where Q = quantity of tracer in the organ; F = blood flow through the organ; Ca and Cv = arterial and venous blood concentration of the tracer.

The Kety-Schmidt equation (Kety 1951) derived from the Fick principle is:

$$Ci(T) = \lambda\, K \int_0^T C_a\, e^{-K(T-t)}\, dt$$

where Ci(T) equals the tissue concentration of the tracer at a given time, T, after injection of the tracer; λ equals the tissue:blood partition coefficient which relates the tracer concentration in the brain to that in the blood and is the ratio of the solubility of the tracer in brain tissue:blood; C_a is the concentration of tracer in the arterial blood; t is the variable, time; and K is a constant defined as:

$$K = mF/W\lambda$$

where F/W equals the rate of blood flow per unit mass of tissue; and m equals a constant (from 0-1) that represents the diffusion equilibrium between blood and tissue. The constant m is a measure of diffusion across the blood brain barrier, so with unrestricted diffusion m = 1.

The general method based on this equation for quantitative determination of blood flow is as follows. The radiolabelled tracer is infused intravenously over a short period (30 s - 1 min) while timed samples of arterial blood are collected. At the end of the infusion period the animal is decapitated and the brain rapidly removed and sectioned. The radioactivity in discrete brain regions is then measured using quantitative autoradiography. Thus the rate of blood flow per unit mass of tissue (F/W) can be determined from the final concentration of tracer in the tissue (Ci(T)) - obtained from the autoradiogram, and the concentration of tracer in arterial blood from time 0 to T - obtained from the arterial blood samples.

Kety and colleagues originally measured CBF in non-primates using the inert gas [^{131}I]trifluoroiodomethane as the tracer (reviewed in Sakurada *et al.* 1978). However there were several technical drawbacks associated with this tracer including difficulty in measuring a volatile gas and the relatively short half-life of ^{131}I. [^{14}C]antipyrine was then used but due to its relatively low lipid solubility it had poor diffusion across the blood-brain barrier ($m<1$) and consequently underestimated CBF. With the introduction of [^{14}C]IAP a compound was found that fulfilled all the requirements for a suitable tracer (unrestricted diffusion across blood-brain barrier, metabolically inert, ability to be labelled with a convenient radioisotope). [^{14}C]IAP has been demonstrated to have a relatively high lipid solvent:water partition coefficient. It is uniformly soluble throughout all brain regions but is slightly more soluble in blood than brain with a brain tissue:blood partition coefficient of 0.79 (0.78-0.80 dependent on method of determination, Sakurada *et al.* 1978).

The main advantage of the [^{14}C]IAP method for determination of local CBF is the high degree of spatial resolution that enables lCBF to be measured in numerous regions throughout the brain. The main disadvantage is that flow can only be measured at one time point since the brain has to be removed immediately following infusion of the tracer. However the temporal resolution can be improved by combining this method with another tracer *e.g.* hexamethylpropyleneamine oxime (see Section 2.4.2.2.) to obtain blood flow measurements at 2 time points in the same rat.

Another limitation of the [^{14}C]IAP method is that due to the high diffusability of the tracer it may underestimate flow in regions with very high blood flows such as the choroid plexus and also fail to detect heterogeneity within a region (*e.g.* cortical columns) due to diffusion of the tracer from regions of high flow to regions of low flow in the delay between decapitation and freezing (Williams *et al.* 1991). Diffusion of the tracer can be minimised by ensuring the brain is dissected out as rapidly as possible.

Practice: [^{14}C]iodoantipyrine determination of local CBF in the rat

The protocol used was based on the method of Sakurada *et al.* 1978.

General Preparation Rats were anaesthetised and polyethylene catheters inserted in the femoral arteries and veins as described in Section 2.2. For rats in which CBF was to be measured under anaesthesia a tracheostomy was performed and the rats were artificially ventilated. For rats intended for conscious CBF measurement no tracheostomy was performed. In these rats local anaesthetic gel was applied to the surgical sites, the skin was sutured and gauze pads covered with more gel taped over the wounds. The anaesthetics were then withdrawn. The rat's torso was enclosed in a surgical stocking and the lower half of the body wrapped in a loose fitting plaster cast. The plaster cast and the rat's hindlimbs were then taped to a lead brick for restraint. The animals were allowed to recover for 2 h before the experimental procedure was initiated.

For both anaesthetised and conscious rats body temperature was monitored via a rectal probe and maintained around 37°C by heating lamps. Blood pressure was continuously monitored (from one arterial catheter) while blood gases were measured at regular intervals. The flow rate from the other arterial catheter was adjusted by means of a small metal cuff to give a drop rate of approximately 10-15 drops/10 s.

Measurement of local CBF A ramped infusion of 50 μCi [^{14}C]IAP (1.5 ml) was administered intravenously over 30 s. During the infusion 18 timed samples of arterial blood were collected onto preweighed filter paper discs held in a perspex carousel. At the end of the 30 s the rat was decapitated using a guillotine and the brain rapidly dissected out. The brain was immersed in isopentane (-42°C) for 10 min. The frozen brain was then mounted on a small metal chuck and coated with embedding medium. Immediately following decapitation the 18 filter paper discs containing the blood samples were placed in 18 preweighed glass vials, sealed and reweighed to obtain the weight of each blood sample. After weighing hydrogen peroxide (0.4 ml) was added to each vial (to bleach the blood sample) followed by distilled water (1 ml), the vials were left at room temperature for 30 min, then 10 ml scintillant was added. The radioactivity in each sample was determined by counting in a liquid scintillation counter (Model 1900CA, Canberra Packard, U.K.), and the number of counts per minute converted to absolute disintegrations per minute (dpm). The mean of 3 sets of counts (dpm) was then used, together with the sample weights, to calculate the ^{14}C concentration (nCi/g) in each of the 18 timed samples and thereby obtain the arterial concentration curve for [^{14}C]IAP.

Tissue processing After freezing and embedding the brain was cut into coronal sections (20 μm) using a cryostat. Tissue sections were thaw mounted onto glass coverslips and dried on a hotplate at 70°C. The coverslips were glued onto pieces of card together with a set of precalibrated ^{14}C standards (44-1880 nCi/g) and apposed to ^{14}C-sensitive film (SB-5, Kodak, U.K.) in sealed X-ray cassettes for 14 days. The concentrations of [^{14}C]IAP in regions of interest on the resultant autoradiograms were then determined as described in Section 2.4.3.

Calculation of local CBF The experimental data (arterial concentration curve for [^{14}C]IAP and final tissue concentrations of [^{14}C]IAP) were entered into a computer program (BBC computer) to calculate absolute blood flow (ml/100 g/min) using a brain tissue:blood partition coefficient of 0.79.

2.4.2.2. Local cerebral blood flow determination using [^{99m}Tc]-D,L-hexamethyl propyleneamine oxime ([^{99m}Tc]HMPAO)

Theory

[^{99m}Tc]HMPAO was originally developed as a SPECT (single photon emission computerised tomography) tracer molecule for measurement of CBF in man. HMPAO fulfils the criteria for such a tracer being a lipophilic, low molecular weight compound that easily crosses the blood-brain barrier and has high first-pass extraction from the blood to brain tissue (Andersen 1989). Once the lipophilic HMPAO has entered the brain it is rapidly converted by glutathione and other reducing agents to a hydrophilic form that can not traverse plasma membranes and becomes trapped within the brain tissue (Andersen 1989). The resultant regional distribution of the trapped tracer is therefore proportional to regional blood flow.

A 4 compartment model for the exchange of HMPAO between blood and brain has been proposed (Andersen 1989). The first and second compartments represent the freely diffusible lipophilic tracer in the blood and brain tissue respectively, while the third and fourth compartments represent the hydrophilic forms of the tracer retained in brain and blood (see Figure 13). The rate constants k_3 and k_5 represent the conversion of lipophilic form to hydrophilic form in brain and blood respectively. The conversion of the lipophilic form to the hydrophilic form is virtually irreversible so that the rate constants (k_4 and k_6) for re-conversion back to the lipophilic form are assumed to be zero. The rate of uptake of HMPAO from the blood to brain (K_1) is determined by the cerebral blood flow (F) and the first-pass extraction rate (E) which is itself variable and dependent on blood flow. The rate

Figure 13 A four compartment model of hexamethylpropyleneamine oxime (HMPAO) uptake in the brain

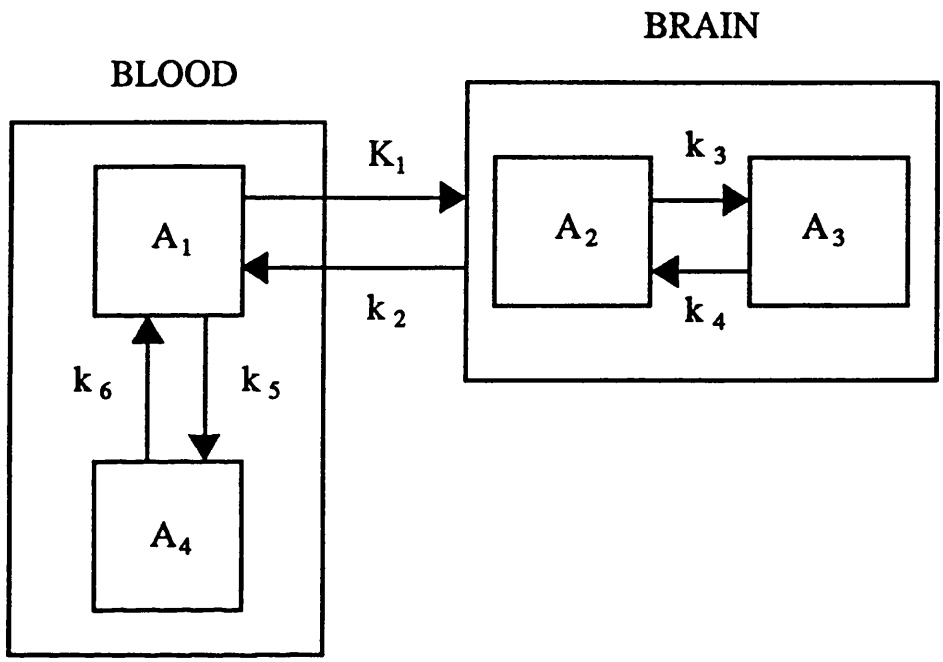

The freely diffusible lipophilic form of the tracer in the blood (A_1), crosses the blood-brain barrier and enters brain tissue (A_2) where it undergoes conversion to a hydrophilic form (A_3) which can not traverse plasma membranes and is retained in the tissue. The conversion of the lipophilic to hydrophilic form of the tracer also occurs in the blood (A_4). The uptake of the tracer from blood to tissue (K_1) is directly related to blood flow. See main text for more details.

A = amount of tracer in each compartment.

K_1 = transfer of HMPAO from blood to tissue.

k_2 to k_6 = first order rate constants for transfer of HMPAO between A_1, A_2, A_3 and A_4.

From Andersen 1989.

constant (k_2) for diffusion of the lipophilic tracer back into the blood is equivalent to K_1 divided by the blood:brain partition coefficient (λ).

The conversion of lipophilic HMPAO to the hydrophilic form within the brain is not instantaneous ($k_3 = 0.8 \pm 0.12$ min^{-1}, Lassen *et al.* 1988). This time lag allows some back diffusion of lipophilic HMPAO into the blood. As k_2 is dependent on blood flow, wash out of the tracer will be higher at higher flow rates resulting in underestimation of CBF in regions of high flow. A correction factor has been derived (Lassen *et al.* 1988) to compensate for this initial preferential back-diffusion of [^{99m}Tc]HMPAO from high flow regions.

Practice

The lipophilic [^{99m}Tc]HMPAO complex is not stable *in vitro* and undergoes conversion to the hydrophilic form with a half-life of 2-4 h (Andersen 1989). As the hydrophilic form can not cross the blood-brain barrier, the [^{99m}Tc]HMPAO complex must be freshly prepared prior to use. Therefore the radio-isotope ^{99m}Tc, in the form of [^{99m}Tc]pertechnetate, was mixed with D,L-HMPAO (Ceretec, Amersham International, U.K.) to form the [^{99m}Tc]HMPAO complex immediately following surgical preparation of the animal in which blood flow was to be measured. The [^{99m}Tc]HMPAO (0.7 ml i.v.) was then administered to the rat within 30 min of reconstitution (to prevent loss of the lipophilic form of the tracer) as recommended by Andersen 1989.

At the end of the experimental period the brain was removed and processed as described in Section 2.4.1. Tissue sections were apposed to [^{3}H]-sensitive film together with a set of precalibrated standards (21330 - 174290 nCi/g ^{99m}Tc tissue equivalent) for a nominal exposure time of 4 h (the exact exposure time being dependent on the delay between decapitation and apposition to the film). Tissue concentrations of [^{99m}Tc]HMPAO on the resultant autoradiograms were determined by densitometry with reference to the standards as described in Section 2.4.3. Unlike the [^{14}C]IAP method of determining CBF, the [^{99m}Tc]HMPAO method does not give an absolute measurement of CBF. Instead relative CBF is estimated by expressing regional [^{99m}Tc]HMPAO uptake (obtained from the autoradiograms) as a percentage of the uptake in a pre-selected reference region - for this study the data was normalised to the cerebellum.

2.4.3. Measurement of autoradiograms

Analysis of all autoradiograms was conducted using the Quantimet 970 imager analyser system (Cambridge Instruments, U.K.). This system firstly measures the optical density of the precalibrated standards (^{3}H or ^{14}C) to obtain a calibration curve of optical density versus ligand concentration (nCi/g tissue). The optical densities of the chosen regions of interest on the autoradiogram were then measured and subsequently converted to the actual tissue concentration of the particular ligand by reference to the standard curve.

For each neuroanatomical region studied 6 measurements of optical density were made from several tissue sections. The mean of these measurements was then converted to the tissue concentration of ligand for each region from each animal with reference to the standards. In studies combining *in vitro* receptor autoradiography with *in vivo* determination of local CBF, care was taken to ensure that optical densities were measured at exactly the same points on the different autoradiograms. For *in vitro* receptor autoradiography optical densities for specific binding were calculated by subtracting the values for nonspecific binding from those for total binding.

2.5. STATISTICAL ANALYSIS

Data in the main text and results tables are presented as means ± standard deviation. Data presented graphically is shown as means ± standard error of the mean to improve the clarity of the figures.

For CBF and ligand binding studies, data was evaluated by either paired or unpaired Student's *t*-tests where appropriate. For analysis of change in blood pressure over time, mean arterial blood pressures were compared by two-way repeated measure ANOVA followed by unpaired Student's *t*-tests with Bonferroni correction for simultaneous multiple comparisons (Wallenstein *et al.* 1980). For the evolution of ischaemic damage study volumes of ischaemic damage for permanent, transient and sham MCA occlusion groups were analysed separately by one-way ANOVA followed by unpaired Student's *t*-tests with Bonferroni correction. In all other histology studies volumes of ischaemic damage were compared by unpaired Student's *t*-tests with Bonferroni correction where appropriate. In all cases differences were considered significant for $p < 0.05$.

3. ALTERATIONS IN LOCAL CEREBRAL BLOOD FLOW FOLLOWING TRANSIENT FOCAL CEREBRAL ISCHAEMIA

3.1. Introduction

The endothelin-1 model of MCA occlusion was specifically designed as a model of *transient* focal ischaemia. It is therefore of critical importance to demonstrate that reperfusion does occur in this model, particularly as restoration of blood flow is not observed (within 3 h of endothelin-1 application) in the superficially similar model described by Sharkey *et al.* 1993. Therefore this study was designed to assess the acute changes in local CBF induced by topical application of endothelin-1 to the MCA in the anaesthetised rat.

In an earlier study it was demonstrated that, in our model, endothelin-1 applied to the MCA induces profound ischaemia followed by spontaneous restoration of blood flow in the caudate nucleus (Macrae *et al.* 1993). This study was conducted using the hydrogen clearance technique and hence was limited to measuring blood flow only at the site of probe placement. The present study was therefore designed to assess endothelin-1-induced changes in CBF throughout the entire cerebral hemispheres using the greater spatial resolution offered by *in vivo* autoradiographical techniques. The combined use of 2 different radio-isotopes ([^{14}C]IAP and [^{99m}Tc]HMPAO) enabled measurement of local CBF at 2 time points following application of endothelin-1 to the MCA. The time points were chosen with reference to the hydrogen clearance study in order to obtain a measure of local CBF at the time of most profound ischaemia (5 min post-endothelin-1 application) and at a time when CBF would be expected to be recovering (2 h post-application of endothelin-1).

3.2. Experimental protocol

Rats underwent transient MCA occlusion (n = 12) induced by topical application of endothelin-1 to the MCA (see Section 2.3.1.). For illustrative comparison one animal was subjected to permanent MCA occlusion while 2 further rats underwent the sham procedure (saline applied to the MCA). Local CBF was measured 5 min and 2 h post-MCA occlusion using the tracers [^{99m}Tc]HMPAO and [^{14}C]IAP respectively. The [^{99m}Tc]HMPAO complex was prepared immediately prior to MCA occlusion and in all cases administered to the rat within 30 min of preparation.

[^{99m}Tc]HMPAO (0.7 ml, 224 MBq ^{99m}Tc) was injected intravenously over 30 s, 4 min post-MCA occlusion to allow for the lag time between administration and brain uptake (approximately 1 min). 2 h post-MCA occlusion local CBF was measured using the standard [^{14}C]IAP protocol described in Section 2.4.2.1. The brain was removed and processed as quickly as possible to prevent excess loss of radioactive tracer due to the relatively short half-life (6 h) of ^{99m}Tc. The frozen brain was cut into coronal sections (20 μm) which were collected onto glass coverslips for autoradiographic determination of local CBF.

For the [^{99m}Tc]HMPAO image of blood flow, the sections were apposed to [^{3}H]-sensitive film for approximately 4-5 h together with a set of precalibrated standards (21330 - 174290 nCi/g ^{99m}Tc tissue equivalent). In addition a set of [^{14}C]-standards was included to assess the degree of contamination by [^{14}C] of the ^{99m}Tc-images. The actual duration of exposure for each individual experiment was determined by the lag time between decapitation and apposition to the film. The [^{99m}Tc]HMPAO film was then developed and the sections stored (behind lead bricks) for 4 days (equivalent to 16 half-lifes for ^{99m}Tc) to allow decay of ^{99m}Tc activity and prevent cross-contamination of ^{99m}Tc onto the ^{14}C image. The sections were then re-apposed to [^{14}C]-sensitive film for 14 days, together with a set of [^{14}C]-standards, to obtain the [^{14}C]IAP image. The scintillation vials were also stored for 4 days (to allow decay of ^{99m}Tc) prior to determination of [^{14}C]-concentration in the arterial blood samples.

3.3. **Results**

Physiological variables measured immediately prior to MCA occlusion and 2 h post-MCA occlusion are shown in Table 2. Individual values were within the normal range and comparable between the 2 time points.

Temporal alterations in cerebral blood flow following transient MCA occlusion

Five min following application of endothelin-1 to the MCA there were reductions in local CBF throughout the hemisphere ipsilateral to the constricted MCA, while by 2 h post-endothelin-1 application local CBF had appreciably increased in those regions which had exhibited the most severe reductions in CBF at the 5 min time point. Autoradiograms (at the same level) 5 min and 2 h following onset of transient MCA occlusion from one animal are shown in Figure 14a-b. The increase in blood flow at the 2 h time point in regions which were densely ischaemic 5 min post-endothelin-1 application is clearly apparent. Although there was some variation between animals with respect to the

topographical distribution and magnitude of the reductions in local CBF following transient MCA occlusion, this same basic pattern of temporal change in CBF was apparent to some extent for all animals studied. In contrast, for the animal subjected to permanent MCA occlusion, blood flow was still very low and not appreciably altered from the 5 min time point 2 h post-MCA occlusion (Figure 14c-d).

The mean values for local CBF 5 min and 2 h post-MCA occlusion are shown in Table 3. Since local CBF measured by the HMPAO technique can not be expressed in absolute units (*i.e.* ml/100 g/min) both the HMPAO-derived values (5 min time point) and the IAP-derived values (2 h time point) are shown normalised to the cerebellum to allow direct comparison of local CBF at the 2 time points (mean absolute blood flow for the cerebellar cortex was 146 ± 50 ml/100 g/min).

5 min post-endothelin-1 application to the MCA the greatest reductions in local CBF were observed in the frontal and sensorimotor cortices (11 - 16% of contralateral value) and dorsolateral caudate nucleus (29% of contralateral value) (Table 3). Moderate reductions in local CBF were found in the parietal cortex, ventromedial caudate nucleus, globus pallidus and genu (38 - 57% of contralateral value) while small, but statistically significant, reductions in flow were present in the thalamus and nucleus accumbens (87 - 91% of contralateral value). Due to heterogeneity in the distribution of the areas of endothelin-1-induced ischaemia, the averaged local CBF values masked more severe reductions in local CBF in a substantial proportion of the animals. For example inspection of the individual data for the dorsolateral caudate nucleus revealed that for 7 of the 12 animals blood flow was reduced to less than 25% of the contralateral value.

By 2 h post-endothelin-1 application local CBF in the core MCA territory had increased - to 29 - 30% of the contralateral value in the frontal and sensorimotor cortices, and 50% of the contralateral value in the dorsolateral caudate nucleus (Table 3). In contrast for regions such as the nucleus accumbens and thalamus which exhibited only minor reductions in local CBF at the 5 min time point, local CBF (expressed as a percentage of the contralateral value) was not appreciably altered at the 2 h time point.

Table 2 Physiological variables for autoradiographical determination of local cerebral blood flow following **transient** MCA occlusion

	Pre-MCAO	Post-MCAO
pH	7.401 ± 0.047	7.386 ± 0.054
Pa CO_2 (mmHg)	38.6 ± 1.8	39.6 ± 2.8
Pa O_2 (mmHg)	174.1 ± 36.7	190.8 ± 27.6
Rectal Temp (°C)	37.11 ± 0.22	36.82 ± 0.34
Glucose (mmol/l)	10.82 ± 2.36	9.89 ± 1.88
Temporalis Temp (°C)	36.70 ± 0.45	——

Physiological variables were determined immediately prior to and 2 h following MCA occlusion (n = 12).

Figure 14 Representative autoradiograms of cerebral blood flow following transient and permanent focal ischaemia

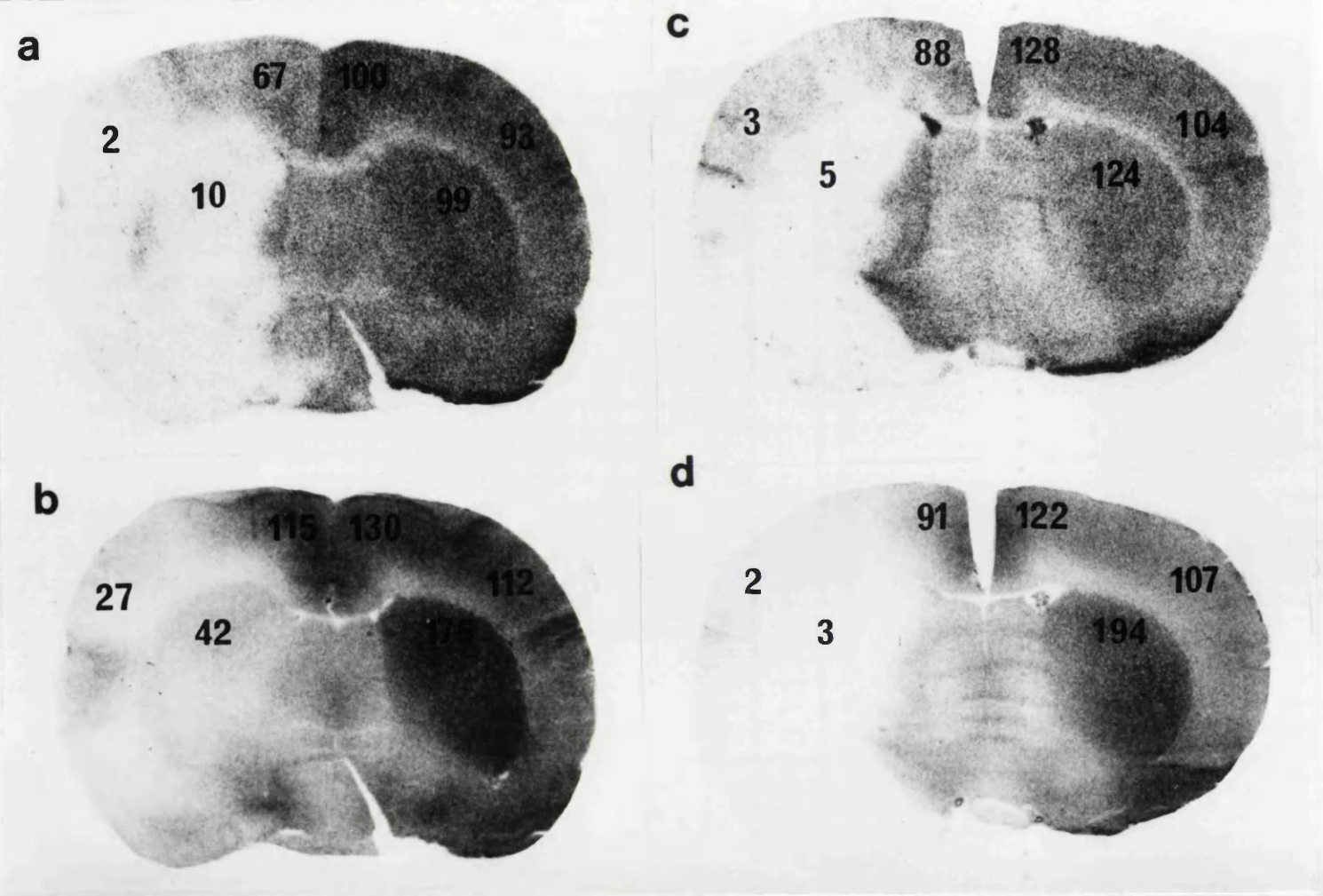

Autoradiograms of lCBF measured 5 min (HMPAO; a,c) and 2 h (IAP; b,d) following transient (a-b) or permanent (c-d) MCA occlusion. Numbers indicate lCBF (normalised to the cerebellum). In both cases CBF was reduced in the frontal cortex and caudate nucleus 5 min post-MCA occlusion, while by 2 h CBF in these same regions had increased following transient MCA occlusion (b), but not permanent MCA occlusion (d). Scale 6:1.

Table 3 Local cerebral blood flow 5 min and 2 h post-onset of **transient** MCA occlusion

REGION	5 min post-MCAO			2 h post-MCAO		
	Ipsilateral	Contralateral	% Contra	Ipsilateral	Contralateral	% Contra
Frontal Cortex	12 ± 15***	111 ± 15	11	35 ± 16***	120 ± 19	29
Sensorimotor Cortex	18 ± 23***	110 ± 15	16	34 ± 17***	114 ± 19	30
Parietal Cortex	53 ± 29***	119 ± 13	45	60 ± 24***	117 ± 20	51
Anterior Cingulate Cortex	109 ± 30	115 ± 14	95	150 ± 42	147 ± 30	102
Caudate Nucleus - dorsolateral	35 ± 26***	120 ± 16	29	90 ± 53***	179 ± 24	50
Caudate Nucleus - ventromedial	46 ± 36***	121 ± 15	38	87 ± 49***	168 ± 20	52
Globus Pallidus	60 ± 40**	106 ± 12	57	76 ± 32**	106 ± 16	72
Nucleus Accumbens	84 ± 12*	94 ± 9	89	82 ± 21	88 ± 16	93
Thalamus - medial	91 ± 13**	100 ± 14	91	98 ± 20**	106 ± 19	92
Thalamus - ventral	87 ± 13***	100 ± 12	87	89 ± 15**	103 ± 19	86
Hypothalamus	81 ± 28	92 ± 13	88	78 ± 13**	82 ± 16	95
Genu of Corpus Callosum	29 ± 11***	64 ± 11	45	50 ± 22**	68 ± 19	74

Local cerebral blood flow (normalised to the cerebellum) in hemispheres ipsilateral and contralateral to MCA occlusion. lCBF was measured 5 min (HMPAO) and 2 h (IAP) following application of endothelin-1 to the MCA. *$p < 0.05$, **$p < 0.01$, ***$p < 0.001$ comparison with contralateral region (paired Student's t-tests).

In contrast to the reductions in local CBF induced by endothelin-1, the sham procedure (saline applied to the MCA) resulted in minimal alterations in local CBF. For example the mean values (n = 2) for local CBF 5 min post-saline application to the MCA (expressed as percentages of the blood flow in the cerebellum) were 127 ± 8 and 140 ± 5 for the frontal cortex (ipsilateral and contralateral to the sham procedure) and 134 ± 4 and 137 ± 4 for the dorsolateral caudate nucleus (ipsilateral and contralateral to the sham procedure).

3.4. Discussion

In this study double label autoradiography was used to measured local CBF at 2 time points following constriction of the MCA induced by endothelin-1. The results demonstrate that there were severe reductions in local CBF in regions such as the frontal cortex and dorsolateral caudate nucleus that receive their blood supply primarily from the MCA 5 min post-application of endothelin-1 to the artery. The magnitude of the reductions in flow in the frontal and sensorimotor cortices (expressed as percentages of the contralateral values) were similar to those previously reported for both permanent MCA occlusion (Tamura *et al.* 1981b) and topical application of endothelin-1 to the MCA (Robinson *et al.* 1990) where local CBF was measured 30 and 10 min post-onset of ischaemia respectively using the IAP technique. Thus the dose of endothelin-1 (25 µl x 10^{-4}M) used in the present study causes reductions in CBF in the MCA territory to levels that have previously been demonstrated to induce ischaemic damage (Tamura *et al.* 1981 a,b). However the present study has also shown that local CBF values in the core MCA territory increase approximately 2-3 fold 2 h post-endothelin-1 application, indicating that a significant degree of reperfusion is present by this time point. The demonstration of reperfusion 2 h following endothelin-1 application to the MCA is in good agreement with the temporal restoration of flow previously reported in this model using the hydrogen clearance technique (Macrae *et al.* 1993). In summary this study has established that application of endothelin-1 to the MCA (as described in Section 2.3.) results in a period of profound ischaemia followed by partial restoration of blood flow by 2 h post-endothelin-1 application, thereby validating this approach as a model of *transient* focal ischaemia.

Although local CBF in the core MCA territory was still reduced at the 2 h time point compared with the corresponding contralateral regions, the observed absolute values for local CBF were well above the flow threshold for irreversible ischaemic damage in the normotensive rat (see Section 5.3.1.). For example the minimum mean absolute value for local CBF (derived from the IAP autoradiograms) obtained at the 2 h time point was 50 ml/100 g/min in the sensorimotor cortex which is approximately twice the ischaemic threshold. Thus although restoration of blood flow was by no means complete at the 2 h

time point, CBF had probably been sufficiently increased to prevent further direct ischaemic damage to the tissue. The demonstration of a significant degree of reperfusion, present as early as 2 h post-onset of ischaemia, lends support to the hypothesis that the dramatic increase in lesion volume that occurs from 4 h to 24 h post-onset of ischaemia in this model (see Section 4.2.) is due to pathological processes associated with reperfusion rather than continued severe ischaemia.

Comparison with alternative models of transient MCA occlusion in the rat

In the present study local CBF (measured by [^{99m}Tc]HMPAO uptake) was reduced to 11 - 16% of the actual contralateral value in core MCA territory such as the frontal and sensorimotor cortices 5 min post-endothelin-1 application. Similar reductions in flow are achieved with MCA occlusion induced by the intraluminal thread method (10 - 15% of contralateral values measured by [^{14}C]IAP autoradiography, Memesawa *et al.* 1992a) or extravascular occlusion with clips (10% of baseline measured by laser Doppler flowmetry, Buchan *et al.* 1992b) or ligatures (21% of baseline measured by laser Doppler flowmetry, Kaplan *et al.* 1991) in tandem with carotid artery occlusion.

2 h following application of endothelin-1 local CBF in the previously ischaemic regions (frontal and sensorimotor cortices and dorsolateral caudate nucleus) had increased to 29 - 50% of the contralateral value demonstrating reperfusion had been initiated. For comparison, in the intraluminal thread model local CBF returns to 32% (cortex) and 47% (caudate) of contralateral values with a 15 min period of reperfusion following 1 h MCA occlusion (Memesawa *et al.* 1992b), and 68% (cortex) and 58% (caudate) after 2 h recirculation (Nagasawa & Kogure 1989). Thus although it may have been surmised that reperfusion in the endothelin-1 model of MCA occlusion would be slower and more progressive than reperfusion following removal of an intraluminal filament this does not appear to be the case. Nagasawa and Kogure suggest the comparatively slow reperfusion in their model is due to marked oedema formation on reperfusion that tends to reduce CBF throughout the brain (Nagasawa & Kogure 1989). In contrast reperfusion following removal of clips or ligatures is associated with an immediate transient hyperaemia (CBF greater than 200% of baseline, Kaplan *et al.* 1991) which is followed by return to baseline flows (Buchan *et al.* 1992b; Kaplan *et al.* 1991). The different haemodynamic patterns of reperfusion observed in the different rat models of transient MCA occlusion will be discussed further in Section 8.2.

It is difficult to relate the CBF changes following experimental transient focal ischaemia to the clinical situation since there is very little data available concerning CBF in the first few hours following resolution of MCA occlusion in man. However it is known that hyperaemia within the previously ischaemic region can frequently occur (44 - 87% of all cases showing reperfusion (Olsen & Lassen 1984; Ringelstein *et al.* 1992) within the first few days following stroke onset and can persist for approximately 2 weeks (Olsen & Lassen 1984; Ringelstein *et al.* 1992). The cause of this prolonged hyperperfusion is unclear - lactate accumulation during the ischaemic phase (Lassen 1966) may contribute to immediate hyperaemia on reperfusion, but is not likely to sustain the hyperaemic state for 2 weeks (Olsen 1986). It is more likely that the hyperperfusion reflects ischaemic damage to the vasculature resulting in loss of the normal vascular reactivity to vasoconstrictive stimuli (Olsen 1986).

The temporal progression of reperfusion in the endothelin-1 model has not yet been studied beyond 4 h post-onset of ischaemia in the anaesthetised rat (Macrae *et al.* 1993). Measurement of local CBF at later time points (*e.g.* 24 and 72 h post-endothelin-1) may yield further information that is pertinent both to the temporal evolution of lesion size within this model and also to clinical stroke.

Methodological considerations for the determination of cerebral blood flow using HMPAO

1) In normal rat brain there is an excellent linear relationship between relative CBF measured by the HMPAO technique and absolute CBF determined by other methods (*e.g.* IAP) up to flows of approximately 100 ml/100 g/min (Bullock *et al.* 1991; Lear 1988). However above this level the HMPAO method can underestimate CBF due to back diffusion of the lipophilic tracer from the brain to the blood. Several authors (Bullock *et al.* 1991; Lear 1988) have utilised the correction algorithm derived by Lassen and colleagues (Lassen *et al.* 1988) to compensate for this phenomenon but we chose not to use this correction factor in the present study for 2 reasons. Firstly, the Lassen correction was originally devised to 'enhance(s) the contrast between high and low flow regions' on an HMPAO image (Lassen *et al.* 1988). Although the correction factor does achieve this aim, and thereby improves the linearisation between CBF measured by HMPAO uptake and other techniques (Lassen *et al.* 1988; Lear 1988), it also increases the spread of the data so that the correlation between the 2 data sets may actually be weaker once the correction factor has been applied (Heiss *et al.* 1990). Therefore we saw no advantage in applying the Lassen correction to quantitative analysis of blood flow data. Secondly, in this study HMPAO uptake was used to assess the ischaemia invoked by endothelin-1-induced

constriction of the MCA. Thus we were primarily concerned with measuring CBF in regions exhibiting pathologically low levels of blood flow. As stated above the HMPAO method accurately reflects CBF up to 100 ml/100 g/min, thus no correction factor was necessary for assessment of blood flow in ischaemic regions.

2) The problem of cross-contamination between the autoradiographic images produced by the 2 radio-isotopes (^{14}C and ^{99m}Tc) must be considered. Contamination of the ^{14}C-image by ^{99m}Tc was prevented by allowing virtual complete decay of ^{99m}Tc before the tissue sections were apposed to ^{14}C-sensitive film. However the possible contamination of the ^{99m}Tc-image by ^{14}C must be addressed. This is of particular importance to the present study since, due to the presence of reperfusion, blood flow in certain regions would be higher at the time of ^{14}C-uptake compared with ^{99m}Tc-uptake and thus the relatively high tissue concentrations of ^{14}C may have resulted in overestimation of CBF on the HMPAO image *i.e.* the severity of the ischaemia induced by endothelin-1 may have been underestimated in regions which were subsequently well reperfused. To assess the degree of contamination, a 'worst-case' analysis was performed using CBF data derived from the HMPAO autoradiogram with the longest exposure time (5.5 h). For this animal the contribution of ^{14}C to the optical density of the regions with densest ischaemia was found to amount to less than the equivalent of 1 ml/100 g/min CBF. Therefore we can conclude that cross-contamination was minimal and that the values of CBF in the ischaemic regions derived from the HMPAO autoradiograms are a true reflection of CBF at the time of HMPAO uptake.

3) Once lipophilic HMPAO has been taken up by brain tissue and converted to the hydrophilic form it is assumed that the tracer is entrapped within the brain. Although conversion of the hydrophilic form of HMPAO back to the lipophilic form is negligible, a small amount of hydrophilic HMPAO may be lost from the brain resulting in underestimation of CBF. Loss of hydrophilic HMPAO may be of particular importance to CBF studies of cerebral ischaemia since it may be surmised that ischaemia induced damage to the blood-brain barrier and cellular membranes could potentially increase the rate of loss of hydrophilic HMPAO. However it has been reported that HMPAO uptake accurately reflects CBF (measured by [^{14}C]IAP) 72 h post-permanent MCA occlusion in the rat (Bullock *et al.* 1991) when blood-brain barrier permeability is increased. Thus loss of hydrophilic HMPAO through a damaged blood-brain barrier does not appear to influence CBF measurement within the sub-acute phase of experimental cerebral ischaemia.

While hypofixation of [^{99m}Tc]HMPAO may be expected in regions of tissue damage, paradoxically increased [^{99m}Tc]HMPAO uptake has been reported in infarcts from patients with sub-acute stroke and evidence of reperfusion (Sperling & Lassen 1993).

[^{99m}Tc]HMPAO uptake in these patients overestimated CBF as measured by ^{133}Xe tomography at the same time point. Thus the actual degree of reperfusion in these patients was more modest than the overt hyperemia suggested by the [^{99m}Tc]HMPAO image. The reasons for hyperfixation of [^{99m}Tc]HMPAO in a reperfused infarct are at present unknown but again may be related to redistribution of the hydrophilic form of the tracer as a consequence of blood-brain barrier damage (Heiss *et al.* 1990). In the present study [^{99m}Tc]HMPAO was used to assess the degree of ischaemia rather than reperfusion, and the tracer was administered within 5 min of endothelin-1 application at a time when the blood-brain barrier is likely to be intact, thus hyperfixation of [^{99m}Tc]HMPAO is not likely to be a confounding influence on the results presented herein.

4. HISTOLOGICAL CHARACTERISATION OF ISCHAEMIC DAMAGE FOLLOWING TRANSIENT AND PERMANENT MCA OCCLUSION

4.1. Assessment of acute ischaemic damage following MCA occlusion

4.1.1. Introduction

The ischaemic damage induced by transient MCA occlusion was first quantified histopathologically in the anaesthetised rat, 4 h following application of endothelin-1 to the MCA. For comparison, the volumes of ischaemic damage following permanent MCA occlusion (4 h duration) or the sham procedure were also determined. The 4 h time point was chosen because: a) maintenance of artificially-ventilated rats under anaesthesia allows physiological parameters (blood pressure, blood gases, body temperature) to be rigorously controlled within strict limits throughout the 4 h period. The impact of these variables on outcome is thus comparable for all animals and b) 4 h is the earliest time point at which the border between viable and ischaemically-damaged tissue can be reliably delineated using the specified histopathological techniques.

4.1.2. Experimental protocol

Rats, maintained under halothane anaesthesia, were subjected to permanent or transient MCA occlusion or the sham procedure as described in Section 2.3.1. Blood pressure was monitored continuously throughout the experiments and rats were killed 4 h post-onset of ischaemia by perfusion fixation. Quantitative histopathology was then used to determine the volumes of ischaemic damage for each group.

4.1.3. Results

4.1.3.1. Physiological Variables

The physiological variables for the 3 separate procedures (permanent, transient and sham MCA occlusion) are shown in Table 4 and were within normal physiological limits for all groups.

Mean values for mean arterial blood pressure (MABP) prior to exposure of the MCA were 88 ± 21, 86 ± 9 and 86 ± 6 mmHg for permanent MCA occlusion, transient MCA occlusion and sham procedure respectively. MABP was not appreciably affected by the surgical procedure (see also Figures 26-27).

Table 4 Physiological variables for 4 h MCA occlusion in the anaesthetised rat

PERMANENT MCAO (n = 6)

	Pre-MCAO	+ 1 HOUR	+ 4 HOUR
pH	7.495 ± 0.042	7.497 ± 0.036	7.442 ± 0.040
Pa CO_2 (mmHg)	37.5 ± 3.2	36.0 ± 1.6	36.7 ± 1.4
Pa O_2 (mmHg)	165.0± 23.0	166.8 ± 12.5	164.7 ± 11.3
Glucose (mmol/l)	9.22 ± 1.04	8.97 ± 0.48	8.63 ± 0.58
Rectal Temp (°C)	36.90 ± 0.55	36.92 ± 0.26	36.88 ± 0.10

TRANSIENT MCAO (n = 12)

	Pre-MCAO	+ 1 HOUR	+ 4 HOUR
pH	7.453 ± 0.040	7.443 ± 0.041	7.425 ± 0.047
Pa CO_2 (mmHg)	37.7 ± 3.1	37.4 ± 3.0	37.8 ± 1.7
Pa O_2 (mmHg)	137.4 ± 23.0	145.3 ± 26.3	154.3 ± 20.1
Glucose (mmol/l)	11.09 ± 1.09	10.27 ± 1.39	9.21 ± 1.12
Rectal Temp (°C)	36.91 ± 0.34	36.97 ± 0.24	37.06 ± 0.23

SHAM PROCEDURE (n = 3)

	Pre-saline	+ 1 HOUR	+ 4 HOUR
pH	7.417 ± 0.040	7.423 ± 0.025	7.437 ± 0.012
Pa CO_2 (mmHg)	36.7 ± 1.5	36.3 ± 3.1	37.0 ± 2.0
Pa O_2 (mmHg)	158.7 ± 8.5	181.3 ± 11.1	174.3 ± 14.6
Glucose (mmol/l)	10.00 ± 1.41	10.37 ± 0.83	9.97 ± 0.57
Rectal Temp (°C)	36.67 ± 0.58	37.23 ± 0.21	37.37 ± 0.32

Physiological variables were measured immediately prior to MCA occlusion (MCAO), and 1 h and 4 h post-MCA occlusion.

4.1.3.2. Quantification of ischaemic damage

Permanent MCA occlusion

Permanent MCA occlusion resulted in a large lesion that extended from the frontal to parietal cortices and also included a large portion of the lateral caudate nucleus (see Figure 15a). The total volumes of ischaemic damage (mean ± S.D.) for hemisphere, cortex and caudate nucleus were 106.6 ± 14.7, 68.5 ± 13.6 and 30.2 ± 4.6 mm^3 respectively.

Neurones within the lesion exhibited the classical signs of ischaemic cell change. The nuclei were shrunken, densely stained and triangular in shape, while the cytoplasm was intensely eosinophillic. The surrounding neuropil was palely stained and spongy in appearance (see Figure 16a).

Transient MCA occlusion

At the 4 h time point the lesion following transient MCA occlusion was smaller than for permanent MCA occlusion but the topographic distribution within the brain was similar for both models (see Figure 15b). The mean volumes of ischaemic damage for hemisphere, cortex and caudate nucleus following transient MCA occlusion were 48.0 ± 26.4, 31.9 ± 22.9 and 12.7 ± 9.6 mm^3 respectively. The histological appearance of neurones and neuropil within the region of ischaemic cell damage following transient MCA occlusion was indistinguishable from permanent MCA occlusion (Figure 16b). Although the mean area of damage at each stereotactic level tended to be less following transient MCA occlusion (particularly in the centre of the lesion), the rostro-caudal extent of ischaemic damage following both permanent and transient MCA occlusion were comparable (see Figure 17).

Sham procedure

The sham operation (involving application of saline to the exposed MCA) resulted in either no apparent lesion, or very minor damage located in the cerebral cortex ventral to the rhinal fissure and corresponding to the site of craniectomy. The mean volumes of ischaemic damage for hemisphere, cortex and caudate nucleus were 0.4 ± 0.7, 0.4 ± 0.7 and 0.0 ± 0.0 mm^3 respectively.

Figure 15 Distribution of tissue damage assessed 4 h following onset of permanent or transient MCA occlusion in the anaesthetised rat

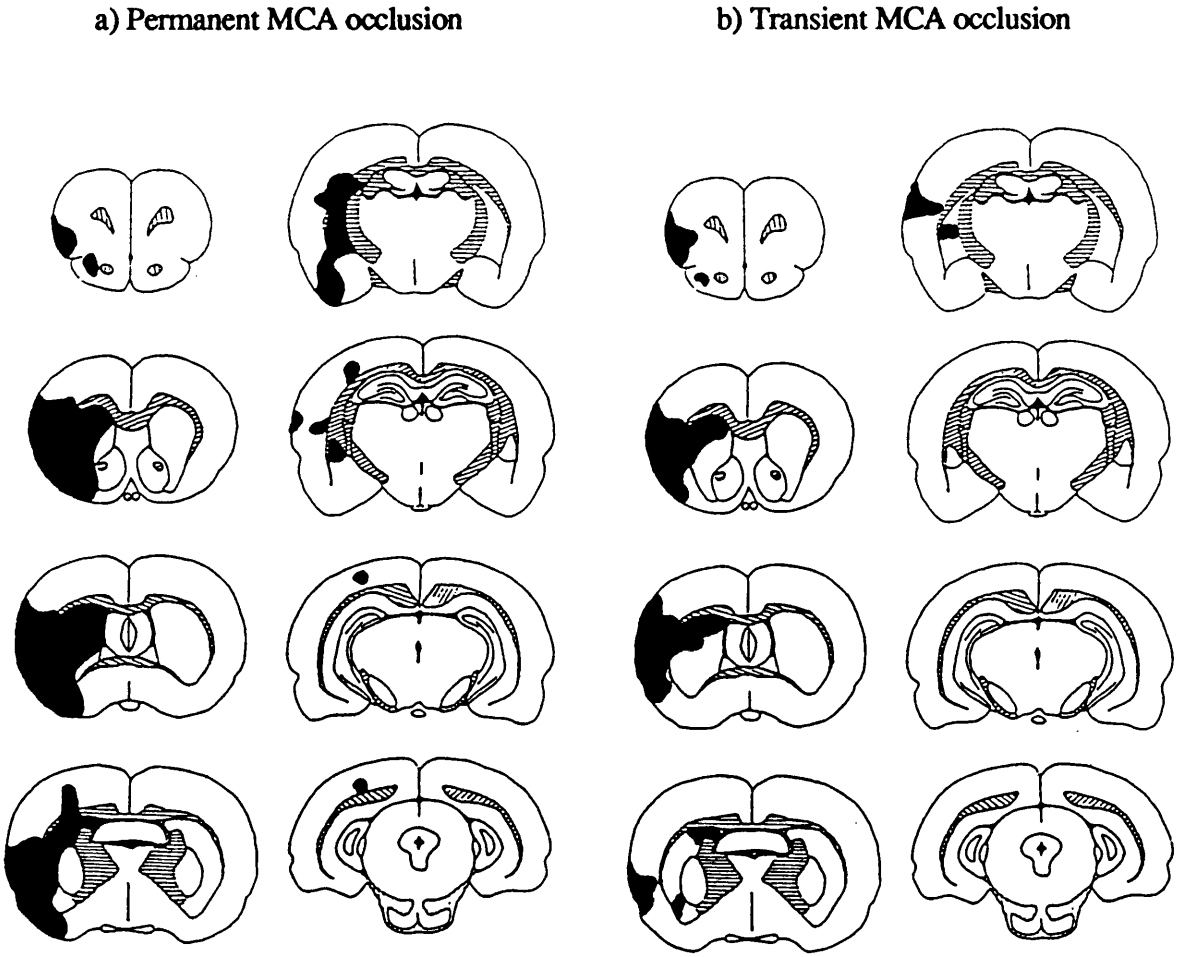

Diagramatic representation of regions showing ischaemic cell change (shaded black) at each of 8 pre-selected stereotactic levels. The figure shows the extent of histological damage for 2 representative animals subjected to a) permanent MCA occlusion or b) transient MCA occlusion. For both models ischaemic damage was located predominantly in frontal and parietal cortices and lateral caudate nucleus.

Figure 16 Ischaemic cell change 4 h following permanent or transient MCA occlusion in the anaesthetised rat

a

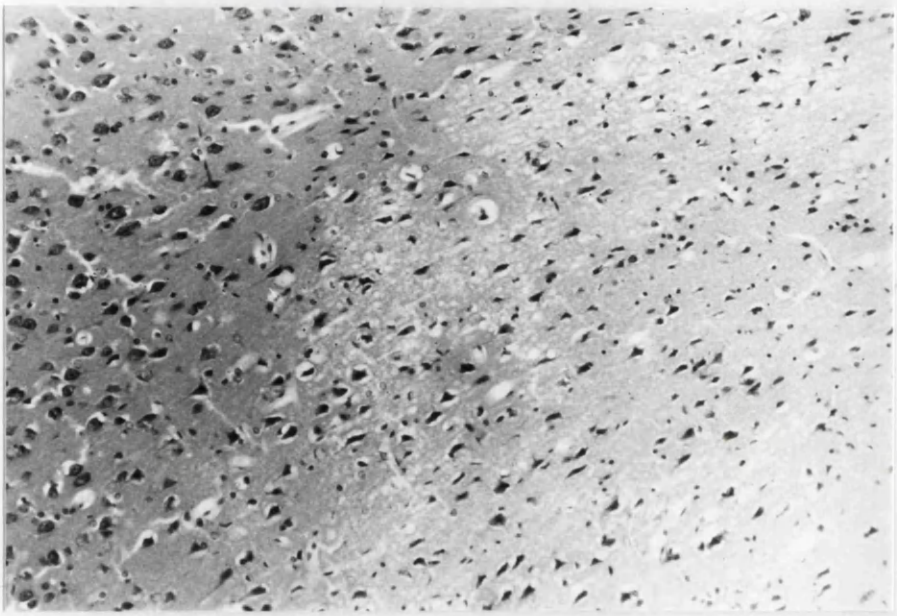

b

The figure shows high power micrographs of the ipsilateral frontal cortex (stained with haematoxylin and eosin) for 2 representative rats subjected to a) permanent and b) transient MCA occlusion. In each case the border between the ischaemic lesion and morphologically normal tissue is clearly visible. Within the lesion neurones that have undergone ischaemic cell change are triangular in shape with intensely stained nuclei. The neuropil surrounding these neurones is pale and spongy in appearance. In contrast neurones within the intact tissue are spherical with less densely stained cytoplasm and nuclei.

Figure 17 Areas of ischaemic damage 4 h following onset of permanent or transient MCA occlusion in the anaesthetised rat

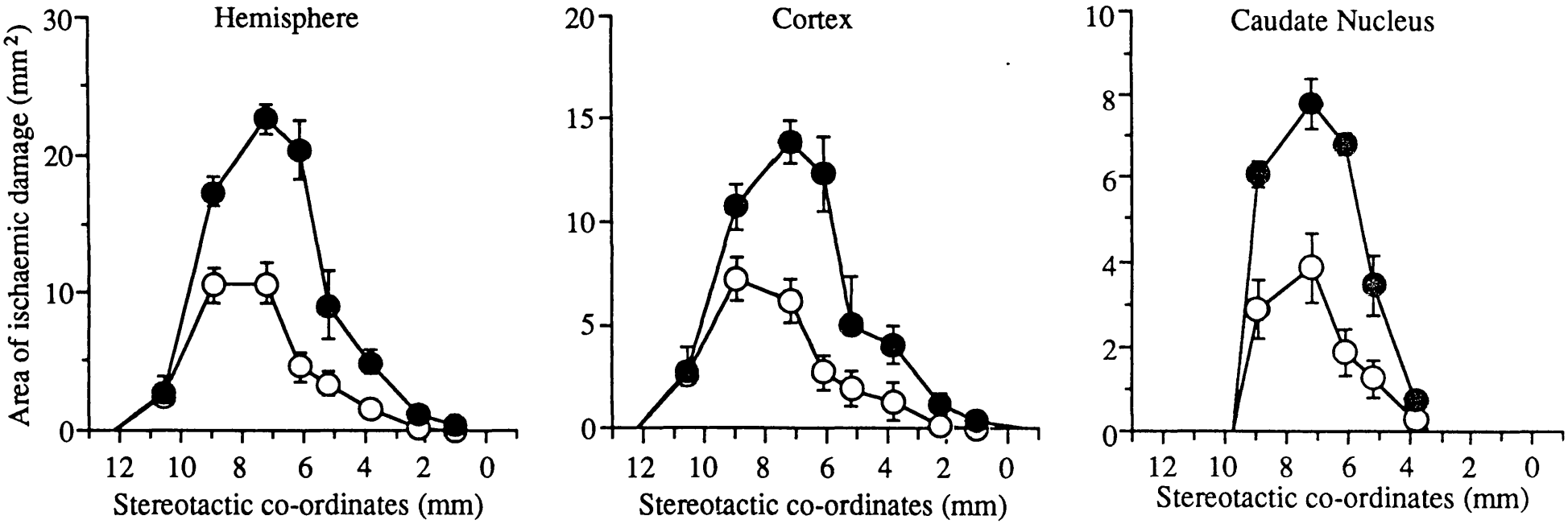

Mean areas of ischaemic damage (mm^2) in whole hemisphere, cortex and caudate nucleus measured at 8 pre-selected stereotactic coronal planes relative to the interaural line (level 0 mm) 4 h following permanent (filled symbols, n = 6) or transient (open symbols, n = 12) MCA occlusion. The mean area of damage was greater for permanent MCA occlusion at each sterotactic level, the difference being particularly pronounced in the centre of the lesion.

4.2. Timecourse for evolution of ischaemic damage following transient and permanent MCA occlusion

4.2.1. Introduction

Having established that transient MCA occlusion induced by endothelin-1 results in a quantifiable lesion 4 h post-application of the peptide, the evolution of ischaemic damage beyond the 4 h time point was then determined. Our hypothesis was that the volume of ischaemic damage following transient MCA occlusion would continue to increase beyond 4 h due to the introduction of additional, as yet undefined, pathological factors during the reperfusion phase. For comparison, separate experiments were again conducted for permanent and sham MCA occlusion at the same time points (4, 24 and 72 h). Rats were allowed to recover consciousness following surgery for the longer survival times (24 and 72 h). Therefore to permit valid comparisons between the 3 time points anaesthetics were also withdrawn following surgery from the 4 h groups. Control of physiological parameters is not possible to the same extent in conscious animals compared to animals maintained in the anaesthetised state. However physiological variables were monitored throughout the survival period so that any observable differences between groups could be taken into account in the interpretation of apparent changes in lesion size over time.

4.2.2. Experimental protocol

Rats were anaesthetised and the right femoral artery cannulated as described in Section 2.2. A permanent, transient (endothelin-1) or sham (saline) MCA occlusion was then performed. Approximately 10-15 min following surgery anaesthetics were withdrawn and the animals allowed to regain consciousness. The rats were killed 4 h, 24 h or 72 h following induction of ischaemia (or application of saline for the sham group). Blood pressure in the 4 h groups was monitored continuously. For the 24 h and 72 h groups blood pressure was monitored for 1 h post-surgery and then for 10-15 min (in conscious animals) at 24 h, 48 h and 72 h post-MCA occlusion where applicable. Blood gases, plasma glucose and rectal temperature were also measured at the 1 h, 24 h, 48 h and 72 h time points. After completion of physiological monitoring rats were returned to the post-operative recovery room. In some animals the cannula did become blocked (inspite of the use of heparin and antibiotics) and hence no physiological data could be obtained for these rats at certain time points. At the end of the specified survival period rats were reanaesthetised and perfusion fixed as described in Section 2.3.2. Quantitative histopathology was used to determine volumes of ischaemic damage at each time point.

4.2.3. Results

4.2.3.1. Physiological variables

Physiological variables for rats allowed to survive for 4, 24 or 72 h post-transient, permanent or sham MCA occlusion are shown in Tables 5, 6 and 7 respectively. For transient MCA occlusion physiological variables immediately prior to MCA occlusion (when rats were anaesthetised) were comparable between the 3 groups. Although the rats were breathing spontaneously under anaesthesia, hypercapnia was not apparent and arterial blood CO_2 levels were similar to those for artificially ventilated rats in other studies. Arterial blood O_2 levels decreased following withdrawal of anaesthetics due to the lower O_2 concentration of atmospheric air. In the 24 h and 72 h groups plasma glucose concentrations were decreased at the 24 h and 48 h time points along with the observed weight loss in the animals, however by 72 h feeding had been resumed and the plasma glucose concentration began to recover. A small increase in rectal temperature was apparent that peaked at 24 h post-MCA occlusion and then subsequently began to decline. Similar changes in physiological variables were noted for both permanent and sham MCA occlusion (see Tables 6 and 7).

The changes in blood pressure following transient MCA occlusion are illustrated in Figure 18. At the time of MCA occlusion (under anaesthesia) mean MABP was similar for the 4 h, 24 h and 72 h groups. Anaesthetics were withdrawn approximately 10-15 min following MCA occlusion. In response to the withdrawal of anaesthetics blood pressure in all 3 groups began to increase, returning to the normal range for the conscious rat by 1 h post-MCA occlusion. MABP was then well maintained at this level throughout the remainder of the survival periods and did not differ appreciably between groups at any comparable time point. Similar patterns of blood pressure response following withdrawal of anaesthetics were observed for permanent (Figure 19) and sham (Figure 20) MCA occlusion and mean values for MABP were comparable between the 4 h, 24 h and 72 h groups in each study.

4.2.3.2. Post-operative behaviour

During the first 24 hours post-MCA occlusion hunching and piloerection were commonly observed in survival animals, but these features resolved themselves with longer survival times. The rats were reluctant to eat and lost weight in the first 2 days post-operatively (probably partly due to impairment of mastication resulting from surgical section of the temporalis muscle), but began to recover weight by the third day. Neither overt hemiparesis nor ipsilateral turning were apparent in recovery animals, although no strict

Table 5 Physiological variables for evolution of ischaemic damage following **transient** MCA occlusion

4 HOUR (n = 10)

	Pre-MCAO	+ 1 HOUR	+ 4 HOUR
pH	7.380 ± 0.027	7.434 ± 0.037	7.444 ± 0.039
Pa CO_2 (mmHg)	39.3 ± 4.1	32.9 ± 4.8	31.3 ± 4.6
Pa O_2 (mmHg)	115.2 ± 20.6	98.7 ± 11.8	100.7 ± 13.6
Glucose (mmol/l)	9.22 ± 1.72	7.04 ± 1.98	7.54 ± 1.72
Rectal Temp (°C)	37.24 ± 0.58	37.44 ± 0.62	37.46 ± 0.63

24 HOUR (n = 9)

	Pre-MCAO	+ 1 HOUR	+ 24 HOUR
pH	7.416 ± 0.034	7.426 ± 0.025	7.453 ± 0.028
Pa CO_2 (mmHg)	39.2 ± 1.86	36.2 ± 1.7	36.8 ± 2.9
Pa O_2 (mmHg)	109.6 ± 7.7	99.9 ± 23.43	87.9 ± 9.8
Glucose (mmol/l)	9.58 ± 1.59	7.79 ± 1.39	7.28± 1.22
Rectal Temp (°C)	37.06 ± 0.17	37.33 ± 0.34	37.69 ± 0.54

72 HOUR (n = 12)

	Pre-MCAO	+ 1 HOUR	+ 24 HOUR	+ 48 HOUR	+ 72 HOUR
pH	7.414 ± 0.045	7.446 ± 0.036	7.460 ± 0.064	7.447 ± 0.015	7.460 ± 0.035
Pa CO_2 (mmHg)	36.8 ± 3.3	36.8 ± 2.2	35.1 ± 2.6	35.3 ± 3.3	37.3 ± 3.2
Pa O_2 (mmHg)	120 ± 21.6	96.2 ± 6.5	99.9 ± 28.3	96.6 ± 7.7	110.3 ± 23.6
Glucose (mmol/l)	8.13 ± 1.72	7.07 ± 1.12	6.44 ± 1.19	5.40 ± 1.12	6.49 ± 1.53
Rectal Temp (°C)	37.26 ± 0.31	37.18 ± 0.41	38.01 ± 0.78	37.9 ± 0.62	37.73 ± 0.61

Rats were anaesthetised at time of MCA occlusion (MCAO) and conscious at all other time points.

Table 6 Physiological variables for evolution of ischaemic damage following **permanent** MCA occlusion

4 HOUR (n = 6)

	Pre-MCAO	+ 1 HOUR	+ 4 HOUR
pH	7.350 ± 0.058	7.382 ± 0.028	7.462 ± 0.031
Pa CO_2 (mmHg)	37.0 ± 3.5	37.2 ± 1.6	36.5 ± 1.6
Pa O_2 (mmHg)	132.5 ± 15.9	126.3 ± 5.5	108.3 ± 25.3
Glucose (mmol/l)	9.02 ± 1.15	8.75 ± 0.77	8.35 ± 0.55
Rectal Temp (°C)	37.17 ± 0.41	37.02 ± 0.10	36.98 ± 0.16

24 HOUR (n = 6)

	Pre-MCAO	+ 1 HOUR	+ 24 HOUR
pH	7.368 ± 0.032	7.420 ± 0.042	7.453 ± 0.058
Pa CO_2 (mmHg)	38.5 ± 2.26	37.2 ± 3.8	37.3 ± 4.1
Pa O_2 (mmHg)	116.8 ± 10.8	90.7 ± 11.0	102.7 ± 19.3
Glucose (mmol/l)	10.13 ± 0.91	7.53 ± 0.83	8.22 ± 1.10
Rectal Temp (°C)	37.08 ± 0.30	37.23 ± 0.33	37.52 ± 0.33

72 HOUR (n = 4)

	Pre-MCAO	+ 1 HOUR	+ 24 HOUR	+ 48 HOUR	+ 72 HOUR
pH	7.420 ± 0.026	7.445 ± 0.019	7.437± 0.032	7.455 ± 0.078	7.405 ± 0.035
Pa CO_2 (mmHg)	41.5 ± 3.4	37.3 ± 5.5	36.7 ± 1.5	34.0 ± 9.9	38.5 ± 3.5
Pa O_2 (mmHg)	109.3 ± 16.8	91.8 ± 11.4	92.7 ± 8.1	96.5 ± 3.5	123.0 ± 8.5
Glucose (mmol/l)	7.70 ± 0.70	6.43 ± 1.05	5.83 ± 1.26	5.80 ± 0.35	7.35 ± 0.49
Rectal Temp (°C)	37.03 ± 0.42	37.10 ± 0.70	37.68 ± 0.39	37.43 ± 0.57	36.98 ± 0.39

Rats were anaesthetised at time of MCA occlusion (MCAO) and conscious at all other time points.

Table 7 Physiological variables for evolution of ischaemic damage following **sham** procedure

4 HOUR (n = 3)

	Pre-Saline	+ 1 HOUR	+ 4 HOUR
pH	7.427 ± 0.006	7.437 ± 0.025	7.463 ± 0.015
Pa CO_2 (mmHg)	39.3 ± 2.5	34.3 ± 1.5	32.7 ± 2.5
Pa O_2 (mmHg)	109.3 ± 4.2	103.3 ± 2.5	98.3 ± 11.1
Glucose (mmol/l)	9.00 ± 1.21	8.47 ± 1.83	8.4 ± 2.35
Rectal Temp (°C)	37.00 ± 0.00	37.13 ± 0.42	37.53 ± 0.50

24 HOUR (n = 4)

	Pre-Saline	+ 1 HOUR	+ 24 HOUR
pH	7.395 ± 0.033	7.490 ± 0.013	7.465 ± 0.029
Pa CO_2 (mmHg)	40.0 ± 2.9	35.5 ± 1.3	39.8 ± 2.5
Pa O_2 (mmHg)	109.3 ± 4.1	83.8 ± 37.5	88.5 ± 7.3
Glucose (mmol/l)	9.65 ± 1.81	9.15 ± 1.68	7.40 ± 1.81
Rectal Temp (°C)	37.23 ± 0.22	37.45 ± 0.55	38.1 ± 0.46

72 HOUR (n = 4)

	Pre-Saline	+ 1 HOUR	+ 24 HOUR	+ 48 HOUR	+ 72 HOUR
pH	7.438 ± 0.021	7.388 ± 0.119	7.429 ± 0.045	7.458 ± 0.063	7.414 ± 0.025
Pa CO_2 (mmHg)	37.8 ± 1.5	36.5 ± 1.7	33.0 ± 7.2	33.3 ± 7.4	34.7 ± 4.9
Pa O_2 (mmHg)	105.8 ± 3.4	90.3 ± 6.1	92.3 ± 7.1	101.7 ± 7.0	97.7 ± 11.2
Glucose (mmol/l)	7.98 ± 0.96	7.13 ± 1.83	5.63 ± 1.64	5.40 ± 1.30	5.65 ± 1.92
Rectal Temp (°C)	37.35 ± 0.62	37.23 ± 0.26	37.93 ± 0.81	38.3 ± 0.22	38.05 ± 0.10

Rats were anaesthetised during the sham operation (saline applied to MCA) and conscious at all other time points.

Figure 18 Mean arterial blood pressure following **transient** MCA occlusion

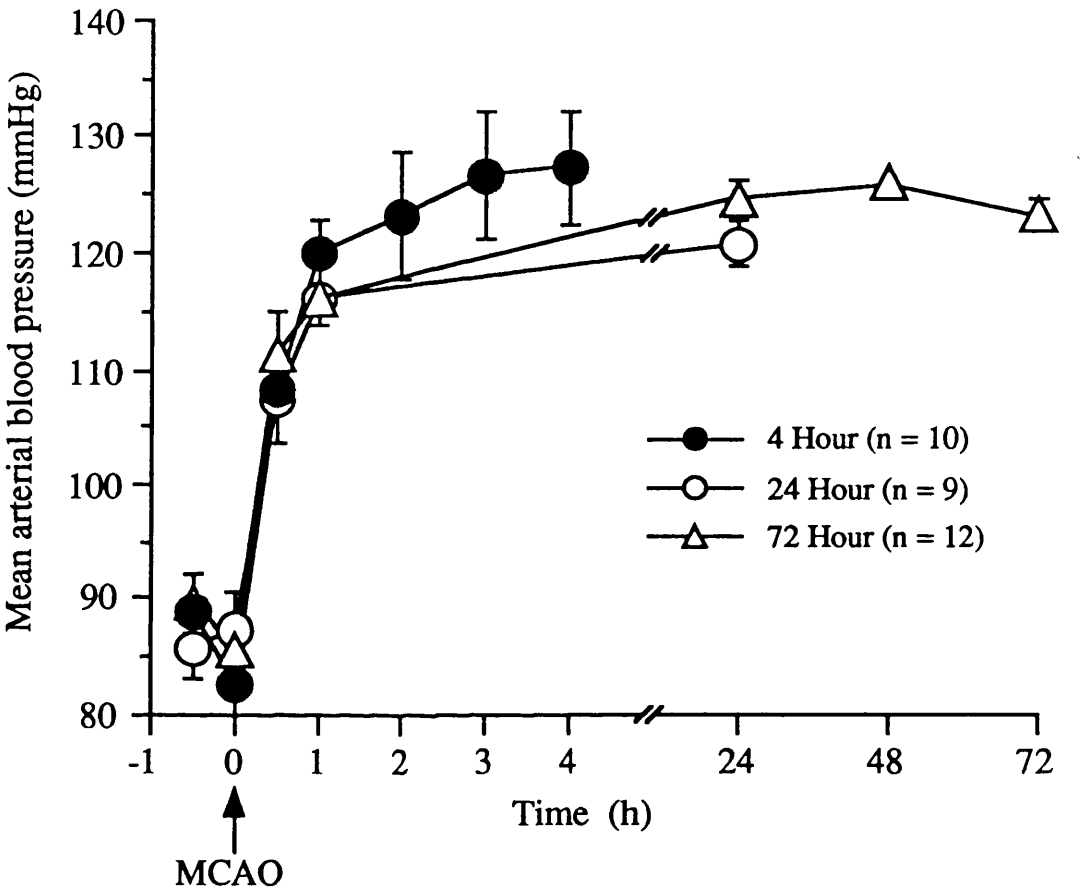

Transient MCA occlusion (MCAO) was performed under halothane anaesthesia. 10-15 min post-MCA occlusion anaesthetics were withdrawn and the rats allowed to recover consciousness. Rats were reanaesthetised and killed by perfusion fixation 4, 24 or 72 h post-MCA occlusion.

Figure 19 Mean arterial blood pressure following **permanent** MCA occlusion

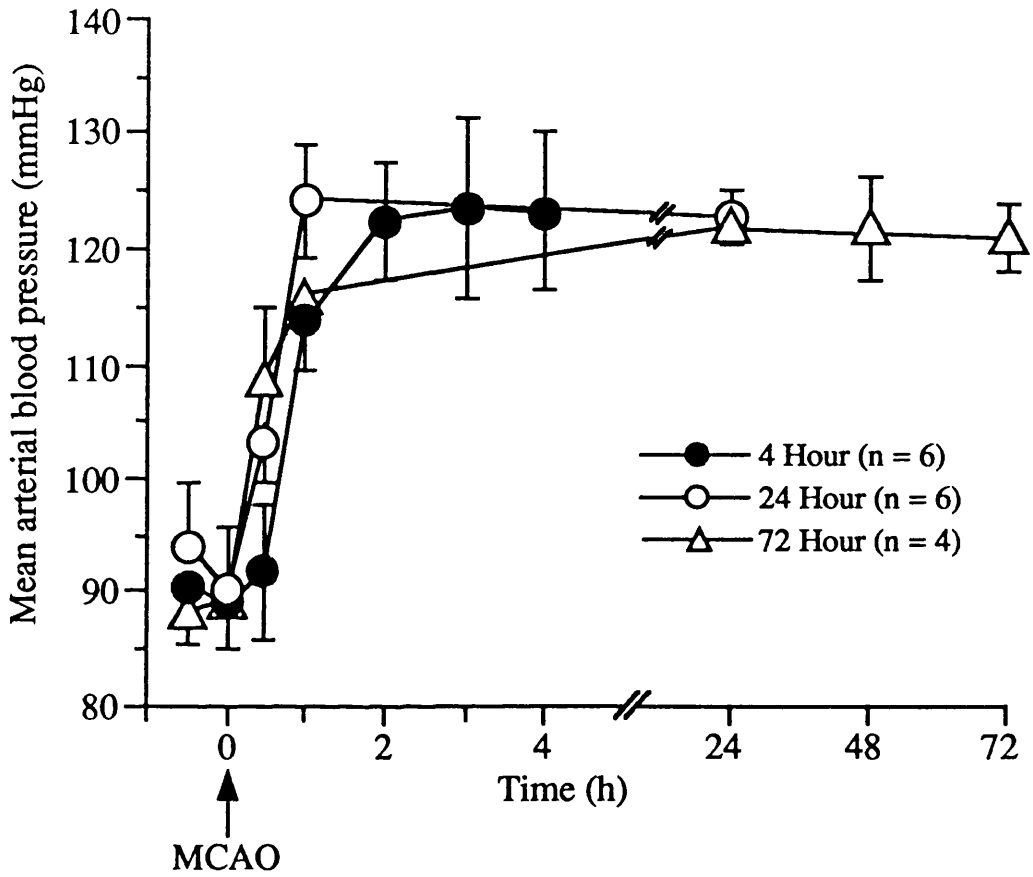

Permanent MCA occlusion (MCAO) was performed under halothane anaesthesia. 10-15 min post-MCA occlusion anaesthetics were withdrawn and the rats allowed to recover consciousness. Rats were reanaesthetised and killed by perfusion fixation 4, 24 or 72 h post-MCA occlusion.

Figure 20 Mean arterial blood pressure following **sham** procedure

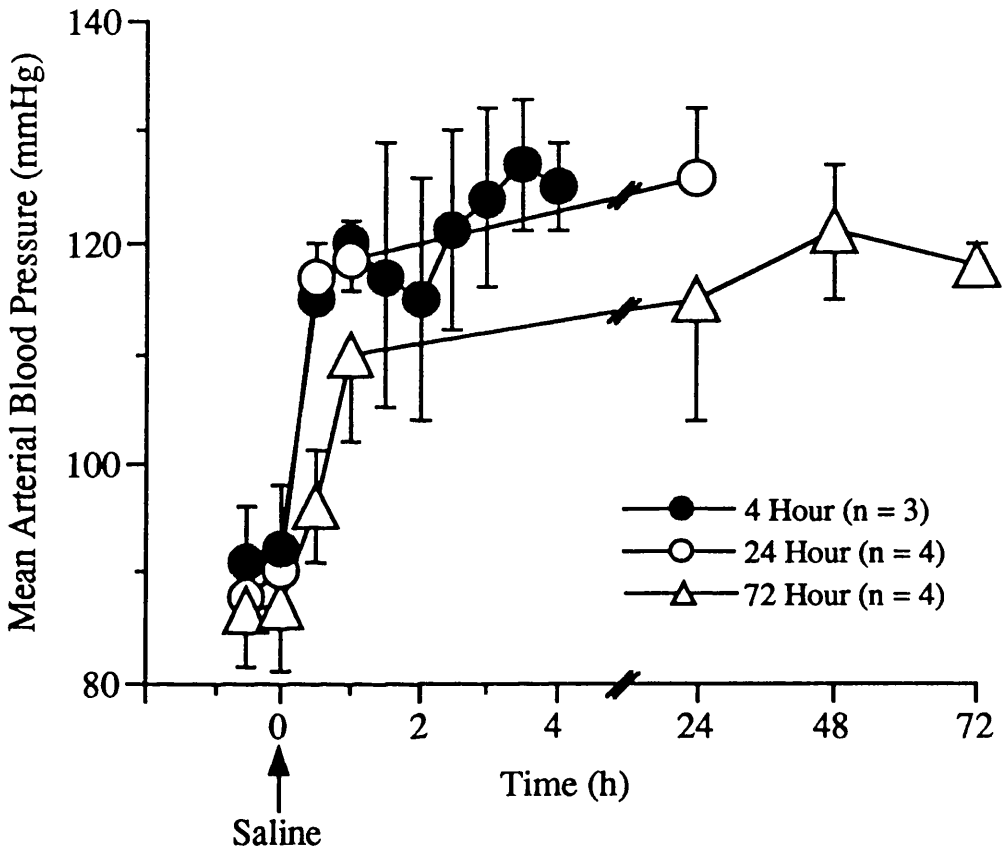

The sham procedure (saline applied to MCA) was performed under halothane anaesthesia. 10-15 min post-saline application anaesthetics were withdrawn and the rats regained consciousness. The animals were reanaesthetised and killed 4, 24 or 72 h post-saline application.

neurological examination was performed. The rats appeared generally apathetic and reluctant to move either spontaneously or in response to touch. A similar response pattern has been reported following selective lesion of the dorsolateral caudate nucleus in humans (Mendez *et al.* 1989). In general symptom severity appeared related to the extent of ischaemic damage so that rats subjected to permanent MCA occlusion were most affected.

4.2.3.3. Evolution of ischaemic damage

Permanent MCA occlusion

Permanent MCA occlusion resulted in a large lesion located predominantly in the frontal, sensorimotor and parietal cortices and the dorsolateral caudate nucleus. The total volume of damage in the 4 h recovery group was 131.1 ± 37.0 mm^3. No further increase in damage was apparent at 24 h or 72 h and there were no significant differences between the volumes of ischaemic damage following permanent MCA occlusion of 4 h, 24 h or 72 h duration for whole hemisphere, cortex or caudate nucleus (see Figure 21). Therefore in this model the volume of ischaemic damage does not increase beyond the 4 h time point. The areas of ischaemic damage at each stereotactic level were also comparable for each time point. Areas of damage following 4 h or 24 h permanent MCA occlusion are shown in Figure 22 (the values for the 72 h group, which were numerically similar to the 4 and 24 h groups, were omitted to improve the clarity of the figure).

Transient MCA occlusion

In contrast to permanent MCA occlusion, the volumes of ischaemic damage in whole hemisphere, cortex and caudate nucleus increased markedly (3 to 4-fold) from 4 h to 24 h post-onset of transient MCA occlusion (see Figure 23). However the volumes of damage at the 72 h time point were smaller than at the 24 h time point, although still increased compared to the volumes of damage 4 h post-onset of transient MCA occlusion. Statistical analysis by one-way ANOVA revealed a significant effect of time on the volumes of ischaemic damage. Subsequent pairwise comparisons showed the volume of damage increased significantly from the 4 h to the 24 h time point. The areas of damage 4 h or 24 h following onset of transient MCA occlusion are shown in Figure 24. These graphs demonstrate that ischaemic damage increased from 4 h to 24 h throughout the rostrocaudal distribution of the MCA territory although the greatest increases were observed in the centre of the lesion.

Figure 21 Evolution of the volume of ischaemic damage following permanent MCA occlusion

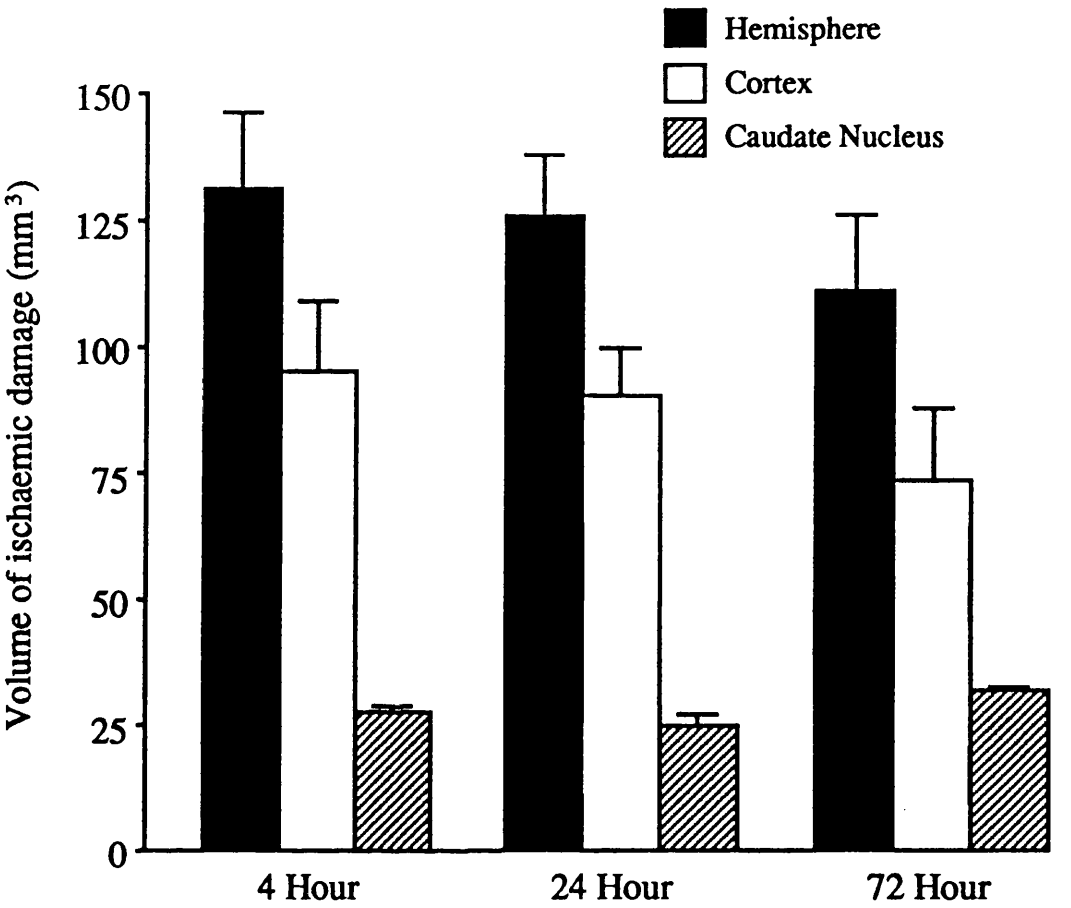

Mean volumes of ischaemic damage in the hemisphere, cerebral cortex and caudate nucleus assessed 4 (n = 6), 24 (n = 6) and 72 (n = 4) h post-permanent MCA occlusion. There were no significant differences between the volumes of damage at any time point ($p > 0.05$, one-way ANOVA).

Figure 22 Evolution of areas of ischaemic damage following **permanent** MCA occlusion

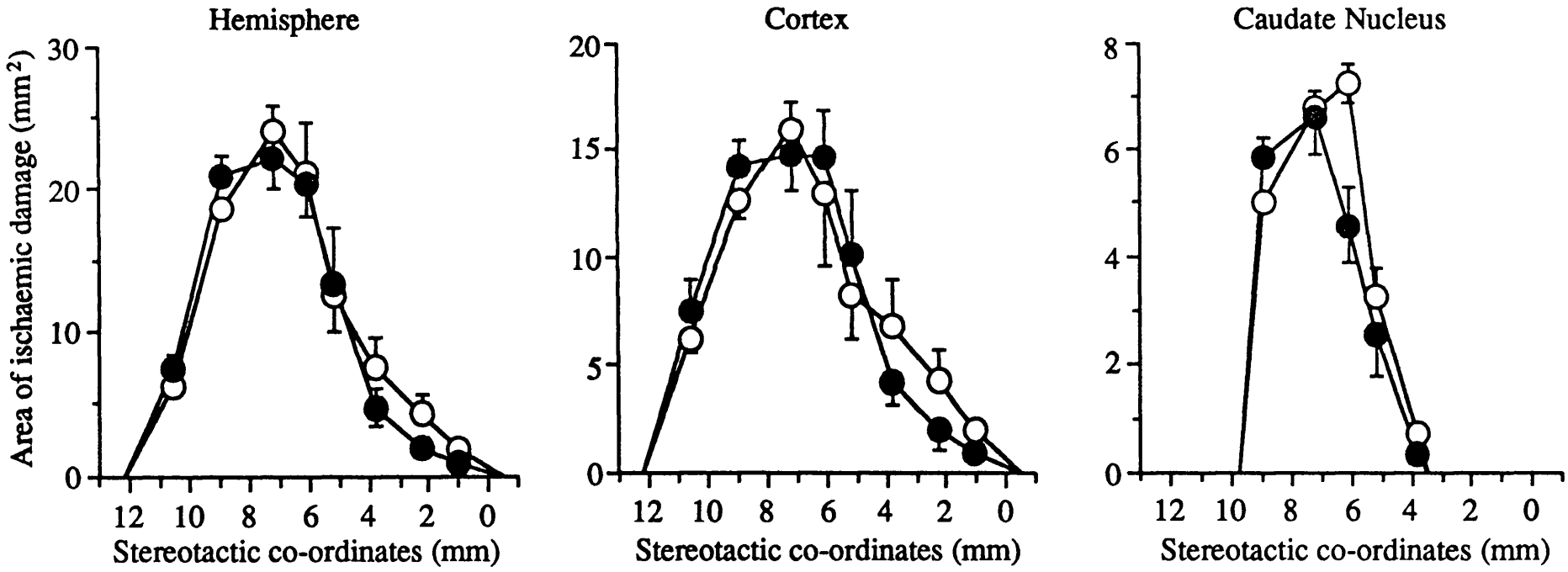

Mean areas of ischaemic damage (mm^2) in the hemisphere, cortex and caudate nucleus assessed 4 h (open symbols, n = 6) and 24 h (filled symbols, n = 6) post-permanent MCA occlusion. The areas of damage at each stereotactic level were comparable between the 2 time points.

Figure 23 Evolution of the volume of ischaemic damage following transient MCA occlusion

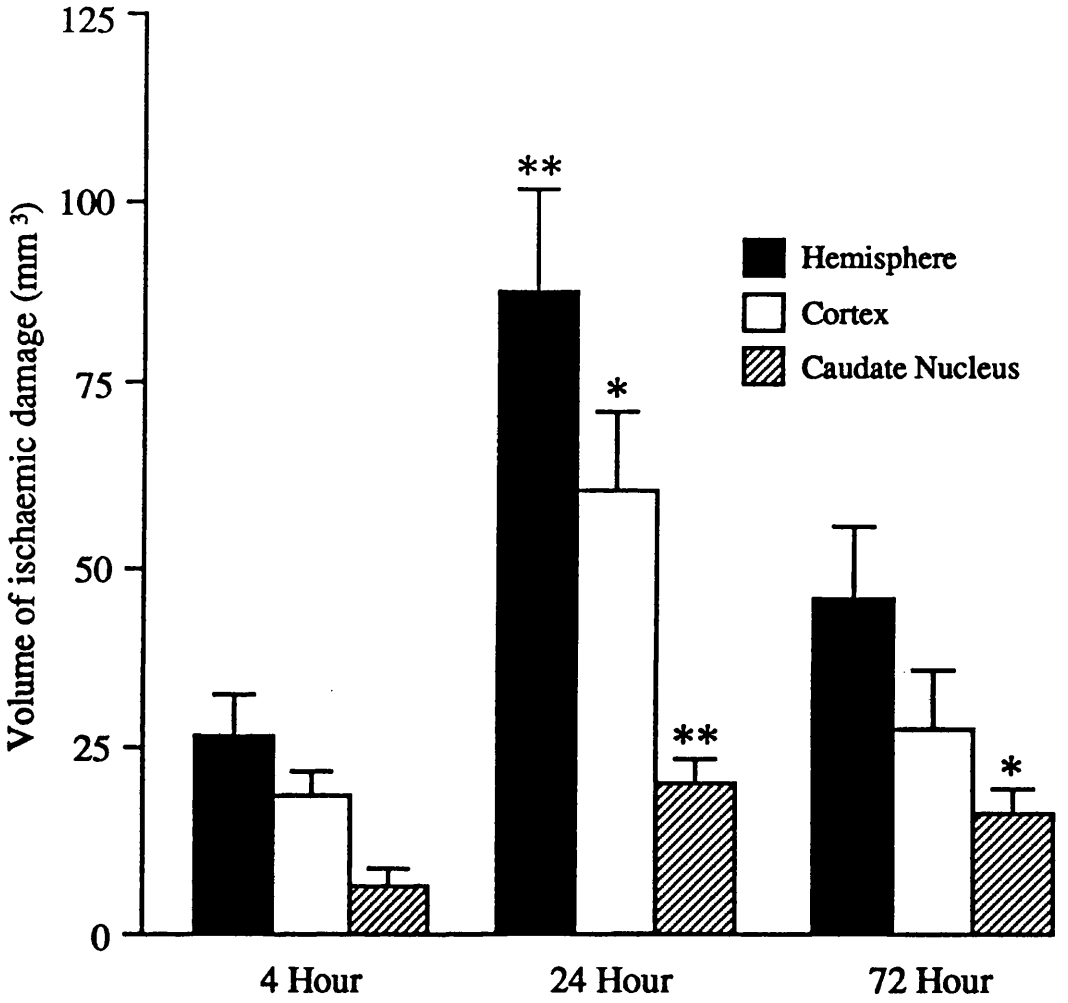

Mean volumes of ischaemic damage in the hemisphere, cerebral cortex and caudate nucleus assessed 4 (n = 10), 24 (n = 9) and 72 (n = 12) h following the onset of transient MCA occlusion. The volumes of damage increased significantly from 4 to 24 h in the hemisphere, cortex and caudate nucleus (one-way ANOVA followed by unpaired Student's t-tests *$p < 0.05$, **$p < 0.01$ compared with 4 h group).

Figure 24 Evolution of areas of ischaemic damage following **transient** MCA occlusion

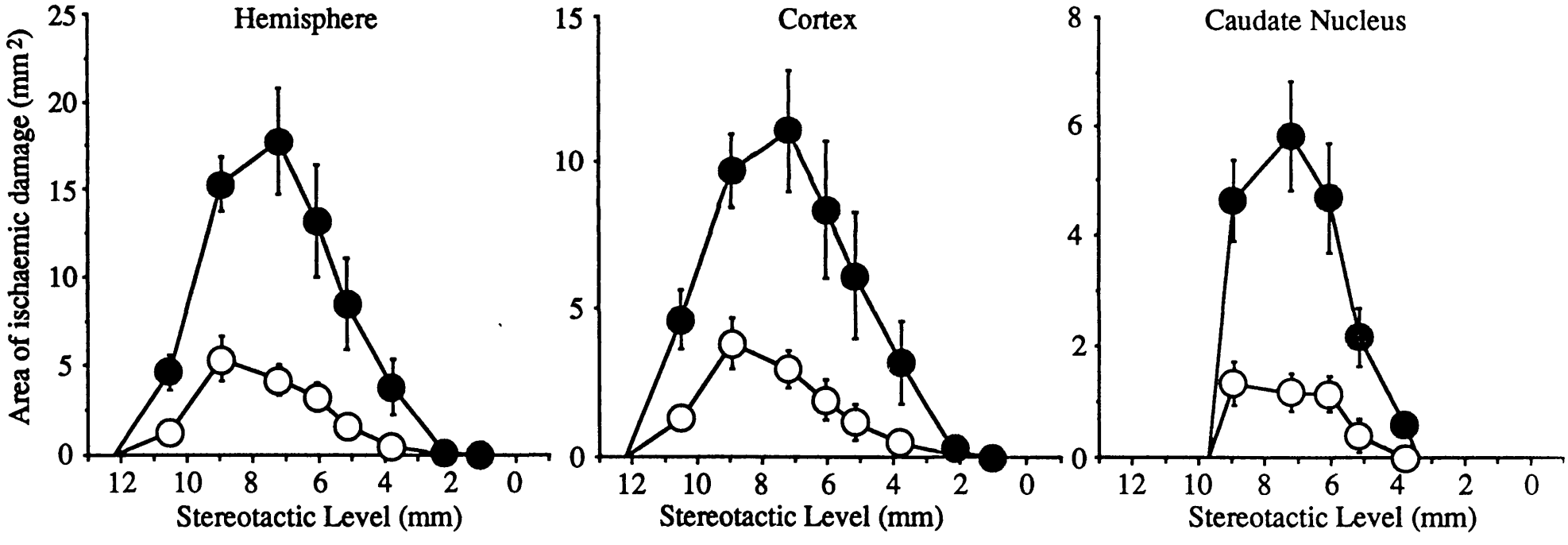

Mean areas of ischaemic damage (mm^2) in the hemisphere, cortex and caudate nucleus assessed 4 h (open symbols, n = 10) and 24 h (filled symbols, n = 9) following the onset of transient MCA occlusion. The areas of damage at 6 of the 8 stereotactic levels were increased in the 24 h group compared to the 4 h group.

Apart from variations in overall size, there were no gross differences between the morphological appearance of lesions following either transient MCA occlusion (4 h and 24 h groups) or permanent MCA occlusion (4 h, 24 h and 72 h groups). In all these animals the lesions exhibited classical ischaemic cell change: shrunken, densely stained cell bodies containing pyknotic nuclei, and spongiform, palely stained neuropil. However the morphological appearance of the lesions in the 72 h transient MCA occlusion group differed in 2 important aspects from all other groups. Firstly pronounced oedema was observed within these brains (despite the fixation procedure), manifested as uniform pallor of the neuropil (which otherwise appeared morphologically normal) surrounding, but outwith, the ischaemic infarct. Secondly in 9 of the 12 animals discrete areas of blood were present, located within the infarct in either the dorsolateral cortex or dorsolateral caudate nucleus (*i.e.* distant from the surgical site). In contrast blood was only observed in 1 of the brains from the 24 h transient MCA occlusion group and in no other animals subjected to either permanent or transient MCA occlusion.

Various physiological factors which have an influence on outcome were examined in an attempt to account for the variability in the results for the 24 h and 72 h time points following transient MCA occlusion. Individual data points were analysed to determine if there was any obvious relationship between blood pressure and/or the degree of initial MCA constriction induced by endothelin-1, and the final volume of ischaemic damage. Rats from the 24 h and 72 h groups were subdivided into those in which endothelin-1 induced only a moderate constriction of the MCA and those in which there was a severe constriction of the artery. Individual volumes of hemispheric damage were then plotted against a) MABP at the time of MCA occlusion and b) MABP 1 h post-MCA occlusion - when blood pressure was increasing following withdrawal of anaesthetics (Figure 25). Firstly these graphs show that, irrespective of blood pressure, there was a tendency for the final volume of ischaemic damage to be greater following a severe constriction in response to endothelin-1 compared to a moderate constriction (mean volumes of damage 73 ± 44 mm^3 and 46 ± 33 mm^3 respectively). Secondly, although the scatterplots revealed no obvious relationship between final lesion volume and MABP at the time of MCA occlusion (anaesthetised MABP, Figure 25a), there was an apparent inverse correlation between blood pressure 1 h post-MCA occlusion (conscious MABP) and final lesion size for rats in which endothelin-1 induced only a moderate constriction (Figure 25b). In these animals higher MABP during recovery resulted in lower volumes of ischaemic damage. No such relationship was apparent for rats with severe MCA constrictions in response to endothelin-1 (Figure 25b).

Figure 25 Transient MCA Occlusion: relationship between ischaemic damage, severity of vasoconstriction and blood pressure.

Scatterplots of individual volumes of hemispheric damage for rats killed 24 h (filled symbols) and 72 h (open symbols) following onset of transient MCA occlusion plotted against individual mean arterial blood pressure (MABP) at a) time of application of endothelin-1 to MCA and b) 1 h post-onset of MCA occlusion. Data is subdivided into moderate (25 % of original diameter) and severe (< 20 % of original diameter) constrictions of the MCA in response to endothelin-1.

There was no obvious relationship between volume of ischaemic damage and MABP at the time of MCA occlusion for either moderate or severe constrictions. In contrast there was a significant inverse correlation between volumes of damage and MABP 1 h post-MCA occlusion for moderate vasoconstriction ($p < 0.01$, Pearson product moment correlation), but no significant relationship for severe vasoconstriction. The dotted lines on the graphs represent lines of best fit calculated by least squares regression analysis.

Figure 25 Transient MCA occlusion: relationships between ischaemic damage, severity of vasoconstriction and blood pressure

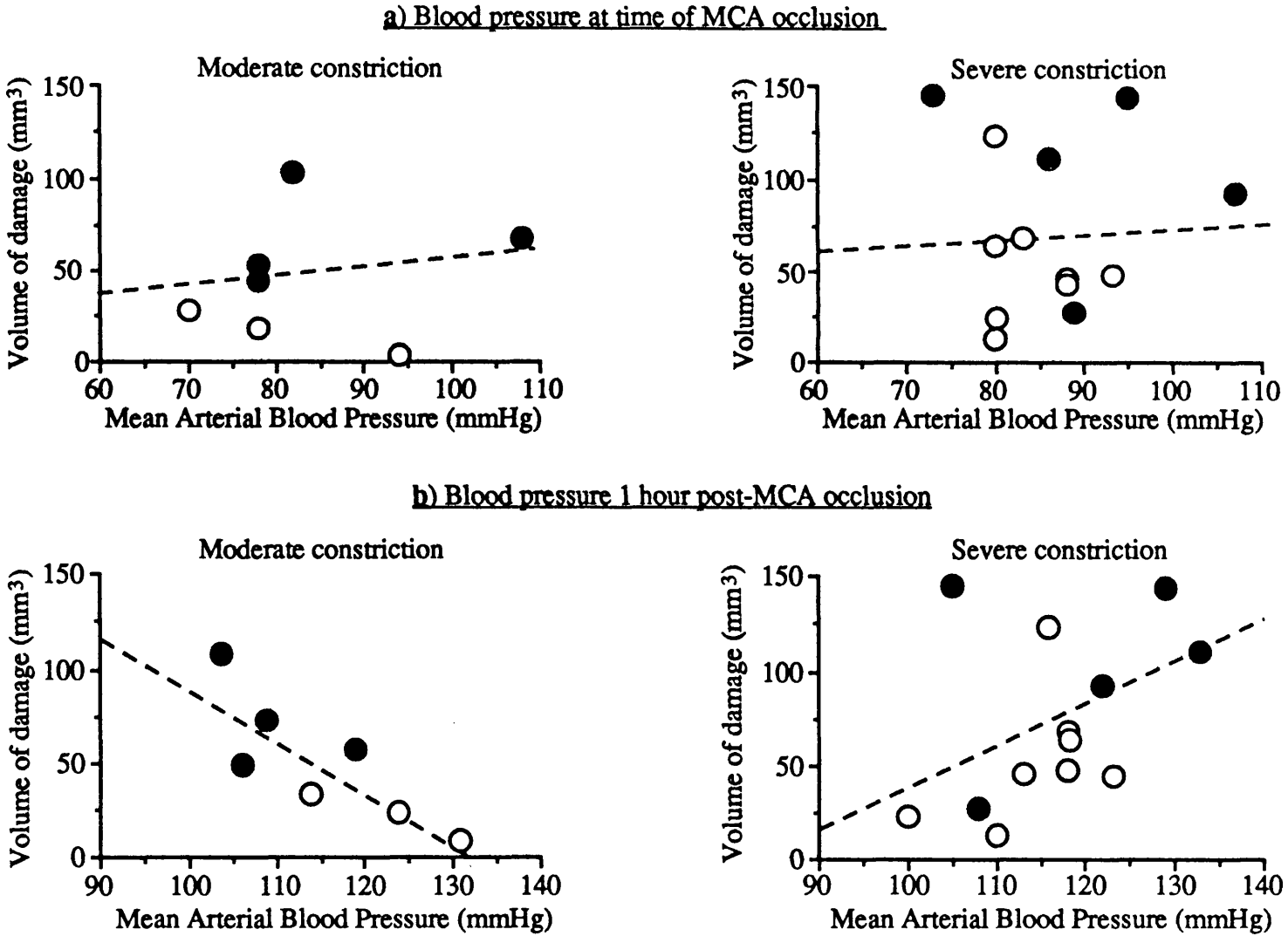

Sham procedure

The sham procedure (saline applied to the MCA) resulted in a very small region of ischaemic damage in less than 40% of the animals located in the cerebral cortex ventral to the rhinal fissure and corresponding to the site of craniectomy. The remainder of the rats showed no ischaemic damage at all. The total volumes of ischaemic damage at the 4 h, 24 h and 72 h time points following sham occlusion were 0 ± 0 mm^3, 0.55 ± 1.1 mm^3 and 1.2 ± 0.85 mm^3 respectively.

4.3. Effect of recovery from anaesthesia on acute outcome following transient and permanent MCA occlusion

4.3.1. Introduction

Comparison of the volumes of ischaemic damage 4 h following transient MCA occlusion revealed the volume of damage was greater for the group maintained under anaesthesia compared to the group allowed to recover consciousness following surgery. This result suggests that some factor associated with the maintenance or withdrawal of anaesthetics directly influences lesion size. Data from the 4 h anaesthetised and recovery groups (for both transient and permanent MCA occlusion) were therefore compared in more detail to further assess the relationship between lesion size and recovery from anaesthesia.

4.3.2. Results

4.3.2.1. Effect of anaesthetic withdrawal on blood pressure

Mean arterial blood pressures at the time of MCA occlusion (when all rats were anaesthetised) were comparable between groups being 91 ± 8 mmHg and 89 ± 4 mmHg for permanent MCA occlusion, anaesthetised and recovery groups respectively and 86 ± 3 mmHg and 84 ± 4 mmHg for transient MCA occlusion, anaesthetised and recovery groups respectively. In the anaesthetised groups MABP remained relatively stable throughout the experimental period (see Figure 26 and 27), while in the recovery groups MABP increased rapidly following withdrawal of anaesthetics. In these groups MABP returned to the normal range for the conscious rat within 1 to 1.5 h of anaesthetic withdrawal. Blood pressure was then well maintained throughout the remainder of the survival period. 4 h post-MCA occlusion the MABP in the recovery groups was 35 mmHg and 45 mmHg higher than the corresponding anaesthetised groups, for permanent and transient MCA occlusion respectively.

Figure 26 Effect of anaesthetic withdrawal on blood pressure following permanent MCA occlusion

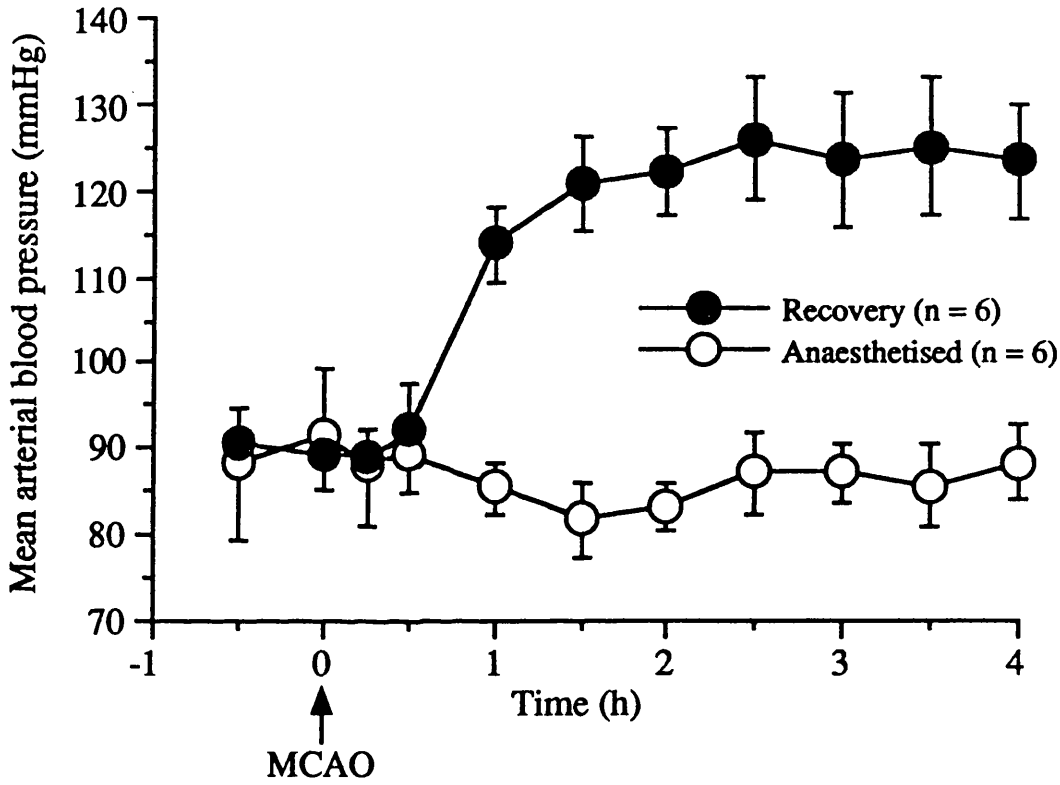

Mean arterial blood pressure pre- and post-permanent MCA occlusion (MCAO) of 4 h duration. Blood pressure for the group maintained under halothane anaesthesia remained relatively stable throughout. In contrast, following withdrawal of anaesthetics (approximately 10-15 min post-MCA occlusion), blood pressure in the recovery group rapidly returned to the normal range for the conscious rat.

Figure 27 Effect of anaesthetic withdrawal on blood pressure following transient MCA occlusion

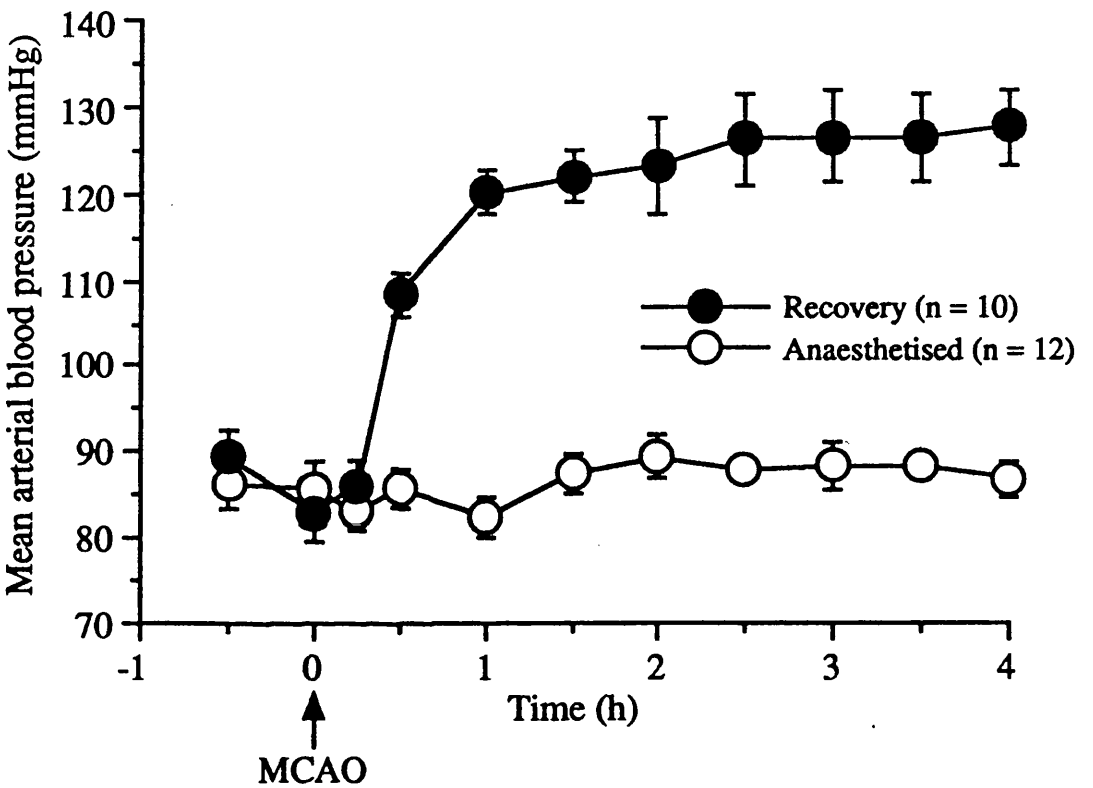

Mean arterial blood pressure pre- and 4 h post-transient MCA occlusion (MCAO). Blood pressure for the group maintained under halothane anaesthesia remained relatively stable, while blood pressure in the recovery group rapidly increased following withdrawal of anaesthetics (approximately 10-15 min post-MCA occlusion).

4.3.2.2. Effect of anaesthetic withdrawal on ischaemic damage

The volumes of ischaemic damage following permanent and transient MCA occlusion of 4 h duration are illustrated in Figure 28 and 29. For permanent MCA occlusion the volumes of ischaemic damage for whole hemisphere, cortex and caudate nucleus were not significantly different between the anaesthetised and recovery groups (Figure 28). In contrast following transient MCA occlusion the total volume of ischaemic damage in the recovery group was reduced by 52% compared to the anaesthetised group (Figure 29). The reduction in volume of ischaemic damage reached significance ($p<0.05$) for the whole hemisphere and caudate nucleus, but not the cerebral cortex.

The areas of hemispheric ischaemic damage in anaesthetised and recovery groups following permanent MCA occlusion were similar at each stereotactic level (Figure 30). In contrast the greater volume of ischaemic damage in the anaesthetised group compared to the recovery group following transient MCA occlusion was reflected in higher mean areas of hemispheric damage, particularly in the centre of the lesion (Figure 31).

Figure 28 Effect of anaesthetic withdrawal on volumes of ischaemic damage following **permanent** MCA occlusion

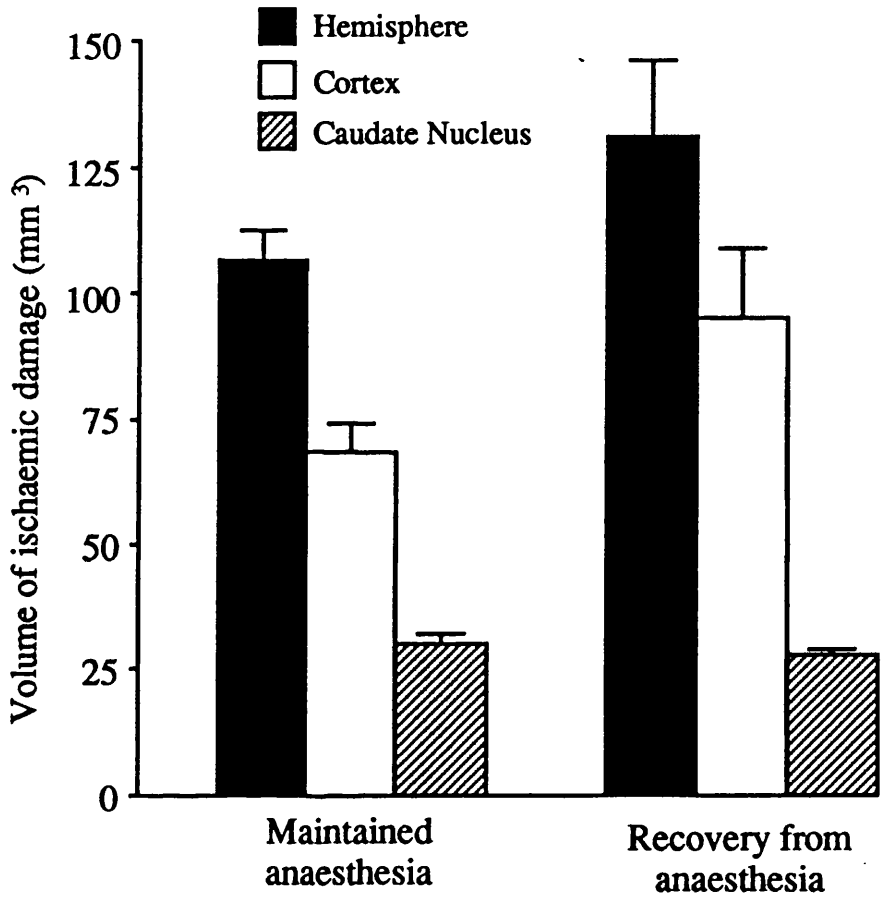

Mean volumes of ischaemic damage (mm^3) in the hemisphere, cerebral cortex and caudate nucleus following permanent MCA occlusion of 4 h duration. The volumes of damage were not significantly different between the anaesthetised (n = 6) and recovery (n = 6) groups ($p > 0.05$ unpaired Student's t-tests).

Figure 29 Effect of anaesthetic withdrawal on volumes of ischaemic damage following **transient** MCA occlusion

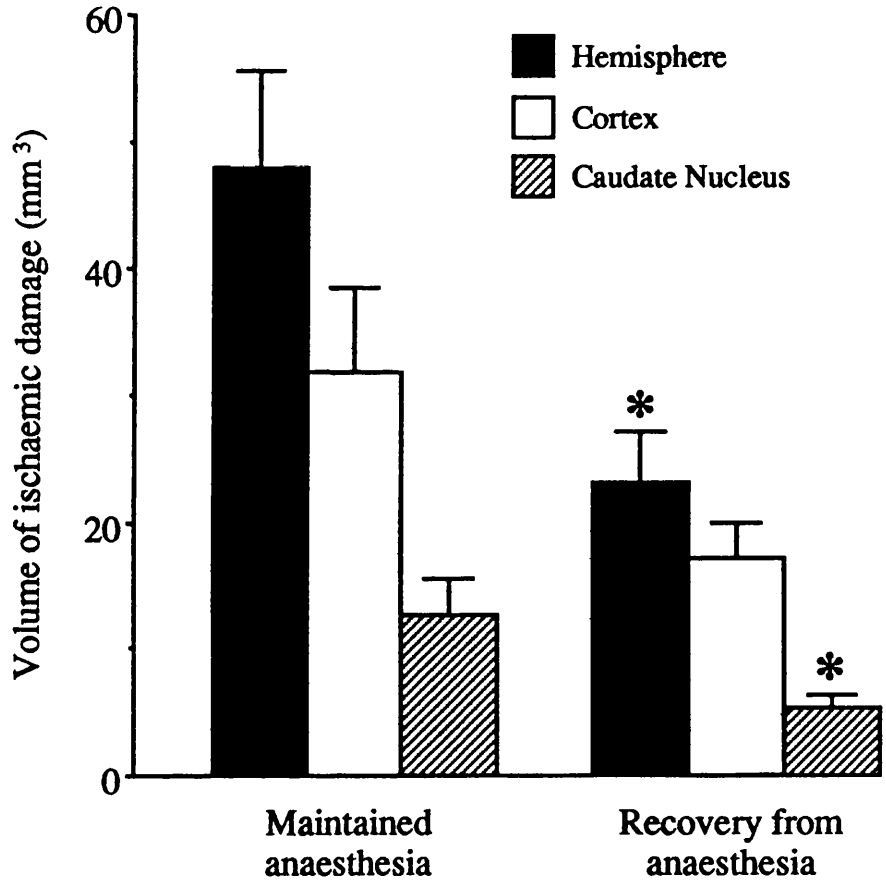

Mean volumes of ischaemic damage (mm^3) in the hemisphere, cerebral cortex and caudate nucleus measured 4 h following the onset of transient MCA occlusion. The volumes of damage were significantly reduced in the recovery group (n = 10) compared with the group maintained under halothane anaesthesia (n = 12). *$p < 0.05$ unpaired Student's t-tests.

Figure 30 Effect of anaesthetic withdrawal on areas of ischaemic damage following **permanent** MCA occlusion

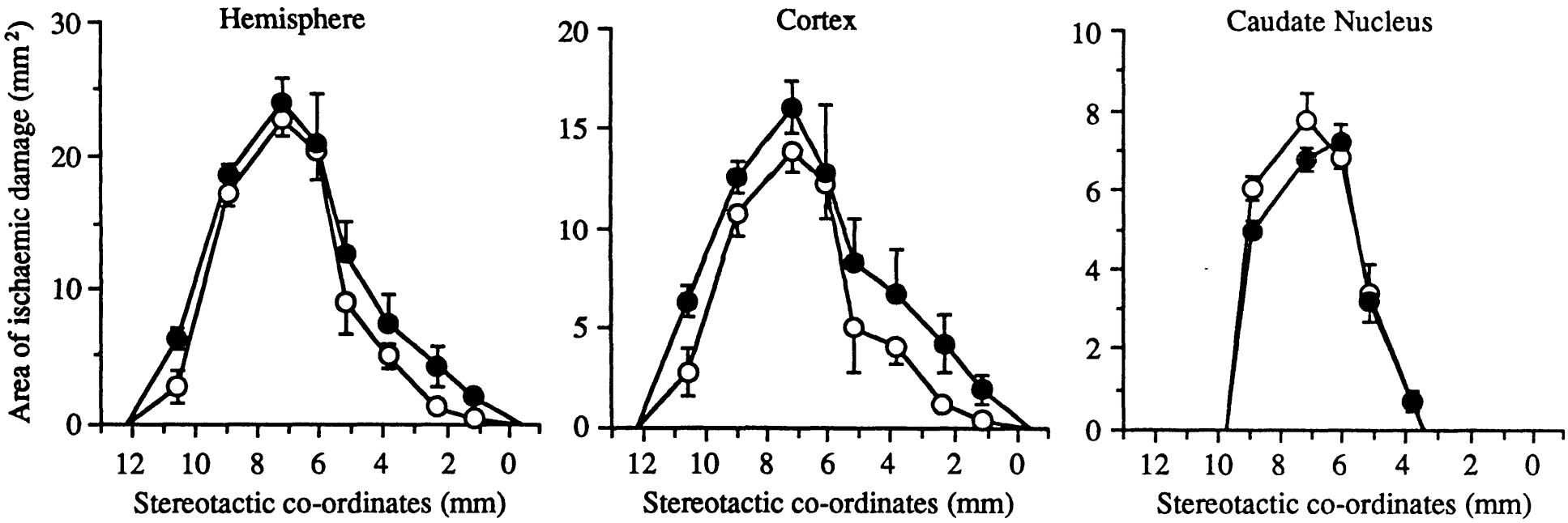

Mean areas of ischaemic damage (mm^2) in the hemisphere, cortex and caudate nucleus following permanent MCA occlusion of 4 h duration. The areas of damage at each stereotactic level were comparable between the anaesthetised (open symbols, n = 6) and recovery (filled symbols, n = 6) groups.

Figure 31 Effect of anaesthetic withdrawal on areas of ischaemic damage following **transient** MCA occlusion

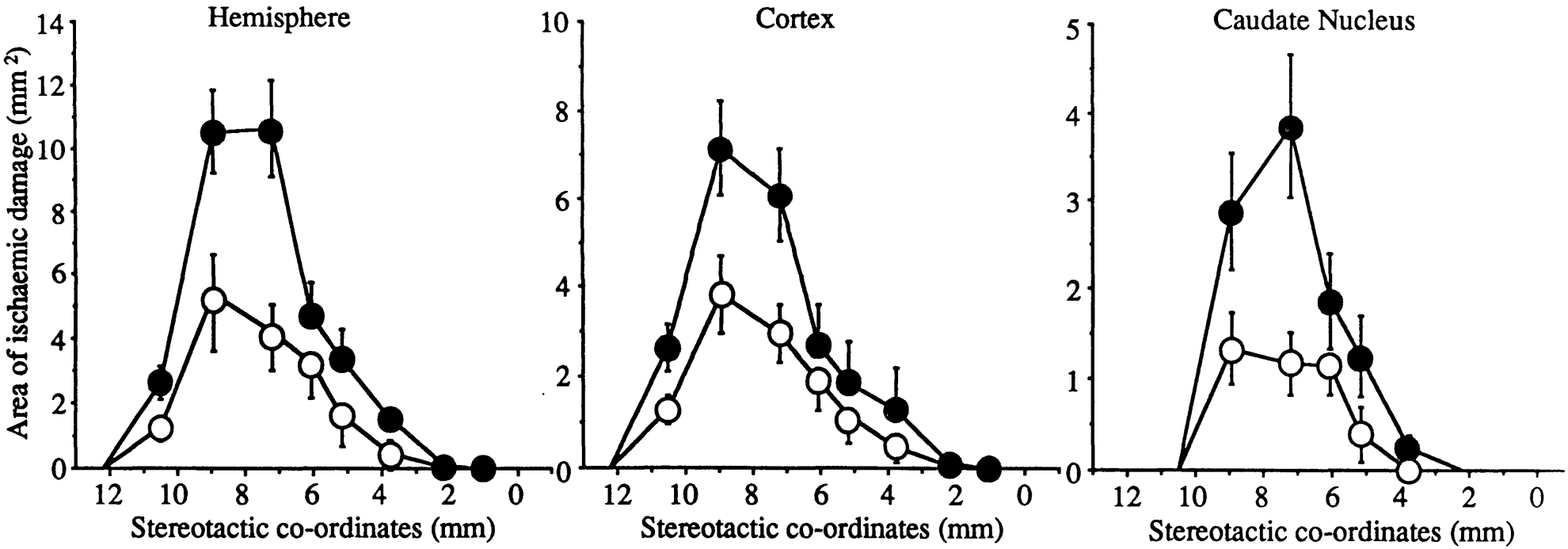

Mean areas of ischaemic damage (mm^2) in the hemisphere, cortex and caudate nucleus 4 h following the onset of transient MCA occlusion. The areas of damage in the anaesthetised group (filled symbols, n = 12) were greater than the recovery group (open symbols, n = 10) for 6 of the 8 stereotactic levels. A similar pattern of increased areas of damage was observed when comparing the 24 h and 4 h recovery groups from the time course study (see Figure 23).

4.4. Discussion

4.4.1. Evolution of ischaemic damage

The results of the time course study show that following *permanent* MCA occlusion, the volume of ischaemic damage remains relatively constant between 4 h and 72 h. This volume of damage does not necessarily represent the absolute maximum amount of tissue that can be recruited to the lesion following permanent MCA occlusion because manipulation of several physiological parameters can influence lesion size *e.g.* transient hypotension further increases the volume of ischaemic damage in this model (Osborne *et al.* 1987). However, under the physiological conditions used in the present study, it can be concluded that the volume of ischaemic damage is already maximal 4 h post-permanent MCA occlusion. In contrast following *transient* MCA occlusion the volume of damage significantly increased from 4 h to 24 h demonstrating that in this model pathological processes are continuing following the onset of reperfusion.

Permanent MCA occlusion

Several studies have purported to evaluate the development of ischaemic damage following permanent MCA occlusion in the rat (Garcia *et al.* 1993; Hakim *et al.* 1992; Nedergaard 1987; Persson *et al.* 1989) but the strength of the conclusions of these studies (with regards to this point only) is questionable due to problems of methodology. Firstly, investigations of the change in volume of ischaemic damage over time should use a method of quantification that compensates for the contribution of oedema to total infarct volume. Direct measurement of infarct volume (*e.g.* from the area of pallor on TTC or cresyl violet stained sections) will include a component of tissue swelling due to brain oedema that can overestimate infarct volume by 20% (Brint *et al.* 1988; Lin *et al.* 1993). Brain oedema (assessed by hemispheric water content) increases progressively after the onset of permanent MCA occlusion reaching its maximum level at 3 days (Gotoh *et al.* 1985). This time course differs from the temporal evolution of ischaemic damage so that apparent fluctuations in infarct volume (measured directly from stained sections) can be the direct result of variations in oedema content of the tissue (Lin *et al.* 1993). The method of quantification used in the present study addresses this problem by measuring the areas of damage from scale drawings rather than directly from the sections so that the confounding influence of tissue swelling is avoided. Secondly, studies of the temporal evolution of ischaemic damage that only analyse selected sections at the centre of the infarct (Garcia *et al.* 1993; Hakim *et al.* 1992) may incompletely characterise the lesion and over- or underestimate changes in total lesion volume. Previous studies have shown that a minimum of 8 stereotactic levels must be analysed to give an accurate asssessment of total

lesion volume (Duverger & Mackenzie 1988; Osborne *et al.* 1987) and therefore this was the number of levels used in the present study.

Persson *et al.* 1989 have reported that infarct area does not reach maximal size until 18 h to 2 days following permanent MCA occlusion. The lesion was then constant until day 7 when a progressive reduction in size was observed due to resorption of oedema and tissue atrophy. However given the small group size (n = 3) and wide time-scale (1 h - 8 h) of the only group of animals killed earlier than 18 h post-MCA occlusion no real conclusions can be drawn from this study concerning the early evolution of ischaemic damage. Nedergaard (1987) found that infarction was clearly demarcated only in the striatum at 4 h and was not obvious in the cortex until 24 h post-MCA occlusion. However this report was primarily directed towards studying selective neuronal necrosis outwith the borders of the main infarct and no real attempt was made to quantify temporal changes in infarct size.

Hakim *et al.* 1992 reported that the area of damage increased in size from 4 to 24 h post-MCA occlusion, but the method of assessing ischaemic damage used in this study - area of pallor on cresyl violet stained sections - can only detect 'frank infarction'. This method is therefore much less sensitive than the morphological assessment used to delineate ischaemic damage in the present study and may have failed to detect early evidence of necrosis. Finally Garcia *et al.* 1993 found the area of ischaemic damage (expressed as percentage of ipsilateral hemispheric area) did not change markedly from 3 to 48 h post-MCA occlusion. In this study there was a late increase in lesion size apparent at 72 h and 96 h that may have reflected changes in hemispheric area due to alterations in oedema content.

In summary none of these published studies was particularly well suited for volumetric assessment of the temporal changes in ischaemic damage following permanent MCA occlusion. However our results have received confirmation from the work of Gill 1992 who has shown, using a similar system of quantitative analysis to our own, that following permanent MCA occlusion the lesion volume is maximal at 4 h and 'the size of the lesion does not change between 4 h and 7 days' (Gill 1992).

Transient MCA occlusion

The majority of studies of the temporal evolution of ischaemic damage following transient focal ischaemia have approached the problem by varying the duration of the initial ischaemic insult and keeping the kill time constant. This approach is directed towards assessing the therapeutic time window in which re-establishment of CBF may be beneficial to patient outcome by salvaging tissue otherwise destined to die. However we were interested in the more fundamental question of whether lesion size increases with time following a period of transient focal ischaemia. Therefore we kept the procedure for induction of ischaemia constant and looked at outcome following increasing periods of reperfusion. We found that the volume of ischaemic damage continued to increase from 4 to 24 h in the endothelin-1 model of transient focal ischaemia. In this model restoration of CBF begins before the 4 h time point (Macrae *et al.* 1993 and see Section 3.3.). Thus the volume of damage is increasing during the reperfusion phase. This result suggests, but can not prove, that secondary mechanisms occuring within the reperfusion phase are contributing to the maturation of lesion size. In the 72 h group the lesion size was smaller, although still numerically greater than at the 4 h time point. Examination of the physiological data revealed no obvious explanation for the difference in lesion size between the 24 h and 72 h groups since blood gases, plasma glucose, body temperature and MABP were similar for both groups (see Table 5 and Figure 18). From studies of permanent MCA occlusion it is known that resorption of the lesion does not become apparent until 7 days post-ischaemia (Persson *et al.* 1989). Thus 72 h is probably too early a time point for actual resorption of the lesion to be occuring and the apparent reduction in lesion size may merely reflect the inherent variability present in this, and indeed all, models of transient focal ischaemia (Macrae 1992 and see Section 8.1.). Despite the fact that mean lesion volume was smaller at 72 h compared to 24 h there was qualitative evidence from the morphological appearance of these lesions that reperfusion injury was continuing from 24 h to 72 h post-transient MCA occlusion. The pronounced oedema in the 72 h group together with the appearance of blood within a substantial proportion of the infarcts, suggestive of haemorrhagic transformation, points to secondary vascular damage occuring late within the reperfusion phase that may be further evidence of reperfusion injury within this model.

To the best of our knowledge there is only one published study directly comparable to the present work in which the period of ischaemia (90 min MCA occlusion (ligature) in tandem with bilateral carotid occlusion (clips)) was kept constant while the reperfusion period was increased (Lin *et al.* 1993). In this study the volume of ischaemic damage (corrected for influence of oedema) did not change with periods of reperfusion of 6, 24, and 72 h, while oedema (assessed as hemispheric water content) increased from 6 to 24 h reperfusion and then subsequently decreased. This result may at first appear to contradict our study in

which the volume of ischaemic damage increased from 4 to 24 h post-MCA occlusion. However our results suggest that the volume of damage reaches its maximal level at some unspecified time between 4 and 24 h post-MCA occlusion which compares well with Lin *et al.* whose earliest time point was 7.5 h post-onset of ischaemia.

In studies where the duration of the initial ischaemia is varied, the final volume of ischaemic damage, as would be expected, is proportional to the length of the ischaemic insult. Studies utilising models of distal MCA occlusion together with unilateral or bilateral carotid artery occlusion have found that the volume of ischaemic damage increases progressively with periods of MCA occlusion from 1 to 3 h duration when outcome is assessed at 24 h (Buchan *et al.* 1992b; Kaplan *et al.* 1991) or 7 days (Hiramatsu *et al.* 1993) post-onset of ischaemia. The volume of damage is maximal after 3-4 h of transient MCA occlusion (with 21-20 h reperfusion), at which point it is equivalent to the volume of damage following 24 h permanent MCA occlusion (Buchan *et al.* 1992b; Kaplan *et al.* 1991). Oedema formation (assessed by the difference in hemispheric volumes) also increases with increased duration of ischaemia (Hiramatsu *et al.* 1993) being equivalent to that observed with 24 h permanent MCA occlusion after 3 h of transient ischaemia (plus 21 h reperfusion) (Kaplan *et al.* 1991). In a study using Koizumi's intraluminal thread technique the volume of ischaemic damage was found to increase with increasing lengths of ischaemia of up to 2 h duration (plus 7 days reperfusion) at which point lesion size was comparable to that for 24 h permanent MCA occlusion (Memezawa *et al.* 1992b). The shorter time frame in this model (2 h versus 3-4 h for extravascular occlusion models) probably reflects the 'massive brain edema' that results in very high mortality rates for rats subjected to ischaemic intervals of 90 min or longer (Memezawa *et al.* 1992b).

4.4.2. Factors influencing outcome in the endothelin-1 model of transient focal ischaemia

Analysis of the individual data from the transient ischaemia time course study revealed 2 important factors that can influence *final* lesion volume in this model. Firstly, the degree of vasoconstriction induced by endothelin-1 influenced lesion size with severe vasoconstriction of the MCA tending to be associated with larger lesions than moderate vasoconstriction. If it is assumed that the degree of ischaemia induced by endothelin-1 is proportional to the severity of the observed vasoconstriction then this result suggests that the severity of the initial ischaemic insult can directly influence final lesion volume. Similarly, in a cat model of transient MCA occlusion the extent of cortical damage was found to be directly related to the degree of reduction in CBF during the ischaemic period (Tamura *et al.* 1980). Secondly, the MABP 1 h following application of endothelin-1 to the MCA was found to be inversely related to lesion volume in rats with a moderate initial

ischaemia. The increase in arterial blood pressure following withdrawal of anaesthetics in these experiments occurs at approximately the same time as the vasoconstrictive action of endothelin-1 is beginning to wane and CBF in the ischaemic region is recovering (Macrae *et al.* 1993). Thus increased MABP at this time may help to re-open the previously constricted artery and improve the quality of reperfusion of the MCA territory. Following a moderate ischaemic insult the net effect of improved reperfusion appears beneficial and reduces the volume of ischaemic damage. However following severe vasoconstriction no such relationship was apparent, suggesting that either reperfusion is not improved by this level of hypertension or that improved reperfusion is not beneficial to outcome following a severe ischaemic insult.

4.4.3. Effect of recovery from anaesthesia on acute outcome following transient and permanent MCA occlusion

Comparison of the volumes of ischaemic damage at the 4 h time point showed that recovery from anaesthesia, concomitant with an increase in MABP of 35-45 mmHg, did not improve *acute* outcome following permanent MCA occlusion but was of benefit in the endothelin-1 model of transient MCA occlusion.

In the context of permanent focal ischaemia hypertension has been proposed as a possible treatment strategy to increase collateral perfusion of the ischaemic region (Yatsu 1982). Phenylephrine-induced hypertension (30-35 mmHg) has been demonstrated to improve cerebral blood flow via the collateral circulation 15 min following permanent MCA occlusion in normotensive rats (Drummond *et al.* 1989). However increasing the hydrostatic pressure gradient to a region where the cerebrovasculature is already compromised by ischaemic damage carries the risks of increased oedema formation (Hatashita & Hoff 1986) and haemorrhagic transformation of the infarct (Olsen 1983). In the present study, despite the elevated MABP in the recovery group, the volumes of ischaemic damage following permanent MCA occlusion did not differ significantly between the anaesthetised and recovery groups. In fact there was a trend for the volume of ischaemic damage to be greater in the recovery group (volumes of hemispheric damage 131 $\pm$ 15 vs 107 $\pm$ 5 mm^3 for recovery and anaesthetised groups respectively) suggesting that the continued presence of halothane anaesthesia may be neuroprotective and that removal of anaesthesia opposes any beneficial effect of the resultant rise in blood pressure. This result is in contrast to Drummond's group who have found, using a different model of permanent MCA occlusion, that hypertension instituted immediately following MCA occlusion, or delayed in onset for 2 hours, significantly reduces the area of ischaemic damage (measured by TTC staining) 4 h post-MCA occlusion in the SHR (Patel *et al.* 1991b). There are 2

possible explanations for this apparent discrepancy. Firstly in the Drummond study rats were maintained under isoflurane anaesthesia while blood pressure was increased with phenylephrine. In our study anaesthesia was withdrawn resulting in a spontaneous rise in blood pressure. Thus the confounding influence of isoflurane anaesthesia, which itself may be neuroprotective, makes direct comparison between the 2 studies difficult. Secondly, the method of inducing MCA occlusion (2 separate ligatures) may have improved the possibility of collateral supply to the ischaemic region compared to the more complete occlusion used in our permanent ischaemia model.

With regards to transient MCA occlusion, phenylephrine-induced hypertension (30 mmHg) initiated during the reperfusion phase following 2 h MCA occlusion (ligatures) in SHR, also improves CBF in the MCA territory (Cole *et al.* 1992) and reduces the area of ischaemic damage following 2 h of reperfusion without aggravation of oedema formation (Patel *et al.* 1991a). These results agree with the present findings where a relative increase in blood pressure reduced the volume of ischaemic damage following transient MCA occlusion. However differences in the mechanism of inducing hypertension, as for permanent MCA occlusion, probably precludes direct comparison of the 2 studies. Drummond's group attribute the beneficial effect of hypertension to reopening of collapsed vessels in the microvasculature thereby improving the quality of reperfusion. It may be however that their method of inducing MCA occlusion (by ligatures) provoked mechanical damage to the MCA so that an increase in intraluminal hydrostatic pressure (induced by the hypertension) was necessary to regain adequate reperfusion through the main MCA itself, and this was the reason for the observed beneficial effect of hypertension. It is interesting to note that the same group have found hypertension induced at the onset of reperfusion following a longer period of ischaemia (3 h) was associated with an increase in blood-brain barrier permeability and hence aggravated oedema formation (Cole *et al.* 1991).

In the present study the rise in blood pressure began within 15 min of endothelin-1 application. Therefore the increase in arterial pressure may have reduced the volume of ischaemic damage by increasing the intraluminal pressure within the MCA, firstly opposing the vasoconstriction induced by endothelin-1 and secondly improving the quality of reperfusion either through the previously constricted MCA and/or by reopening collapsed capillaries. Future studies aimed at measuring local CBF at early and late time points following withdrawal of anaesthetics post-MCA occlusion could address this issue.

In this discussion it has been assumed that the difference in volumes of ischaemic damage between the anaesthetised and recovery groups following transient MCA occlusion is a result of the difference in blood pressure between the 2 groups. An alternative explanation is that continued halothane anaesthesia is detrimental to outcome compared with rats from

which halothane is withdrawn. This explanation appears unlikely since halothane anaesthesia maintained during the ischaemic phase of transient global (Baughman *et al.* 1988) or transient focal (Warner *et al.* 1993) ischaemia markedly reduces neuronal damage compared to nitrous oxide or 'awake' controls.

Combining the information gained from the acute (4 h) study and the time course study it appears that increased blood pressure (and therefore it is proposed improved reperfusion) is beneficial to outcome when volumes of damage are assessed at a relatively early time point (4 h) following transient MCA occlusion when the ischaemic phase is the major contributor to lesion size. However at later time points, when the reperfusion phase may also be contributing to maturation of the lesion (as evidenced by the marked increase in volume of ischaemic damage from 4 h to 24 h), improved reperfusion may not be beneficial to outcome (providing the initial ischaemic insult was relatively severe). Thus secondary pathological mechanisms associated with improved early reperfusion (*e.g.* increased free radical production) may be the causative factor leading to the delayed increase in damage observed at the 24 h time point.

5. ALTERATIONS IN FORSKOLIN AND D_1 RECEPTOR BINDING FOLLOWING PERMANENT FOCAL AND GLOBAL CEREBRAL ISCHAEMIA IN THE RAT

5.1. Forskolin and D_1 receptor binding following permanent focal cerebral ischaemia, and relationship with cerebral blood flow

5.1.1. Introduction

Post-ischaemic alterations in second messenger systems have been widely studied using models of global ischaemia (*e.g.* Daval *et al.* 1989; Onodera & Kogure 1989), in contrast there is a paucity of data available for focal ischaemia. This study was therefore designed to assess the effects of focal reductions in CBF (induced by permanent MCA occlusion) on the adenylate cyclase second messenger system utilising *in vitro* autoradiographical techniques and the ligands [^{3}H]forskolin (to map adenylate cyclase) and [^{3}H]SCH23390 (to map D_1 dopamine receptors that are coupled to adenylate cyclase via a stimulatory G protein). Ligand binding was assessed at 2 time points following MCA occlusion to determine whether significant alterations in binding could be detected at an earlier time point than irreversible damage to neurones: 1) 2 h - *i.e.* before the border between normal and abnormal tissue can be reliably defined using standard histopathological techniques and 2) 24 h - when gross infarction is present.

The changes in local CBF following permanent MCA occlusion are well characterised (Tamura *et al.* 1981b; Bolander *et al.* 1989). In these models the continued presence of collateral blood supply maintains a range of blood flows (Hakim *et al.* 1992) that is in contrast to the uniform severity of a global ischaemic insult. This range of flows gives the opportunity to study the relationship between CBF and alterations in binding sites in more detail. To do this, in the present study *in vivo* autoradiographical determination of local CBF 2 h post-MCA occlusion was combined with *in vitro* autoradiography to obtain measurements of CBF and ligand binding within the same animals.

5.1.2. Experimental protocol

Rats underwent permanent MCA occlusion of 2 or 24 h duration. The general surgical preparation and induction of MCA occlusion were as described in Sections 2.2. and 2.3.1., with the exception that the femoral artery was not cannulated in the 24 h survival group. Local CBF was measured immediately prior to sacrifice in the 2 h group using a 30 s ramped infusion of [^{14}C]IAP as described in Section 2.4.2.1. The brains were then

rapidly removed, frozen in isopentane (-42°C) and sectioned in a cryostat. Consecutive sections (20 μm) were taken for [^{3}H]forskolin binding, [^{3}H]SCH23390 binding and determination of local CBF. For the 24 h group rats were reanaesthetised 24 h post-MCA occlusion, decapitated and the brains processed as for the 2 h group except that sections were taken for histology rather than CBF determination. These sections were fixed in 10% formaldehyde then stained with cresyl violet. Forskolin and SCH23390 binding protocols were performed as described in Section 2.4.1. Optical densities of regions of interest on the autoradiograms were measured using computer-assisted densitometry (Section 2.4.3.).

For qualitative assessment of the relationship between loss of ligand binding and histological evidence of infarction at 24 h, areas of infarcted tissue were drawn from the cresyl violet stained sections using a light microscope with a drawing tube attachment and compared to the areas of forskolin and D_1 receptor loss (for 24 h group) traced from the densitometer screen.

Flow threshold for loss of forskolin binding

The relationship between local CBF and forskolin binding 2 h post-permanent MCA occlusion was investigated in the ipsilateral dorsolateral caudate nucleus. Six individual measurements of optical density, corresponding to a range of blood flows, were made for each rat. [^{3}H]Forskolin and [^{14}C]IAP autoradiograms were superimposed to ensure optical density was measured at exactly the same point on each section. A graph of forskolin binding (represented as a percentage of the binding in the contralateral caudate nucleus for each individual animal) versus caudate blood flow was then constructed to obtain the blood flow threshold for loss of forskolin binding sites.

5.1.3. Results

Physiological variables measured immediately prior to MCA occlusion and 2 h post-MCA occlusion are shown in Table 8 and were comparable for the 2 time points.

Table 8 Physiological variables for autoradiographical determination of cerebral blood flow and ligand binding following **permanent** MCA occlusion

	Pre-MCAO	Post-MCAO
pH	7.473 ± 0.019	7.532 ± 0.014
Pa CO_2 (mmHg)	35.0 ± 1.5	34.9 ± 1.0
Pa O_2 (mmHg)	148.3 ± 11.2	137.2 ± 6.8
Rectal Temp (°C)	37.05 ± 0.23	37.08 ± 0.30
MABP (mmHg)	102 ± 8	102 ± 7

Physiological variables were determined immediately prior to and 2 h following MCA occlusion (n = 6).

Cerebral blood flow following permanent MCA occlusion

Local CBF was reduced throughout the hemisphere ipsilateral to the occluded MCA (Table 9). The greatest reductions in CBF were seen in frontal, sensorimotor and parietal cortices (19 - 26% of contralateral values) and dorsolateral caudate nucleus (6% of contralateral value). Moderate reductions in CBF were observed in the ipsilateral anterior cingulate cortex, ventromedial caudate nucleus and nucleus accumbens (60 - 71% of contralateral values), while small, but still statistically significant, reductions in CBF were found in the ipsilateral septum, globus pallidus, thalamus and hypothalamus. No areas of hyperperfusion were observed at this time point following permanent MCA occlusion.

Forskolin binding sites

Representative autoradiograms, at the level of the caudate nucleus, of [^{3}H]forskolin binding 2 and 24 h post-permanent MCA occlusion are shown in Figure 32. In the hemisphere contralateral to the occluded MCA, the highest levels of binding sites were located in the caudate nucleus and olfactory tubercle, while binding in the cerebral cortex was lower. The level of non-specific binding was less than 5% of the total for both cortex and caudate nucleus. In the ipsilateral hemisphere a reduction in forskolin binding sites in the dorsolateral caudate nucleus was clearly visible to the naked eye 2 h post-MCA occlusion (Figure 32a). By 24 h post-MCA occlusion forskolin binding was clearly reduced in both the caudate nucleus and overlying cerebral cortex (Figure 32c).

The mean values for forskolin binding sites 2 and 24 h post-permanent MCA occlusion are shown in Tables 10 and 11. Forskolin binding was significantly reduced only in the ipsilateral dorsolateral caudate nucleus 2 h post-occlusion (60% reduction compared with contralateral value) and was further reduced at 24 h post-MCA occlusion in this region (94% reduction). Forskolin binding was also significantly reduced in the frontal and sensorimotor cortices (by 74 and 63% respectively) at the 24 h time point.

Table 9 Local cerebral blood flow 2 h post-**permanent** MCA occlusion

REGION	Local cerebral blood flow (ml/100g/min)	
	Ipsilateral	Contralateral
Frontal Cortex	37 ± 10**	156 ± 57
Sensorimotor Cortex	32 ± 11***	171 ± 46
Parietal Cortex	47 ± 15**	183 ± 35
Anterior Cingulate Cortex	111 ± 34**	186 ± 35
Caudate Nucleus		
Dorsolateral	10 ± 4***	166 ± 66
Ventromedial	102 ± 13**	159 ± 31
Globus Pallidus	99 ± 25*	119 ± 32
Septum	90 ± 12*	99 ± 11
Nucleus Accumbens	107 ± 7**	150 ± 23
Thalamus		
Medial	109 ± 14**	142 ± 15
Ventral	113 ± 14*	135 ± 9
Hypothalamus	91 ± 11*	99 ± 13
Internal Capsule	65 ± 15	62 ± 14
Genu of Corpus Callosum	43 ± 15***	62 ± 13

Local cerebral blood flow in hemispheres ipsilateral and contralateral to MCA occlusion. *$p < 0.05$, **$p < 0.01$, ***$p < 0.001$ comparison with contralateral region (paired Student's t-tests).

Figure 32 Representative autoradiograms of [^{3}H]forskolin binding 2 and 24 h post-**permanent** MCA occlusion

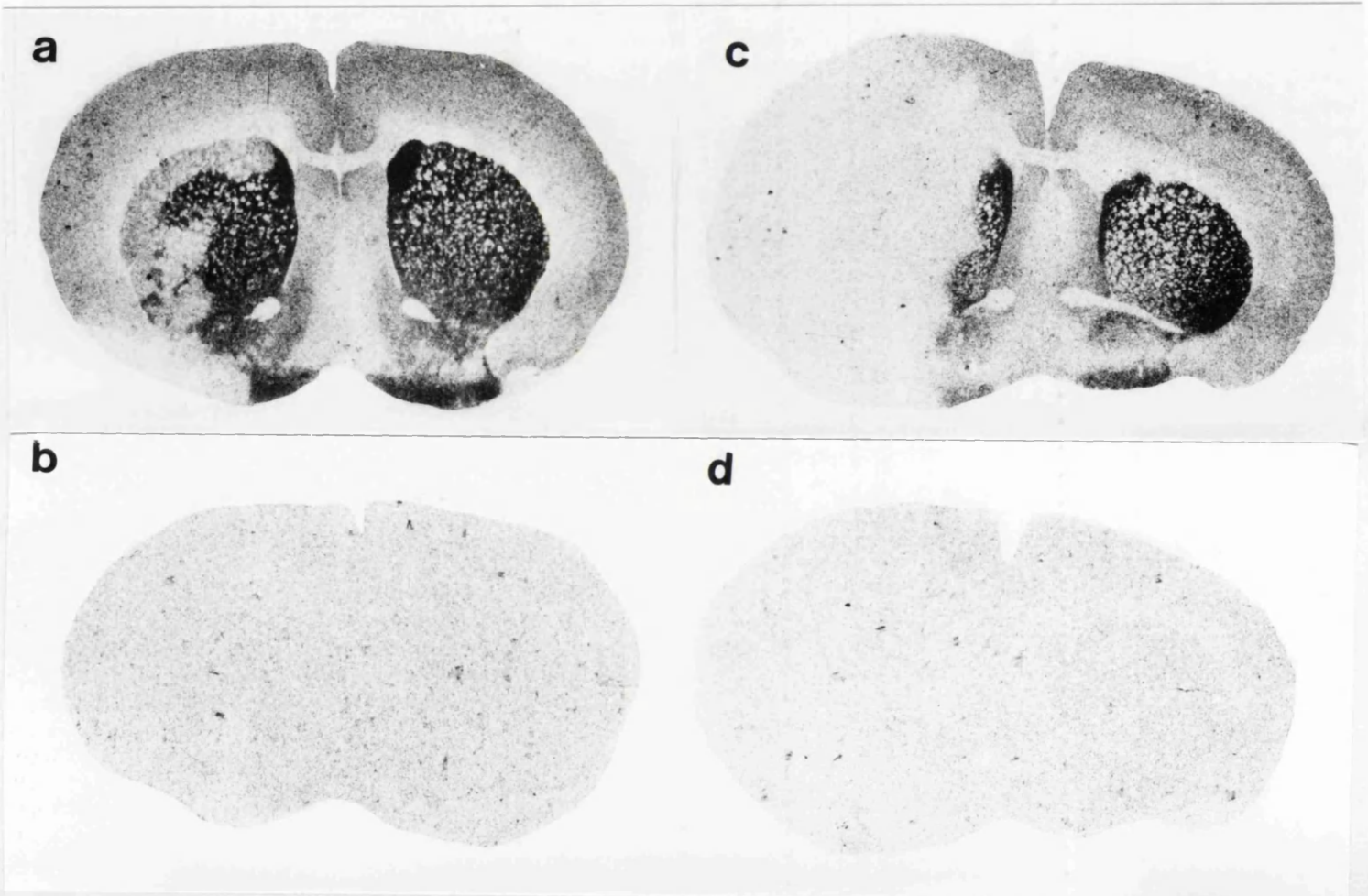

Autoradiograms of [^{3}H]forskolin binding 2 h (a-b) and 24 h (c-d) following permanent MCA occlusion. The figure shows total binding (a,c) and non-specific binding (b,d) at each time point. Note the reduction in forskolin binding sites in the dorsolateral caudate nucleus at 2 h (a) and the widespread loss of forskolin binding sites in the dorsolateral caudate nucleus and cerebral cortex 24 h post-MCA occlusion (c). Scale 6:1.

Table 10 [^{3}H]Forskolin and [^{3}H]SCH23390 binding 2 h post-**permanent** MCA occlusion

REGION	[^{3}H]Forskolin (pmol/g tissue)		[^{3}H]SCH23390 (pmol/g tissue)	
	Ipsilateral	Contralateral	Ipsilateral	Contralateral
Frontal Cortex	67.6 ± 32.3	66.5 ± 27.5	8.4 ± 2.7	9.9 ± 4.4
Sensorimotor Cortex	69.0 ± 34.6	72.9 ± 32.9	11.8 ± 2.6	11.9 ± 4.1
Parietal Cortex	62.7 ± 27.0	67.4 ± 27.6	10.0 ± 3.2	9.8 ± 2.5
Anterior Cingulate Cortex	98.7 ±38.3	95.4 ± 33.9	17.6 ± 3.4	16.5 ± 3.7
Caudate Nucleus				
Dorsolateral	86.7 ± 26.1**	215.4 ± 72.8	109.9 ±31.2**	138.9 ± 41.5
Ventromedial	219.7 ± 81.2	210.4 ± 71.0	135.3 ± 31.8	141.4 ± 31.2
Globus Pallidus	102.5 ± 35.9	103.3 ± 33.4	16.9 ± 6.4	17.8 ± 7.9
Septum	64.4 ± 25.7	68.7 ± 30.2	15.3 ± 4.8	17.6 ± 6.9
Nucleus Accumbens	190.2 ± 79.9	198.1 ± 84.3	129.1 ± 45.8	138.4 ± 53.1
Thalamus				
Medial	64.9 ± 24.6	62.8 ± 23.5	12.5 ± 4.2	12.0 ± 3.8
Ventral	47.4 ± 14.5	45.3 ± 14.2	4.5 ± 2.7	4.1 ± 3.1
Hypothalamus	49.5 ± 21.2	44.0 ± 19.5	9.2 ± 3.1	9.8 ± 2.5
Internal Capsule	14.7 ± 7.1	12.8 ± 8.2	3.2 ± 3.0	2.9 ± 2.8
Genu of Corpus Callosum	22.6 ± 11.8	22.5 ± 10.8	3.2 ± 2.2	4.3 ± 2.2

Ligand binding in hemispheres ipsilateral and contralateral to MCA occlusion. **$p < 0.01$ comparison with contralateral region (paired Student's t-tests).

Table 11 [^{3}H]Forskolin and [^{3}H]SCH23390 binding 24 h post-**permanent** MCA occlusion

REGION	[^{3}H]Forskolin (pmol/g tissue)		[^{3}H]SCH23390 (pmol/g tissue)	
	Ipsilateral	Contralateral	Ipsilateral	Contralateral
Frontal Cortex	22.8 ± 23.1**	87.6 ± 17.4	10.4 ± 2.7	14.1 ± 4.8
Sensorimotor Cortex	33.0 ± 32.6**	89.5 ± 14.4	11.1 ± 2.1	15.2 ± 4.4
Anterior Cingulate Cortex	92.2 ± 19.0	93.0 ± 15.9	21.5 ± 3.5	21.1 ± 3.9
Caudate Nucleus				
Dorsolateral	15.6 ± 10.9***	270.5 ± 89.2	105.9 ± 22.2**	153.6 ± 39.5
Ventromedial	233.8 ± 23.3	244.6 ± 76.5	156.8 ± 37.5	149.6 ± 42.5
Globus Pallidus	84.0 ± 37.0	96.2 ± 40.9	22.5 ± 3.8	24.2 ± 4.5
Septum	70.0 ± 7.9	72.2 ± 10.6	24.1 ± 8.9	23.3 ± 8.8
Nucleus Accumbens	246.6 ± 71.2	243.1 ± 56.5	151.3 ± 44.9	129.7 ± 76.4
Genu of Corpus Callosum	18.9 ± 13.9	19.6 ± 20.2	8.3 ± 4.9	8.1 ± 6.3

Ligand binding in hemispheres ipsilateral and contralateral to MCA occlusion. ***$p < 0.001$, **$p < 0.01$ comparison with contralateral region (paired Student's t-tests).

D_1 receptor binding sites

Representative autoradiograms, at the level of the caudate nucleus, of [^{3}H]SCH23390 binding 2 and 24 h post-permanent MCA occlusion are shown in Figure 33. In the contralateral hemisphere the highest levels of binding were observed in the caudate nucleus and nucleus accumbens, while binding throughout the cerebral cortices was relatively low. The level of specific binding in the caudate nucleus was approximately 90% of the total amount bound. In contrast to the reductions in forskolin binding, alterations in SCH23390 binding in the ipsilateral hemisphere were not obvious to the naked eye but were present in the dorsolateral caudate nucleus.

The mean values for D_1 receptor binding sites 2 and 24 h post-permanent MCA occlusion are shown in Tables 10 and 11. 2 h post-MCA occlusion there was a small, but significant, reduction in the level of D_1 dopamine receptor binding in the dorsolateral caudate nucleus (20% reduction). This reduction was smaller in magnitude than the 60% reduction in forskolin binding in the same region at the same time point. 24 h post-occlusion the dorsolateral caudate nucleus was still the only region to show a significant reduction in D_1 dopamine receptor binding. Unlike the progressive reduction in forskolin binding, there was no significant difference between the levels of D_1 dopamine receptor binding at 2 and 24 h post-MCA occlusion. These comparative changes in forskolin and D1 receptor binding in the frontal cortex and dorsolateral caudate nucleus are illustrated in Figures 34 and 35.

24 h post-MCA occlusion the boundary between normal tissue and the area of infarction was clearly demarcated on cresyl violet stained sections. The infarct appeared as an area of pallor that included the dorsolateral caudate nucleus and overlying cerebral cortex. The areas of reduced forskolin and D_1 receptor binding sites in the dorsolateral caudate nucleus 24 h post-occlusion were found to match this area of pallor, while the area of reduced forskolin binding in the cerebral cortex also matched the infarct.

Figure 33 Representative autoradiograms of [^{3}H]SCH23390 binding 2 and 24 h post-**permanent** MCA occlusion

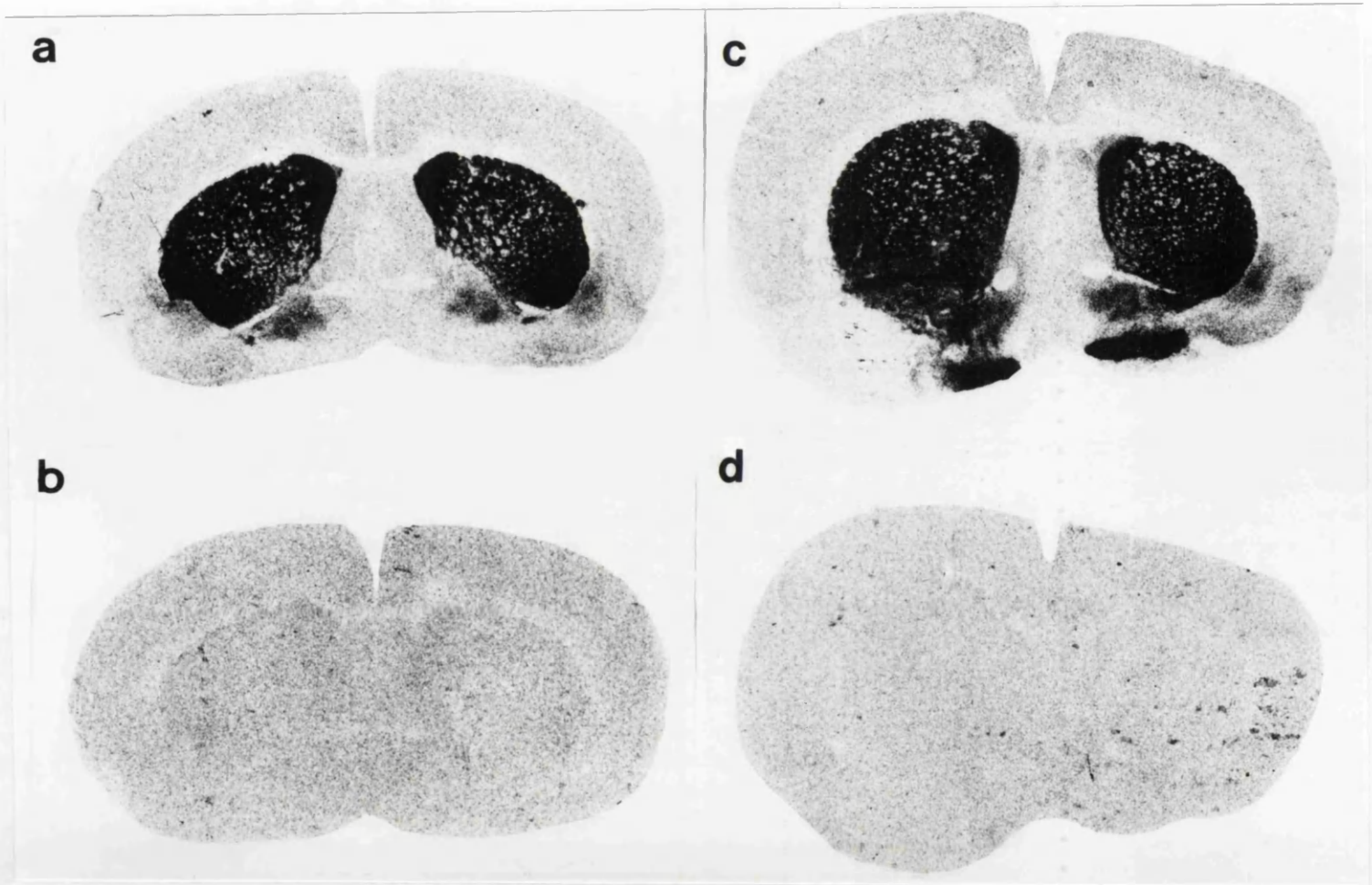

Autoradiograms of [^{3}H]SCH23390 binding 2 h (a-b) and 24 h (c-d) following permanent MCA occlusion. The figure shows total binding (a,c) and non-specific binding (b,d) at each time point. Scale 6:1.

Figure 34 [^{3}H]Forskolin binding in the frontal cortex and caudate nucleus 2 and 24 h post-permanent MCA occlusion

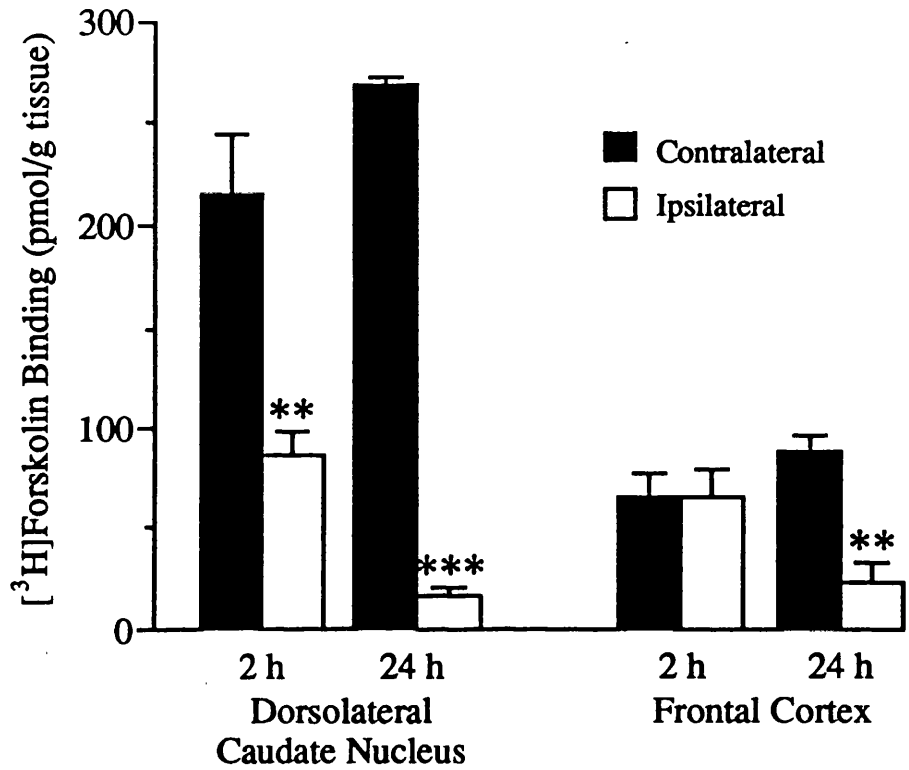

[^{3}H]Forskolin binding was substantially reduced in the dorsolateral caudate nucleus 2 h post-MCA occlusion, and was further reduced to only 6% of contralateral value by 24 h. In contrast [^{3}H]forskolin binding in the frontal cortex was only significantly reduced 24 h post-MCA occlusion. **p<0.01, ***p<0.001 comparison with contralateral region (paired Student's t-tests).

Figure 35 [^{3}H]SCH23390 binding in the frontal cortex and caudate nucleus 2 and 24 h post-permanent MCA occlusion

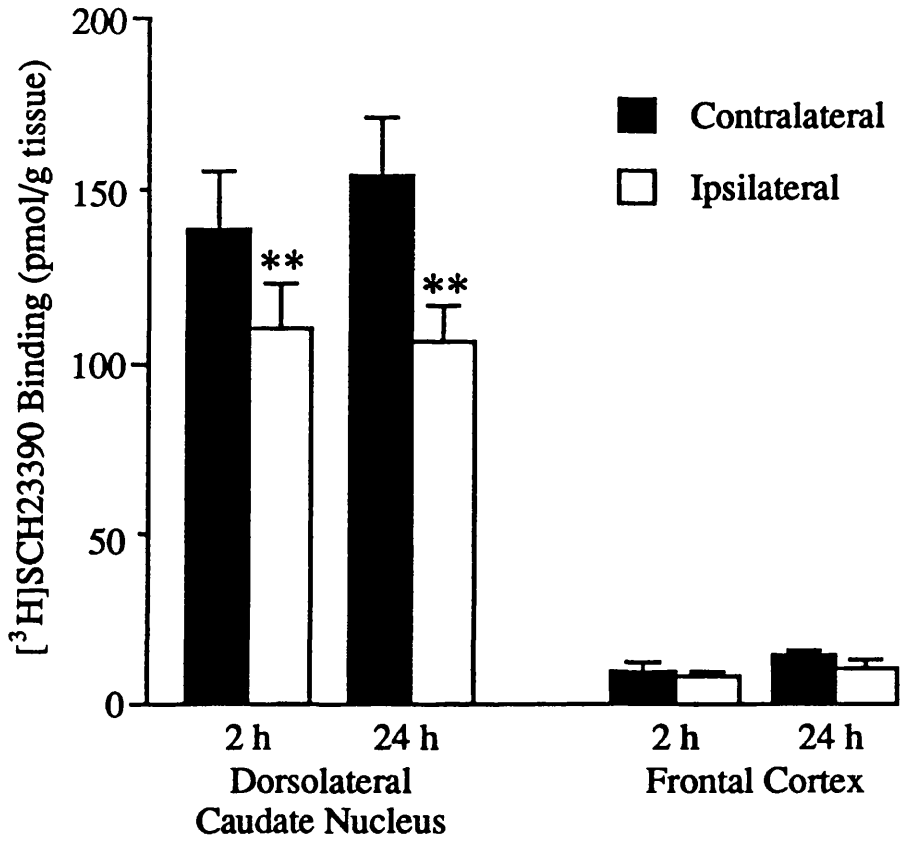

[^{3}H]SCH23390 binding in the dorsolateral caudate nucleus was decreased by 20% 2 h post-MCA occlusion. Unlike forskolin binding there was no progressive reduction in binding from 2 to 24 h. There was no significant alteration in the level of [^{3}H]SCH23390 binding in the frontal cortex either 2 or 24 h post-MCA occlusion. **$p < 0.01$ comparison with contralateral region (paired Student's t-tests).

Relationship between blood flow and forskolin binding in the caudate nucleus

Visual inspection of the CBF and [^{3}H]forskolin autoradiograms revealed that forskolin binding in some parts of the dorsolateral caudate nucleus was preserved despite marked reductions in blood flow in the corresponding [^{14}C]IAP autoradiogram (Figure 36). The subsequent analysis of the relationship between blood flow and forskolin binding in the caudate nucleus is shown in Figure 37. Forskolin binding was represented as a percentage of the corresponding contralateral value because of the heterogeneous distribution of forskolin binding sites within the caudate nucleus. Inspection of Figure 37 reveals that blood flows well below the mean contralateral value of 166 ml/100 g/min could be tolerated without significant loss of forskolin binding sites at the 2 h time point. However when blood flow fell below approximately 34 ml/100 g/min reductions in forskolin binding began to occur, and blood flows below 25 ml/100 g/min (with one exception) were associated with at least a 20% reduction in forskolin binding sites.

Figure 36 Autoradiograms showing conservation of [^{3}H]forskolin binding sites in regions of less severe hypoperfusion

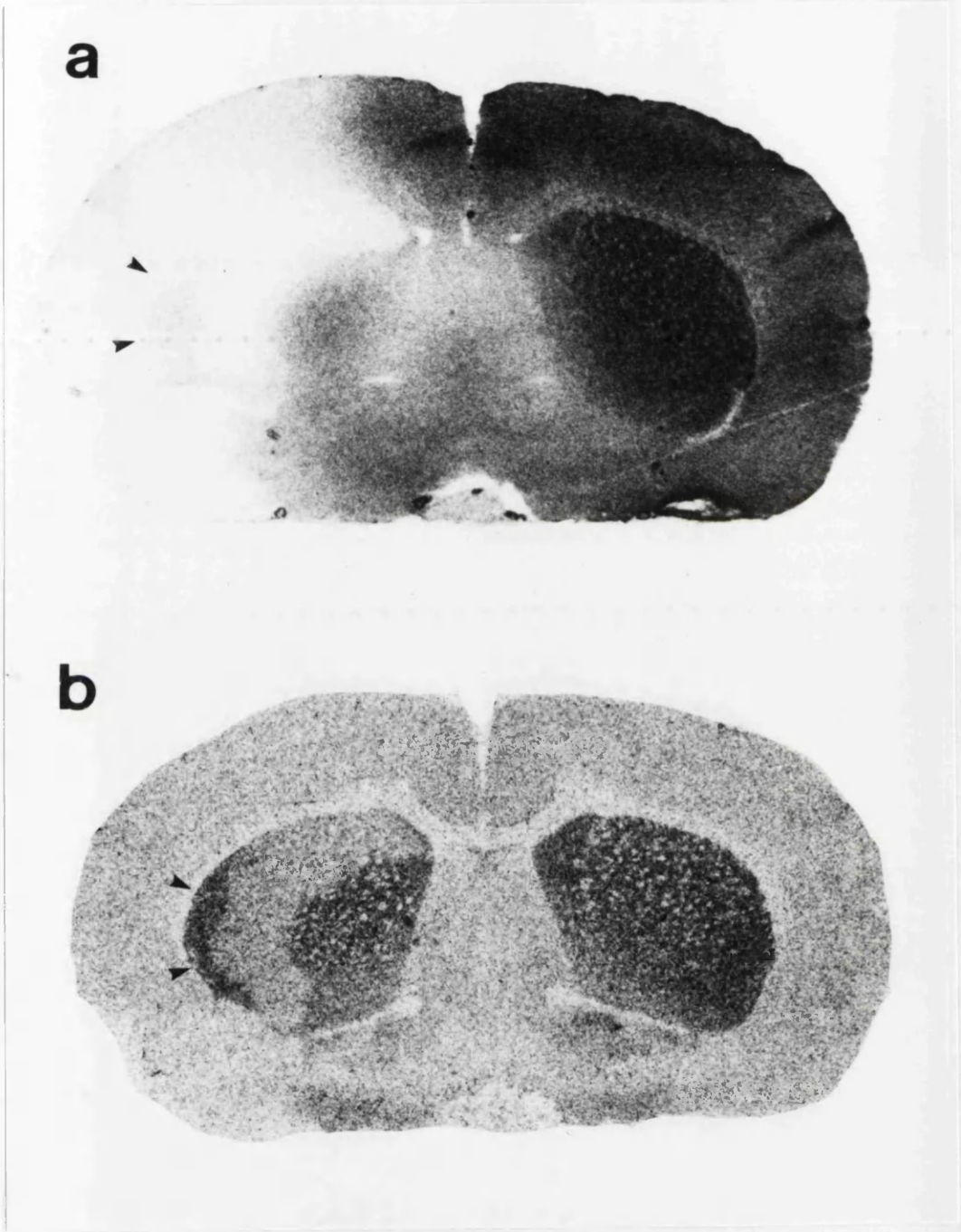

Autoradiograms of consecutive sections from an animal 2 h post-permanent MCA occlusion showing a) local cerebral blood flow measured by [^{14}C]iodoantipyrine and b) [^{3}H]forskolin binding. Note the area of conserved forskolin binding sites corresponding to an area of less profound hypoperfusion (arrowheads on a and b). Scale 8:1.

Figure 37 Blood flow threshold for loss of [^{3}H]forskolin binding sites from the caudate nucleus following **permanent** MCA occlusion

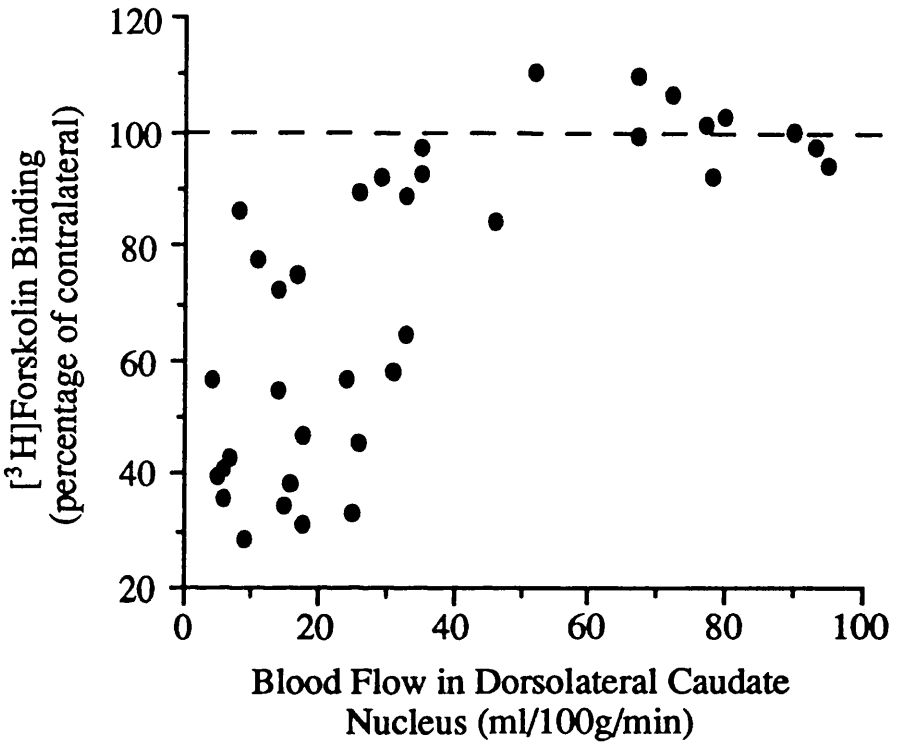

The graph shows the relationship between forskolin binding sites and blood flow in the ipsilateral dorsolateral caudate nucleus 2 h post-permanent MCA occlusion. Each point represents an individual pair of measurements for forskolin binding and blood flow made at corresponding locations on consecutive autoradiograms.

5.2. Forskolin and D_1 receptor binding following permanent global ischaemia

5.2.1. Introduction

In this study the impact of a permanent *global* ischaemic insult on cortical and striatal second messenger associated binding sites was investigated using *in vitro* autoradiography. The aim of this work was to assess the effect of a complete absence of cerebral blood flow on forskolin and D_1 receptor binding sites, and also to gain more information on the relative time courses for reductions in these binding sites following cerebral ischaemia.

5.2.2. Experimental protocol

Rats (n = 5 per group) were subjected to irreversible global ischaemia of 0 to 4 h duration (see Section 2.3.3.). Consecutive cryostat sections (20 μm) from the level of the caudate nucleus were processed for [^{3}H]forskolin and [^{3}H]SCH23390 binding as described in Section 2.4.1. In addition saturation analysis was performed using sections from a control brain and a brain subjected to 4 h ischaemia. Sections were incubated with [^{3}H]forskolin over the concentration range 2 - 150 nM or [^{3}H]SCH23390 over the range 0.25 - 20 nM and processed for autoradiography as described above.

5.2.3. Results

Forskolin binding sites

Representative autoradiograms, at the level of the caudate nucleus, of [^{3}H]forskolin binding following decapitation and incubation of the head at 37°C for 0, 1 or 4 h are shown in Figure 38. [^{3}H]Forskolin binding in the caudate nucleus decreased rapidly after the onset of global ischaemia, being reduced by 35% (compared with control) after 15 min and 87% after 4 h (Figure 39). At the 4 h time point [^{3}H]forskolin binding in the caudate nucleus had reached a level similar to that observed in the frontal cortex (see Figures 38 and 39). The rate of reduction in [^{3}H]forskolin binding in the frontal cortex was much slower with a significant reduction only observed 4 h post-onset of ischaemia, when the level of binding was reduced by 53% compared with control (Figure 39).

Figure 38 Representative autoradiograms of [^{3}H]forskolin binding following permanent **global** ischaemia

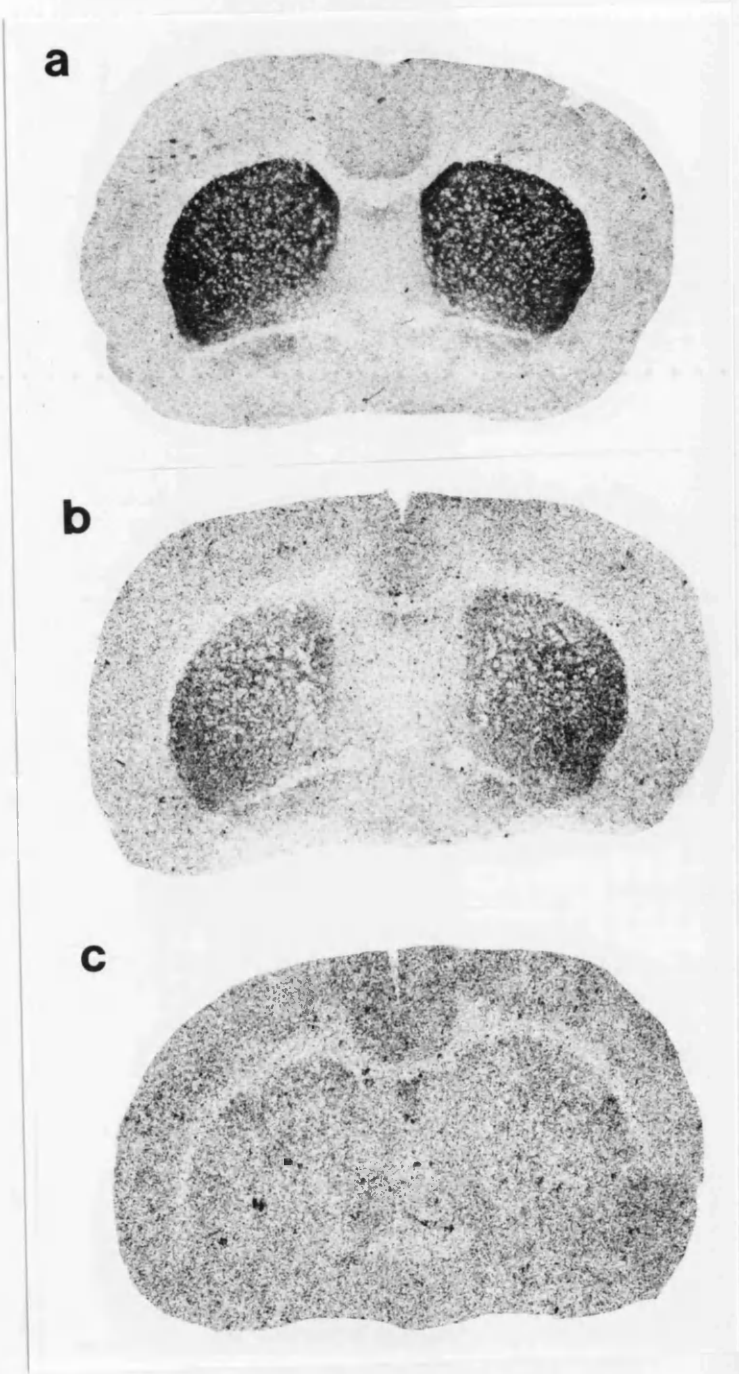

Autoradiograms of [^{3}H]forskolin binding 0 h (a), 1 h (b) and 4 h (c) following onset of global (decapitation) ischaemia. Note the progressive, bilateral loss of forskolin binding sites in the caudate nucleus with increasing duration of ischaemia, so that by 4 h the level of binding in the caudate nucleus is comparable to that in the cerebral cortex. Scale 5:1.

Figure 39 Progressive loss of [^{3}H]forskolin binding sites following permanent **global** ischaemia

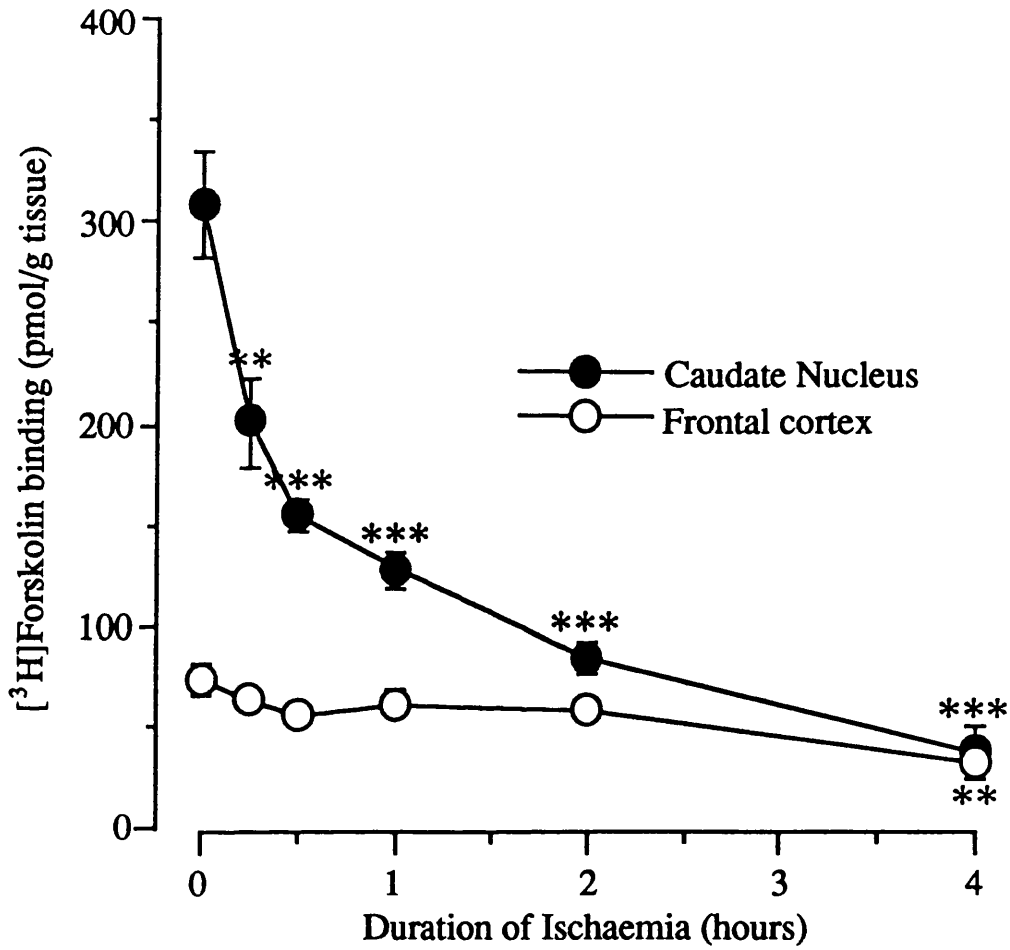

Forskolin binding in the caudate nucleus decreased rapidly and progressively with increasing durations of global ischaemia so that by 4 h the level of binding in the caudate nucleus was comparable to that in the frontal cortex. **$p < 0.01$, ***$p < 0.001$ comparison with time 0 (unpaired Student's t-tests).

Saturation data and Scatchard analysis for control and 4 h ischaemic brain are shown in Figures 40 and 41. There was a 52% reduction in the number of high affinity forskolin binding sites in the caudate nucleus 4 h post-ischaemia (control B_{max} = 849 pmol/g, 4 h ischaemia B_{max} = 414 pmol/g), while in the frontal cortex ischaemia had a minimal effect on the number of binding sites (control B_{max} = 289 pmol/g, 4 h ischaemia B_{max} = 284 pmol/g). K_d values for both caudate nucleus and frontal cortex were increased following 4 h ischaemia indicating a decrease in affinity for forskolin binding sites in both regions (caudate nucleus: control K_d = 23 nM, 4 h ischaemia K_d = 83 nM; frontal cortex: control K_d = 38 nM, 4 h ischaemia K_d = 67 nM).

D_1 receptor binding sites

Representative autoradiograms, at the level of the caudate nucleus, of [^{3}H]SCH23390 binding following 0, 1 and 4 h of global ischaemia are shown in Figure 42. [^{3}H]SCH23390 binding in the caudate nucleus had significantly decreased by 23% 15 min following onset of global ischaemia (Figure 43). However, unlike forskolin binding, there was no further decrease in the level of [^{3}H]SCH23390 binding which remained at approximately 80% of control value throughout the 4 h of the experiment. The level of [^{3}H]SCH23390 binding in the frontal cortex was very low (compared to forskolin) and did not show any significant changes over time.

Saturation data and Scatchard analysis for SCH23390 binding to D_1 dopamine receptors in the caudate nucleus are shown in Figures 44 and 45. There was a small (15%) reduction in the number of D_1 dopamine receptors following 4 h ischaemia (control B_{max} = 192 pmol/g, 4 h ischaemia B_{max} = 163 pmol/g), but no appreciable change in affinity (control K_d = 1.4 nM, 4 h ischaemia K_d = 1.3 nM). The level of [^{3}H]SCH23390 specific binding in the frontal cortex was too low to enable Scatchard analysis to be performed on this data.

Figure 40 Saturation analysis of [^{3}H]forskolin binding sites in the caudate nucleus and frontal cortex following permanent global ischaemia

Sections from control (n = 1) and 4 h ischaemic (n = 1) brain were incubated with increasing concentrations of [^{3}H]forskolin (2 - 150 nM). Non-specific binding was assessed in adjacent sections by the addition of unlabelled forskolin (20 μM). Specific binding was calculated by subtracting non-specific binding from total binding.

Figure 40 Saturation analysis of [^{3}H]forskolin binding sites in the caudate nucleus and frontal cortex following permanent **global** ischaemia

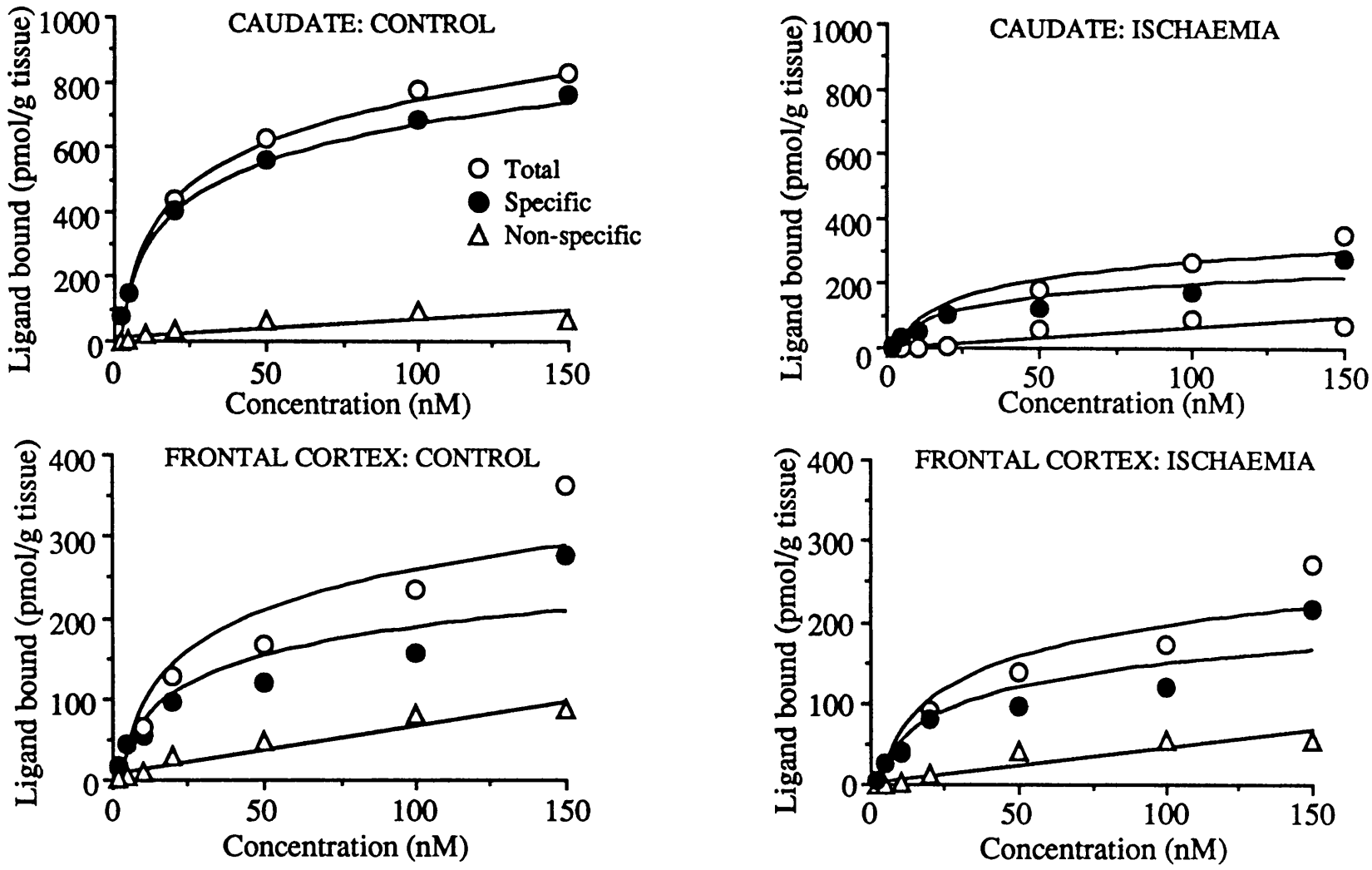

Figure 41 Scatchard analysis of saturation data for [^{3}H]forskolin binding in the caudate nucleus and frontal cortex following permanent **global** ischaemia

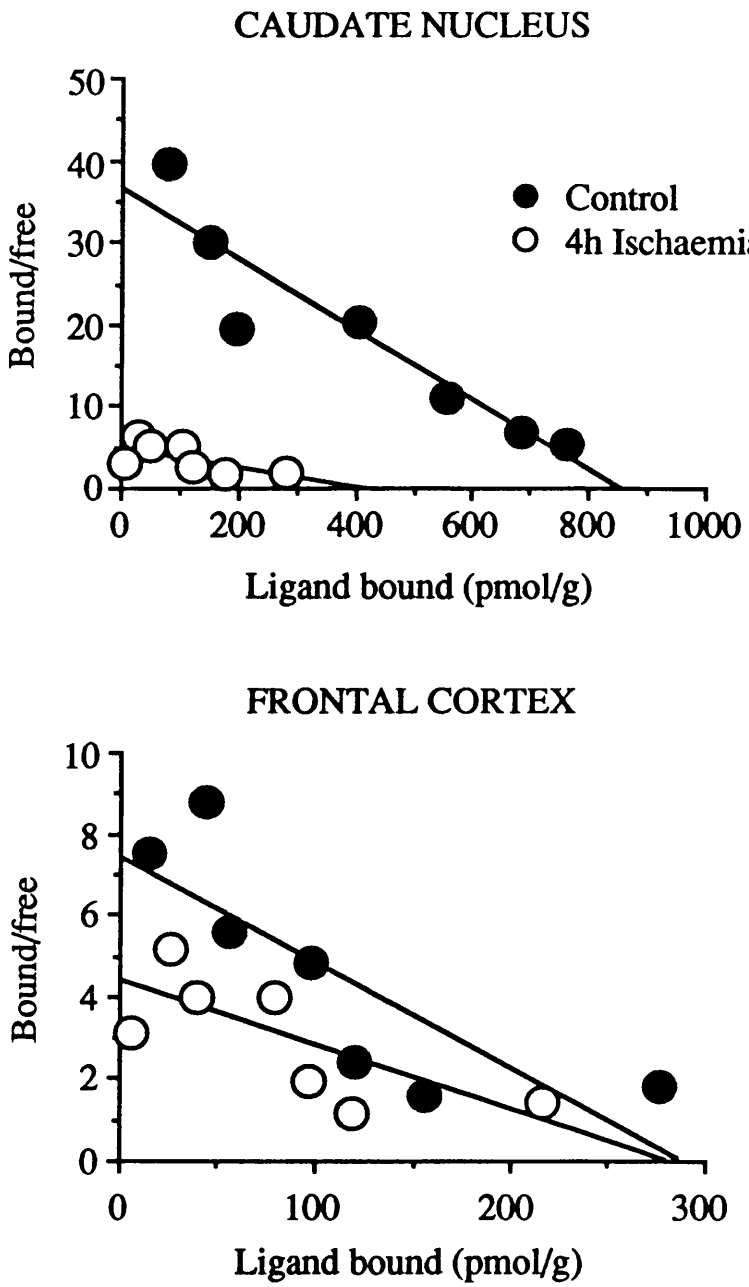

Sections from control and 4 h ischaemic brain were incubated with increasing concentrations of [^{3}H]forskolin (2 - 150 nM). B_{max} and K_d were determined using linear regression analysis and are shown in main text.

Figure 42 Representative autoradiograms of [^{3}H]SCH23390 binding following permanent **global** ischaemia

Autoradiograms of [^{3}H]SCH23390 binding 0 h (a), 1 h (b) and 4 h (c) following onset of global (decapitation) ischaemia. Note that SCH23390 binding is bilaterally reduced in the caudate nucleus 1 h post-onset of ischaemia but that there was no further loss of binding sites at the 4 h time point. Scale 6:1.

Figure 43 Reduction in [^{3}H]SCH23390 binding sites following permanent **global** ischaemia

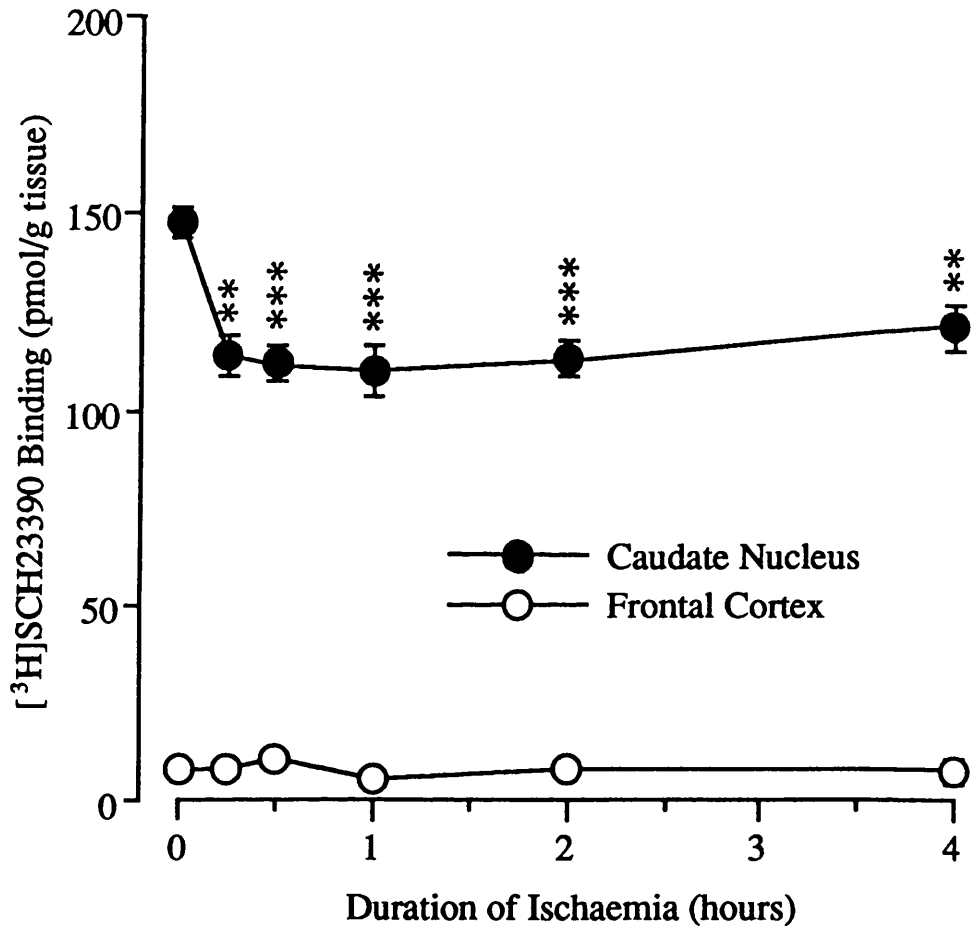

[^{3}H]SCH23390 binding in the caudate nucleus was reduced by approximately 20% following 15 min global ischaemia. No further reduction in binding was apparent with increasing periods of ischaemia. The lower level of binding in the frontal cortex was not significantly altered by up to 4 h of global ischaemia. **$p < 0.01$, ***$p < 0.001$ comparison with time 0 (unpaired Student's t-tests).

Figure 44 Saturation analysis of [^{3}H]SCH23390 binding sites in the caudate nucleus following permanent **global** ischaemia

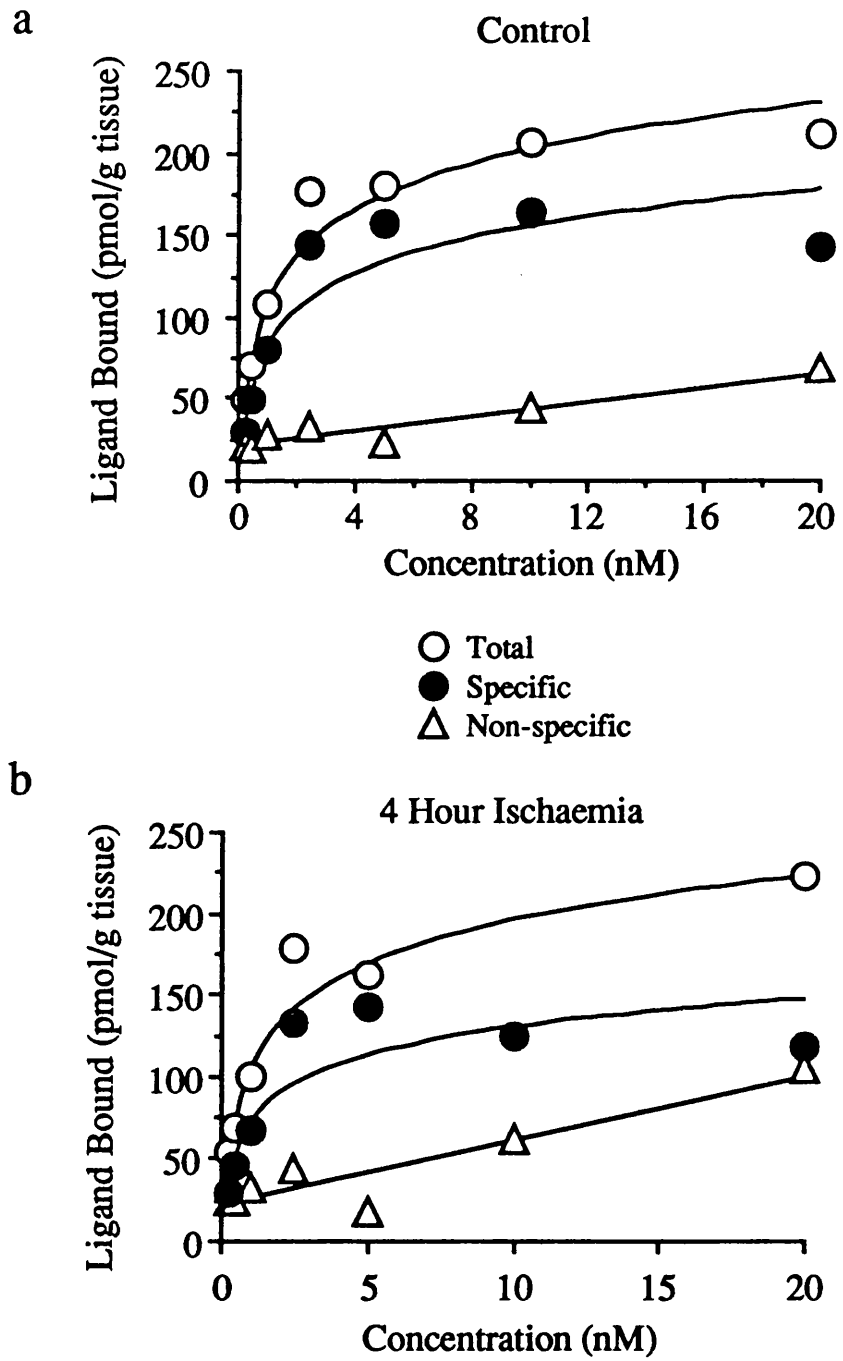

Sections from a control brain (a) and one subjected to 4 h ischaemia (b) were incubated with increasing concentrations of [^{3}H]SCH23390 (0.25 - 20 nM). Non-specific binding was assessed in adjacent sections by addition of piflutixol (10 μM). Specific binding was determined by subtraction of non-specific binding from total binding.

Figure 45 Scatchard analysis for [^{3}H]SCH23390 binding sites in the caudate nucleus following permanent **global** ischaemia

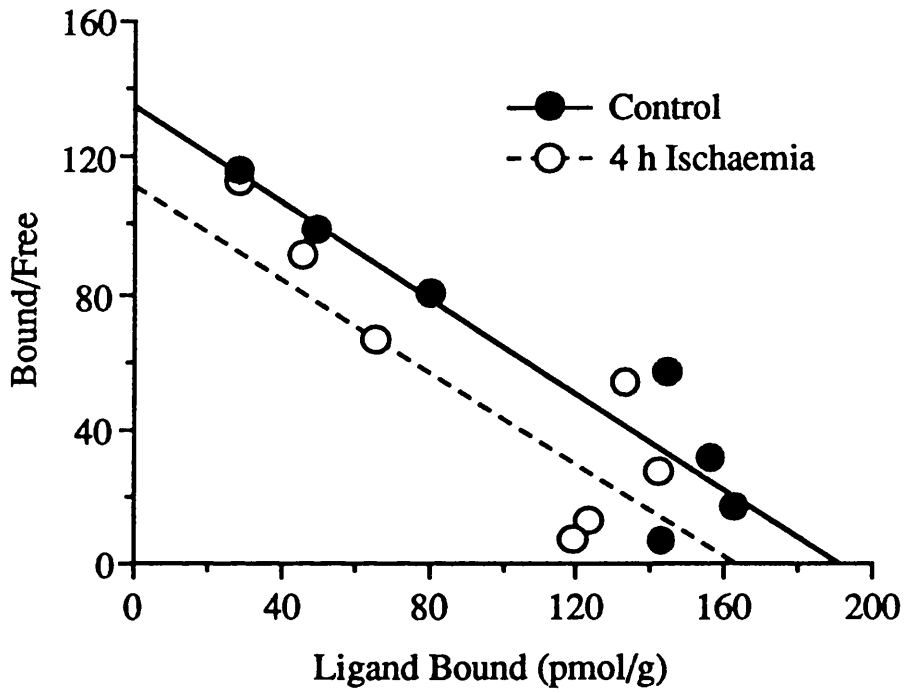

Sections from control and 4 h ischaemic brain were incubated with increasing concentrations of [^{3}H]SCH23390 (0.25 - 20 nM). B_{max} and K_d were determined using linear regression analysis, and values are given in the main text.

5.3. Discussion

5.3.1. Post-ischaemic reductions in second messenger-associated binding sites and neurotransmitter receptors

The present study was one of the first in the literature to examine second messenger systems in a model of focal cerebral ischaemia. The use of 2 separate ligands (forskolin and SCH23390) allowed us to assess the effect of permanent focal ischaemia at 2 distinct levels within the neurotransmitter-adenylate cyclase system. Although forskolin also binds, independently of adenylate cyclase, to several other membrane proteins including glucose transporters and ion channels (Laurenza *et al.* 1989), it has low affinity for these alternative sites (Laurenza *et al.* 1989). Furthermore it has been reported (Gerhart *et al.* 1991) that the glucose transporter site in rat brain is unaffected by ischaemia. Therefore it can be assumed that the observed post-ischaemic alterations in forskolin binding do reflect changes in the adenylate cyclase system.

Changes in ligand binding have been widely studied following transient global ischaemia in rats and gerbils (Daval *et al.* 1989; Hara *et al.* 1991; Onodera & Kogure 1989; Onodera *et al.* 1989). In these models selective neuronal necrosis becomes apparent in specific brain regions (*e.g.* CA1 region of the hippocampus) 3-7 days following recirculation (Kirino *et al.* 1982). The time course for reduction in forskolin binding sites in these models appears to parallel this neuronal loss since very small (Hara *et al.* 1991; Onodera & Kogure 1989) or no (Araki *et al.* 1991) reductions in binding are apparent within 2 h of the onset of reperfusion, while appreciable reductions (36 - 50%) only occur after 3-7 days (Araki *et al.* 1991; Hara *et al.* 1991; Onodera & Kogure 1989). In contrast in the present study a 60% reduction in striatal forskolin binding sites was observed only 2 h post-onset of focal ischaemia, while a recent study has reported significant reductions in striatal forskolin binding as early as 30 min post-permanent MCA occlusion (Wallace *et al.* 1991). These early reductions in forskolin binding sites are greater in magnitude than any change reported up to 7 days following transient global ischaemia. Thus reductions in forskolin binding sites (in certain regions) following permanent focal ischaemia appear to proceed much faster than for any neuroanatomical region following transient global ischaemia. However in the present study no significant reductions in forskolin binding sites were apparent in the frontal or sensorimotor cortices at the 2 h time point. This suggests that changes in forskolin binding could be used as a reliable early indicator of tissue likely to proceed to irreversible ischaemic damage within the caudate nucleus, but not the cerebral cortex. However by 24 h post-permanent MCA occlusion the areas of reduced forskolin binding sites matched the areas of cell damage assessed by histological staining in both the

caudate nucleus and cerebral cortex. Thus at this late time point assay of forskolin binding sites could be used as an alternative indicator of tissue infarction than the more traditional histological methods.

The decapitation model of global ischaemia was included in this study to investigate in more detail the time course for reductions in forskolin and D_1 dopamine receptor binding following cerebral ischaemia. The global ischaemia study confirmed the major findings of the focal ischaemia work and has given insight into the interpretation of those results. Firstly, reductions in forskolin binding sites proceeded more quickly than reductions in D_1 dopamine receptor binding sites following both global and focal ischaemia. Forskolin binding in the caudate nucleus was significantly reduced at the earliest time point in both studies (15 min or 2 h) and continued to decrease over time. In contrast to forskolin, D_1 dopamine receptor binding did not show a progressive reduction over time. D_1 dopamine receptor binding was reduced at the earliest time points but did not decrease further at the 4 h or 24 h time point respectively. Thus D_1 dopamine receptor binding appears more resistant to cerebral ischaemia than forskolin binding. This may reflect the subcellular localisation of the binding sites: the intracellular second messenger site (forskolin) appears to be more vulnerable than the neurotransmitter receptor site (D_1 dopamine) located on the outside of the plasma membrane. The majority of the D_1 dopamine receptor sites maintained their integrity even after 24 h of permanent focal ischaemia when neuronal necrosis must be present. This suggests that D_1 dopamine binding will only show appreciable reductions when neurones undergo lysis and the membrane structure disintegrates. Our results have been confirmed by a study of post-mortem delay in which rat brains, subjected to a controlled cooling curve, showed only a 20 % reduction in D_1 dopamine receptor binding levels in the caudate nucleus after 24 h (Gilmore *et al.* 1991).

Secondly, reductions in both forskolin and D_1 dopamine receptor binding proceed faster in the caudate nucleus than the frontal cortex. From the focal cerebral ischaemia studies it may be surmised that the vulnerability of striatal forskolin binding sites reflects the more severe reduction in CBF observed in this region compared to the frontal cortex. However the results of the global ischaemia study demonstrate that this can not be the entire explanation since both frontal cortex and caudate nucleus are exposed to the same degree of ischaemia (*i.e.* total absence of blood flow) in this model. It is possible that striatal forskolin binding sites differ functionally and/or structurally from cortical forskolin binding sites, and this difference renders them more vulnerable to ischaemic damage. The differential sensitivity of forskolin binding sites to ischaemia may reflect regional differences in the expression of G protein-subtypes. Within the rat brain high levels of

mRNA controlling the expression of the G_s-like protein G_{olf} are found in the caudate nucleus while other brain regions, including the cortex, exhibit much lower expression of this mRNA (Drinnan *et al.* 1991). This molecular variation may underlie observed differences between high affinity forskolin binding sites in the caudate nucleus and other brain regions (Poat *et al.* 1988) and their vulnerability to cerebral ischaemia. Alternatively the caudate nucleus may contain the same relatively resistant forskolin binding sites as the cortex, and an additional population of sites which are peculiarly vulnerable to ischaemia. However the Scatchard analysis showed no clear evidence of 2 distinct populations of forskolin binding sites in the caudate nucleus.

5.3.2. Cerebral blood flow following permanent MCA occlusion, and relationship with loss of forskolin binding sites

The hypoperfusion observed following permanent MCA occlusion in this study is qualitatively and quantitatively similar to previous reports in this model (Tamura *et al.* 1981b). The regions with the most profound reductions in blood flow were located in core MCA territory *e.g.* frontal and sensorimotor cortices and dorsolateral caudate nucleus. Structures that receive blood supply from the anterior cerebral artery as well as the MCA *e.g.* ventromedial caudate nucleus and anterior cingulate cortex showed smaller reductions in flow. In contrast to the original study (Tamura *et al.* 1981b) no hyperperfusion was observed in the ipsilateral globus pallidus. This may reflect the different time points at which local CBF was measured in the 2 studies (30 min compared with 2 h post-MCA occlusion in the present study). The values for regions contralateral to the occlusion were similar to those obtained previously for sham operated rats (Tamura *et al.* 1981b) validating the use of the contralateral hemisphere as a control group in the present study.

Flow thresholds for focal cerebral ischaemic damage

The CBF threshold for development of irreversible ischaemic damage is dependent not only on the severity of the ischaemic insult, but also on its duration (Jones *et al.* 1981; Hakim *et al.* 1992). Thus severe reductions in blood flow produce minimal damage if the ischaemia is of very short duration, while comparatively mild reductions in flow can cause irreversible damage if sustained for a sufficient length of time. Therefore direct comparison of thresholds obtained in different studies is strictly only valid when comparing identical models at the same time point. However because the volume of ischaemic damage following permanent MCA occlusion is maximal by 3 to 4 h post-onset of ischaemia (see Section 4.2.) studies assessing infarction at, or beyond, this time point can be compared.

In primates the critical CBF threshold for irreversible damage is approximately 17 ml/100 g/min (Jones *et al.* 1981) while in normotensive rats the threshold is considerably higher at 24-25 ml/100 g/min (Bolander *et al.* 1989; Tyson *et al.* 1984). The higher CBF threshold in rats reflects the 3-fold higher basal CBF in this species compared with primates. This high basal CBF is dictated by the higher cerebral metabolic rate necessary to sustain the 3-fold greater neuronal density in the rat brain (Jacewicz *et al.* 1992).

In the present study detailed analysis of the relationship between forskolin binding and blood flow in the caudate nucleus revealed that flow must fall below 34 ml/100 g/min before reductions in forskolin binding become apparent. In addition blood flow below 25 ml/100 g/min is always associated with at least a 15% loss of forskolin binding sites. These values are in good agreement with the thresholds for irreversible tissue damage in the rat discussed above. In particular Tyson *et al.* (1984) reported some histologically abnormal areas in the caudate nucleus when blood flow was less than 35 ml/100 g/min, whereas flows below 25 ml/100 g/min were always associated with histological damage. Bearing in mind the different time points of these 2 studies, it appears that the flow threshold for loss of striatal forskolin binding sites at 2 h post-MCA occlusion is a good predictor of irreversible damage at 4 h in the same model.

6. THE CEREBROVASCULAR EFFECTS OF L-NAME IN THE INTACT RAT

6.1. Introduction

The aim of this study was to assess the importance of endogenous NO in cerebral circulatory control. In order to do this NO production was inhibited by systemic adminstration of the NOS inhibitor L-NAME, and the resultant reductions in local CBF were determined using the *in vivo* [^{14}C]IAP technique. Firstly a dose-response curve (0.3 - 30 mg/kg) for L-NAME-induced reductions in CBF was obtained in conscious rats. The duration of action of the highest dose (30 mg/kg) was then followed over the course of 3 h. Finally the comparative effect of L-NAME on blood presure and CBF in conscious and anaesthetised rats was assessed. In addition to the primary aim of this study, a fuller understanding of the cerebrovascular effects of the NO synthase inhibitor L-NAME obtained from this work will aid interpretation of the observed effects of L-NAME against cerebral ischaemic damage *in vivo* (see Section 7).

6.2. Dose-dependency of response to L-NAME

6.2.1. Experimental protocol

L-NAME (0.3, 3, 30 mg/kg i.v.) or saline (1 ml/kg i.v.) was administered to conscious rats 30 min prior to [^{14}C]IAP determination of local CBF. [^{14}C]IAP was administered as a ramped infusion over 30 s during which time approximately 18 timed samples of arterial blood were collected as described in Section 2.4.2. The arterial concentration curve for [^{14}C]IAP was determined from the timed blood samples as described previously, but the tissue content of [^{14}C]IAP was measured using liquid scintillation analysis of micro-dissected tissue samples instead of autoradiography. Following decapitation the brain was removed from the skull onto an ice-cooled glass plate and 13 neuroanatomical regions were rapidly dissected out. The regions studied were cerebellum, medulla oblongata, inferior colliculus, superior colliculus, thalamus, hypothalamus, hippocampus, caudate nucleus, nucleus accumbens, frontal cortex, parietal cortex, occipital cortex and olfactory bulbs. The tissue samples were placed in preweighed glass vials which were immediately capped and reweighed. Soluene 350 (1 ml) was added to each vial prior to placement in a water bath (50°C) for approximately 12 h to dissolve the tissue samples. 0.5 ml acetic acid (2N) in toluene and 10 ml scintillant were then added to each vial and the radioactivity content determined by liquid scintillation counting as for blood samples (see Section 2.4.2.1.).

6.2.2. Results

6.2.2.1. Physiological variables

Physiological variables pre-L-NAME or saline administration are shown in Table 12. Arterial blood gases and plasma glucose were comparable between groups.

L-NAME (0.3,3 30 mg/kg i.v.) induced a dose-related hypertensive response as shown in Figure 46. All 3 doses elicited a significant increase in MABP, the magnitude of which increased with increasing dose. At the 30 mg/kg dose of L-NAME rats appeared sedated and less sensitive to external stimuli.

6.2.2.2. Dose-dependency of reductions in cerebral blood flow

The reductions in CBF induced by L-NAME were also found to be dose-related and are represented in Table 13 as a percentage of each contemporaneous saline control group. For the 0.3 mg/kg dose of L-NAME there was a trend to reduce CBF, but this did not reach significance for any of the 13 regions studied. With 3 mg/kg L-NAME the reductions in CBF attained significance in 6 of the 13 regions (cerebellum, inferior colliculus, superior colliculus, hypothalamus, occipital cortex and olfactory bulbs), while for 30 mg/kg L-NAME significant reductions in CBF were achieved for 11 of the 13 regions. The data for 5 selected regions is illustrated in Figure 47. From this graph the dose-dependency of the hypoperfusion induced by L-NAME can be clearly seen in regions such as the cerebellum and medulla oblongata. In addition the statistical significance of the reductions in flow, for all 5 regions, was greater for the 30 mg/kg dose of L-NAME than for the lower doses. However for the frontal cortex and caudate nucleus the magnitude of the observed reductions in flow were comparable between the 3 and 30 mg/kg doses of L-NAME.

Table 12 Physiological variables for the dose-dependency of the vascular effects of L-NAME

	SALINE (n = 9)	L-NAME 0.3 mg/kg (n = 5)	L-NAME 3 mg/kg (n = 5)	L-NAME 30 mg/kg (n = 6)
pH	7.435 ± 0.016	7.426 ± 0.035	7.436 ± 0.017	7.399 ± 0.027
Pa CO_2 (mmHg)	39.4 ± 2.9	40.0 ± 2.9	39.4 ± 1.5	42.0 ± 3.0
Pa O_2 (mmHg)	84.6 ± 3.9	92.2 ± 6.8	85.4 ± 6.4	87.2 ± 4.3
Glucose (mmol/l)	9.00 ± 1.13	8.82 ± 2.01	8.28 ± 1.39	8.26 ± 0.57
Rectal Temp (°C)	37.13 ± 0.40	36.90 ± 0.22	37.18 ± 0.85	37.08 ± 0.24

Physiological variables were measured immediately prior to administration of L-NAME (0.3, 3 or 30 mg/kg i.v.) or saline (1 ml/kg i.v.). Local cerebral blood flow was subsequently determined 30 min post-drug administration.

Figure 46 Dose-dependency of the pressor response to L-NAME in the conscious rat

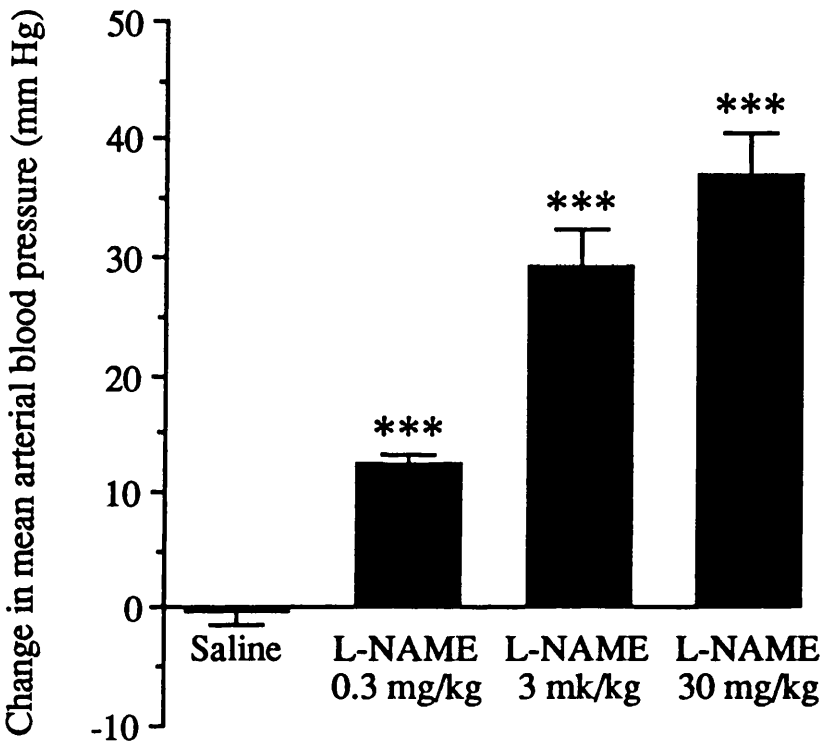

Change in mean arterial blood pressure measured 30 min following L-NAME (0.3 - 30 mg/kg i.v.) or saline administration in conscious rats. ***$p < 0.001$ compared with saline control (unpaired Student's t-tests). Base-line mean arterial blood pressures prior to drug or vehicle administration were 135 ± 6, 135 ± 4, 134 ± 1 and 131 ± 6 (mean ± S.D.) for saline and 0.3, 3 and 30 mg/kg L-NAME groups respectively.

Table 13 Dose-dependency of the effect of L-NAME on local cerebral blood flow in neuroanatomically defined regions of the brain in the conscious rat

Neuroanatomical Region	Dose of L-NAME		
	0.3 mg/kg	3 mg/kg	30 mg/kg
Cerebellum	92 ± 8	76 ± 6 *	70 ± 8 ***
Medulla	96 ± 9	86 ± 8	76 ± 5 **
Inferior Colliculus	91 ± 15	73 ± 10 *	80 ± 8 **
Superior Colliculus	86 ± 12	68 ± 11 *	85 ± 19 *
Hypothalamus	87 ± 12	68 ± 11 *	67 ± 16 **
Thalamus	80 ± 13	73 ± 16	70 ± 8 **
Hippocampus	91 ± 13	80 ± 21	76 ± 6 *
Caudate Nucleus	86 ± 11	78 ± 12	81 ± 14 *
Nucleus Accumbens	79 ± 18	74 ± 24	63 ± 5 **
Frontal Cortex	87 ± 11	75 ± 13	74 ± 11 *
Parietal Cortex	86 ± 12	75 ± 12	84 ± 16
Occipital Cortex	74 ± 9	60 ± 9 *	83 ± 12
Olfactory Bulbs	88 ± 9	75 ± 8 *	79 ± 9 **

Local cerebral blood flow was measured 30 min following administration of L-NAME (0.3, 3 and 30 mg/kg i.v.) or saline (n = 5-6 per group) in the conscious rat. Data is represented as percentages of the mean CBF values for individual saline control groups.

***$p < 0.001$, **$p < 0.01$, *$p < 0.05$ compared with relevant saline control group (unpaired Student's t-tests).

Figure 47 Dose-dependency of the cerebrovascular response to L-NAME in the conscious rat

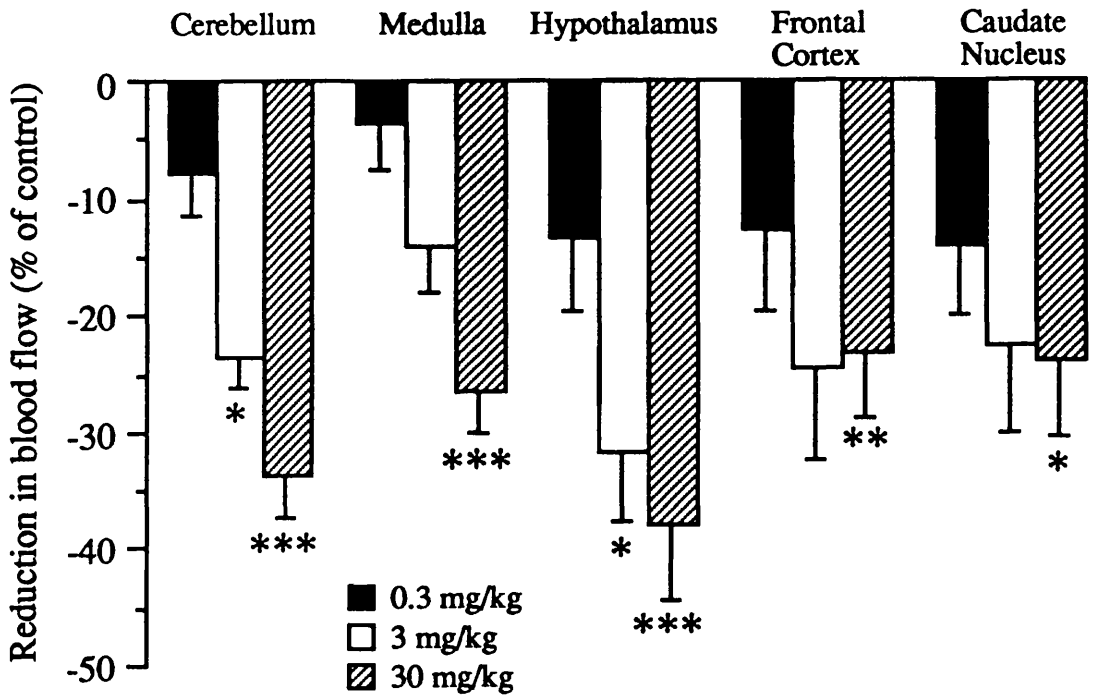

Percentage reduction in cerebral blood flow in selected neuroanatomically defined regions of the brain measured 30 min following 0.3, 3 or 30 mg/kg L-NAME i.v. Data was compared to individual saline control groups by unpaired Student's t-tests. *$p < 0.05$, **$p < 0.02$, ***$p < 0.001$.

6.3. Time course for effect of L-NAME on cerebral blood flow

6.3.1. Experimental Protocol

Local CBF was measured, in separate groups of conscious rats, 15, 30, 60 and 180 min after injection of L-NAME (30 mg/kg i.v.) or saline (1 ml/kg i.v.). The whole tissue method described in Section 6.2. was used to determine the tissue concentrations of [^{14}C]IAP, and CBF was then calculated for each of the 13 neuroanatomical regions studied.

6.3.2. Results

6.3.2.1. Physiological variables

Physiological variables pre-drug administration were within the normal ranges and are shown in Table 14.

As in the previous study (Section 6.2.), L-NAME induced a rapid and highly significant increase in MABP compared with the relevant saline control group. For experiments of 180 min duration subsequent pairwise comparisons showed this difference was significant at all timepoints studied (Figure 48a). MABP declined slightly from its maximal value 60 min post-drug, but was still elevated (by over 30 mmHg) 180 min following administration of the single dose of L-NAME.

In the conscious rat L-NAME (30 mg/kg) induced a significant hypothermic response, even with the presence of heating lamps, exhibited as a slow progressive reduction in rectal temperature that was most marked at the 60 min and 180 min time points (*e.g.* mean rectal temperatures were 35.5 ± 0.17 and 37.1 ± 0.3 in L-NAME and saline groups respectively, 60 min post-drug or saline administration).

6.3.2.2. Time course for reductions in cerebral blood flow

CBF was significantly reduced by L-NAME in the majority of regions at each time point post-drug administration (15-180 min, see Table 15). The reductions in CBF did not decrease in magnitude over time, and CBF was still significantly reduced in all 13 regions at the 180 min time point (see Table 15 and Figure 48b). The reductions in CBF were similar in magnitude for all regions of interest (*e.g.* 37-43% for 180 min group).

Table 14 Physiological variables for the time course of the effect of L-NAME on local cerebral blood flow in the conscious rat

	Pre-drug values for 15 min group		Pre-drug values for 30 min group	
	SALINE (n = 4)	L-NAME (n = 8)	SALINE (n = 4)	L-NAME (n = 6)
pH	7.424 ± 0.007	7.377 ± 0.042	7.418 ± 0.026	7.399 ± 0.027
Pa CO_2 (mmHg)	41.7 ± 0.6	40.6 ± 3.1	41.0 ± 2.9	42.0 ± 3.0
Pa O_2 (mmHg)	80.1 ± 3.3	84.5 ± 6.7	83.1 ± 1.8	87.2 ± 4.3
Glucose (mmol/l)	9.06 ± 0.48	9.58 ± 1.42	7.95 ± 0.55	8.26 ± 0.57
Rectal Temp (°C)	37.17 ± 0.72	36.95 ± 0.33	37.30 ± 0.35	37.08 ± 0.24

	Pre-drug values for 60 min group		Pre-drug values for 120 min group	
	SALINE (n = 4)	L-NAME (n = 6)	SALINE (n = 4)	L-NAME (n = 6)
pH	7.423 ± 0.026	7.431 ± 0.052	7.429 ± 0.022	7.435 ± 0.051
Pa CO_2 (mmHg)	42.3 ± 2.4	41.0 ± 6.2	37.7 ± 5.6	40.0 ± 2.4
Pa O_2 (mmHg)	88.3 ± 8.0	86.0 ± 8.6	92.5 ± 6.6	92.7 ± 8.0
Glucose (mmol/l)	9.90 ± 2.35	8.47 ± 1.38	9.50 ± 2.05	9.05 ± 1.76
Rectal Temp (°C)	37.05 ± 0.25	36.93 ± 0.48	36.75 ± 0.79	37.12 ± 0.65

Physiological variables were measured immediately prior to administration of L-NAME (30 mg/kg i.v.) or saline (1 ml/kg i.v.). Local cerebral blood flow was determined 15 min, 30 min, 1 h or 3 h following drug treatment.

Figure 48 Prolonged maintenance of the pressor and cerebrovascular effects of L-NAME in the conscious rat

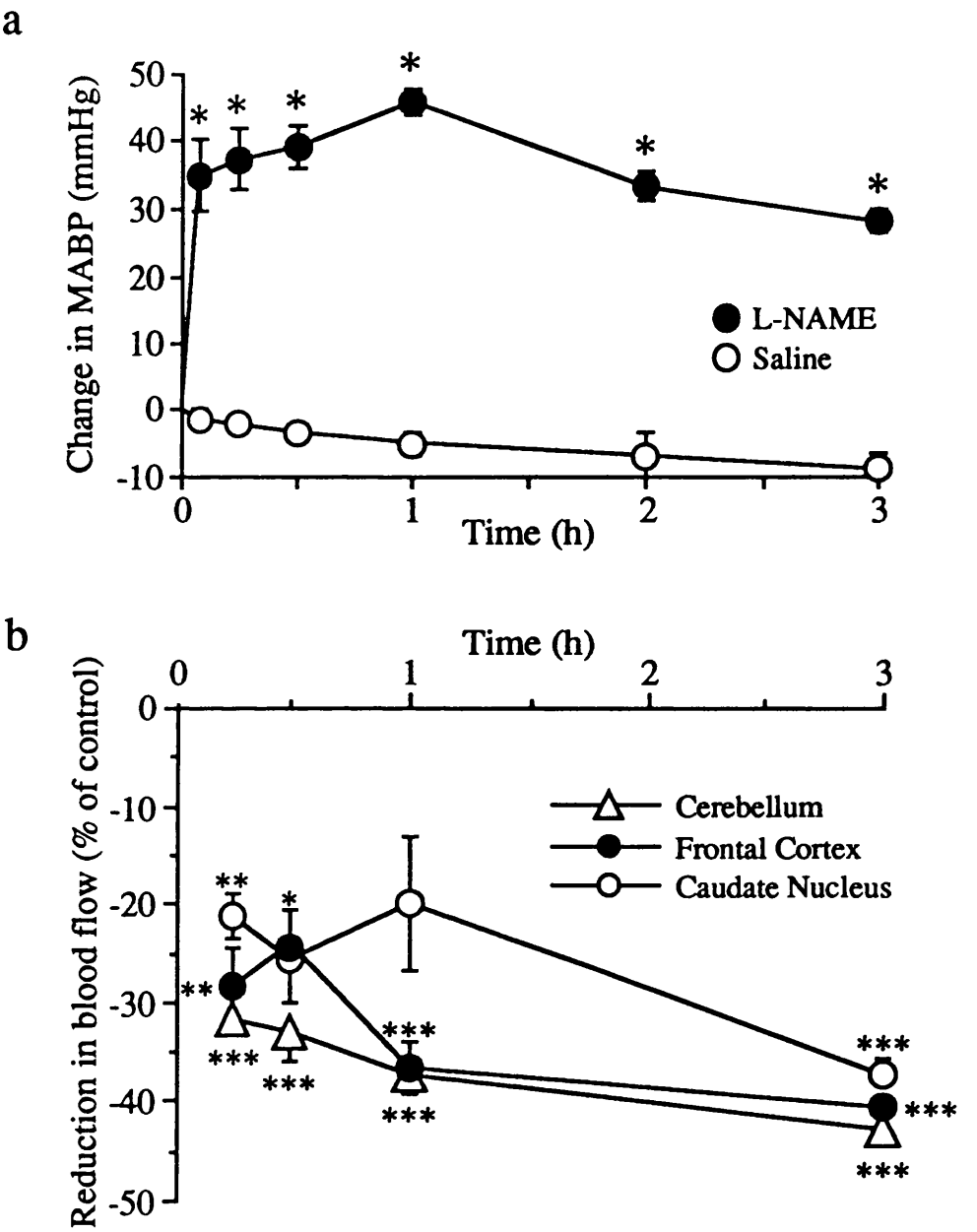

Temporal profile of peripheral and central responses following administration of L-NAME (30 mg/kg i.v. at time 0): a) Change in mean arterial blood pressure (MABP) and b) Reductions in cerebral blood flow (CBF) expressed as percentage of relevant saline control.

*p<0.05, **p<0.01, ***p<0.001 compared with appropriate saline control group (statistical analysis by a) two-way repeated measure ANOVA followed by unpaired Student's t-tests with Bonferroni correction for blood pressure data b) unpaired Student's t-tests for blood flow data).

Table 15 Time course of effect of L-NAME on local cerebral blood flow in neuroanatomically defined regions of the brain in the conscious rat

Neuroanatomical Region	15 min		30 min		60 min		180 min	
	Saline	L-NAME	Saline	L-NAME	Saline	L-NAME	Saline	L-NAME
Cerebellum	82 ± 10	56 ± 6 ***	89 ± 10	62 ± 7 ***	82 ± 10	52 ± 5 ***	79 ± 8	45 ± 2 ***
Medulla	79 ± 6	59 ± 3 ***	80 ± 8	61 ± 4 **	79 ± 10	56 ± 7 ***	76 ± 8	47 ± 5 ***
Inferior Colliculus	113 ± 14	85 ± 8 ***	110 ± 16	88 ± 9 **	121 ± 6	91 ± 7 ***	117 ± 12	72 ± 10 ***
Superior Colliculus	91 ± 16	65 ± 3 ***	85 ± 14	73 ± 16 *	97 ± 12	73 ± 17 ***	94 ± 8	58 ± 5 ***
Hypothalamus	78 ± 6	50 ± 8 ***	79 ± 14	53 ± 13 **	75 ± 6	51 ± 12 *	73 ± 8	42 ± 5 ***
Thalamus	87 ± 9	65 ± 9 **	92 ± 14	65 ± 7 **	86 ± 16	75 ± 19	94 ± 9	42 ± 4 ***
Hippocampus	72 ± 6	44 ± 6 ***	67 ± 14	51 ± 4 *	76 ± 14	50 ± 7 ***	72 ± 8	44 ± 5 ***
Caudate Nucleus	77 ± 14	60 ± 6 **	76 ± 12	62 ± 11 *	82 ± 12	66 ± 17	84 ± 12	52 ± 5 **
Nucleus Accumbens	67 ± 14	47 ± 6 **	79 ± 18	50 ± 4 **	82 ± 22	51 ± 12 ***	65 ± 8	38 ± 7 **
Frontal Cortex	98 ± 11	70 ± 12 **	98 ± 12	73 ± 11 *	110 ± 21	70 ± 7 **	109 ± 15	65 ± 7 ***
Parietal Cortex	98 ± 16	91 ± 20	109 ± 16	92 ± 17	123 ± 24	86 ± 10 **	127 ± 23	78 ± 11 **
Occipital Cortex	100 ± 9	63 ± 11 ***	103 ± 15	86 ± 13	121 ± 17	87 ± 14 **	115 ± 18	74 ± 8 **
Olfactory Bulbs	80 ± 10	59 ± 6 ***	77 ± 10	61 ± 7 **	86 ± 10	64 ± 15 *	86 ± 6	53 ± 5 ***

Local cerebral blood flow (ml/100g/min) was measured in separate groups of animals 15, 30, 60 and 180 min following administration of L-NAME (30 mg/kg i.v.) or saline in the conscious rat. ***$p < 0.001$, **$p < 0.01$, *$p < 0.05$ compared with relevant saline control group (unpaired Student's t-tests).

6.4. Comparison of the effect of L-NAME on cerebral blood flow in anaesthetised and conscious rats

6.4.1. Experimental Protocol

Conscious and halothane-anaesthetised rats were prepared for [^{14}C]IAP measurement of local CBF as described in Section 2.4.2.1. Local CBF was measured 30 min after administration of L-NAME (30 mg/kg) or 1ml/kg saline i.v. using a 30 s ramped infusion of [^{14}C]IAP. Following decapitation the brains were processed for autoradiography.

6.4.2. Results

6.4.2.1. Physiological variables

Physiological variables measured immediately prior to administration of L-NAME (30 mg/kg i.v.) or saline are shown in Table 16. Values for all animals were within the normal ranges for conscious and halothane-anaesthetised rats.

The changes in MABP following administration of L-NAME (30 mg/kg) or saline in conscious and halothane-anaesthetised rats are shown in Figure 49. In the conscious rat L-NAME induced a rapid and significant elevation in MABP ($p < 0.001$) compared to the saline control group. Subsequent pairwise comparisons revealed significant differences ($p < 0.05$) between L-NAME and saline treated rats at all time points following drug administration, and MABP at the 30 min time point was 32 ± 12 mmHg (mean ± S.D.) greater than the pre-drug value. In contrast under halothane anaesthesia the pressor response to L-NAME was markedly reduced so that MABP did not differ significantly ($p > 0.05$) between the L-NAME and saline groups. MABP at the 30 min time point was only 12 ± 11 mmHg above the pre-L-NAME level. This represents approximately one-third of the pressor response observed with the same dose of L-NAME in conscious rats.

6.4.2.2. Cerebrovascular effect of L-NAME

L-NAME significantly reduced CBF in all 16 of the neuroanatomical regions studied in both conscious and halothane-anaesthetised rats (Table 17). The hypoperfusion induced by L-NAME was rather uniform throughout the brain. Reductions in CBF for the conscious group ranged between 21 and 41%, while for halothane anaesthetised rats L-NAME reduced CBF by 36 to 50%. The cerebrovascular conductance values for all 16 regions of interest were similarly significantly reduced following L-NAME treatment in both conscious and halothane-anaesthetised rats (Table 17).

Table 16 Physiological variables for the effect of L-NAME on cerebral blood flow in conscious and anaesthetised rats

CONSCIOUS

	SALINE (n = 7)	L-NAME (n = 6)
pH	7.435 ± 0.030	7.431 ± 0.037
Pa CO_2 (mmHg)	39.1 ± 2.9	39.1 ± 3.2
Pa O_2 (mmHg)	85.6± 6.2	82.4 ± 3.4
Glucose (mmol/l)	9.00 ± 1.41	9.36 ± 0.93
Rectal Temp (°C)	36.77 ± 0.48	37.07 ± 0.52

HALOTHANE

	SALINE (n = 6)	L-NAME (n = 6)
pH	7.410 ± 0.044	7.96 ± 0.088
Pa CO_2 (mmHg)	39.0 ± 1.8	37.8 ± 1.9
Pa O_2 (mmHg)	166.2 ± 16.7	160.6 ± 16.2
Glucose (mmol/l)	9.42 ± 0.65	9.28 ± 0.87
Rectal Temp (°C)	37.30 ± 0.25	37.08 ± 0.38

Physiological variables were measured immediately prior to administration of L-NAME (30 mg/kg i.v.) or saline (1 ml/kg i.v.).

Figure 49 Effect of L-NAME on blood pressure in conscious and anaesthetised rats

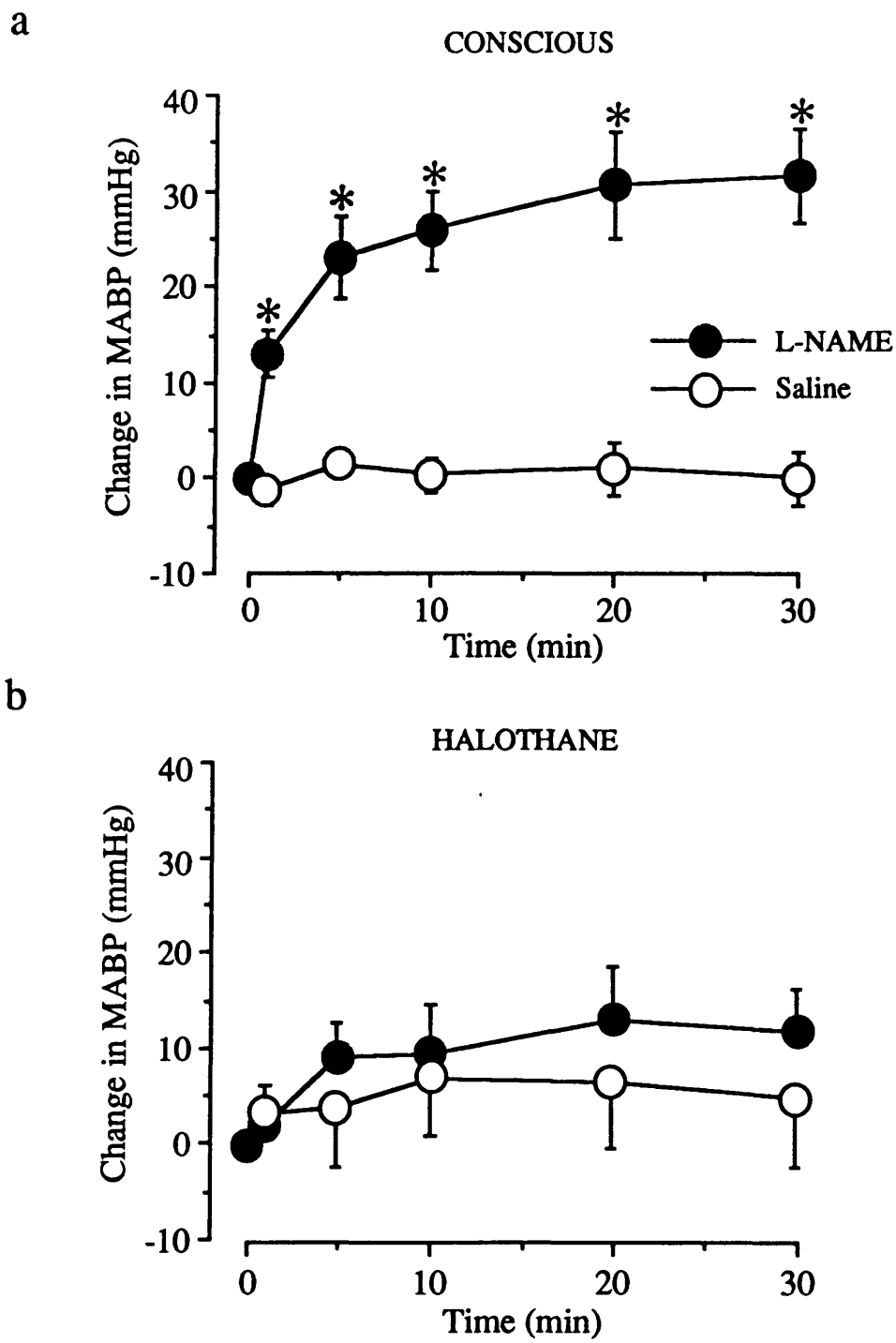

Change in mean arterial blood pressure (MABP) following L-NAME (30 mg/kg i.v.) or saline in: a) conscious (n = 6 L-NAME group, n = 7 saline group) and b) halothane-anaesthetised rats (n = 6 both groups). *$p<0.05$, 2-way repeated measure ANOVA followed by Student's unpaired t-test with Bonferroni correction for comparison of saline and L-NAME treated rats at each time point.

Table 17 Effect of L-NAME on local cerebral blood flow and cerebrovascular conductance in neuroanatomically defined regions of the brain in anaesthetised and conscious rats

	Cerebral Blood Flow (ml/100g/min)				Cerebrovascular Conductance (ml/100g/min/mmHg)			
	CONSCIOUS		HALOTHANE		CONSCIOUS		HALOTHANE	
Region	Saline (n = 7)	L-NAME (n = 6)	Saline (n = 6)	L-NAME (n = 6)	Saline (n = 7)	L-NAME (n = 6)	Saline (n = 6)	L-NAME (n = 6)
Olfactory Bulbs	147 ± 23	104 ± 16**	152 ± 56	90 ± 22*	1.13 ± 0.14	0.65 ± 0.14***	1.39 ± 0.32	0.73 ± 0.19**
Frontal Cortex	170 ± 33	131 ± 17*	208 ± 64	133 ± 42*	1.27 ± 0.25	0.81 ± 0.16**	1.93 ± 0.53	1.06 ± 0.35**
Parietal Cortex	203 ± 40	134 ± 27*	197 ± 58	119 ± 36*	1.43 ± 0.22	0.84 ± 0.23***	1.86 ± 0.61	0.95 ± 0.30**
Occipital Cortex	222 ± 76	131 ± 22**	204 ± 48	120 ± 43**	1.58 ± 0.63	0.81 ± 0.17*	1.91 ± 0.37	0.96 ± 0.37**
Nucleus Accumbens	148 ± 27	106 ± 18**	193 ± 64	111 ± 42*	1.11 ± 0.19	0.66 ± 0.17***	1.78 ± 0.36	0.89 ± 0.34**
Caudate Nucleus	147 ± 29	112 ± 17*	225 ± 72	136 ± 44*	1.10 ± 0.22	0.70 ± 0.16**	2.09 ± 0.60	1.08 ± 0.35**,†
Globus Pallidus	82 ± 17	65 ± 9*	117 ± 40	66 ± 20*	0.63 ± 0.13	0.40 ± 0.08**	1.11 + 0.47	0.53 ± 0.16*
Thalamus mediodorsal	184 ± 26	126 ± 12***	175 ± 56	102 ± 38*	1.39 ± 0.18	0.78 ± 0.13***	1.62 ± 0.39	0.82 ± 0.31**
Thalamus ventrolateral	152 ± 29	113 ± 18**	162 ± 45	97 ± 25*	1.13 ± 0.21	0.70 ± 0.15**	1.52 ± 0.43	0.77 ± 0.21**
Hypothalamus	106 ± 5	71 ± 6***	125 ± 36	69 ± 19**	0.81 ± 0.04	0.44 ± 0.06***	1.17 ± 0.27	0.56 ± 0.17***
Hippocampus	114 ± 28	89 ± 18	163 ± 60	92 ± 25*	0.85 ± 0.19	0.55 ± 0.14**	1.48 ± 0.33	0.73 ± 0.21***
Dentate Gyrus	112 ± 16	88 ± 16*	152 ± 52	84 ± 19*	0.82 ± 0.10	0.54 ± 0.13**	1.39 ± 0.30	0.67 ± 0.16***
Superior Colliculus	150 ± 35	122 ± 11	202 ± 53	102 ± 20**	1.13 ± 0.25	0.76 ± 0.12**	1.87 ± 0.34	0.82 ± 0.19***
Inferior Colliculus	281 ± 71	191 ± 30*	279 ±106	147 ± 41*	2.18 ± 0.55	1.18 ± 0.22**	2.56 ± 0.74	1.17 ± 0.33**
Cerebellum grey matter	123 ± 23	89 ± 13**	142 ± 43	73 ± 16**	0.93 ± 0.19	0.55 ± 0.11**	1.34 + 0.48	0.58 ± 0.13**
Cerebellum white matter	65 ± 14	48 ± 11**	77 ± 26	41 ± 11*	0.49 ± 0.12	0.30 ± 0.08**	0.72 ± 0.25	0.32 ± 0.10**

L-NAME (30 mg/kg i.v.) or saline was administered 30 min prior to local cerebral blood flow measurement in conscious and halothane-anaesthetised rats. *$p < 0.05$, **$p < 0.01$, ***$p < 0.001$ comparison with relevant saline group, † $p < 0.05$ comparison between L-NAME groups (statistical comparisons by unpaired t-tests).

6.5. Discussion

6.5.1. Peripheral vascular response to nitric oxide synthase inhibition

In the conscious rat L-NAME elicited a dose-related hypertensive response. The magnitude of this response is in agreement with previous studies (Gardiner *et al.* 1990a; Rees *et al.* 1990) and demonstrates that NO maintains the basal vasodilatory tone of the peripheral vasculature. In addition we have shown that halothane anaesthesia significantly attenuates the pressor response to L-NAME. This phenomenon was also observed in other studies designed to investigate the effect of L-NAME on ischaemic damage in anaesthetised rats (see Section 7). The influence of anaesthetic agents on the pressor response to NOS inhibitors has also been reported by other groups (Aisaka *et al.* 1991; Greenblatt *et al.* 1992; Wang *et al.* 1991). These studies have confirmed that halothane anaesthesia reduces the elevation in MABP induced by NOS inhibition, and also shown that other anaesthetic agents (*e.g.* pentobarbital) can increase the pressor response to L-NAME. The mechanism by which halothane reduces the pressor response is not known, but can not be wholly dependent on its inherent vasodilator properties since other volatile anaesthetics which produce a similar degree of hypotension to halothane actually potentiate the hypertensive action of NOS inhibitors (Wang *et al.* 1991). In addition this effect appears selective for NOS inhibitors as halothane only minimally reduces the pressor response to noradrenaline and angiotensin II (Pang *et al.* 1992). Interestingly halothane has also been reported to reduce the vasodilation induced by NO in isolated large conductance vessels (Muldoon *et al.* 1988). Thus halothane appears to reduce the physiological response to both NO and NOS inhibitors. However regional variations in the vascular response to NOS inhibition (Greenblatt *et al.* 1992) cautions against direct comparison of *in vitro* studies with *in vivo* control mechanisms in the whole animal.

6.5.2. Central vascular response to nitric oxide synthase inhibition

Prior to the initiation of this study no detailed report concerning the regional distribution, dose-dependency and duration of action of NOS inhibition on local CBF had been published. Before the identification of EDRF as NO, an endothelium derived factor was known to control the relaxation of central vessels (Rosenblum 1986). This fact together with the subsequent demonstration that NOS inhibitors could constrict cerebral vessels *in vivo* (Faraci 1990; Gotoh *et al.* 1991; Rosenblum *et al.* 1990) suggested that NO may mediate regulation of vascular tone centrally as well as peripherally. The results of the present study have shown that this is indeed the case.

In the conscious rat, L-NAME elicited sustained, dose-dependent reductions in CBF throughout the brain. Reductions in CBF of the same magnitude have subsequently been reported for both conscious (Tanaka *et al.* 1991) and anaesthetised (Kozniewska *et al.* 1992; Prado *et al.* 1992) rats using similar doses of NOS inhibitors. If NOS inhibitors had no effect on the cerebrovasculature, the increase in arterial blood pressure induced by NOS inhibition would lead to autoregulatory constriction of cerebral blood vessels in an attempt to maintain constant CBF. The fact that CBF is actually decreased following NOS inhibition demonstrates that these drugs have a direct constrictive action on cerebral vessels and confirms that basal NO production is involved in the maintenance of resting CBF in the rat.

NOS is located within all cellular elements of the CNS including endothelium (Bredt *et al.* 1990), vascular smooth muscle (Katusic 1991), intrinsic and extrinsic peri-vascular neurones (Regidor *et al.* 1993; Iadecola *et al.* 1993) and glia (Murphy *et al.* 1990). All of these sources of NO could potentially influence cerebrovascular tone. However the hetergeneous distribution of neuronal NOS (highest in cerebellum, lowest in medulla oblongata (Bredt *et al.* 1990; Forstermann *et al.* 1990)) does not match the homogeneity of the observed reductions in local CBF suggesting that endothelial NOS may be of greater importance than intraparenchymal NOS in controlling the basal tone of the cerebral circulation. Furthermore the response to NOS inhibition is dependent on vessel size, being greater in large arteries than arterioles regardless of brain region (Faraci 1991), suggesting the reductions in CBF observed following administration of NOS inhibitors are mediated primarily by constriction of the main cerebral vessels rather than the microcirculation. In this regard the NOS-containing neurones that originate in the sphenopalantine ganglion and innervate the cerebral arteries (Iadecola *et al.* 1993; Nozaki *et al.* 1993) may also be an important regulator of global CBF. The intrinsic NOS-containing neurones within the brain (Regidor *et al.* 1993) may be more involved in the control of localised changes in blood flow in response to stimulation of particular neuronal pathways.

In the anaesthetised cat a heterogeneous reduction in regional CBF following L-nitro-arginine has been reported (Kovach *et al.* 1992) leading the authors to suggest involvement of neuronal NO in the control of basal cerebrovascular tone in this species. However this argument is not supported by the regional distribution of neuronal NOS which does not match the reported reductions in rCBF in the cat. However some species differences do appear to exist with regards to the relative importance of NO for control of basal tone since L-nitroarginine has no significant effect on CBF in the rabbit (Faraci & Heistad 1992).

In the present study the time course for L-NAME-induced reductions in local CBF was monitored for 3 h following administration of a single dose of L-NAME (30 mg/kg). The reductions in CBF were still maximal at the 3 h time point accentuating the prolonged inhibition of NO production achieved by treatment with NOS inhibitors. Other studies have demonstrated similarly prolonged cerebrovascular responses to NOS inhibition (Kovach *et al.* 1992; Prado *et al.* 1992) with reports of reduced CBF 24 h post-infusion of L-nitroarginine in the rat (quoted in Prado *et al.* 1992) and 48 h post-infusion of L-NAME in the goat (Fernandez *et al.* 1993). In addition subsequent *ex vivo* assay of cerebral vessel reactivity following systemic administration of L-nitroarginine has shown NO-dependent relaxations to be impaired (Kovach *et al.* 1992). All of this data is consistent with the irreversible inhibition of central NOS activity that has been reported to occur following systemic administration of NOS inhibitors (Dwyer *et al.* 1991).

6.5.3. Halothane anaesthesia and cerebrovascular effect of L-NAME

Halothane anaesthesia did not dramatically alter the cerebral hypoperfusion induced by L-NAME since significant reductions in local CBF were observed in both conscious and halothane-anaesthetised rats. However the hypertension induced by L-NAME in conscious rats makes direct comparison of CBF between conscious and anaesthetised rats difficult. Therefore conductance values were calculated to compensate for the difference in blood pressure between L-NAME treated rats in the conscious and halothane groups. These results showed that, following L-NAME treatment, there were no significant differences in the cerebrovascular conductances for conscious and halothane-anaesthetised rats. Therefore the degree of cerebral vasoconstriction induced by L-NAME is equivalent in the 2 groups.

The results of this study have demonstrated that halothane anaesthesia reduces the peripheral vasoconstrictive action of the NOS inhibitor L-NAME but does not affect the central response. This differential action may reflect the different subcellular localisations of NOS in the brain and periphery. Within peripheral endothelial cells NOS is located in both the plasma membrane and cytoplasm (Forstermann *et al.* 1991), while in the brain NOS is predominantly cytosolic (Matsumoto *et al.* 1993). Halothane, like other general anaesthetics, induces membrane perturbations that may prevent interaction of L-NAME with membrane NOS while leaving cytosolic NOS unaffected, resulting in attenuation of the peripheral rather than the central response to L-NAME.

6.5.4. The choice of L-NAME as the inhibitor of nitric oxide synthase

L-NAME was chosen as the *in vivo* inhibitor of central NOS in these studies in preference to N^G-monomethyl-L-arginine (L-NMMA), the first widely available NOS inhibitor, for several reasons. L-NMMA acts in part indirectly by inhibiting L-arginine uptake into neurones and endothelium (Bogle *et al.* 1992; Westergaard *et al.* 1993). This compound is also metabolised to L-arginine (Hecker *et al.* 1990) and can therefore actually promote NO synthesis (Archer & Hampl 1992). Furthermore L-NMMA is a more potent inhibitor of inducible NOS than constitutive NOS (Gross *et al.* 1990; Lambert *et al.* 1991) so is not ideally suited to studies of constitutive NOS in neuronal or endothelial cells. In contrast N^G-nitro-L-arginine (L-NA) is a more potent inhibitor of constitutive NOS than L-NMMA (Moore *et al.* 1990), and is not metabolised to L-arginine (Hecker *et al.* 1990). However because L-NA has low solubility in saline, its methyl ester derivative L-NAME was instead used in the present studies. L-NA and L-NAME are similar in potency, and are more potent inhibitors of neuronal and endothelial NOS than L-NMMA *in vitro* (East & Garthwaite 1990; Moore *et al.* 1990) and *in vivo* (Babbedge *et al.* 1993; Rees *et al.* 1990). *In vivo* L-NAME is rapidly converted to L-NA (Schwarzacher & Raberger 1992) by an esterase, so the actions of L-NAME are probably mediated by L-NA which itself does not undergo further metabolism (Krejcy *et al.* 1993). The presence of a guanidino-nitro group means L-NA and L-NAME can cross the blood-brain barrier more easily than other arginine analogs such as L-NMMA, and systemic administration of L-NA has been demonstrated to inhibit brain NOS activity in rats (Dwyer *et al.* 1991).

6.5.5. The putative role of nitric oxide as an endogenous vasodilator in the cerebrovasculature

The identification of NO as the EDRF controlling the response to acetyl choline in the CNS has been disputed (Rosenblum 1992), and it may be that $EDRF_{ACh}$ is actually a NO-containing compound such as a nitrosothiol rather than NO itself (Myers *et al.* 1990; Rosenblum 1992). The mode of action of 'NOS inhibitors', particularly L-NMMA, has also been questioned. In the mouse cerebral circulation L-NMMA may act by activating arachidonic acid metabolism thereby generating superoxide which scavenges NO resulting in vasoconstriction (Rosenblum *et al.* 1992). However this response appears to be species-specific for the mouse since 'NOS inhibitors' in the presence of cyclooxygenase inhibitors or superoxide dismutase still produce significant vasoconstriction in both rats and cats (Rees *et al.* 1990; Wei *et al.* 1992). This fact together with the demonstration that coadministration of L-arginine and L-NAME reverses the cerebrovascular response to L-NAME (Prado *et al.* 1992) justifies our conclusion that L-NAME reduces CBF by inhibiting basal production of NO.

7. THE CONTRIBUTIONS OF GLUTAMATE AND NITRIC OXIDE TO ISCHAEMIC AND EXCITOTOXIC DAMAGE

7.1. Effect of MK-801 pre-treatment on ischaemic damage following transient MCA occlusion

7.1.1. Introduction

The role of glutamate in the pathophysiology of permanent focal cerebral ischaemia is well established (see Section 1.4.3.), but its role in transient ischaemia-reperfusion injury remains to be as fully defined. As a first step towards elucidation of the role of glutamate in focal ischaemia-reperfusion injury the neuroprotective efficacy of the non-competitive NMDA receptor antagonist MK-801 was assessed on acute outcome (4 h) following transient MCA occlusion in the anaesthetised rat. The 4 h, anaesthetised paradigm was chosen because it allows monitoring and control of physiological variables (including blood pressure) which can influence outcome in the endothelin-1 model of transient ischaemia (see Section 4.1.4.).

7.1.2. Experimental protocol

A bolus injection of MK-801 (0.12 mg/kg i.v.) was administered either 1 h or 2.5 h prior to transient MCA occlusion induced by application of endothelin-1 to the MCA. The bolus was immediately followed by an infusion of MK-801 (108 μg/kg/h at 0.6 ml/h i.v.) that continued throughout the experimental period. The control group received a bolus injection of saline (1 ml/kg i.v.) 1 h prior to endothelin-1 application that was followed by continuous infusion of saline (0.6 ml/h i.v.). Blood pressure and rectal temperature were monitored throughout. Temporalis muscle temperature was measured at the time of endothelin-1 application. Blood gases and plasma glucose were measured at one hourly intervals following MCA occlusion. 4 h post-MCA occlusion the rats were perfusion fixed and the volumes of ischaemic damage in the 3 groups assessed by quantitative histopathology as previously described (Section 2.3.4.).

7.1.3. Results

7.1.3.1. Physiological variables

Physiological variables prior to drug or vehicle administration, and pre- and post-MCA occlusion are shown in Table 18. There were no major differences between groups for any variable tested. In particular temporalis muscle temperatures at the time of endothelin-1 application to the MCA were similar in all groups. Plasma glucose levels tended to decline with time probably reflecting the relatively long duration of these experiments.

Immediately following administration of the bolus dose of MK-801 there was a rapid and significant reduction in mean arterial blood pressure in both MK-801 groups (Figure 50). MABP returned to basal level 30 min before MCA occlusion for the group in which MK-801 treatment was initiated 2.5 h pre-MCA occlusion. In contrast significant hypotension persisted until 30 min after MCA occlusion for the group in which MK-801 treatment was initiated only 1 h before the onset of ischaemia.

7.1.3.2. Effect of MK-801 on ischaemic damage

MK-801 treatment initiated 2.5 h pre-transient MCA occlusion markedly, and significantly, reduced the volumes of ischaemic damage in the whole hemisphere and caudate nucleus by 71 and 85% respectively (Figure 51). The volume of ischaemic damage in the cerebral cortex was reduced by 61% but this just failed to reach statistical significance at the 5% level. In contrast MK-801 treatment initiated 1 h pre-MCA occlusion did not significantly alter the volume of ischaemic damage in the whole hemisphere or cortex. There was a trend for reduction in the volume of damage in the caudate nucleus, but this was also not statistically significant.

MK-801 treatment initiated 2.5 h pre-MCA occlusion reduced the areas of ischaemic damage in hemisphere, cortex and caudate nucleus throughout the rostrocaudal extent of the lesion (Figure 52). The areas of damage in the caudate nucleus following the 1 h MK-801 pre-treatment were intermediate between the control and 2.5.h MK-801 group reflecting the trend for reduced volume of damage in this region following 1 h MK-801 pre-treatment. In contrast the 1 h MK-801 treatment tended to increase the cortical areas of damage towards the caudal part of the lesion compared with the saline control group (Figure 52).

Table 18 Physiological variables for effect of MK-801 against ischaemic damage induced by **transient** MCA occlusion

CONTROL (n = 10)

	PRE-SALINE	MCAO	+ 1 HOUR	+ 4 HOUR
pH	7.432 ± 0.045	7.401 ± 0.064	7.400 ± 0.032	7.392 ± 0.052
Pa CO_2 (mmHg)	34.4 ± 2.1	39.1 ± 3.2	37.1 ± 3.6	37.8 ± 2.7
Pa O_2 (mmHg)	170.3 ± 18.3	176.5 ± 25.2	173.9 ± 14.5	184.2 ± 23.6
Glucose (mmol/l)	9.25 ± 1.86	9.05 ± 1.61	9.16 ± 1.48	8.17 ± 1.25
Rectal Temp (°C)	36.98 ± 0.25	37.01 ± 0.19	37.00 ± 0.19	36.99 ± 0.17
Temporalis Temp (°C)		36.67 ± 0.29		

MK-801 1 h pre-MCAO (n = 9)

	PRE-MK-801	MCAO	+ 1 HOUR	+ 4 HOUR
pH	7.444 ± 0.059	7.404 ± 0.053	7.420 ± 0.039	7.413 ± 0.054
Pa CO_2 (mmHg)	36.2 ± 3.4	37.1 ± 2.7	36.6 ± 3.5	37.1 ± 2.5
Pa O_2 (mmHg)	176.9 ± 20.6	176.0 ± 21.7	180.2 ± 27.1	184.9 ± 14.9
Glucose (mmol/l)	9.10 ± 1.23	8.40 ± 1.73	8.03 ± 1.17	6.92 ± 1.02
Rectal Temp (°C)	36.92 ± 0.29	37.11 ± 0.29	36.92 ± 0.48	37.14 ± 0.14
Temporalis Temp (°C)		36.68 ± 0.29		

MK-801 2.5 h pre-MCAO (n = 9)

	PRE-MK-801	MCAO	+ 1 HOUR	+ 4 HOUR
pH	7.428 ± 0.035	7.403 ± 0.025	7.392 ± 0.032	7.406 ± 0.048
Pa CO_2 (mmHg)	36.9 ± 2.5	38.2 ± 2.6	35.7 ± 3.0	37.3 ± 2.9
Pa O_2 (mmHg)	181.8 ± 39.4	179.1 ± 29.1	176.7± 26.7	173.8 ± 21.6
Glucose (mmol/l)	8.70 ± 0.97	7.57 ± 1.00	7.20 ± 1.01	6.94 ± 0.62
Rectal Temp (°C)	36.94 ± 0.24	37.01 ± 0.08	36.99 ± 0.15	36.96 ± 0.10
Temporalis Temp (°C)		36.41 ± 0.28		

Treatment with MK-801 (0.12 mg/kg bolus then 108 µg/kg/h at 0.6 ml/h i.v.) or an equivalent volume of saline was initiated either 1 h or 2.5 h pre-MCA occlusion. Physiological variables were measured immediately prior to drug administration, immediately prior to MCA occlusion and 1 h and 4 h post-MCA occlusion.

Figure 50 Effect of MK-801 on mean arterial blood pressure pre- and post-transient MCA occlusion

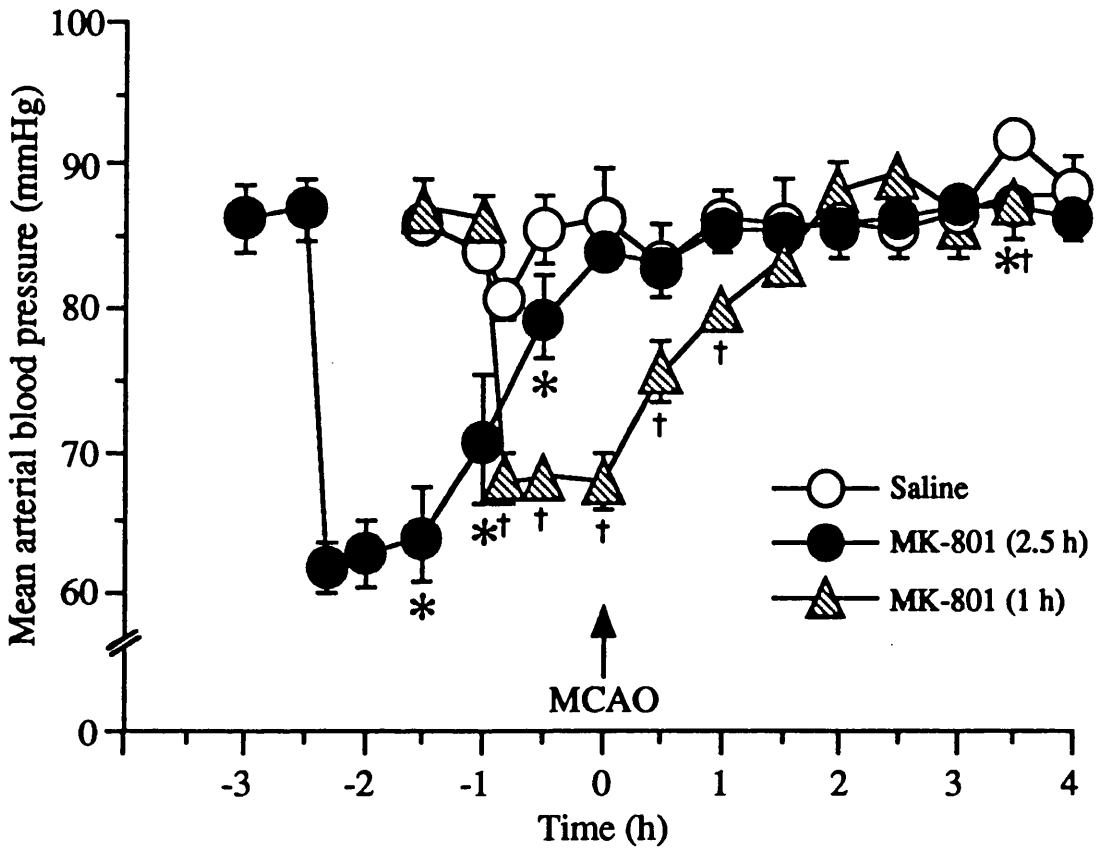

MK-801 was administered as a bolus (0.12 mg/kg i.v.) followed by continuous infusion (108 μg/kg/h at 0.6 ml/h). Treatment was started either 2.5 h or 1 h pre-MCA occlusion (MCAO). Both dosing schedules resulted in significant reductions in mean arterial blood pressure (MABP), but while MABP had returned to pre-drug levels by the time of MCAO for the 2.5 h group it was still significantly reduced for the 1 h pre-treatment group. *$p < 0.05$, †$p < 0.05$ comparison with saline control at same time point for 2.5 h and 1 h groups respectively.

Figure 51 Effect of MK-801 on volume of ischaemic damage induced by transient MCA occlusion

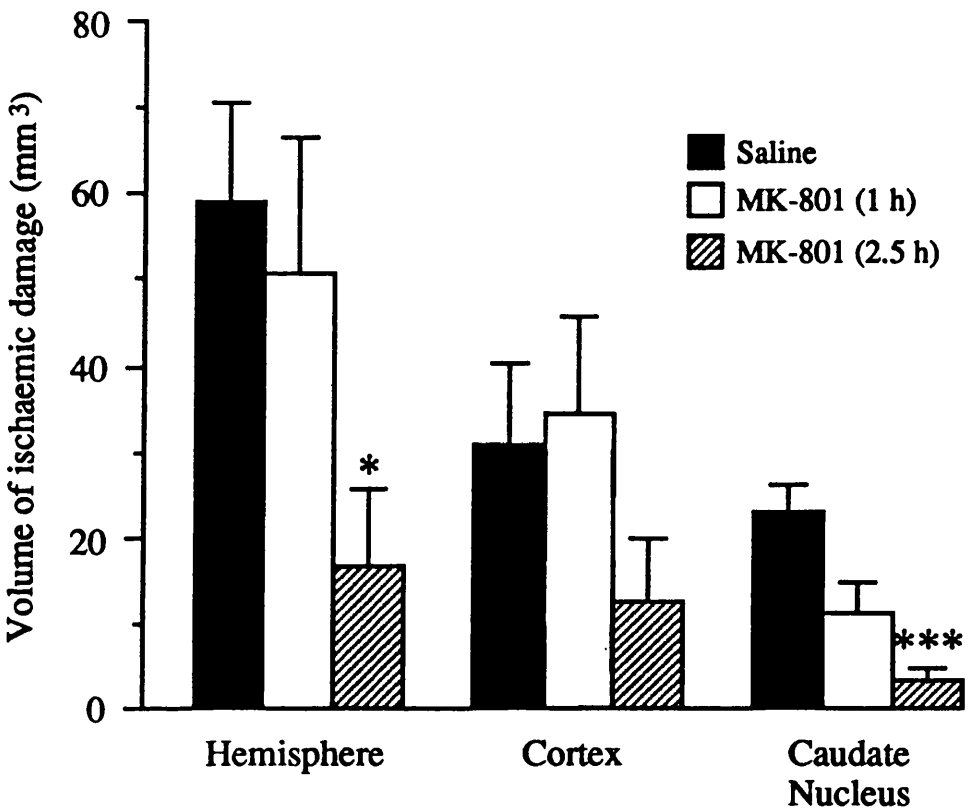

MK-801 pre-treatment (0.12 mg/kg bolus followed by 108 μg/kg/h at 0.6 ml/h i.v.) initiated 2.5 h pre-MCA occlusion significantly reduced the mean volumes of ischaemic damage in the whole hemisphere and caudate nucleus. In contrast MK-801 treatment initiated only 1 h pre-MCA occlusion did not significantly alter the mean volumes of ischaemic damage in hemisphere, cortex or caudate nucleus. *$p < 0.05$, ***$p < 0.001$ compared with saline control group respectively (unpaired Student's t-test with Bonferroni correction).

Figure 52 Effect of MK-801 on areas of ischaemic damage following **transient** MCA occlusion

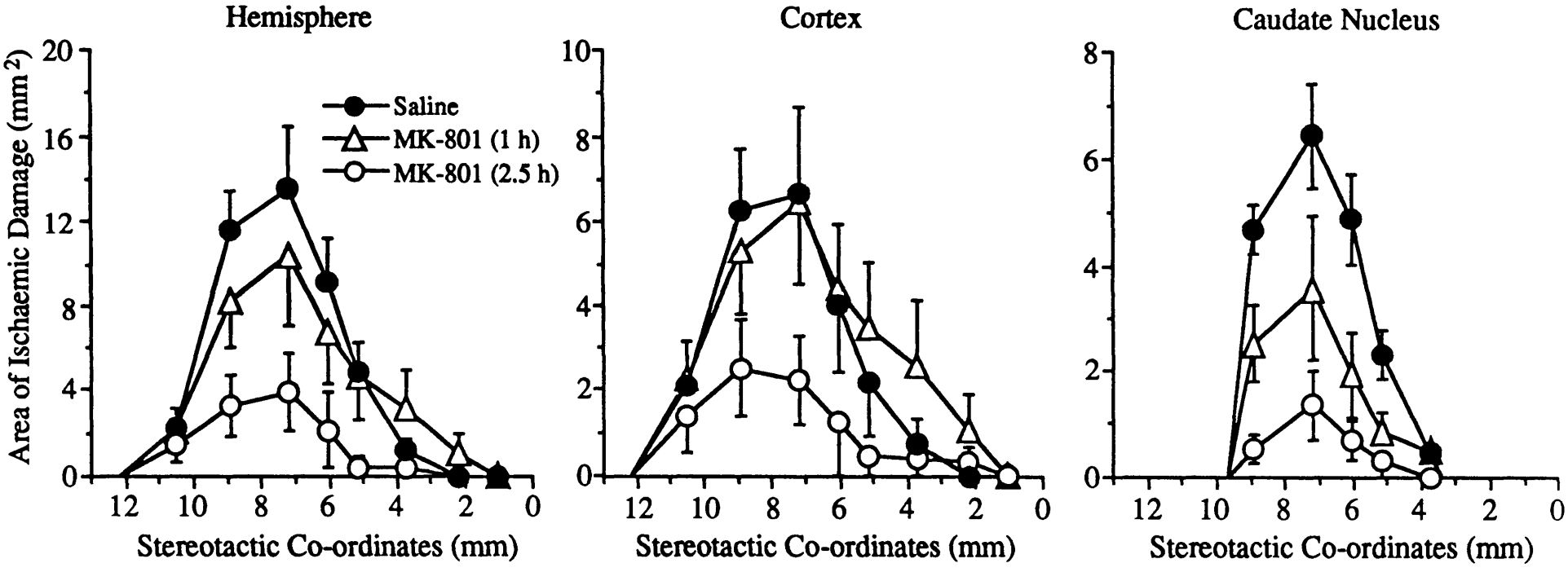

MK-801 (0.12 mg/kg bolus, then 108 μg/kg/h at 0.6 ml/h i.v.) administered 2.5 h pre-transient MCA occlusion reduced the mean areas of damage in the hemisphere, cortex and caudate nucleus compared to the saline control. While MK-801 treatment inititated only 1 h pre-MCA occlusion had an intermediate effect on the areas of damage in the caudate nucleus and did not reduce the areas of damage in the cortex.

7.1.4. Discussion

In halothane-anaesthetised rats bolus injection of 0.5 mg/kg MK-801 (a dose that significantly reduces the volume of ischaemic damage following permanent MCA occlusion, Park *et al.* 1988; Roussel *et al.* 1992a) induces an immediate and relatively prolonged hypotension where MABP falls below 60 mmHg (Park *et al.* 1988; Park *et al.* 1989). Transient hypotension of this magnitude can significantly increase the volume of ischaemic damage (Osborne *et al.* 1987) and blood-brain barrier permeability (Tyson *et al.* 1982) following permanent MCA occlusion. In view of this, and the apparent relationship between outcome and MABP following transient MCA occlusion (see Section 4.1.4.), we wished to avoid the confounding influence of MK-801-induced hypotension in the present study. MK-801 was therefore administered as a low bolus dose followed by a continuous intravenous infusion using a dosing schedule previously demonstrated to transiently reduce MABP below 75 mmHg for less than 15 min while providing significant neuroprotection against permanent MCA occlusion (Gill *et al.* 1991). However despite the use of this dosing schedule a relatively prolonged hypotension was still observed in the present study. This result was in contrast to the Gill *et al.* study where MK-801 treatment was initiated immediately following MCA occlusion. This suggests an interaction between MK-801 and the surgical procedure involved in exposing the MCA prolongs the hypotensive action of the drug. A similar phenomenon has been observed with bolus administration of MK-801: MABP remains significantly depressed (below 75 mmHg for 3.5 h) when MK-801 is administered pre-MCA occlusion whereas MABP returns to control level within 60 min when the drug is given post-MCA occlusion (Park *et al.* 1988). To compensate for the prolonged hypotensive response a second group of animals was included in the study in which MK-801 infusion was started 2.5 h pre-MCA occlusion to ensure that MABP had returned to control levels by the time of MCA occlusion. The infusion rate employed in the current study attains steady state plasma levels of MK-801(18.9 ng/ml) within 60 min (Gill *et al.* 1991; Willis *et al.* 1991), therefore the plasma concentrations of MK-801 at the time of MCA occlusion should have been equivalent in both MK-801 groups, the only difference being the relative MABP.

In this study the MK-801 infusion initiated 2.5 h prior to MCA occlusion significantly reduced the volume of ischaemic damage while the 1 h pre-MCA occlusion infusion did not. Thus the lower MABP at the onset of ischaemia in the 1 h group (68 ± 6 mmHg compared to 84 ± 4 mmHg) appears to have increased the severity of the ischaemic insult (as for permanent MCA occlusion, Osborne *et al.* 1987) and directly counteracted the neuroprotective action of the drug. Significant neuroprotection was demonstrated in the caudate nucleus following the 2.5 h pre-treatment with MK-801. In contrast to this result

ischaemic damage in the caudate nucleus following permanent MCA occlusion in the rat is usually resistant to MK-801 (Gill *et al.* 1991; Roussel *et al.* 1992a) although a very small neuroprotective effect has been reported (Park *et al.* 1990). The lack of efficacy of MK-801 against striatal damage following permanent focal ischaemia is usually attributed to the absence of collateral supply to this region (Gill *et al.* 1991). In the context of transient MCA occlusion the restoration of blood supply to the caudate nucleus allows the potential salvage of the tissue as demonstrated in the present study.

In addition to its peripheral action on blood pressure MK-801 has marked effects on cerebral glucose metabolism and CBF, which differ in conscious and anesthetised rats (Kurumaji & McCulloch 1989; Nehls *et al.* 1990; Park *et al.* 1989; Roussel *et al.* 1992b), and which could potentially influence outcome following cerebral ischaemia. In conscious rats MK-801 increases local CBF in specific regions including the neocortex and caudate nucleus while minimally affecting other regions (Nehls *et al.* 1990; Roussel *et al.* 1992b). In contrast under halothane anaesthesia MK-801 induces widespread homogeneous reductions in local CBF (of approximately 37%) in the majority of brain regions including cortex and caudate nucleus (Park *et al.* 1989). However following MCA occlusion in halothane-anaesthetised rats and cats, MK-801 does not invoke further reductions in CBF in the MCA territory beyond the control level of ischaemia (Dezsi *et al.* 1992; Greenberg *et al.* 1991; Park *et al.* 1989). Therefore the cerebrovascular effects of MK-801 are likely to have less impact on outcome following experimental ischaemia in which halothane anaesthesia is maintained (as in the present study) compared with studies in which animals are allowed to regain consciousness.

MK-801 administered either during ischaemia and reperfusion, or immediately prior to onset of ischaemia, significantly reduces the amount of damage following 2-3 h transient MCA occlusion combined with 22 or 3 h reperfusion in normotensive rats (Buchan *et al.* 1992a; Yang *et al.* 1991 respectively). However in these models the animals were conscious for most of the ischaemic period and all of the reperfusion phase, and the beneficial action of MK-801 has been attributed to the observed increase in blood flow in the ischaemic core region (Buchan *et al.* 1992a). To the best of our knowledge the present study is the first (for normotensive rats) in which halothane anaesthesia was maintained throughout both the ischaemic and reperfusion periods and in which therefore MK-801 probably does not significantly influence CBF in the MCA territory. Therefore the present results represent the first study of transient focal cerebral ischaemia in the normotensive rat to demonstrate a beneficial effect of MK-801 pre-treatment that is independent of the cerebrovascular effects of the drug and probably mediated by its antiexcitotoxic action. This result has been confirmed by studies in halothane-anaesthetised cats. MK-801 (1

mg/kg), administered during a 2 h period of MCA occlusion, significantly reduces the volume of hemispheric damage (by 29%) assessed after 4 h reperfusion, without altering CBF in the peripheral MCA territory during either the ischaemic or reperfusion phases (Dezsi *et al.* 1992). Similar results have been obtained (2mg/kg MK-801) with a 1 h period of MCA occlusion followed by 3 h reperfusion (Greenberg *et al.* 1991).

In SHR, where MK-801 does not improve CBF in the ischaemic core of conscious rats (Buchan *et al.* 1992a), pre-treatment with MK-801 or the alternative non-competitive NMDA antagonist ketamine, does not significantly alter ischaemic damage assessed 24 or 96 h following a 2 h period of transient MCA occlusion (Buchan *et al.* 1992a; Panetta *et al.* 1989; Ridenour *et al.* 1991). However it is also more difficult to demonstrate significant neuroprotection with MK-801 against permanent MCA occlusion in this strain (Roussel *et al.* 1992a) due to the inefficient collateral circulation. In contrast to MK-801, the AMPA antagonist NBQX has been reported to reduce the volume of ischaemic damage at 24 h following 2 h transient MCA occlusion in SHR (Buchan *et al.* 1991b), apparently without altering CBF. A more dramatic, long term protective effect of the non-selective AMPA/kainate antagonist DNQX has also been reported in which DNQX administered prior to, and immediately following, onset of ischaemia significantly reduced brain atrophy measured 1 month following 60 min transient MCA occlusion induced by the intraluminal thread technique (Hara *et al.* 1993).

Glutamate-induced excitotoxic mechanisms are one of the main mediators of ischaemic injury following permanent focal ischaemia as evidenced by the marked increase in extracellular glutamate (Butcher *et al.* 1990) and the repeated demonstration of efficacy of a wide range of glutamate receptor antagonists in animal models of permanent MCA occlusion (Bullock *et al.* 1990; Gill *et al.* 1991; Park *et al.* 1988; Simon & Shiraishi 1990). However following transient MCA occlusion the volume of ischaemic damage continues to increase after the onset of reperfusion (see Section 4.1.2.) suggesting that secondary mechanisms, other than glutamate, contribute to outcome in these models. However glutamate released during the ischaemic phase may indirectly lead to reperfusion injury by 'priming' the brain to increase oxygen radical and NO production at the onset of reperfusion. Thus the observed beneficial effect of MK-801 pre-treatment in the endothelin-1 model of transient focal ischaemia may be due to direct antagonism of glutamate-induced excitotoxicity in the ischaemic phase and consequential prevention of glutamate-induced production of free radicals and other potentially neurotoxic molecules in the reperfusion phase.

Following MCA occlusion extracellular glutamate levels in the cortex rapidly increase reaching a peak approximately 30-60 min post-onset of ischaemia with subsequent decline towards basal levels despite the persistence of the occlusion (Butcher *et al.* 1990; Ginsberg *et al.* 1992; Graham *et al.* 1990). With the onset of reperfusion only a small, very transient, increase in the extracellular concentration of glutamate occurs (Ginsberg *et al.* 1992), thus the direct contribution of glutamate to injury is likely to be less during the reperfusion phase compared with the ischaemic phase of the insult. Consequently glutamate receptor antagonists may be less efficacious when administered post-onset of reperfusion compared to the pre-ischaemic dosing schedule used in the present experiment. Future studies using the endothelin-1 model of transient ischaemia could address this issue, although the effects of MK-801 on blood pressure and CBF in the conscious rat discussed above will make experimental design and interpretation difficult.

7.2. Effect of L-NAME pre-treatment on ischaemic damage following transient and permanent MCA occlusion

7.2.1. Introduction

The demonstration that under certain conditions NO synthase inhibitors can antagonise glutamate toxicity *in vitro* (see Section 1.6) raised the possibility that these drugs would be efficacious against ischaemic damage *in vivo*. The potential neuroprotective action of the NO synthase inhibitor L-NAME was therefore assessed in a series of experiments in anaesthetised rats killed 4 h post-onset of transient or permanent MCA occlusion.

7.2.2. Experimental protocol

In the first series a relatively high dose of L-NAME (30 mg/kg s.c.) was administered 30 min pre- and 30 min post-permanent MCA occlusion only. Control rats received an equivalent volume of saline (1 ml/kg s.c.). Blood pressure and rectal temperature were monitored throughout, while blood gases and plasma glucose were measured at one hourly intervals. 4 h post-MCA occlusion rats were killed by perfusion fixation and volumes of ischaemic damage determined using quantitative histopathology.

In the second series of experiments a lower dose of L-NAME (3 mg/kg i.v.), or an equivalent volume of saline (1 ml/kg i.v.), was adminstered 30 min prior to induction of permanent or transient MCA occlusion. Physiological variables were monitored as above and in addition temporalis muscle temperature was measured at the time of MCA occlusion. Rats were killed 4 h post-MCA occlusion and the brains processed for quantitative histopathology.

7.2.3. Results

7.2.3.1. Physiological variables

Physiological variables for the 3 separate studies are shown in Tables 19, 20 and 21 and were within the normal ranges for all groups.

Table 19 Physiological variables for effect of L-NAME (30 mg/kg) against ischaemic damage induced by **permanent** MCA occlusion

CONTROL (n = 9)

	PRE-SALINE	MCAO	+ 1 HOUR	+ 4 HOUR
pH	7.433 ± 0.037	7.452 ± 0.036	7.470 ± 0.045	7.443 ± 0.045
Pa CO_2 (mmHg)	37.4 ± 2.7	37.0 ± 0.4	37.0 ± 4.1	37.6 ± 2.5
Pa O_2 (mmHg)	144.1 ± 22.1	136.0 ± 17.0	153.3 ± 27.6	167.8 ± 21.0
Rectal Temp (°C)	37.05 ± 0.14	36.98 ± 0.42	36.90 ± 0.18	36.91 ± 0.18
Glucose (mmol/l)	10.78 ± 1.05	10.53 ± 2.10	9.75 ± 1.98	10.25 ± 1.35

L-NAME (n = 9)

	PRE-L-NAME	MCAO	+ 1 HOUR	+ 4 HOUR
pH	7.460 ± 0.064	7.448± 0.078	7.421 ± 0.063	7.383 ± 0.045
Pa CO_2 (mmHg)	37.2 ± 1.6	36.8 ± 1.4	36.3 ± 3.0	38.3 ± 2.4
Pa O_2 (mmHg)	149.4 ± 19.4	155.2 ± 17.8	152.8 ± 16.4	147.1 ± 12.8
Rectal Temp (°C)	37.15 ± 0.24	37.06 ± 0.57	37.21 ± 0.33	37.06 ± 0.36
Glucose (mmol/l)	10.52 ± 2.10	9.91 ± 1.17	9.65 ± 1.04	8.32 ± 2.04

L-NAME (30 mg/kg s.c.) or saline was administered 30 min pre- and 30 min post-permanent MCA occlusion (MCAO) in the anaesthetised rat.

Table 20 Physiological variables for effect of L-NAME (3 mg/kg) against ischaemic damage induced by **permanent** MCA occlusion

CONTROL (n = 5)

	PRE-SALINE	MCAO	+ 1 HOUR	+ 4 HOUR
pH	7.392 ± 0.056	7.395 ± 0.028	7.387 ± 0.027	7.405 ± 0.041
Pa CO_2 (mmHg)	35.2 ± 2.7	36.7 ± 2.2	39.7 ± 5.3	37.0 ± 2.6
Pa O_2 (mmHg)	201.3 ± 24.9	212.3 ± 32.1	209.3 ± 20.9	220.5 ± 32.0
Glucose (mmol/l)	8.90 ± 1.38	8.60 ± 1.10	8.12 ± 0.73	8.17 ± 0.95
Rectal Temp (°C)	37.1 ± 0.11	37.02 ± 0.28	37.12 ± 0.21	37.00 ± 0.00
Temporalis Temp (°C)	36.72 ± 0.34	36.52 ± 0.66		

L-NAME (n = 6)

	PRE-L-NAME	MCAO	+ 1 HOUR	+ 4 HOUR
pH	7.393 ± 0.051	7.390± 0.037	7.368 ± 0.048	7.387 ± 0.062
Pa CO_2 (mmHg)	37.2 ± 1.7	36.0 ± 4.1	35.0 ± 4.2	34.8 ± 2.0
Pa O_2 (mmHg)	203.5 ± 26.6	204.0 ± 25.0	198.7 ± 31.2	208.0 ± 24.9
Glucose (mmol/l)	8.37 ± 0.76	9.02 ± 0.36	8.70 ± 0.70	8.15 ± 0.72
Rectal Temp (°C)	37.15 ± 0.27	37.27 ± 0.27	37.07 ± 0.23	37.03 ± 0.08
Temporalis Temp (°C)	36.40 ± 0.13	36.78 ± 0.39		

L-NAME (3 mg/kg i.v.) or saline was administered 30 min prior to permanent MCA occlusion (MCAO) in the anaesthetised rat.

Table 21 Physiological variables for effect of L-NAME (3 mg/kg) against ischaemic damage induced by **transient** MCA occlusion

CONTROL (n = 14)

	PRE-SALINE	MCAO	+ 1 HOUR	+ 4 HOUR
pH	7.417 ± 0.024	7.391 ± 0.027	7.391 ± 0.033	7.409 ± 0.035
Pa CO_2 (mmHg)	37.6 ± 3.2	39.0 ± 3.8	37.1 ± 3.7	37.0 ± 2.8
Pa O_2 (mmHg)	175.2 ± 27.9	171.3 ± 30.1	176.6 ± 24.6	183.6 ± 21.5
Glucose (mmol/l)	9.47 ± 1.13	9.58 ± 1.42	8.74 ± 1.06	8.00 ± 1.00
Rectal Temp (°C)	36.86 ± 0.23	37.16 ± 0.30	37.11 ± 0.41	37.04 ± 0.17
Temporalis Temp (°C)		36.63 ± 0.40		

L-NAME (n = 14)

	PRE-L-NAME	MCAO	+ 1 HOUR	+ 4 HOUR
pH	7.415 ± 0.051	7.384 ± 0.046	7.379 ± 0.021	7.384 ± 0.043
Pa CO_2 (mmHg)	36.1 ± 3.5	35.2 ± 2.4	38.4 ± 2.3	36.8 ± 3.1
Pa O_2 (mmHg)	168.5 ± 23.7	166.9 ± 19.7	173.9 ± 25.9	177.6 ± 25.5
Glucose (mmol/l)	9.31 ± 0.99	8.71 ± 1.12	7.94 ± 0.80	7.60 ± 1.06
Rectal Temp (°C)	37.05 ± 0.37	37.06 ± 0.39	37.00 ± 0.32	37.04 ± 0.12
Temporalis Temp (°C)		36.54 ± 0.24		

L-NAME (3 mg/kg i.v.) or saline was administered 30 min prior to transient MCA occlusion (MCAO) in the anaesthetised rat.

In the first series of experiments repeat dosing of the higher dose of L-NAME (30 mg/kg 30 min pre- and post-permanent MCA occlusion) resulted in a moderate hypertensive effect (see Figure 53). Statistical analysis revealed a significant drug-time interaction ($p = 0.01$) for this study that resulted in significant differences in MABP between the L-NAME and saline groups at 4 time points following the second dose of L-NAME (2-way repeated measure ANOVA followed by unpaired Student's t-tests with Bonferroni correction). In contrast the lower dose of L-NAME (3 mg/kg administered 30 min pre-MCA occlusion only) did not significantly alter MABP in either the transient or permanent MCA occlusion model (Figures 54 and 55).

7.2.3.2. Effect of L-NAME on ischaemic damage

Permanent MCA occlusion

L-NAME (30 mg/kg 30 min pre- and post-permanent MCA occlusion) did not significantly alter the volume of ischaemic damage in whole hemisphere, cortex or caudate nucleus (Figure 56). In fact the total volume of ischaemic damage was marginally greater in the L-NAME group compared to the saline control. In contrast the lower dose of L-NAME (3 mg/kg) significantly reduced the volume of ischaemic damage following permanent MCA occlusion in whole hemisphere and cortex (Figure 57) although the effect was relatively small (the total volume of tissue salvaged was 12 mm^3 representing a 16% reduction in the total volume of ischaemic damage). The volume of ischaemic damage in the caudate nucleus was not significantly altered by L-NAME pre-treatment.

The modest neuroprotective effect of L-NAME (3 mg/kg) in the volumetric assessment of ischaemic damage was paralled by only minor reductions in the areas of ischaemic damage in the hemisphere and cortex, while it had no effect on areas of damage in the caudate nucleus (Figure 58).

Transient MCA occlusion

The anti-ischaemic efficacy of L-NAME (3 mg/kg) in this model was similar in magnitude to that observed for permanent MCA occlusion. L-NAME reduced the volumes of ischaemic damage in the whole hemisphere, cortex and caudate nucleus by 29%, 26% and 33% respectively following transient MCA occlusion (Figure 59), with the total volume of tissue salvaged being 16 mm^3. However these reductions did not reach statistical significance because of the greater variability encountered in this model compared to the permanent MCA occlusion model.

Figure 53 Effect of L-NAME (30 mg/kg) on blood pressure pre- and post-permanent MCA occlusion

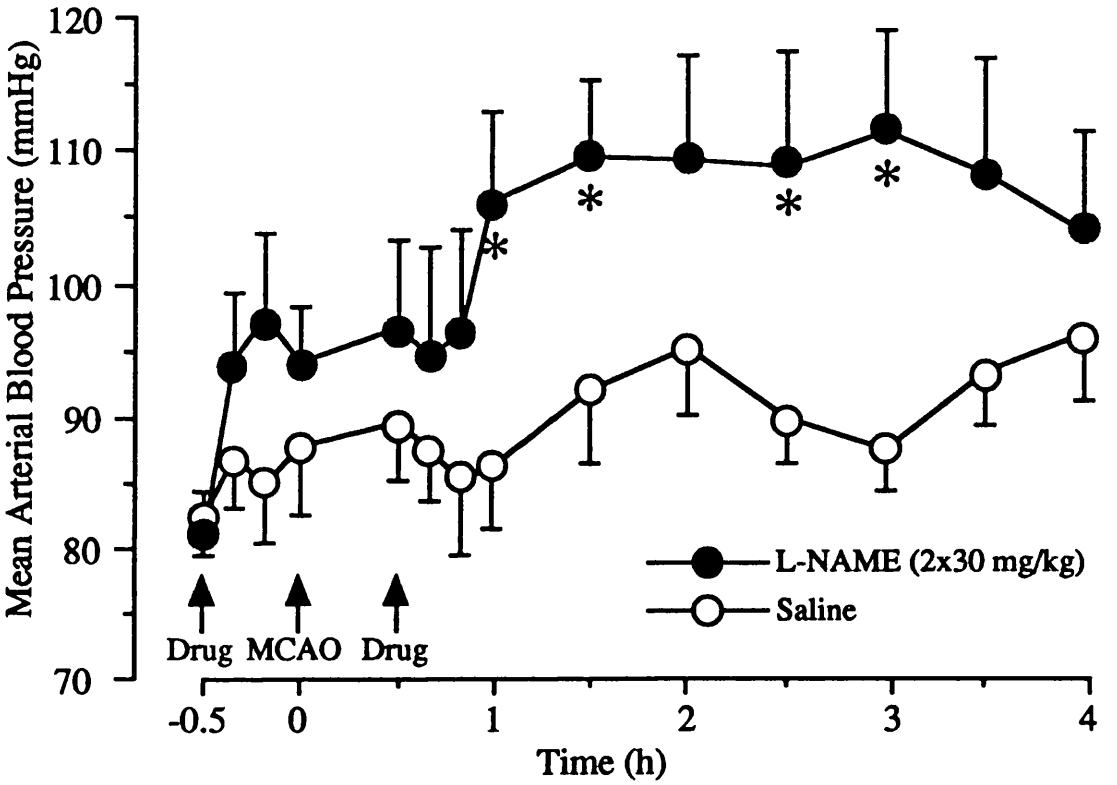

L-NAME (30 mg/kg s.c.) or saline was administered 30 min pre- and 30 min post-MCA occlusion (MCAO) in the anaesthetised rat. Mean arterial blood pressure was significantly increased (*$p < 0.05$) following the second dose of L-NAME.

Figure 54 Effect of L-NAME (3 mg/kg) on blood pressure pre- and post-permanent MCA occlusion

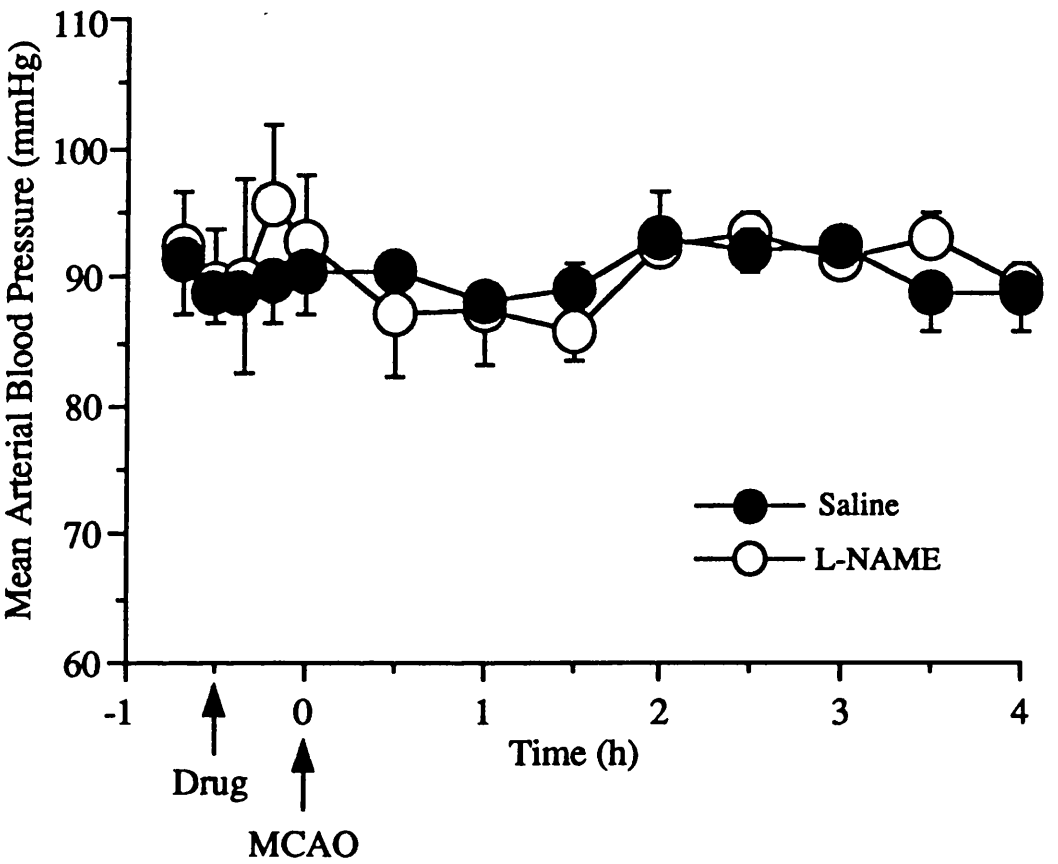

L-NAME (3 mg/kg i.v.) or saline was administered 30 min prior to permanent MCA occlusion (MCAO) in the anaesthetised rat. In this study L-NAME had no significant effect on mean arterial blood pressure.

Figure 55 Effect of L-NAME (3 mg/kg) on blood pressure pre- and post-transient MCA occlusion

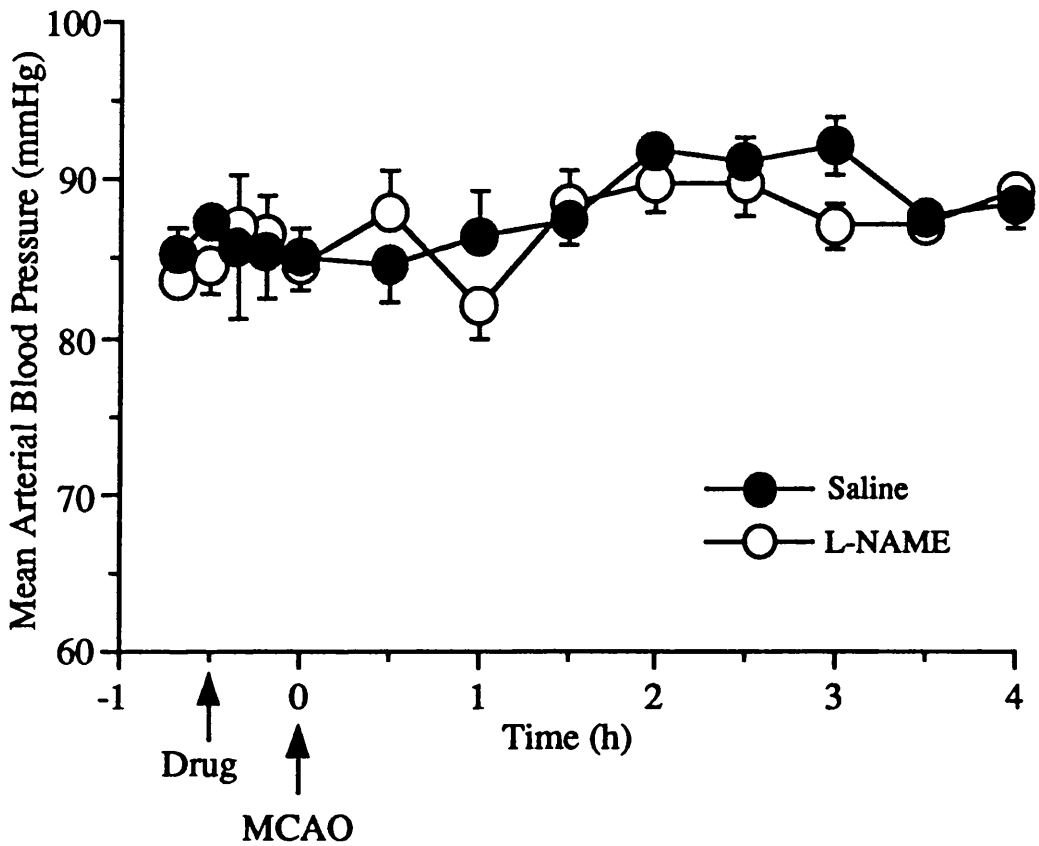

L-NAME (3 mg/kg i.v.) or saline was administered 30 min prior to transient MCA occlusion (MCAO) in the anaesthetised rat. In this study L-NAME had no significant effect on mean arterial blood pressure.

Figure 56 Effect of L-NAME (30 mg/kg) on volume of ischaemic damage induced by **permanent** MCA occlusion

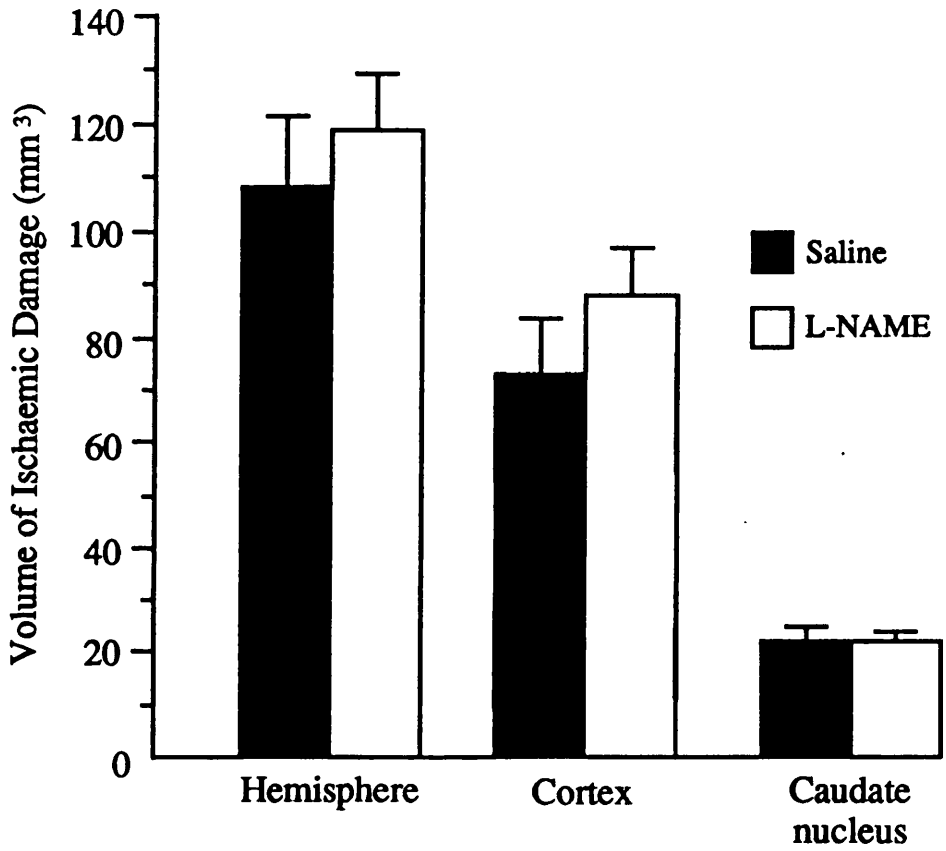

L-NAME (30 mg/kg s.c., n = 9) or saline (n = 9) was administered 30 min pre- and 30 min post-MCA occlusion. This relatively high dose of L-NAME did not significantly alter the mean volumes of ischaemic damage in hemisphere, cortex or caudate nucleus ($p > 0.05$ unpaired Student's t-tests).

Figure 57 Effect of L-NAME (3 mg/kg) on volume of ischaemic damage induced by permanent MCA occlusion

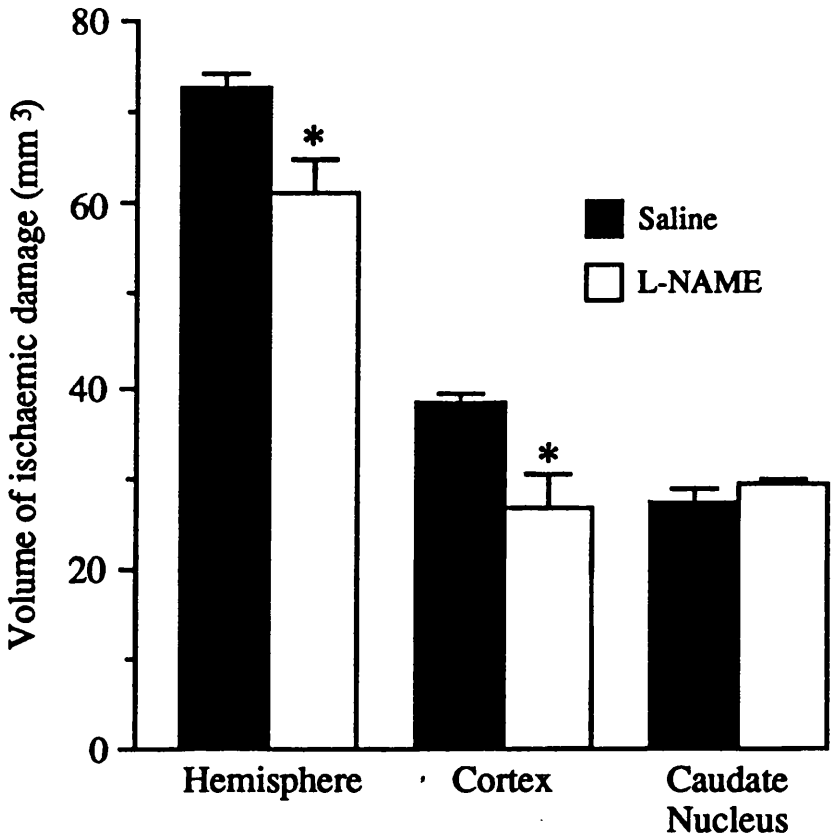

L-NAME (3 mg/kg i.v., n = 6) or saline (n = 5) was administered 30 min prior to permanent MCA occlusion in the anaesthetised rat. This relatively low dose of L-NAME significantly reduced the mean volumes of ischaemic damage in the whole hemisphere and cerebral cortex compared with saline control (*$p < 0.05$, unpaired Student's t-tests).

Figure 58 Effect of L-NAME (3 mg/kg) on areas of ischaemic damage following **permanent** MCA occlusion

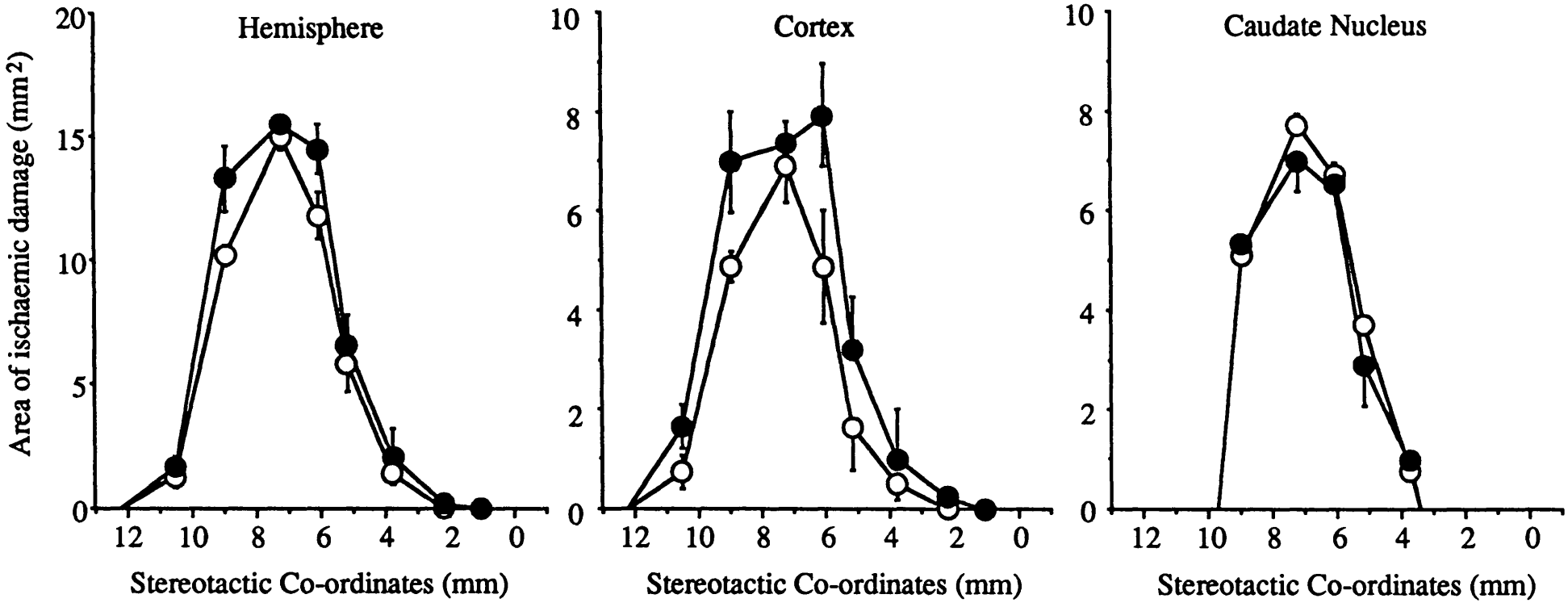

L-NAME (3 mg/kg i.v., open symbols) or saline (closed symbols) was administered 30 min prior to permanent MCA occlusion in the anaesthetised rat. L-NAME marginally reduced the mean areas of damage in the hemisphere and cerebral cortex, while having no obvious effect on areas of damage in the caudate nucleus.

Figure 59 Effect of L-NAME (3 mg/kg) on volume of ischaemic damage induced by **transient** MCA occlusion

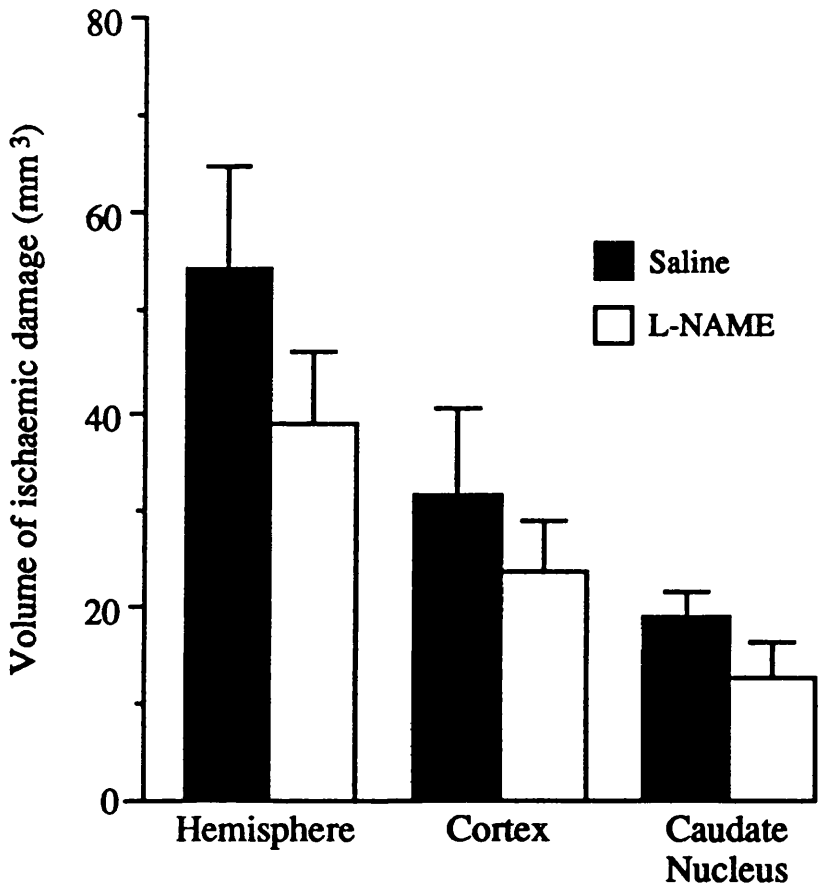

L-NAME (3 mg/kg i.v., n = 14) or saline (n = 14) was administered 30 min prior to transient MCA occlusion in the anaesthetised rat. L-NAME did not significantly reduce the volume of ischaemic damage compared to the saline control ($p > 0.05$ unpaired Student's t-tests).

7.2.4. Discussion

In the first pharmacoprotection study utilising permanent MCA occlusion L-NAME had no neuroprotective effect, whereas in the second series of experiments the drug had a signficant neuroprotective action. The difference between the 2 studies lies in the treatment paradigms employed: with 3 mg/kg L-NAME a significant, if comparatively moderate, reduction in ischaemic damage was achieved, but increasing the dose to 2 x 30 mg/kg resulted in the abolition of this beneficial effect.

The results presented in the preceding chapter demonstrated that the cerebral vasoconstrictive action of L-NAME is dose-dependent with 30 mg/kg producing significantly greater hypoperfusion than 3 mg/kg in the conscious rat (see Section 6.1.). Therefore the more severe vasoconstrictive response elicited by 2 x 30 mg/kg L-NAME in the current study (assuming a similar dose-response relationship is maintained in anaesthetised, ischaemic animals) may have further reduced blood flow to the MCA territory resulting in a more severe ischaemic insult that directly counteracted the neuroprotective action of the drug exhibited at the lower dose (3 mg/kg). However even at 3mg/kg the degree of neuroprotection achieved with L-NAME (12 mm^3 tissue salvaged) is smaller than that observed for MK-801 (0.5 mg/kg) pre-treatment in the same model (41 mm^3 of tissue salvaged, Park *et al.* 1988) suggesting that the contribution of NO to permanent focal ischaemic injury is less than that of glutamate. Following MCA occlusion there is an acute transient elevation in NO that reaches its peak within 5 minutes of the onset of ischaemia and declines to basal levels within one hour (Trifiletti *et al.* 1992; Malinski *et al.* 1993). Thus during severe ischaemia NO production can not be maintained despite the more prolonged elevation in extracellular glutamate (Butcher *et al.* 1990). This may reflect chronic depletion of oxygen and energy supplies since continued production of NO necessitates continued supply of adequate levels of oxygen (as substrate, see Rengasamy & Johns 1991) and ATP (to regenerate the cofactor NADPH). Therefore neuronal NO may not be a major contributor to ischaemic damage in the acute post-ischaemic period following permanent MCA occlusion and this, together with the vasoconstriction induced by L-NAME, may explain the very modest neuroprotective effect of L-NAME observed following 4 h permanent MCA occlusion in the present series of experiments.

With the onset of reperfusion (and the restoration of energy supplies) following transient MCA occlusion there is a slow, progressive increase in NO production that is maintained for at least 1 h (Malinski *et al.* 1993). Thus the potential for NO-mediated injury would appear greater in the context of transient MCA occlusion followed by reperfusion than for permanent MCA occlusion. However our results do not support this premise since in the

present studies 3 mg/kg L-NAME had a broadly similar effect on ischaemic damage following both transient and permanent MCA occlusion (the volumes of tissue salvaged were 16 and 12 mm^3 respectively). The only difference being that, due to the greater variability in the transient model relative to the permanent model (see Section 8.2), the comparable reduction in ischaemic damage did not attain statistical significance.

In addition, as for permanent MCA occlusion, the efficacy of L-NAME pre-treatment was smaller than that observed for MK-801 pre-treatment in the same model (16 and 42 mm^3 of tissue salvaged by L-NAME and MK-801 respectively). Thus the cerebrohypoperfusion induced by L-NAME during the ischaemic phase may have again detracted from the direct anti-excitotoxic action of the drug in the transient MCA occlusion model. In addition several other factors may have contributed to the modest efficacy of L-NAME in this study. Firstly L-NAME pre-treatment was observed to facilitate the vasoconstriction of the MCA elicited by endothelin-1. L-NAME may therefore have increased the severity of the initial ischaemic insult compared to saline controls by removing a tonic basal NO-mediated vasodilatation. Enhancement of the vasomotor response to endothelin-1 by L-NAME has also been reported for other vascular beds (Gardiner *et al.* 1990b; Lerman *et al.* 1992). Secondly L-NAME may have adverse effects during the reperfusion phase that follows a period of transient ischaemia. NO synthase inhibitors enhance leucocyte adherence to vascular endothelium (Ma *et al.* 1993) and may therefore impair restoration of blood flow to ischaemic regions (see also Section 1.4.5). Furthermore it has recently been demonstrated that L-NAME pre-treatment results in prolonged elevation of extracellular glutamate levels in the reperfusion phase following transient global ischaemia (Zhang, J. *et al.* 1993). The mechanism behind this effect remains to be established, but it has been suggested that prevention of NO formation may prolong the half-life of superoxide and promote superoxide-induced glutamate release (Zhang, J. *et al.* 1993). The effect of NO synthase inhibition on glutamate levels during focal ischaemia/reperfusion has not yet been investigated, but enhancement of extracellular glutamate levels in the reperfusion phase may be another factor detracting from the inherent neuroprotective action of L-NAME in the endothelin-1 model of transient focal ischaemia.

In summary these experiments have demonstrated that the anti-ischaemic efficacy of L-NAME in both transient and permanent acute focal ischaemia is comparatively weak, and that careful choice of the dosing schedule is necessary to prevent loss of this small neuroprotective effect.

In the past 2 years several studies concerning the anti-ischaemic efficacy of L-NAME and other NOS inhibitors have been published in the scientific literature. The results of these studies have been diverse, ranging from marked beneficial effects of NOS inhibition on focal ischaemic damage to significant exacerbation of lesion size. In the following paragraphs I shall attempt to explain these discrepant findings and relate them to the moderate neuroprotective effect of L-NAME obtained in the current thesis.

The observation that inhibitors of NOS antagonise glutamate toxicity *in vitro* (Dawson *et al.* 1991) led directly to investigation of the possible role of NO in the pathophysiology of cerebral ischaemic damage. Elevated levels of extracellular glutamate observed during ischaemia *in vivo* (Butcher *et al.* 1990) were postulated to lead to an increase in neuronal NO production via an increase in intracellular Ca^{2+} and activation of constitutive NO synthase. The first published reports concerning the potential neuroprotective actions of NOS inhibitors were encouraging. Repeated dosing of L-nitroarginine or L-NAME throughout long survival periods was reported to dramatically reduce the volume of ischaemic damage following permanent MCA occlusion in mice (Nowicki *et al.* 1991) and rats (Buisson *et al.* 1992). However subsequent studies in which NOS inhibitors were dosed prior to and/or immediately following MCA occlusion have been unable to confirm these findings with NOS inhibition reported to have no effect (Xue *et al.* 1992a) or exacerbate (Yamamoto *et al.* 1992; Zhang, F. *et al.* 1993) ischaemic damage. The different dosing schedules employed by these 2 groups of studies may explain the discrepant results suggesting that late production of NO is detrimental to outcome while early NO production may be of benefit.

Although investigation of the role of NO in cerebral ischaemic damage was initiated by the hypothesis that excess glutamate stimulated neuronal production of NO, it now appears that endothelial and inducible NOS may be of greater importance than the neuronal form of the enzyme in dictating outcome following ischaemia. Endothelial-derived NO, produced immediately after onset of ischaemia (Tominaga *et al.* 1993), may be beneficial to outcome by inducing vasodilation and improving CBF to the ischaemic region. This effect can be augmented by exogenously-derived NO since administration of the NO donor sodium nitroprusside (Zhang, F. *et al.* 1993) or the NO precursor L-arginine (Morikawa *et al.* 1992c) immediately following permanent MCA occlusion improve CBF in the ischaemic region and reduce infarct size 24 h post-onset of ischaemia (Morikawa *et al.* 1992b; Zhang, F. *et al.* 1993). As discussed above inhibition of endothelial NO production promotes cerebrovasoconstriction. Furthermore NOS inhibitors also potentiate platelet aggregation (Radomski *et al.* 1987) and induce red blood cell stasis in brain capillaries leading to 'ischaemic microregions' (Prado *et al.* 1992). All of these responses may cause further

reduction in flow through the MCA and also impair collateral blood flow to the ischaemic region. Thus non-selective inhibition of NO synthesis in the immediate post-ischaemic period appears detrimental to outcome. The consequences of such endothelial NOS inhibition may be greater in SHR than normotensive rat strains. It is known that cytokine production is increased in SHR compared to normotensive rats (Hallenbeck *et al.* 1991) and that elevated levels of cytokines can switch vessels from an active anti-coagulant state to a procoagulant state where introduction of any further anticoagulant factor can induce severe ischaemia (Hallenbeck *et al.* 1991). Inhibition of NOS may be such a factor and this may explain why L-nitroarginine has been reported to increase ischaemic damage following permanent MCA occlusion in the SHR (Yamamoto *et al.* 1992).

In contrast to the immediate increase in endothelial-derived NO which is of potential benefit in cerebral ischaemia, NO produced several hours or days following the onset of permanent focal ischaemia may directly contribute to ischaemic injury. A potential source of this late NO production may be iNOS in activated microglia (Boje & Arora 1992; Chao *et al.* 1992) and invading macrophages from the periphery (Fabian & Rea 1993) which first appear in appreciable numbers 1-7 days post-permanent MCA occlusion (Garcia & Kamijyo 1974; Morioka *et al.* 1993). In contrast to the transient increase in NO production that occurs following activation of cNOS, the release of NO from iNOS can be sustained over several days and occurs at approximately 500 times the rate of release of NO from endothelial NOS (reviewed in Nathan 1992). Thus this much larger source of NO may have greater cytotoxic potential than the comparatively small amount of NO produced by neurones and endothelial cells. NO released directly from macrophages is toxic to endothelial cells (Palmer *et al.* 1992) and can promote oedema formation through peroxidation of membrane lipids (See Section 1.6.8.). Therefore it is possible that prolonged inhibition of NO synthesis actually improves outcome following permanent focal ischaemia by reducing oedema formation rather than by directly affecting neuronal survival. The studies that reported beneficial effects of chronic NOS inhibition (Buisson *et al.* 1992; Nowicki *et al.* 1991) assessed infarct volume by measuring areas of damage on non-fixed tissue sections. As discussed in Section 4.4. tissue swelling due to brain oedema can significantly contribute to lesion size (Lin *et al.* 1993) and the apparent reductions in infarct volume achieved with NOS inhibition may actually reflect reductions in oedema content of the tissue. In support of this hypothesis repeated treatment with L-nitroarginine has been demonstrated to reduce oedema (assessed by hemispheric water content) 48 h post-permanent MCA occlusion (Nagafuji *et al.* 1992).

Another factor that may contribute to the dramatic efficacy of repeated dosing of NOS inhibitors in conscious animals following permanent MCA occlusion (Buisson *et al.* 1992;

Nowicki *et al.* 1991) is drug-induced hypothermia. We have found that, even with heating lamps, L-NAME reduces body temperature in the conscious rat by approximately 2°C (see Section 6.2.). In the absence of an external heat source multiple dosing of NOS inhibitors may reduce body temperature sufficiently to give marked neuroprotection against focal ischaemic damage (see Section 8.1.). In our acute 4 h models of MCA occlusion body temperature was actively maintained around 37°C by means of heating blankets and, in addition, temporalis muscle temperature was not significantly altered by L-NAME (see Tables 20 and 21). Therefore the moderate neuroprotective action of L-NAME observed in the present studies is not due to hypothermia, whereas this variable can not be excluded as a causative factor for the more dramatic reductions in ischaemic damage previously reported in the conscious rat.

From the above discussion it is evident that NO synthase inhibitors induce a variety of physiological responses that can impact directly on final infarct size. The hypertension induced by low doses of NOS inhibitors in conscious animals and repeated dosing of higher doses in halothane-anaesthetised rats (as in the present study) might be expected to improve CBF to ischaemic regions and thereby reduce ischaemic damage. However the direct central vasoconstrictive action of NOS inhibitors reduces CBF in both conscious and halothane-anaesthetised rats (see Section 6.3.) so that hypertension is not likely to be an important factor. In contrast the cerebral hypoperfusion induced by inhibition of endothelial NOS is likely to be of critical importance to outcome since NOS inhibitors may reduce blood flow in the ischaemic penumbra to below the critical threshold for development of permanent neuronal damage, thereby negating any beneficial actions of these compounds. The potential therapeutic utility of NOS inhibitors as anti-ischaemic agents will therefore depend on the development of selective drugs that allow inhibition of neuronal and inducible NOS (potentially detrimental in ischaemia) while conserving endothelial NOS (potentially beneficial in ischaemia). This may prove possible in the near future as these 3 types of NOS are the products of separate genes (Bredt *et al.* 1991; Lamas *et al.* 1992; Xie *et al.* 1992) and more selective NOS inhibitors are already being developed (Moore *et al.* 1993). When available a selective neuronal NOS inhibitor, that does not facilitate endothelin-1 vasoconstriction, may prove more efficacious in both the endothelin-1 model of transient MCA occlusion and the permanent MCA occlusion model.

7.3. Effect of L-NAME and MK-801 on glutamate toxicity *in vivo*

7.3.1. Introduction

The neuroprotective effect of L-NAME against ischaemic damage in our models of transient and permanent MCA occlusion was more modest than might have been expected from the results of *in vitro* studies of glutamate toxicity (Dawson *et al.* 1991). The lack of dramatic efficacy of L-NAME *in vivo* probably reflects the diverse physiological functions of the drug, particularly its cerebrovascular effects, discussed in Section 6.2.4. Therefore to directly assess the anti-excitotoxic effect of L-NAME *in vivo* required a model where cerebrohypoperfusion induced by the drug would have less impact on outcome. The neuroprotective effect of L-NAME was therefore investigated in the novel model of glutamate toxicity *in vivo* recently developed at the Wellcome Surgical Institute (Landolt *et al.* 1993), and directly compared to the efficacy of MK-801 in the same model.

7.3.2. Experimental protocol

The comparative neuroprotective efficacies of L-NAME and MK-801 against pure excitotoxic damage were evaluated using the glutamate toxicity model described in more detail in Section 2.3.4. L-NAME (10mg/kg i.v.), MK-801 (0.5 mg/kg i.v.) or an equivalent volume of vehicle (5.5 % glucose solution, 1ml/kg i.v.), were adminstered 30 min prior to the start of the glutamate infusion. Blood pressure and rectal temperature were monitored continuously, while blood gases and plasma glucose were measured at regular intervals (1h) throughout the experiment. 4 h post-onset of glutamate infusion the rats were killed by decapitation and the volumes of neuronal damage quantified as described previously (Section 2.3.4).

The assessment of L-NAME in this model was part of a larger study (Fujisawa *et al.* 1993) comparing the relative efficacies of L-NAME, MK-801, the AMPA antagonist NBQX (30 mg/kg 30 min pre- and 30 min post-onset of glutamate perfusion) and the kappa opioid agonist CI-977 (0.3 mg/kg 30 min pre- and 30 min post-onset of glutamate perfusion) against glutamate toxicity *in vivo*. The inclusion of NBQX in the study necessitated the use of 5.5% glucose solution as the vehicle.

7.3.3. Results

7.3.3.1. Physiological variables

Physiological variables immediately prior to L-NAME (10mg/kg i.v.) or MK-801 (0.5 mg/kg i.v.) administration, glutamate infusion, and 1 and 4 h post-glutamate infusion are shown in Table 22 and were comparable between groups. L-NAME induced significant but moderate hypertension in this study (Figure 60), while MK-801 tended to reduce MABP, although this effect was not significant (Figure 60).

7.3.3.2. Neuroprotective effect of L-NAME and MK-801

In the vehicle control group the glutamate infusion induced neuronal injury in the parietal cortex that was clearly visible as an area of pallor on the haematoxylin and eosin stained sections (Fig 61a). At higher magnification neurones within the lesion neurones appeared shrunken and darkly stained with triangulated nuclei. The region of neuronal injury extended both rostrally and caudally from the probe site by approximately 1.5 mm in each direction (Figure 61b). Both L-NAME and MK-801 reduced the area of damage at each stereotactic level (Figure 61b) and significantly reduced the total volume of neuronal damage measured 4 h post-glutamate infusion compared with control (Figure 62). The magnitude of the reductions in lesion volume achieved with L-NAME and MK-801 were similar, being 27% and 30% respectively.

Table 22 Physiological variables for effect of L-NAME and MK-801 against glutamate toxicity in vivo

CONTROL (n = 10)

	VEHICLE	0 HOUR	+ 1 HOUR	+ 4 HOUR
pH	7.49 ± 0.03	7.48 ± 0.03	7.45 ± 0.06	7.44 ± 0.03
Pa CO_2 (mmHg)	39 ± 3	39 ± 3	39 ± 3	37 ± 3
Pa O_2 (mmHg)	172 ± 19	181 ± 19	180 ± 22	171 ± 35
Glucose (mmol/l)	9.8 ± 1.2	9.4 ± 0.95	9.1 ± 0.6	10.0 ± 1.3
Rectal Temp (°C)	37.0 ± 0.3	37.2 ± 0.3	37.2 ± 0.3	37.2 ± 0.3

L-NAME (n = 5)

	L-NAME	0 HOUR	+ 1 HOUR	+ 4 HOUR
pH	7.46 ± 0.03	7.46 ± 0.03	7.44 ± 0.06	7.38 ± 0.09
Pa CO_2 (mmHg)	38 ± 6	36 ± 3	36 ± 3	36 ± 3
Pa O_2 (mmHg)	168 ± 50	175 ± 34	195 ± 25	189 ± 24
Glucose (mmol/l)	9.3 ± 0.6	8.1 ± 1.2	8.8 ± 1.0	10.0 ± 1.2
Rectal Temp (°C)	36.9 ± 0.3	37.1 ± 0.4	37.1 ± 0.2	37.0 ± 0.3

MK-801 (n = 5)

	MK-801	0 HOUR	+ 1 HOUR	+ 4 HOUR
pH	7.47 ± 0.05	7.47 ± 0.03	7.44 ± 0.06	7.44 ± 0.05
Pa CO_2 (mmHg)	39 ± 6	38 ± 5	41 ± 3	35 ± 7
Pa O_2 (mmHg)	165 ± 41	174 ± 15	182 ± 23	173 ± 22
Glucose (mmol/l)	9.8 ± 1.2	8.8 ± 1.2	8.8 ± 0.9	9.7 ± 0.8
Rectal Temp (°C)	37.0 ± 0.2	37.2 ± 0.3	37.0 ± 0.3	37.0 ± 0.4

L-NAME (10mg/kg i.v.), MK-801 (0.5 mg/kg i.v.) or vehicle (5.5% glucose, 1ml/kg i.v.) were administered 30 min pre-glutamate infusion. Physiological variables were measured immediately prior to drug or vehicle administration, immediately prior to start of glutamate infusion (0 hours) and 1 and 4 h after start of glutamate infusion.

Figure 60 Glutamate toxicity *in vivo*: effect of L-NAME and MK-801 on blood pressure

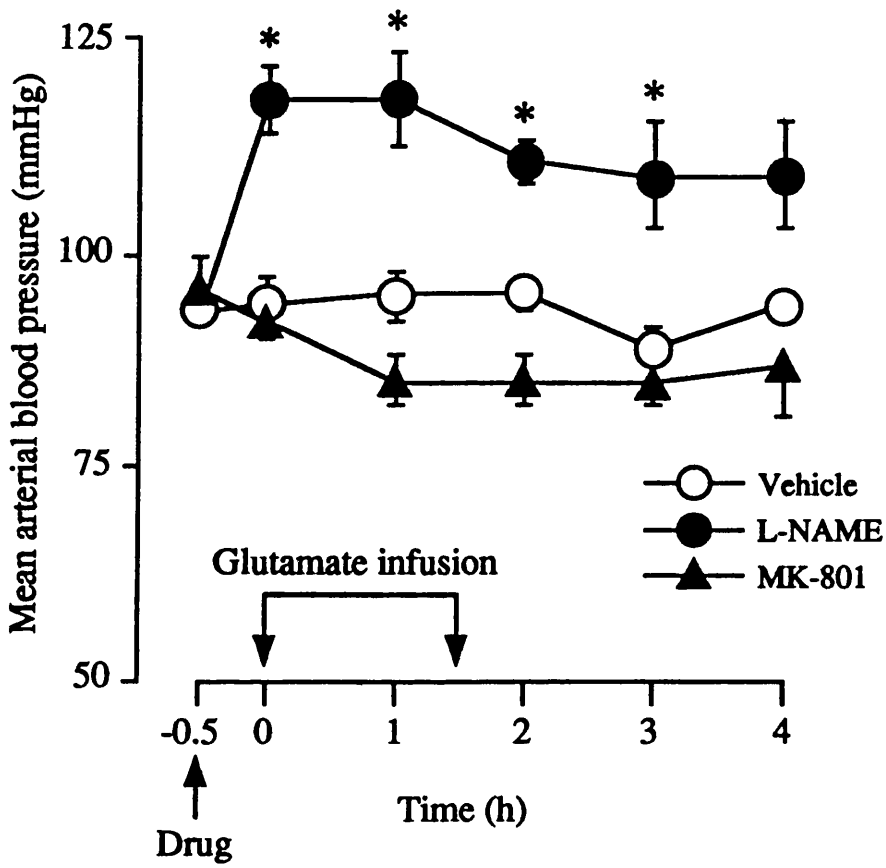

L-NAME (10 mg/kg i.v., n = 5), MK-801 (0.5 mg/kg i.v., n = 5) or vehicle (5.5% glucose i.v., n = 10) were administered 30 min pre-glutamate infusion. L-NAME moderately and significantly increased blood pressure while MK-801 tended to decrease it although this response was not significant. *$p < 0.05$ compared with vehicle control at each time point (two-way, repeated measure ANOVA followed by unpaired Student's t-tests with Bonferroni correction).

Figure 61 Glutamate toxicity *in vivo*: histological appearance of lesion, and areas of neuronal damage following pre-treatment with L-NAME, MK-801 or vehicle

a) Histological appearance of the lesion 4 h post-onset of glutamate infusion.
Representative coronal section demonstrating the lesion induced by perfusion of glutamate (0.5 M at 1.5 µl/min for 90 min) into the right parietal cortex. The section illustrated was taken from a control animal (5.5% glucose i.v., 30 min pre-glutamate infusion) and represents the area of neuronal damage at the centre of the lesion. The lesion is clearly defined as a region of pallor on the haematoxylin and eosin stained section. At higher magnification neurones within the lesion appeared shrunken and densely stained.

b) Areas of damage assessed 4 h post-onset of glutamate infusion.
Glutamate induced a reproducible lesion, that extended both rostrally and caudally from the probe site (assigned stereotactic co-ordinate 0 mm). L-NAME (10 mg/kg i.v., n = 5) or MK-801 (0.5 mg/kg i.v., n = 5) administered 30 min prior to the start of the glutamate infusion reduced the areas of damage throughout the rostral-caudal extent of the lesion compared to the vehicle control (5.5% glucose, n = 10).

Figure 61 Glutamate toxicity *in vivo*: histological appearance of lesion, and areas of neuronal damage following pre-treatment with L-NAME, MK-801 or vehicle

a

b

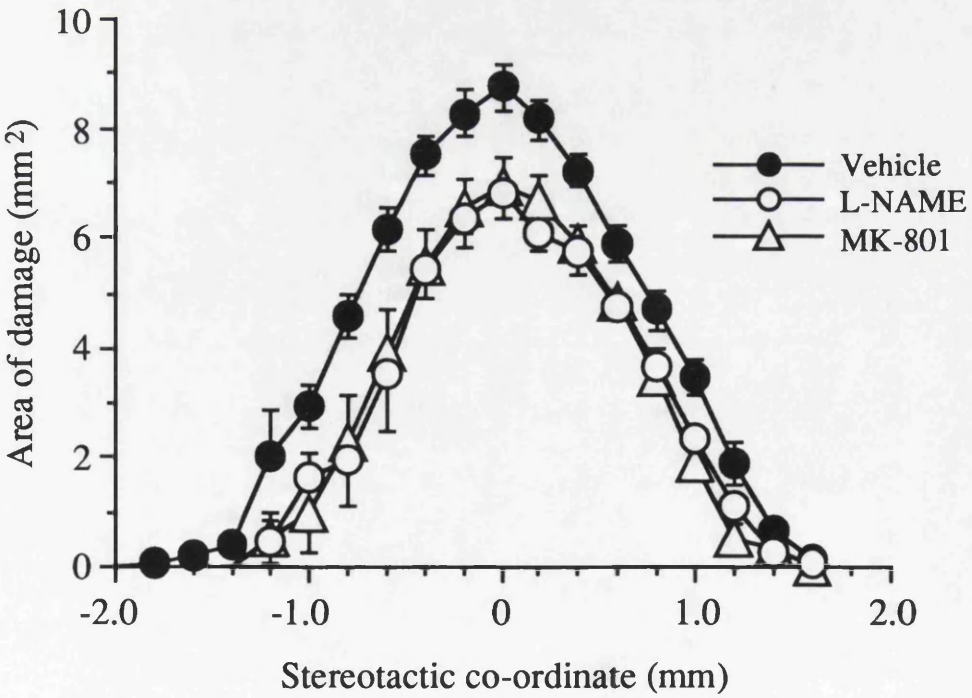

Figure 62 Glutamate toxicity *in vivo*: volumes of neuronal damage following L-NAME or MK-801 pre-treatment

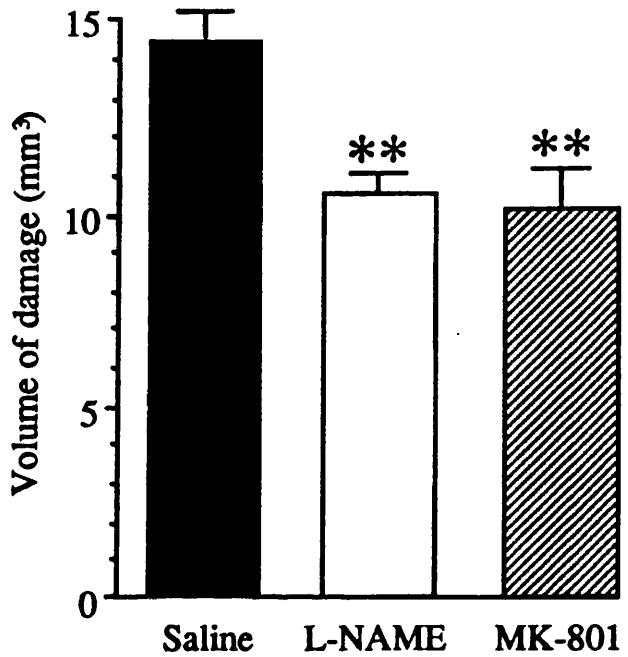

L-NAME (10 mg/kg i.v.) administered 30 min pre-glutamate infusion (0.5 M at 1.5 µl/min for 90 min) reduced the volume of cortical damage assessed 4 h post-onset of glutamate infusion. In this model, the protection achieved with L-NAME was equivalent to that observed with MK-801 (0.5 mg/kg i.v., 30 min pre-glutamate). **$p < 0.01$ compared with vehicle control (unpaired Student's t-tests).

7.3.4. Discussion

In this study 30% of the tissue potentially at risk from the glutamate infusion was salvaged by pre-treatment with MK-801. This result is in concordance with *in vitro* studies of glutamate excitotoxicity (see Section 1.4.3) and demonstrates the expected involvement of the NMDA receptor in glutamate toxicity *in vivo*. However, also in agreement with *in vitro* work, this result shows that other glutamate receptor subtypes also partly mediate glutamate toxicity since 70% of the lesion was unaffected by MK-801 pre-treatment. In this regard the AMPA receptor appears to be of equal importance to the NMDA receptor because, in a parallel experiment, the AMPA antagonist NBQX also significantly reduced the volume of damage by approximately 30% compared with control (Fujisawa *et al.* 1993).

The direct pharmacological antagonism of glutamate-induced neuronal injury observed with MK-801 and NBQX is of minor importance in terms of advancement of our knowledge of the excitotoxic cascade of neuronal injury, but did serve to validate the glutamate toxicity model. Of greater theoretical importance was the demonstration that L-NAME also gave significant neuroprotection against glutamate toxicity *in vivo* and, furthermore, the dose chosen (10mg/kg) was similar in efficacy to MK-801(0.5 mg/kg). Thus in this model NO appears to be an important mediator of glutamate-induced neuronal injury. This result is of potential clinical importance because it shows that pharmacological intervention with NO synthase inhibitors can allow successful interruption of the excitotoxic cascade downstream from the post-synaptic glutamate receptors thereby leaving normal excitatory neurotransmission relatively intact and circumventing potential therapeutic disadvantages associated with antagonism of either the NMDA or AMPA receptor.

Although both NMDA and AMPA receptor-activated events contribute to glutamate-induced damage in this model, stimulation of NO production probably occurs predominantly via the NMDA receptor since, in a similar model, pre- and post-treatment with L-NAME has been demonstrated to reduce hippocampal damage induced by focal injection of NMDA but not AMPA (Moncada *et al.* 1992). Thus it is likely that influx of Ca^{2+} through the NMDA receptor-gated ion channel is primarily responsible for activation of NO synthase and increased NO production following the pathway illustrated in Figure 10 (Section 1.6.5).

The comparative neuroprotective efficacy of L-NAME in acute focal cerebral ischaemia and glutamate toxicity *in vivo* can be directly assessed in our models because the experiments were performed under broadly similar conditions (Sprague-Dawley rats maintained under halothane anaesthesia, physiological variables constantly monitored and controlled, rats

killed 4 h post-glutamate administration/onset of MCA occlusion). The results of these 2 studies have shown that L-NAME is equipotent with MK-801 in reducing neuronal damage in the glutamate toxicity model, but is much less efficacious than MK-801 against permanent focal ischaemic damage. There are 2 possible explanations for this discrepancy which may be associated with the conservation of CBF in the glutamate toxicity model and which have been addressed in the preceding section (Section 7.2.). Firstly NO is likely to be of greater importance as a mediator of neurotoxicity in situations where its synthesis is not compromised by reduced blood flow such as the reperfusion phase of transient MCA occlusion or the glutamate toxicity model, rather than permanent MCA occlusion where depletion of oxygen and ATP supplies preclude prolonged production of NO. Secondly, the contribution of cardiovascular and cerebrovascular parameters to final outcome is likely to be of less importance in the glutamate toxicity model compared with models of cerebral ischaemia. Thus the cerebral hypoperfusion induced by L-NAME, that may have tended to exacerbate neuronal damage following MCA occlusion, appears to have much less impact on outcome following glutamate infusion, allowing a significant neuroprotective effect of the drug to be demonstrated in the glutamate toxicity model.

In the glutamate toxicity study L-NAME induced a significant hypertensive response despite the presence of continued halothane anaesthesia. This result is in contrast to other experiments in which halothane anaesthesia markedly attenuated the pressor response to L-NAME (see Sections 6.3. and 7.2.3.) and is probably due to the lower concentration of halothane (0.5-0.7%) used by Dr Fujisawa.

8. GENERAL DISCUSSION

8.1. Comparison of permanent and transient MCA occlusion in the rat

This thesis has been primarily concerned with the evaluation of a new model of transient MCA occlusion in the rat utilising the potent vasoconstrictor peptide endothelin-1. This model was specifically designed to investigate the pathophysiology of transient focal ischaemic damage since the more well established models of permanent MCA occlusion can not fully address the complexities of focal ischaemia-reperfusion injury. In the course of the completion of my investigations it has become increasingly apparent that outcome following transient MCA occlusion differs in many important aspects from outcome following permanent MCA occlusion. Some of the most important differences between transient and permanent MCA occlusion will be discussed below and are summarised in Table 23. The existence of these differences emphasises the importance of developing valid models of transient focal ischaemia in order that the pathophysiology of clinical embolic stroke, where reperfusion is more common than persistence of the occlusion (Mohr *et al.* 1986), can be more fully investigated and understood.

The fundamental theoretical difference between transient and permanent MCA occlusion concerns the mechanisms of tissue damage in the 2 models. In both cases the ischaemic cascade mediates injury during the initial ischaemic insult. This complex cascade involves the interaction of several different pathways that lead ultimately to cell death. However in addition to these mechanisms of injury the reperfusion phase that follows transient MCA occlusion introduces additional processes (*e.g.* free radical and leucocyte-mediated events) that can also contribute to cellular injury. Thus the mechanisms of tissue damage are more complex for a transient ischaemic insult compared to a permanent ischaemic insult.

Differences in the temporal evolution of ischaemic damage following transient and permanent MCA occlusion lend support to the hypothesis that the reperfusion phase contributes to tissue damage in the transient MCA occlusion model. The results presented in Section 4 demonstrated that for permanent MCA occlusion the volume of damage was maximal 4 h post-onset of ischaemia whereas for transient MCA occlusion the volume of damage continued to increase from 4 h to 24 h post-onset of ischaemia.

It is also evident that key physiological variables such as blood pressure and brain temperature can influence the extent of tissue damage to a greater degree for transient compared to permanent MCA occlusion. For example with transient MCA occlusion the increase in blood pressure associated with anaesthetic withdrawal was found to reduce the volume of ischaemic damage, while the reduction in blood pressure induced by MK-801, if

Table 23 Summary of the major differences between models of permanent and transient MCA occlusion in the rat

	Permanent MCA Occlusion	Transient MCA Occlusion
Mechanisms of damage	Comparatively few	More complex
Temporal evolution of tissue damage	Maximal by 4 h	Increases up to 24 h
Blood pressure	Sensitive	Highly sensitive
Brain temperature	Sensitive	Highly sensitive
Statistical power	Good	Weaker
Potential volume of salvagable tissue	Approximately 50 %	Up to 100 %
Anatomical distribution of salvagable tissue	Cerebral cortex	Cerebral cortex and caudate nucleus

present at the time of MCA occlusion, inhibited the neuroprotective action of the drug. In contrast for permanent MCA occlusion anaesthetic withdrawal did not significantly alter the volume of damage, and previous studies have shown that MK-801 pre-treatment is highly neuroprotective in this model despite the presence of drug-induced hypotension at the time of MCA occlusion (Park *et al.* 1989).

In addition outcome following transient MCA occlusion is more sensitive to alterations in brain temperature than permanent MCA occlusion. Moderate hypothermia (30-33°C) maintained during the ischaemic phase and first hour of reperfusion has been shown to reduce the volume of ischaemic damage following transient MCA occlusion compared to normothermic or hyperthermic (39°C) controls (Chen *et al.* 1993; Morikawa *et al.* 1992a; Ridenour *et al.* 1992), whereas transient hypothermia of the same magnitude is not protective against permanent MCA occlusion (Morikawa *et al.* 1992a; Ridenour *et al.* 1992). More profound transient hypothermia (24°C, Onesti *et al.* 1991) or moderate hypothermia (32°C) maintained for the entire duration of the ischaemic insult (Xue *et al.* 1992b) is normally necessary to demonstrate protection in models of permanent focal ischaemia. However one study has reported that transient hypothermia (33°C for 1 h) delayed up to 1 h post-permanent MCA occlusion can significantly reduce ischaemic damage (assessed by TTC staining, Kader *et al.* 1992).

The sensitivity of transient focal ischaemic damage to variations in brain temperature is further illustrated by reports that moderate hypothermia (30-32°C) initiated 1-3 h after the onset of reperfusion significantly reduces volume of ischaemic damage by approximately 50 % (Xue *et al.* 1992b; Zhang, R.L. *et al.* 1993). The fact that delayed hypothermia initiated 3 h after the onset of reperfusion can give such dramatic protection further emphasises the importance of events occuring during the reperfusion phase to the evolution of tissue injury in models of transient focal ischaemia.

The long-standing assumption that the cerebroprotective effect of hypothermia is related to suppression of cerebral metabolic rate is questionable (Todd & Warner 1992). The protection achieved by progressively increasing levels of hypothermia does not parallel observed changes in metabolic rate, energy metabolite depletion or lactic acid accumulation (Dietrich 1992; Todd & Warner 1992). Instead recent evidence suggests the neuroprotective effect of intra-ischaemic hypothermia derives from inhibition of the ischaemia-induced elevation of extracellular glutamate (Busto *et al.* 1989; Graf *et al.* 1992). In contrast protection afforded by hypothermia initiated during reperfusion may be vascular in origin. Alterations in blood-brain barrier permeability and leucocyte accumulation following transient global ischaemia are temperature-dependent, being significantly increased at 39°C and attenuated at 33°C (Dietrich *et al.* 1990). The early deleterious

increase in blood-brain barrier permeability following transient focal ischaemia is also suppressed by post-ischaemic hypothermia (28-30°C, Huang *et al.* 1993). This response may in turn be partly due to hypothermia-induced attenuation of post-ischaemic hyperaemia (Morikawa *et al.* 1992a) which is known to mediate the initial opening of the blood-brain barrier following resolution of arterial occlusion (Kuroiwa *et al.* 1989).

The well-documented protective action of hypothermia on outcome following transient focal ischaemia, coupled with the fact that both MK-801 and L-NAME induce hypothermia in conscious animals, made it imperative to monitor brain temperature in the pharmacoprotection studies included in this thesis to ensure that any observed beneficial effect was not due to drug-induced hypothermia. Therefore ipsilateral temporalis muscle temperature was continously measured during MCA exposure and occlusion. Unlike rectal temperature, temporalis muscle temperature correlates closely with intraparenchymal brain temperature following MCA occlusion (Onesti *et al.* 1991) and therefore provides a good estimate of brain temperature. In our experiments, where rectal temperature was controlled by external heating, temporalis muscle temperature was not significantly altered by either L-NAME or MK-801 pre-treatment. In these studies intra- and inter-experimental temporalis muscle temperature was relatively consistent suggesting that variations in brain temperature were not a major contributor to overall variability in lesion size in the endothelin-1 model of transient focal ischaemia. However cerebral hypothermia may be of greater importance in dictating outcome in some alternative models of transient focal ischaemia. For example when ischaemia is induced by MCA occlusion in tandem with bilateral carotid artery occlusion, the interruption of carotid arterial blood flow causes a more profound reduction in brain temperature than that observed in our model (subdural temperature 2-3°C below rectal temperature, Moyer *et al.* 1992), which if not prevented, significantly reduces lesion size (Moyer *et al.* 1992).

Statistical power and variability in volumes of ischaemic damage

One of the most important criteria for the development of animal models of focal cerebral ischaemia (both permanent and transient) is that the model should achieve a reproducible lesion with an acceptable degree of variability so that different treatment strategies can be evaluated. The greater the degree of variability in a model the greater the possibility that a true difference between lesion size in control and drug groups will not be detected by statistical testing - a 'type II' error.

The presence of the collateral circulation in the rat introduces a certain level of variability into models of permanent focal ischaemia. Incorporation of a period of reperfusion into the design introduces additional variability, over and above that associated with the ischaemic

phase, due to a whole series of physiological parameters (cerebral blood flow, blood pressure, temperature, biochemical mediators such as nitric oxide discussed above and in various parts of this thesis) that can directly influence neuronal damage and/or oedema formation following the restoration of blood flow. Therefore models of transient focal ischaemia are inherently associated with a greater degree of variability in lesion size than models of permanent focal ischaemia.

For any particular model power analysis can be used to estimate the number of animals per group necessary to avoid a type II error and detect a specified difference in lesion size between control and drug groups. Using the results for the 4 h paradigm in the anaesthetised rat, the group sizes necessary to detect a 50% reduction in lesion size, at the 5% level of significance, with a power of 80% (*i.e.* 80% probability of detecting the true difference between the sample means and rejecting the null hypothesis of equal means) were calculated for both transient and permanent MCA occlusion (Table 24a). The mean volumes of hemispheric damage for control rats from the 3 separate studies utilising this paradigm in the transient occlusion model were relatively consistent (Table 24a). However the variability in lesion size (estimated by the standard deviation) is rather high, particularly for the control group from the L-NAME study. This is reflected in the large group sizes estimated by power analysis to be necessary to detect a 50% reduction in lesion volume (n = 19-34) compared with n = 2 for the model of permanent MCA occlusion (Table 24a). As there was no significant difference between the volumes of ischaemic damage in the 3 transient ischaemia studies they were combined to give an overall estimate of the variability in this model. This shows that, on average, groups of 26 would be required to demonstrate a statistically significant 50% reduction in lesion size utilising the 4 h paradigm in the anaesthetised rat (Table 24a). Furthermore power analysis predicts that groups with n = 78 would be necessary to statistically detect the observed 29% reduction in hemispheric damage achieved with L-NAME in the transient ischaemia study. The practicalities of conducting such a large experiment precluded its inclusion in the current thesis. However this analysis does not invalidate the present results achieved with smaller group sizes. In particular it can be concluded that pre-treatment with MK-801 is more efficacious than L-NAME pre-treatment (at the doses used) when volumes of ischaemic damage are assessed 4 h post-onset of transient MCA occlusion. Although the group sizes discussed above appear quite large it should be noted that power analysis gives conservative estimates of the number of animals required and that statistical significance can frequently be demonstrated with smaller experimental groups. For example the statistically significant 70% reduction in lesion size observed with MK-801 in the transient ischaemia study was achieved with an average group size of only 9, while power analysis suggested n of 13 would be required.

Table 24 Power analysis for selected models of transient and permanent MCA occlusion

Sample sizes necessary to detect a 50% reduction in lesion volume were calculated for 80% power at the 0.05 level of significance ($\beta = 0.2$; $\alpha = 0.05$).

Volumes of hemispheric damage (mean ± S.D.) assessed 4 h or 24 h post-onset of transient MCA occlusion and sample sizes are shown for:

a) Endothelin-1 model (4 h duration in the anaesthetised Sprague-Dawley (S-D) rat): i) untreated ii) saline control group from the MK-801 study iii) saline control group from the L-NAME study and iv) the overall mean of the 3 studies combined, compared with permanent MCA occlusion of 4 h duration.

b) and c) Endothelin-1 model ('ET-1', 24 h duration in the S-D rat) compared with representative studies from the published literature using normotensive and spontaneously hypertensive (SHR) rat strains.

Table 24 Power analysis for selected models of transient and permanent MCA occlusion

a) Volumes of ischaemic damage assessed 4 h post-onset of transient and permanent MCA occlusion in the anaesthetised rat

	Transient MCA Occlusion				Permanent MCAO
	Untreated	MK-801 control	L-NAME control	Combined	Untreated
Volume of ischaemic damage (mm^3)	48 ± 26 (n = 12)	59 ± 37 (n = 10)	54 ± 40 (n = 14)	53 ± 34 (n = 36)	107 ± 15 (n = 6)
Sample size to detect 50% reduction	n = 19	n = 25	n = 34	n = 26	n = 2

b) Volumes of ischaemic damage assessed 24 h post-onset of transient MCA occlusion (normotensive strains)

	ET-1 (S-D)	Buchan *et al.* 1992 (Wistar; clip occlusion)			Hiramatsu *et al.* 1993 (S-D; clip occlusion)		
Duration of ischaemia (min)	—	60	120	180	60	120	180
Volume of ischaemic damage (mm^3)	87 ± 42	21 ± 13	150 ± 29	211 ± 34	71 ± 79	133 ± 107	177 ± 20
Sample size to detect 50% reduction	n = 15	n = 25	n = 34	n = 26	n = 78	n = 41	n = 1

c) Volumes of ischaemic damage assessed 24 h post-onset of transient MCA occlusion (SHR)

	Buchan *et al.* 1992 (SHR; clip occlusion)			Kaplan *et al.* 1991 (SHR; hook occlusion)		
Duration of ischaemia (min)	60	120	180	60	120	180
Volume of ischaemic damage (mm^3)	15 ± 25	93 ± 65	217 ± 28	33 ± 21	100 ± 23	183 ± 29
Sample size to detect 50% reduction	n = 180	n = 31	n = 1	n = 25	n = 3	n = 12

Although all models of transient focal ischaemia are more variable than their permanent counterparts, this comparative lack of power must be balanced against the maximum degree of pharamacoprotection that could potentially be demonstrated in the 2 types of model. For permanent MCA occlusion, tissue in the core ischaemic region will always be destined to die due to depletion of oxygen and energy supplies. Only the 'penumbral' region - the border zone between densely ischaemic and normally perfused tissue, where flow is less severely reduced - will be amenable to pharmacological intervention. This means that even the most efficacious of drugs such as MK-801 can only protect approximately 50% of the total tissue at risk. In contrast for transient MCA occlusion, the restoration of blood flow (providing it is initiated before ischaemic damage becomes irreversible) renders 100% of the affected tissue potentially salvagable. This is illustrated by the fact that tissue damage in the caudate nucleus, an end-artery region, can be successfully reduced by pharmacological intervention prior to transient MCA occlusion (*e.g.* with MK-801, Section 7.1.) whereas previous studies have shown that in the presence of permanent MCA occlusion this region is more resistant to neuroprotective agents. Therefore the 'ideal' drug is likely to reduce the total volume of tissue damage to a greater extent following transient compared with permanent MCA occlusion, and consequently the difference in power between the 2 models will be of less practical importance.

The results of the pharmacoprotection studies utilising L-NAME do not appear to support this view since the neuroprotective effect of the drug was broadly similar for both permanent and transient MCA occlusion. However in these studies outcome was only assessed in the acute post-ischaemic period. By extending the endpoint from 4 h to 24 h post-onset of transient ischaemia the contribution of reperfusion injury to the maturation of the lesion would be enhanced, and the volume of potentially salvagable tissue thereby increased. Thus it may prove more feasible to use 24 h as the endpoint for future studies of potential neuroprotective agents in the endothelin-1 model of transient focal ischaemia. From Table 24b it can be seen that, if damage is assessed at 24 h, a group size of only 15 is required to detect a 50% reduction in lesion size. In the present studies we did not use the 24 h time point because 1) it is more difficult to control physiological variables over 24 h in the conscious rat compared with 4 h in the anaesthetised rat and 2) both drugs tested (L-NAME and MK-801) have significant effects on blood pressure and/or cerebral blood flow in the conscious rat that may contribute to apparent anti-ischaemic efficacy and make interpretation of the results difficult. However careful choice of dosing schedules and regular post-operative monitoring of physiological variables may make these problems surmountable in the future.

8.2. Comparison of different models of transient MCA occlusion in the rat

In this section I shall compare the endothelin-1 model of transient MCA occlusion to the alternative models of transient focal ischaemia described in the literature. For most of these models lesion volume is assessed at least 24 h following the onset of the ischaemic insult (Buchan *et al.* 1992b; Kaplan *et al.* 1991). Table 24b-c shows the volumes of ischaemic damage and sample sizes necessary to detect a 50% reduction in lesion size for representative studies in which the MCA was transiently occluded (using clips, ligatures or hooks combined with unilateral or bilateral common carotid artery occlusion) for periods of 60-240 min and volumes of ischaemic damage were assessed 24 h post-onset of occlusion. A previous analysis of the variability associated with different rat models of transient focal cerebral ischaemia concluded that a 3 h period of occlusion was necessary to reduce the variability to acceptable levels (Hiramatsu *et al.* 1993). From Table 24 it can be seen that 3 h occlusion does dramatically reduce variability and required sample size. However the volume of ischaemic damage following 3 h of transient ischaemia in these models is equivalent to 24 h of permanent MCA occlusion (Buchan *et al.* 1992b; Kaplan *et al.* 1991). Thus the volume of damage is already maximal by the 3 h time point (purely due to the ischaemic insult) and the contribution of reperfusion injury can not be assessed. Therefore to study ischaemic-reperfusion injury an initial period of ischaemia of less than 3 h duration is advisable. When compared to models utilising normotensive rat strains and periods of ischaemia of less than 3 h duration, it can be seen from Table 24 that smaller group sizes are required for the endothelin-1 model than for the alternative models of transient focal cerebral ischaemia. Thus the variability associated with the endothelin-1 model (at the 24 h time point) compares favourably with that of other methods of transient MCA occlusion described in the literature.

One of the main advantages of the endothelin-1 model of transient MCA occlusion is that induction of ischaemia does not involve mechanical damage to the vasculature. In models utilising extravascular occlusion (Buchan *et al.* 1992b; Kaplan *et al.* 1991) the clips or ligatures used to induce occlusion may cause damage to the MCA resulting in variability in the degree of reflow through the vessel when the occluder is removed (Tamura *et al.* 1980). Models of intravascular occlusion may also cause vascular damage when the filament is advanced from the common carotid artery through the internal carotid artery to occlude the origin of the MCA. Insertion of a catheter into the common carotid artery is known to cause loss of endothelial cells and immediate reduction in NO-mediated vasodilation which is followed by a later increase in NO production 24 h post-insult due to induction of NO synthase in the vascular smoooth muscle (Joly *et al.* 1992). Thus occlusion of the MCA by insertion of a filament may cause initial loss of vasodilatory mechanisms that would

normally be employed to counteract ischaemia, and secondly, following reperfusion, endothelial damage and/or increased NO production that may contribute to the massive cerebral oedema observed in these models (Koizumi *et al.* 1989; Memesawa *et al.* 1992b). An advantage of the intravascular models often cited is the fact that no craniectomy is necessary to induce MCA occlusion so that any increase in intracranial pressure in reponse to oedema formation will not be artificially ameliorated by the opening in the skull (Nagasawa & Kogure 1989). This is indeed the case, but the gross oedema induced by this method results in very high mortality rates (Koizumi *et al.* 1989; Memesawa *et al.* 1992) probably directly related to increased intracranial pressure. Thus the model is not ideally suited to long term studies of ischaemia-reperfusion injury. In contrast the endothelin-1 model is associated with very low mortality rates.

Models of extravascular occlusion normally utilise distal MCA occlusion resulting in a lesion located predominantly in the cerebral cortex with little striatal involvement. These models do not therefore closely mimic human stroke since, in man, the most common site for MCA occlusion is proximal to the lenticulo-striate branches resulting in consistent damage to the caudate nucleus (Ringelstein *et al.* 1992; Saito *et al.* 1987). The location of the lesion induced by MCA occlusion is of importance because recent evidence suggests the caudate nucleus responds differently to ischaemia-reperfusion injury than the cerebral cortex (Abe *et al.* 1988; Matsumiya *et al.* 1991). Models of transient distal MCA occlusion can not be used to elucidate the differential mechanisms underlying cortical and striatal damage, whereas the endothelin-1 model, which induces a lesion in both cortex and caudate nucleus, could be used for this purpose. In the present study both L-NAME and MK-801 had a greater neuroprotective effect on striatal damage compared with cortical damage following transient MCA occlusion lending support to the idea that the caudate nucleus is more susceptible to reperfusion injury and/or more amenable to pharmacological intervention than the cortex.

Another difference between the endothelin-1 model and other models of transient MCA occlusion concerns the dynamics of restoration of blood flow. In models where the MCA is mechanically occluded removal of the occluder can result in an immediate absolute hyperaemia in the previously ischaemic region in a substantial proportion of animals (Shigeno *et al.* 1985; Tamura *et al.* 1990). During ischaemia blood vessels are probably maximally dilated due to acidosis (Lassen 1966). Rapid re-opening of the occluded MCA causes a rush of blood through the dilated vessels resulting in "haemodynamic" damage to the blood-brain barrier and increased oedema formation (Kuroiwa *et al.* 1985; Kuroiwa *et al.* 1989; Tamura *et al.* 1980). Following subsidence of hyperaemia normal blood-brain

barrier function is temporarily restored (Kuroiwa *et al.* 1985; Shigeno *et al.* 1985), until a second later opening of the blood-brain barrier occurs due to ischaemia-reperfusion injury to the vasculature (Kuroiwa *et al.* 1985). In the absence of hyperaemia, or when hyperaemia is actively suppressed by modulating the degree of arterial re-opening, the initial transient opening of the blood-brain barrier does not occur (Kuroiwa *et al.* 1989; Tamura *et al.* 1980). In contrast to other models, restoration of blood flow in the endothelin-1 model of transient MCA occlusion is slow and progressive (Macrae *et al.* 1993) so that the artifactual opening of the blood-brain barrier observed in other models will not influence outcome in the endothelin-1 model.

8.3. Concluding remarks and future studies

In both experimental MCA occlusion and clinical stroke early reperfusion is essential if tissue is to be salvaged and functional recovery optimised. However the restoration of blood flow can invoke a further cascade of pathological events which, if not interrupted, may cause additional 'reperfusion injury' to the tissue. The fundamental premise that separate and/or additional pathological processes contribute to outcome following transient as opposed to permanent focal cerebral ischaemia has been repeatedly demonstrated within this thesis with the observation that outcome in the transient (endothelin-1) model differs in several important aspects from that in the permanent MCA occlusion model (reviewed in Section 8.1.).

To address the problem of reperfusion injury models of transient focal cerebral ischaemia are being increasingly utilised in experimental studies of stroke. In this regard the endothelin-1 model of transient focal ischaemia, extensively characterised in this thesis, compares favourably with the alternative rat models described in the literature, both in terms of variability in lesion size and the absence of mechanical damage to the endothelium that can occur following intra- or extra-vascular occlusion with filaments or clips.

One of the most important questions arising from my investigations concerns the nature of the biochemical mediators of reperfusion injury. As discussed in the Introduction to this thesis one of the most obvious candidates for this role are oxygen free radicals. A series of experiments has therefore been initiated to assess the contribution of free radicals to ischaemic-reperfusion injury in the endothelin-1 model by 1) measuring the levels of free radicals produced and 2) determining the neuroprotective efficacy of a free radical scavenger in this model. Future studies could also be directed towards further investigation of the reperfusion phase of the endothelin-1 model by measuring CBF at later time intervals than 2 h following endothelin-1 application to the MCA.

In conclusion the investigations reported in this thesis have established that topical application of endothelin-1 to the MCA is a viable model of transient focal cerebral ischaemia in the rat. This novel approach, in tandem with other experimental models, will hopefully allow the concept of reperfusion injury to be more fully investigated and understood in the near future.

REFERENCES

Abe, K., Araki, T. & Kogure, K. (1988) Recovery from edema and of protein synthesis differs between the cortex and caudate following transient focal cerebral ischemia in rats. *J. Neurochem.* **51**, 1470-1476.

Agullo, L. & Garcia, A. (1991) Norepinephrine increases cyclic GMP in astrocytes by a mechanism dependent on nitric oxide synthesis. *Eur. J. Pharmacol.* **206**, 343-346.

Agullo, L. & Garcia, A. (1992) Different receptors mediate stimulation of nitric oxide-dependent cyclic GMP formation in neurons and astrocytes in culture. *Biochem. Biophys. Res. Commun.* **182**, 1362-1368.

Aisaka, K., Mitani, A., Kitajima, Y., Ohno, T. & Ishihara, T. (1991) Difference in pressor responses to N^G-monomethyl-L-arginine between conscious and anaesthetized rats. *Japan J. Pharmacol.* **56**, 245-248.

Albanese, V., Tommasino, C., Spadaro, A. & Tomasello, F. (1980) A transbasisphenoidal approach for selective occlusion of the middle cerebral artery in rats. *Experientia* **36**, 1302-1304.

Alcala, H., Gado, M. & Torack, R.M. (1978) The effect of size, histologic elements, and water content on the visualization of cerebral infarcts. *Arch. Neurol.* **35**, 1-8.

Andersen, A.R. (1989) ^{99m}Tc-D,L,-Hexamethylene-propyleneamine oxime (^{99m}Tc-HMPAO): Basic kinetic studies of a tracer of cerebral blood flow. *Cerebrovasc. Brain Metabol. Rev.* **1**, 288-318.

Aoki, E., Semba, R., Mikoshiba, K. & Kashiwamata, S. (1991) Predominant localization in glial cells of free L-arginine. Immunocytochemical evidence. *Brain Res.* **547**, 190-192.

Araki, T., Kato, H., Hara, H. & Kogure, K.(1991) Postischemic alteration of [^{3}H]forskolin binding sites in selectively vulnerable areas: an autoradiographic study of gerbil brain. *Neurosci. Lett.* **125**, 159-162.

Araki, N., Greenberg, J.H., Uematsu, D., Sladky, J.T. & Reivich, M. (1992) Effect of superoxide dismutase on intracellular calcium in stroke. *J. Cereb. Blood Flow Metabol.* **12**, 43-52.

Archer, S.L. & Hampl, V. (1992) N^G-Monomethyl-L-arginine causes nitric oxide synthesis in isolated arterial rings: trouble in paradise. *Biochem. Biophys. Res. Comm.* **188**, 590-596.

Babbedge, R.C., Hart, S.L. & Moore, P.K. (1993) Anti-nociceptive activity of nitric oxide synthase inhibitors in the mouse: dissociation between the effect of L-NAME and L-NMMA. *J. Pharm. Pharmacol.* **45**, 77-79.

Barone, F.C., Schmidt, D.B., Hillegass, L.M., Price, W.J., White, R.F., Feuerstein, G.Z., Clark, R.K., Lee, E.V., Griswold, D.E. & Sarau, H.M. (1992) Reperfusion increases neutrophils and leukotriene B4 receptor binding in rat focal ischemia. *Stroke* **23**, 1337-1348.

Baughman, V.L., Hoffman, W.E., Miletich, D.J., Albrecht, R.F. & Thomas, C. (1988) Neurologic outcome in rats following incomplete cerebral ischemia during halothane, isoflurane, or N_2O. *Anesthesiology* **69**, 192-198.

Beckman, J.S., Beckman, T.W., Chen, J., Marshall, P.A. & Freeman, B.A. (1990) Apparent hydroxyl radical production by peroxynitrite: implications for endothelial injury from nitric oxide and superoxide. *Proc. Natl. Acad. Sci. USA* **87**, 1620-1624.

Bederson, J.B., Pitts, L.H., Tsuji, M., Nishimura, M.C., Davis, R.L. & Bartkowski, H.M. (1986) Rat middle cerebral artery occlusion: Evaluation of the model and development of a neurologic examination. *Stroke* **17**, 472-476.

Benveniste, H., Drejer, J., Schousboe, A. & Diemer, N.H. (1984) Elevations of the extracellular concentrations of glutamate and aspartate in rat hippocampus during transient cerebral ischemia monitored by intracerebral microdialysis. *J. Neurochem.* **43**, 1369-1374.

Benveniste, H., Jorgensen, M.B., Diemer, N.H. & Hansen, A.J. (1988) Calcium accumulation by glutamate receptor activation is involved in hippocampal cell damage after ischemia. *Acta Neurol. Scand.* **78**, 529-536.

Betz, A.L. (1985) Identification of hypoxanthine transport and xanthine oxidase activity in brain capillaries. *J. Neurochem.* **44**, 574-579.

Betz, A.L., Randall, J. & Martz, D. (1991) Xanthine oxidase is not a major source of free radicals in focal ischemia. *Am. J. Phys.* **260**, H563-H568.

Bogle, R.G., Moncada, S., Pearson, J.D. & Mann, G.E. (1992) Identification of inhibitors of nitric oxide synthase that do not interact with the endothelial cell L-arginine transporter. *Br. J. Pharmacol.* **105**, 768-770.

Bohme, G.A, Bon, C., Stutzmann, J.-M., Doble, A. & Blanchard, J.-C. (1991) Possible involvement of nitric oxide in long-term potentiation. *Eur. J. Pharmacol.* **199**, 379-381.

Boje, K.M. & Arora, P.K. (1992) Microglial-produced nitric oxide and reactive nitrogen oxides mediate neuronal cell death. *Brain Res.* **587**, 250-256.

Boje, K.M. & Skolnick, P. (1992) Nitric oxide does not mediate the neurotrophic effects of excitatory amino acids in cultured cerebellar granule neurons. *Eur. J. Pharmacol.* **212**, 151-158.

Bolander, H.G., Persson, L., Hillered, L., d'Argy, R., Ponten, U. & Olsson, Y. (1989) Regional cerebral blood flow and histopathological changes after middle cerebral artery occlusion in rats. *Stroke* **20**, 930-937.

Bondy, S.C. & Lee, D.K. (1993) Oxidative stress induced by glutamate receptor agonists. *Brain Res.* **610**, 229-233.

Bralet, J., Schreiber, L. & Bouvier, C. (1992) Effect of acidosis and anoxia on iron delocalization from brain homogenates. *Biochem. Pharmacol.* **43**, 979-983.

Bredt, D.S. & Snyder, S.H. (1989) Nitric oxide mediates glutamate-linked enhancement of cGMP levels in the cerebellum. *Proc. Natl. Acad. Sci. USA* **86**, 9030-9033.

Bredt, D.S. & Snyder, S.H. (1990) Isolation of nitric oxide synthetase, a calmodulin-requiring enzyme. *Proc. Natl. Acad. Sci. USA* **87**, 682-685.

Bredt, D.S. & Snyder, S.H. (1992) Nitric oxide, a novel neuronal messenger. *Neuron* **8**, 3-11.

Bredt, D.S., Hwang, P.M. & Snyder, S.H. (1990) Localization of nitric oxide synthase indicating a neural role for nitric oxide. *Nature* **347**, 768-770.

Bredt, D.S., Hwang, P.M., Glatt, C.E., Lowenstein, C., Reed, R.R. & Snyder, S.H. (1991) Cloned and expressed nitric oxide synthase structurally resembles cytochrome P-450 reductase. *Nature* **351**, 714-718.

Bredt, D.S., Ferris, C.D. & Snyder, S.H. (1992) Nitric oxide synthase regulatory sites. Phosphorylation by cyclic AMP-dependent protein kinase; protein kinase C, and calcium/calmodulin protein kinase; identification of flavin and calmodulin binding sites. *J. Biol. Chem.* **267**, 10976-10981.

Brint, S., Jacewicz, M., Kiessling, M., Tanabe, J. & Pulsinelli, W. (1988) Focal brain ischemia in the rat: methods for reproducible neocortical infarction using tandem occlusion of the distal middle cerebral and ipsilateral common carotid arteries. *J. Cereb. Blood Flow Metabol.* **8**, 474-485.

Bromont, C., Marie, C. & Bralet, J. (1989) Increased lipid peroxidation in vulnerable brain regions after transient forebrain ischemia in rats. *Stroke* **20**, 918-924.

Brown, A.W. (1977) Structural abnormalities in neurones. *J. Clin. Path.* **30**, S11, 155-169.

Buchan, A.M. & Pulsinelli, W.A. (1990) Hypothermia but not the N-methyl-D-aspartate antagonist MK-801 attenuates neuronal damage in gerbils subjected to transient global ischemia. *J. Neurosci.* **10**, 311-316.

Buchan, A.M., Li, H. & Pulsinelli, W.A. (1991a) The N-methyl-D-aspartate antagonist MK-801 fails to protect against neuronal damage caused by transient, severe forebrain ischemia in adult rats. *J. Neurosci.* **11**, 1049-1056.

Buchan, A.M., Xue, D., Huang, Z.-G., Smith, K.H. & Lesiuk, H. (1991b) Delayed AMPA receptor blockade reduces cerebral infarction induced by focal ischemia. *NeuroReport* **2**, 473-476.

Buchan, A.M., Slivka, A. & Xue, D. (1992a) The effect of the NMDA receptor antagonist MK-801 on cerebral blood flow and infarct volume in experimental stroke. *Brain Res.* **574**, 171-177.

Buchan, A.M., Xue, D. & Slivka, A. (1992b) A new model of temporary focal neocortical ischemia in the rat. *Stroke* **23**, 273-279.

Buisson, A., Plotkine, M. & Boulu, R.G. (1992) The neuroprotective effect of a nitric oxide inhibitor in a rat model of focal cerebral ischaemia. *Br. J. Pharmacol.* **106**, 766-767.

Bullock, R., Graham, D.I., Chen, M.-H., Lowe, D. & McCulloch, J. (1990) Focal cerebral ischemia in the cat: pretreatment with a competitive NMDA receptor antagonist, D-CPP-ene. *J. Cereb. Blood Flow Metabol.* **10**, 668-674.

Bullock, R., Patterson, J. & Park, C. (1991) Evaluation of ^{99m}Tc-hexamethylpropyleneamine oxime cerebral blood flow mapping after actue focal ischemia in rats. *Stroke* **22**, 1284-1290.

Busto, R., Dietrich, W.D.,Globus, M. Y.-T., Valdes, I., Scheinberg, P. & Ginsberg, M.D. (1987) Small differences in intra-ischemic brain temperature critically determine the extent of ischemic neuronal injury. *J. Cereb. Blood Flow Metabol.* **7**, 729-738.

Busto, R., Globus, M. Y.-T., Dietrich, W.D., Martinez, E., Valdes, I. & Ginsberg, M.D. (1989) Effect of mild hypothermia on ischemia-induced release of neurotransmitters and free fatty acids in rat brain. *Stroke* **20**, 904-910.

Butcher, S.P., Bullock, R., Graham, D.I. & McCulloch, J. (1990) Correlation between amino acid release and neuropathologic outcome in rat brain following middle cerebral artery occlusion. *Stroke* **21**, 1727-1733.

Buxton, I.L.O., Cheek, D.J., Eckman, D., Westfall, D.P., Sanders, K.M. & Keef, K.D. (1993) N^G-Nitro L-arginine methyl ester and other alkyl esters of arginine are muscarininc receptor antagonists. *Circ. Res.* **72**, 387-395.

Carter, C., Rivy, J.-P. & Scatton, B. (1989) Ifenprodil and SL 82.0715 are antagonists at the polyamine site of the N-methyl-D-aspartate (NMDA) receptor. *Eur. J. Pharmacol.* **164**, 611-612.

Castoldi, A.F., Manzo, L. & Costa, L.G. (1993) Cyclic GMP formation induced by muscarinic receptors is mediated by nitric oxide synthesis in rat cortical primary cultures. *Brain Res.* **610**, 57-61.

Cazevieille, C., Muller, A., Meynier, F. & Bonne, C. (1993) Superoxide and nitric oxide cooperation in hypoxia/reoxygenation-induced neuron injury. *Free Rad. Biol. Med.* **14**, 389-395.

Chan, P.H. (1992) Antioxidant-dependent amelioration of brain injury: role of CuZn-superoxide dismutase. *J.Neurotrauma* **9**, S2, S417-S423.

Chan, P.H. & Fishman, R.A. (1980) Transient formation of superoxide radicals in polyunsaturated fatty acid-induced brain swelling. *J. Neurochem.* **35**, 1004-1007.

Chan, P.H., Fishman, R.A., Caronna, J., Schmidley, J.W., Prioleau, G. & Lee, J. (1983) Induction of brain edema following intracerebral injection of arachidonic acid. *Ann. Neurol.* **13**, 625-632.

Chan, P.H., Schmidley, J.W., Fishman, R.A. & Longar, S.M. (1984) Brain injury, edema, and vascular permeability changes induced by oxygen-derived free radicals. *Neurology* **34**, 315-320.

Chan, P.H., Chen, S.F. & Yu, A.C.H. (1988) Induction of intracellular superoxide radical formation by arachidonic acid and by polyunsaturated fatty acids in primary astrocytic cultures. *J. Neurochem.* **50**, 1185-1193.

Chan, P.H., Chu, L., Chen, S.F., Carlson, E.J. & Epstein, C.J. (1990) Reduced neurotoxicity in transgenic mice overexpressing human copper-zinc-superoxide dismutase. *Stroke* **21**, SIII, III80-III82.

Chao, C.C., Hu, S., Molitor,T.W., Shaskan, E.G. & Peterson, P.K. (1992) Activated microglia mediate neuronal injury via a nitric oxide mechanism. *J. Immunol.* **149**, 2736-2741.

Chen, H., Chopp, M. & Bodzin, G. (1992) Neutropenia reduces the volume of cerebral infarct after trasnient middle certebral artery occlusion in the rat. *Neurosci. Res. Comm.***11**, 93-99.

Chen, J., Chang, B., Williams, M. & Murad, F. (1991) Sodium nitroprusside degenerates cultured rat striatal neurons. *NeuroReport* **2**, 121-123.

Chen, Q., Chopp, M., Bodzin, G. & Chen, H. (1993) Temperature modulation of cerebral depolarization during focal cerebral ischemia in rats: correlation with ischemic injury. *J. Cereb. Blood Flow Metabol.* **13**, 389-394.

Chen, S.T., Hsu, C.Y., Hogan E.L., Maricq, H. & Balentine, J.D. (1986) A model of focal ischemic stroke in the rat: reproducible extensive cortical infarction. *Stroke* **17**, 738-743.

Cheung, J.Y., Bonventre, J.V., Malis, C.D. & Leaf, A. (1986) Calcium and ischemic injury. *New Engl. J. Med.* **314**, 1670-1676.

Cho, H.J., Xie, Q.-W., Calaycay, J., Mumford, R.A., Swiderek, K.M., Lee, T.D. & Nathan, C. (1992) Calmodulin is a subunit of nitric oxide synthase from macrophages. *J. Exp. Med.* **176**, 599-604.

Choi, D.W. (1987) Ionic dependence of glutamate neurotoxicity. *J. Neurosci.* **7**, 369-379.

Choi, D.W., Koh, J.-Y. & Peters, S. (1988) Pharmacology of glutamate neurotoxicity in cortical cell culture: attenuation by NMDA antagonists. *J. Neurosci.* **8**, 185-196.

Chuang, D.-M., Lin, W.-W. & Lee, C.Y. (1991) Endothelin-induced activation of phosphoinositide turnover, calcium mobilization, and transmitter release in cultured neurons and neurally related cell types. *J. Cardiovasc. Pharmacol.* **17**, S7, S85-S88.

Cole, D.J., Matsumara, J.S., Drummond, J.C., Schultz, R.L. & Wong, M.H. (1991) Time- and pressure-dependent changes in blood-brain barrier permeability after temporary middle cerebral artery occlusion in rats. *Acta Neuropath.* **82**, 266-273.

Cole, D.J., Matsumara, J.S., Drummond, J.C. & Schell, R.M. (1992) Focal cerebral ischemia in rats: effects of induced hypertension, during reperfusion, on CBF. *J. Cereb. Blood Flow Metabol.* **12**, 64-69.

Cooper, D.M.F. (1986) Guanine nucleotide regulatory proteins and signal transduction in the CNS - multiple mechanisms. *Clin. Neuropharmacol.* **9**, S4, 6-8.

Corasaniti, M.T., Tartaglia, R.L., Melino, G., Nistico, G. & Finazzi-Agro, A. (1992) Evidence that CHP100 neuroblastoma cell death induced by N-methyl-D-aspartate involves L-arginine-nitric oxide pathway activation. *Neurosci. Lett.* **147**, 221-223.

Courtney, M.J., Lambert, J.J. & Nicholls, D.G. (1990) The interactions between plasma membrane depolarization and glutamate receptor activation in the regulation of cytoplasmic free calcium in cultured cerebellar granule cells. *J. Neurosci.* **10**, 3873-3879.

Coyle, P. & Jokelainen, P.T. (1982) Dorsal cerebral arterial collaterals of the rat. *Anat. Rec.* **203**, 397-404.

Crowell, R.M., Olsson, Y., Klatzo, I. & Ommaya, A. (1970) Temporary occlusion of the middle cerebral artery in the monkey: clinical and pathological observations. *Stroke* **1**, 439-448.

Dalal, P.M., Shah, P.M. & Aiyar, R.R. (1965) Arteriographic study of cerebral embolism. *Lancet* 2, 358-361.

Daval, J-L., Von Lubitz, D.K.J.E., Deckert, J., Redmond, D.J. & Marangos, P.J. (1989) Protective effect of cyclohexyladenosine on adenosine A_1-receptors, guanine nucleotide and forskolin binding sites following transient brain ischemia: a quantitative autoradiographic study. *Brain Res.* **491**, 212-226.

Davenport, A.P. & Morton, A.J. (1991) Binding sites for ^{125}I ET-1, ET-2, ET-3 and vasoactive intestinal contractor are present in adult rat brain and neurone-enriched primary cultures of embryonic brain cells. *Brain Res.* **554**, 278-285.

Dawson, V.L., Dawson, T.M., London, E.D., Bredt , D.S. & Snyder, S.H. (1991) Nitric oxide mediates glutamate neurotoxicity in primary cortical cultures. *Proc. Natl. Acad. Sci. USA* **88**, 6368-6371.

Dawson, V.L., Dawson, T.M., Bartley, D.A., Uhl, G.R. & Snyder, S.H. (1993) Mechanisms of nitric oxide-mediated neurotoxicity in primary brain cultures. *J. Neurosci.* **13**, 2651-2661.

Deguchi, T. & Yoshioka, M. (1982) L-Arginine identified as an endogenous activator for soluble guanylate cyclase from neuroblastoma cells. *J. Biol. Chem.* **257**, 10147-10151.

Del Zoppo, G.J., Schmid-Schonbein, G.W., Mori, E., Copeland, B.R. & Chang, C.-M. (1991) Polymorphonuclear leukocytes occlude capillaries follwing middle cerebral artery occlusion and reperfusion in baboons. *Stroke* **22**, 1276-1283.

Demerle-Pallardy, C., Lonchampt, M.O., Chabrier, P.E. & Braquet, P. (1992) Absence of implication of L-arginine/nitric oxide pathway on neuronal cell injury induced by L-glutamate or hypoxia. *Biochem. Biophys. Res. Comm.* **181**, 456-464.

Dezsi, L., Greenberg, J.H., Hamar, J., Sladky, J., Karp, A. & Reivich, M. (1992) Acute improvement in histological outcome by MK-801 following focal cerebral ischemia and reperfusion in the cat independent of blood flow changes. *J. Cereb. Blood Flow Metabol.* **12**, 390-399.

Dickie, B.G.M., Lewis, M.J. & Davies, J.A. (1992) NMDA-induced release of nitric oxide potentiates aspartate overflow from cerebellar slices. *Neurosci. Lett.* **138**, 145-148.

Dietrich, W.D. (1992) The importance of brain temperature in cerebral injury. *J. Neurotrauma* **9**, S2, S475-S485.

Dietrich, W.D., Busto, R., Halley, M. & Valdes, I. (1990) The importance of brain temperature in alterations of the blood-brain barrier following cerebral ischemia. *J. Neuropathol. Exp. Neurol.* **49**, 486-497.

Douglas, S.A., James, S. & Hiley, C.R. (1991) Endothelial modulation and changes in endothelin pressor activity during hypoxia in the rat isolated perfused superior mesenteric arterial bed. *Br. J. Pharmacol.* **103**, 1441-1448.

Drinnan, S.L., Hope, B.T., Snutch, T.P. & Vincent, S.R. (1991) G_{olf} in the basal ganglia. *Mol. Cell. Neurosci.* **2**, 66-71.

Drummond, J.C., Oh, Y.-S., Cole, D.J. & Shapiro, H.M. (1989) Phenylephrine-induced hypertension reduces ischemia following middle cerebral artery occlusion in rats. *Stroke* **20**, 1538-1544.

Duverger, D. & MacKenzie, E. (1988) The quantification of cerebral infarction following focal ischemia in the rat: influence of strain, arterial pressure, blood glucose concentration, and age. *J. Cereb. Blood Flow Metabol.* **8**, 449-461.

Duverger, D., Viossat, I., Chabrier, P.-E., Pirotzky, E. & Braquet. P. (1992) Ischemie cerebrale focale chez le rat: quantification de l'endotheline tissulaire. *Circulation et Metabolisme du Cerveau* **9**, 85-93.

Dwyer, M.A., Bredt, D.S. & Snyder, S.H.(1991) Nitric oxide synthase: irreversible inhibition by L-N^G-nitroarginine in brain in vitro and in vivo. *Biochem. Biophys. Res. Commun.* **176**, 1136-1141.

East, S.J. & Garthwaite, J. (1990) Nanomolar N^G-nitroarginine inhibits NMDA-induced cyclic GMP formation in rat cerebellum. *Eur. J. Pharmacol.* **184**, 311-313.

East, S.J. & Garthwaite, J. (1991) NMDA receptor activation in rat hippocampus induces cyclic GMP formation through the L-arginine-nitric oxide pathway. *Neurosci. Lett.* **123**, 17-19.

East, S.J., Batchelor, A.M. & Garthwaite, J. (1991) Selective blockade of N-methyl-D-aspartate receptor function by the nitric oxide donor, nitroprusside. *Eur. J. Pharmacol.* **209**, 119-121.

Edvinsson, L., Emson, P., McCulloch, J., Tatemoto, K. & Uddman, R. (1984) Neuropeptide Y: Immunocytochemical localisation to and effect upon feline pial arteries and veins in vitro and in situ. *Acta Physiol. Scand.***122**, 155-163.

Eguchi, S., Hirata, Y., Imai, T. & Marumo, F. (1993) Endothelin receptor subtypes are coupled to adenylate cyclase via different guanyl nucleotide-binding proteins in vasculature. *Endocrinology* **132**, 524-529.

Eklof, B & Siesjo, B.K. (1972) The effect of bilateral carotid artery ligation upon the blood flow and energy state of the rat brain. *Acta Physiol. Scand.* **86**, 155-165.

Emori, T., Hirata, Y. & Marumo, F. (1991) Endothelin-3 stimulates prostacyclin production in cultured bovine endothelial cells. *J. Cardiovasc. Pharmacol.* **17**, S7, S140-S142.

Fabian, R.H. & Rea, H.C. (1993) Neuronal toxicity by macrophages in mixed brain cell culture is augmented by antineuronal IgG and dependent upon nitric oxide synthesis. *J. Neuroimmunol.* **44**, 95-102.

Faraci, F.M. (1989) Effects of endothelin and vasopressin on cerebral blood vessels. *Am. J. Physiol.* **257**, H799-H803.

Faraci, F.M. (1990) Role of nitric oxide in regulation of basilar artery tone in vivo. *Am. J. Physiol.* **259**, H1216-H1221.

Faraci, F.M. (1991) Role of endothelium-derived relaxing factor in cerebral circulation: large arteries vs. microcirculation. *Am. J. Physiol.* **261**, H1038-H1042.

Faraci, F.M. & Breese, K.R. (1993) Nitric oxide mediates vasodilation in response to activation of N-methyl-D-aspartate receptors in brain. *Circ. Res.* **72**, 476-480.

Faraci, F.M. & Heistad, D.D. (1992) Does basal production of nitric oxide contribute to regulation of brain-fluid balance? *Am. J. Physiol.* **262**, H340-H344.

Feldman, P.L., Griffith, O.W., Hong, H. & Stuehr, D.J. (1993) Irreversible inactivation of macrophage and brain nitric oxide synthase by L-N^G-methylarginine requires NADPH-dependent hydroxylation. *J. Med. Chem.* **36**, 491-496.

Fernandez, N., Garcia, J.L., Garcia-Villalon, A.L., Monge, L., Gomez, B. & Dieguez, G. (1993) Cerebral blood flow and cerebrovascular reactivity after inhibition of nitric oxide synthesis in conscious goats. *Br. J. Pharmacol.* **110**, 428-434.

Floyd, R.A. & Carney, J.M. (1992) Free radical damage to protein and DNA: mechanisms involved and relevant observations on brain undergoing oxidative stress. *Ann. Neurol.* **32**, S1, S22-S27.

Folbergrova, J., Kiyota, Y., Pahlmarkm K., Memezawa, H., Smith, M.-L. & Siesjo, B.K. (1993) Does ischemia with reperfusion lead to oxidative damage to proteins in the brain? *J. Cereb. Blood Flow Metabol.* **13**, 145-152.

Forstermann, U., Gorsky, L.D., Pollock, J.S., Schmidt, H.H.H.W., Heller, M. & Murad, F. (1990) Regional distribution of EDRF/ NO-synthesizing enzyme(s) in rat brain. *Biochem. Biophys. Res. Commun.* **168**, 727-732.

Forstermann, U., Pollock, J.S., Schmidt, H.H.H.W., Heller, M. & Murad, F. (1991) Calmodulin-dependent endothelium-derived relaxing factor/nitric oxide synthase activity is present in the particulate and cytosolic fractions of bovine aortic endothelial cells. *Proc. Natl. Acad. Sci. USA* **88**, 1788-1792.

Frandsen, A., Drejer, J. & Schousboe, A. (1989) Direct evidence that excitotoxicity in cultured neurons is mediated via N-methyl-D-aspartate (NMDA) as well as non-NMDA receptors. *J. Neurochem.* **53**, 297-299.

Freeman, B.A. & Crapo, J.D. (1982) Free radicals and tissue injury. *Lab. Invest.* **47**, 5, 412-426.

Frelin, C., Ladoux, A., Marsault, R. & Vigne, P. (1991) Functional properties of high- and low-affinity receptor subtypes for endothelin-3. *J. Cardiovasc. Pharmacol.* **17**, S7, S131-S133.

Fujimori, H. & Pan-Hou, H. (1991) Effect of nitric oxide on L-[^{3}H]glutamate binding to rat brain synaptic membranes. *Brain Res.* **554**, 355-357.

Fujisawa, H., Landolt, H., Macrae, I.M. & Bullock, R. (1993) Glutamate neurotoxicity in vivo: the effect of ischaemia and ionic concentrations in extracellular fluid. *J. Cereb. Blood Flow Metabol.* **13**, S1, S784.

Furchgott, R.F. & Zawadzki, J.V. (1980) The obligatory role of endothelial cells in the relaxation of arterial smooth muscle by acetylcholine. *Nature* **288**, 373-376.

Fuxe, K., Anggard, E., Lundgren, K., Cintra, A., Agnati, L.F., Galton, S. & Vane, J. (1989a) Localization of [^{125}I]endothelin-1 and [^{125}I]endothelin-3 binding sites in the rat brain. *Acta Physiol. Scand.* **137**, 563-564.

Fuxe, K., Cintra, A., Andbjer, B., Anggard, E., Goldstein, M. & Agnati, L.F. (1989b) Centrally administered endothelin-1 produces lesions in the brain of the male rat. *Acta Physiol. Scand.* **137**, 155-156.

Fuxe, K., Kurosawa, N., Cintra, A., Hallstrom, A., Goiny, M., Rosen, L., Agnati, L.F. & Ungerstedt, U. (1992) Involvement of local ischemia in endothelin-1 induced lesions of the neostriatum of the anaesthetized rat. *Exp. Brain Res.* **88**, 131-139.

Gally, J.A., Montague, P.R., Reeke, G.N.& Edelman, G.M. (1990) The NO hypothesis: Possible effects of a short-lived, rapidly diffusible signal in the development and function of the nervous system. *Proc. Natl. Acad. Sci. USA* **87**, 3547-3551.

Garcia, J.H. (1984) Experimental ischemic stroke: a review. *Stroke* **15**, 5-12.

Garcia, J.H. & Kamijyo, Y. (1974) Cerebral Infarction. Evolution of histopathological changes after occlusion of a middle cerebral artery in primates. *J. Neuropath. Exp. Neurol.* **33**, 408-421.

Garcia, J.H., Yoshida, Y., Chen, H., Li, Y., Zhang, Z.G., Lian, J., Chen, S. & Chopp, M. (1993) Progression from ischemic injury to infarct following middle cerebral artery occlusion in the rat. *Am. J. Pathol.* **142**, 623-635.

Gardiner, M., Smith, M.-L., Kagstrom, E., Shohami, E. & Siesjo, B.K. (1982) Influence of blood glucose concentration on brain lactate accumulation during severe hypoxia and subsequent recovery of brain energy metabolism. *J. Cereb. Blood Flow Metabol.* **2**, 429-438.

Gardiner, S.M., Compton, A.M., Kemp, P.A. & Bennett, T.(1990a) Regional and cardiac haemodynamic effects of N^G-nitro-L-arginine methyl ester in conscious, Long Evans rats. *Br. J. Pharmacol.* **101**, 625-631.

Gardiner, S.M., Compton, A.M., Kemp, P.A. & Bennett, T.(1990b) Regional and cardiac haemodynamic responses to glyceryl trinitrate, acetylcholine, bradykinin and endothelin-1in conscious rats: effects of N^G-nitro-L-arginine methyl esters. *Br. J. Pharmacol.* **101**, 632-639.

Garthwaite, G. & Garthwaite, J. (1988) Cyclic GMP and cell death in rat cerebellar slices. *Neurosci.* **26**, 321-326.

Garthwaite, J. (1990) Nitric oxide synthesis linked to activation of excitatory neurotransmitter receptors in the brain. In *Nitric oxide from L-arginine: a bioregulatory system,* ed. Moncada, S. & Higgs, E.A., pp 115-137, Amsterdam, Elsevier Science Publishers.

Garthwaite, J. (1991) Glutamate, nitric oxide and cell-cell signalling in the nervous system. *Trends Neurosci.* **14**, 60-67.

Garthwaite, J., Charles, S.L., Chess-Williams, R. (1988) Endothelium-derived relaxing factor release on activation of NMDA receptors suggests role as intercellular messenger in the brain. *Nature* **336**, 385-388.

Garthwaite, J., Southam, E. & Anderton, M. (1989) A kainate receptor linked to nitric oxide synthesis from arginine. *J. Neurochem.* **53**, 1952-1954.

Gasic, G.P. & Hollmann, M. (1992) Molecular neurobiology of glutamate receptors. *Annu. Rev. Physiol.* **54**, 507-536.

Gehlert, D.R., Dawson, T.M., Yamamura, H.I. & Wamsley, J.K.(1985) Quantitative autoradiography of [^{3}H]forskolin binding sites in the rat brain. *Brain Res.* **361**, 351-360.

Gehlert, D.R. (1986) Regional modulation of [^{3}H]forskolin binding in the rat brain by guanylyl-5'-imidodiphosphate and sodium fluoride: comparison with the distribution of guanine nucleotide binding sites. *J. Pharmacol. Exp. Ther.* **239**, 952-958.

Gemba, T., Matsunaga, K. & Ueda, M. (1992) Changes in extracellular concentrations of amino acids in the hippocampus during cerebral ischemia in stroke-prone SHR, stroke-resistant SHR and normotensive rats. *Neurosci. Lett.* **135**, 184-188.

Gerhart, D.Z., Djuricic, B. & Drewes, L.R. (1991) Quantitative immunocytochemistry (image analysis) of glucose transporters in the normal and postischemic rodent hippocampus.*J.Cereb. Blood Flow Metabol.* **11**, 440-448.

Gill, R. (1992) The pharmacology of excitatory amino acid antagonists in focal cerebral ischaemia in the rat. PhD Thesis, University of London.

Gill, R. & Woodruff, G.N. (1990) The neuroprotective actions of kynurenic acid and MK-801 in gerbils are synergistic and not related to hypothermia. *Eur. J. Pharmacol.* **176**, 143-149.

Gill, R., Brazell, C., Woodruff, G.N. & Kemp, J.A. (1991) The neuroprotective action of dizocilpine (MK-801) in the rat middle cerebral artery occlusion model of focal ischaemia. *Br. J. Pharmacol.* **103**, 2030-2036.

Gill, R., Nordholm, L. & Lodge, D. (1992) The neuroprotective actions of 2,3-dihydroxy-6-nitro-7-sulfamoyl-benzo(F)quinoxaline (NBQX) in a rat focal ischaemia model. *Brain Res.* **580**, 35-43.

Gilman, S.C., Bonner, M.J. & Pellmar, T.C. (1992) Peroxide effects on [^{3}H]L-glutamate release by synaptosomes isolated from the cerebral cortex. *Neurosci. Lett.* **140**, 157-160.

Gilmore, J.H., Lawler, C.P., Eaton, A.M. & Mailman, R.B. (1991) Postmortem stability of dopamine D_1 receptors and D_1 receptor mRNA. *Soc. Neurosci. Abstr.* **17**, 86.

Ginsberg, M.D. & Busto, R. (1989) Rodent models of cerebral ischemia. *Stroke* **20**, 1627-1642.

Ginsberg, M.D., Watson, B.D., Busto, R., Yoshida, S., Prado, R., Nakayama, H., Ikeda, M., Dietrich, W.D. & Globus, M.Y.-T. (1988) Peroxidative damage to cell membranes following cerebral ischemia. A cause of ischemic brain injury? *Neurochem. Pathol.* **9**, 171-193.

Ginsberg, M.D., Takagi, K. & Globus, M. Y.-T. (1992) Release of neurotransmitters in cerebral ischemia: relevance to neuronal injury. In *Pharmacology of cerebral ischemia 1992*, ed. Krieglstein, J. & Oberpichler-Schwenk, H., pp 177-189, Stuttgart, Wissenschaftliche Verlagsgesellschaft mbH.

Giuffrida, R., Bellomo, M., Polizzi, G. & Malatino, L.S. (1992) Ischemia-induced changes in the immunoreactivity for endothelin and other vasoactive peptides in the brain of the mongolian gerbil. *J. Cardiovasc. Pharmacol.* **20**, S12, S41-S44.

Giulian, D., Woodward, J., Young, D.G., Krebs, J.F. & Lachman, L.B. (1988) Interleukin-1 injected into mammalian brain stimulates astrogliosis and neovascularization. *J. Neurosci.* **8**, 2485-2490.

Goldberg, M.P., Weiss, J.H., Pham, P.-C. & Choi, D.W. (1987) N-Methyl-D-aspartate receptors mediate hypoxic neuronal injury in cortical culture. *J. Pharmacol. Exp. Ther.* **243**, 784-791.

Goldman, R.S., Finkbeiner, S.M. & Smith, S.J. (1991) Endothelin induces a sustained rise in intracellular calcium in hippocampal astrocytes. *Neurosci. Lett.* **123**, 4-8.

Gotoh, F., Fukuuichi, Y., Amano, T., Yamawaki, T., Ito, N., Muramatsu, K., Shirai, T., Takahashi, K. & Gotoh, J. (1991) Role of endothelium-derived relaxing and contracting factors in feline cerebral microcirculation. *Stroke* **22**, 144.

Gotoh, O., Asano, T., Koide, T. & Takakura, K. (1985) Ischemic brain edema following occlusion of the middle cerebral artery in the rat. I: The time courses of the brain water, sodium and potassium contents and blood-brain barrier permeability to ^{125}I-albumin. *Stroke* **16**, 101-109.

Gotoh, O., Mohamed, A.A., McCulloch, J., Graham, D.I., Harper, A.M. & Teasdale, G.M. (1986) Nimodipine and the haemodynamic and histopathological consequences of middle cerebral artery occlusion in the rat. *J.Cereb. Blood Flow Metabol.* **6**, 321-331.

Goy, M.F. (1991) cGMP: the wayward child of the cyclic nucleotide family. *Trends Neurosci.* **14**, 293-299.

Graf, R., Matsumoto, K., Risse, F., Rosner, G & Heiss, W.-D. (1992) Effect of mild hypothermia on glutamate accumulation in cat focal ischemia. *Stroke* **23**, 150.

Graham, D.I. (1977) Pathology of hypoxic brain damage in man. *J. Clin. Path.* **30**, S11, 170-180.

Graham, D.I. (1988) Vascular & hypoxic disorders. In *An introduction to neuropathology*, ed. Hume Adams, J. & Graham, D.I., pp 57-82, Edinburgh, Churchill Livingstone.

Graham, S.H., Shiraishi, K., Panter, S.S., Simon, R.P. & Faden, A.I. (1990) Changes in extracellular amino acid neurotransmitters produced by focal cerebral ischemia. *Neurosci. Lett.* **110**, 124-130.

Greenberg, D.A., Chan, J. & Sampson, H.A. (1992) Endothelins and the nervous system. *Neurology* **42**, 25-31.

Greenberg, J.H., Uematsu, D., Araki, N. & Reivich, M. (1991) Intracellular calcium and pathophysiological changes in cerebral ischaemia. *Arzneim.-Forsch./Drug Res.* **41** (I),3a, 324-332.

Greenblatt, E.P., Loeb, A.L. & Longnecker, D.E. (1992) Endothelium-dependent circulatory control - a mechanism for the differing peripheral vascular effects of isoflurane versus halothane. *Anesthesiol.* **77**, 1178-1185.

Grogaard, B., Schurer, L., Gerdin, B. & Arfors, K.E. (1989) Delayed hypoperfusion after incomplete forebrain ischemia in the rat. The role of polymorphonuclear leukocytes. *J. Cereb. Blood Flow Metabol.* **9**, 500-505.

Gross, P.M., Wainman, D.S., Esinosa, F.J., Nag, S. & Weavers, D.F. (1992) Cerebral hypermetabolism produced by intraventricular endothelin-1 in rats: inhibition by nimodipine. *Neuropeptides* **21**, 211-223.

Gross, S.S., Stuehr, D.J., Aisaka, K., Jaffe, E.A., Levi, R. & Griffith, O.W. (1990) Macrophage and endothelial cell nitric oxide synthesis: cell-type selective inhibition by N^G-aminoarginine, N^G-nitroarginine and N^G-methylarginine. *Biochem. Biophys. Res. Comm.* **170**, 96-103.

Grotta, J.C., Picone, C.M., Dedman, J.R., Rhoades, H.M., Strong, R.A., Earls, R.M. & Yao, L.P. (1990) Neuronal protection correlates with prevention of calcium-calmodulin binding in rats. *Stroke* **21**, SIII, III28-III31.

Gryglewski, R.J., Palmer, R.M.J. & Moncada, S. (1986) Superoxide anion is involved in the breakdown of endothelium-derived vascular relaxing factor. *Nature* **320**, 454-456.

Hadani, M., Young, W. & Flamm, E.S. (1988) Nicardipine reduces calcium accumulation and electrolyte derangements in regional cerebral ischemia in rats. *Stroke* **19**, 1125-1132.

Hagberg, H., Andersson, P., Butcher, S., Sandberg, M., Lehmann, A. & Hamberger, A. (1986) Blockade of N-methyl-D-aspartate-sensitive acidic amino-acid receptors inhibits ischemia-induced accumulation of purine catabolites in the rat striatum. *Neurosci. Lett.* **68**, 311-316.

Hakim, A.M., Hogan, M.J. & Carpenter, S. (1992) Time course of cerebral blood flow and histological outcome after focal cerebral ischemia in rats. *Stroke* **23**, 1138-1144.

Hall, E.D. (1993) Cerebral ischaemia, free radicals and antioxidant protection. *Biochem. Soc. Trans.* **21**, 334-339.

Hallenbeck, J.M., Dutka, A.J., Vogel, S.N., Heldman, E., Doron, D.A. & Feuerstein, G. (1991) Lipopolysaccharide-induced production of tumor necrosis factor activity in rats with and without risk factors for stroke. *Brain Res.* **541**, 115-120.

Halliwell, B. (1989) Oxidants and the central nervous system: some fundamental questions. *Acta Neurol. Scand.* **126**, 23-33.

Halsey, J.H., Conger, K.A., Garcia, J.H. & Sarvary, E. (1991) The contribution of reoxygenation to ischemic brain damage. *J. Cereb. Blood Flow Metabol.* **11**, 994-1000.

Hamilton, M.G., Frew, R. & Lundy, P.M. (1989) Effect of endothelin on Ca^{2+} influx, intracellular free Ca^{2+} levels and ligand binding to N and L type Ca^{2+} channels in rat brain. *Biochem. Biophys. Res. Comm.* **162**, 1332-1338.

Hara, H., Nagasawa, H. & Kogure, K. (1990) Nimodipine prevents postischemic brain damage in the early phase of focal cerebral ischemia. *Stroke* **21**, SIV, IV102-IV104.

Hara, H., Onodera, H., Kato, H., Araki, T. & Kogure, K.(1991) Autoradiographic analysis of second messenger and neurotransmitter system receptors in the gerbil hippocampus following transient forebrain ischemia *Brain Res.* **545**, 87-96.

Hara, H., Harada, K. & Sukamoto, T. (1993) Chronological atrophy after transient middle cerebral artery occlusion in rats. *Brain Res.* **618**, 251-260.

Harris, R.J., Symon, L., Branston, N.M., Bayhan, M. (1981) Changes in extracellular calcium activity in cerebral ischemia. *J. Cereb. Blood Flow Metabol.* **1**, 203-210.

Hartley, D.M., Kurth, M.C., Bjerkness, L., Weiss, J.H. & Choi, D.W. (1993) Glutamate receptor-induced Ca^{2+} accumulation in cortical cell culture correlates with subsequent neuronal degeneration. *J. Neurosci.* **13**, 1993-2000.

Hatashita, S. & Hoff, J.T. (1986) Role of a hydrostatic pressure gradient in the formation of early ischemic brain edema. *J. Cereb. Blood Flow Metabol.* **6**, 546-552.

He, Y.Y., Hsu, C.Y., Ezrin, A.M. & Miller, M.S. (1993) Polyethylene glycol-conjugated superoxide dismutase in focal cerebral ischemia-reperfusion. *Am. J. Physiol.* **265**, H252-H256.

Hecker, M., Mitchell, J.A., Harris, H.J., Katsura, M., Thiermann, C. & Vane, J.R. (1990) Endothelial cells metabolize N^G-monomethyl-L-arginine to L-citrulline and subsequently to L-arginine. *Biochem. Biophys. Res. Comm.* **167**, 1037-1043.

Heiss, W.-D., Herholz, K., Podreka, I., Neubauer, I. & Pietrzyk, U. (1990) Comparison of [^{99m}Tc]HMPAO SPECT with [^{18}F]fluoromethane PET in cerebrovascular disease. *J. Cereb. Blood Flow Metabol.* **10**, 687-697.

Hieda, H.S. & GomezSanchez, C.E. (1990) Hypoxia increases endothelin release in bovine endothelial cells in culture, but epinephrine, norepinephrine, serotonin, histamine and angiotensin II do not. *Life Sci.* **47**, 247-251.

Hillered, L., Hallstrom, A., Segersvard, S., Persson, L. & Ungerstedt, U. (1989) Dynamics of extracellular metabolites in the striatum after middle cerebral artery occlusion in the rat monitored by intracerebral microdialysis. *J. Cereb. Blood Flow Metabol.* **9**, 607-616.

Hiramatsu, K., Kassell, N.F., Goto, Y., Soleau, S. & Lee, K.S. (1993) A reproducible model of reversible, focal, neocortical ischemia in Sprague-Dawley rat. *Acta Neurochir.* **120**, 66-71.

Hirata, Y., Emori, T., Eguchi, S., Kanno, K., Imai, T., Ohta, K. & Marumo, F. (1993) Endothelin receptor subtype-B mediates synthesis of nitric oxide by cultured bovine endothelial cells. *J. Clin. Invest.* **91**, 1367-1373.

Hirosumi, J., Ouchi, Y., Watanabe, M., Kusonoki, J., Nakamura, T. & Orimo, H. (1988) Effect of superoxide and lipid peroxide on cytosolic free calcium concentration in cultured pig aortic endothelial cells. *Biochem. Biophys. Res. Comm.* **152**, 301-307.

Hogg, N., Darley-Usmar, V.M., Wilson, M.T. & Moncada, S. (1992) Production of hydroxyl radicals from the simultaneous generation of superoxide and nitric oxide. *Biochem. J.* **281**, 419-424.

Hogg, N., Darley-Usmar, V.M., Wilson, M.T. & Moncada, S. (1993) The oxidation of alpha-tocopherol in human low-density lipoprotein by the simultaneous generation of superoxide and nitric oxide. *FEBS Lett.* **326**, 199-203.

Hope, B.T., Michael, G.J., Knigge, K. & Vincent, S.R. (1991) Neuronal NADPH diaphorase is a nitric oxide synthase. *Proc. Natl. Acad. Sci. USA.* **88**, 2811-2814.

Hori, S., Komatsu, Y., Shigemoto, R., Mizuno, N. & Nakanishi, S. (1992) Distinct tissue distribution and cellular localization of two messenger ribonucleic acids encoding different subtypes of rat endothelin receptors. *Endocrinology* **130**, 1885-1895.

Horio, T., Kohno, K., Yokokawa, K., Murakawa, K.-I., Yasunari, K., Fujiwara, H., Kurihara, N. & Takeda, T. (1991) Effect of hypoxia on plasma immunoreactive endothelin-1 concentration in anesthetized rats. *Metabol.* **40**, 999-1001.

Hosli, E. & Hosli. L. (1991) Autoradiographic evidence for endothelin receptors on astrocytes in cultures of rat cerebellum, brainstem and spinal cord. *Neurosci. Lett.* **129**, 55-58.

Hossmann, K.-A. (1989) Calcium antagonists for the treatment of brain ischemia: a critical appraisal. In *Pharmacology of cerebral ischemia 1988*, ed. Krieglstein, J., pp 53-63, Stuttgart, Wissenschaftliche Verlagsgesellschaft mbH.

Hossmann, K.-A., Paschen, W. & Csiba, L (1983) Relationship between calcium accumulation and recovery of cat brain after prolonged cerebral ischemia. *J. Cereb. Blood Flow Metabol.* **3**, 346-353.

Huang, Z.-G., Preston, E., Xue, D. & Buchan, A.M. (1993) Blood-brain barrier damage after temporary focal ischemia is reduced by moderate post-ischemic hypothermia. *Stroke* **24**, 164.

Hudgins, W.R. & Garcia, J.H. (1970) Transorbital approach to the middle cerebral artery of the squirrel monkey: a technique for experimental cerebral infarction applicable to ultrastructural studies. *Stroke* **1**, 107-111.

Iadecola, C., Beitz, A.J., Renno, W., Xu, X., Mayer, B. & Zhang, F. (1993) Nitric oxide synthase-containing neural processes on large cerebral arteries and cerebral microvessels. *Brain Res.* **606**, 148-155.

Ignarro, L.J. (1990a) Biosynthesis and metabolism of endothelial derived nitric oxide. *Ann. Rev. Pharmacol. Toxicol.* **30**, 535-560.

Ignarro, L.J. (1990b) Heme-dependent activation of cytosolic guanylate-cyclase by L-arginine-derived nitric oxide represents a novel transduction mechanism for transcellular signaling. *Eur. J. Pharmacol.* **183**, 1624-1625.

Iino, M., Ozawa, S. & Tsuzuki, K. (1990) Permeation of calcium through excitatory amino acid receptor channels in cultured rat hippocampal neurones. *J. Physiol.* **424**, 151-165.

Imaizumi, S., Woolworth, V., Fishman, R.A. & Chan, P.H. (1989) Superoxide dismutase activities and their role in focal cerebral ischemia. *J. Cereb. Blood Flow Metabol.* **9**, S1, S217.

Imaizumi, S., Woolworth, V., Fishman, R.A. & Chan, P.H. (1990) Liposome-entrapped superoxide dismutase reduces cerebral infarction in cerebral ischemia in rats. *Stroke* **21**, 1312-1317.

Inoue, A., Yanagisawa, M., Kimura, S., Kasuya, Y., Miyauchi, T, Goto, K. & Masaki, T. (1989) The human endothelin family: three structurally and pharmacoloigcally distinct isopeptides predicted by three separate genes. *Proc. Natl. Acad. Sci. USA* **86**, 2863-2867.

Irino, T., Taneda, M. & Minami, T. (1977) Sanguineous cerebrospinal fluid in recanalized cerebral infarction. *Stroke* **8**, 22-24.

Izumi, Y., Benz, A.M., Clifford, D.B. & Zorumski, C.F. (1992) Nitric oxide inhibitors attenuate N-methyl-D-aspartate excitotoxicity in rat hippocampal slices. *Neurosci. Lett.* **135**, 227-230.

Izumi, Y., Benz, A.M., Clifford,D.B. & Zorumski, C.F. (1993) Neurotoxic effects of sodium nitroprusside in rat hippocampal slices. *Exp. Neurol.* **121**, 14-23.

Jacewicz, M., Tanabe, J. & Pulsinelli, W.A. (1992) The CBF threshold and dynamics for focal cerebral infarction in spontaneously hypertensive rats. *J. Cereb. Blood Flow Metabol.* **12**, 359-370.

Jansen, I., Fallgren, B. & Edvinsson, L. (1989) Mechanisms of action of endothelin on isolated feline cerebral arteries: in vitro pharamacology and electrophysiology. *J. Cereb. Blood Flow Metabol.* **9**, 743-747.

Joly, G.A., Schini, V.B. and Vanhoutte, P.M. (1992) Balloon injury and interleukin-1ß induce nitric oxide synthase activity in rat carotid arteries. *Circ. Res.* **71**, 331-338.

Jones, C.R., Hiley, C.R., Pelton, J.T. & Mohr, M. (1989) Autoradiographic visualization of the binding sites for [^{125}I]endothelin in rat and human brain. *Neurosci. Lett.* **97**, 276-279.

Jones, T.H., Morawetz, R.B., Crowell, R.M., Marcoux, F.W., Fitzgibbon, R.M., DeGirolami, U. & Ojemann, R.G. (1981) Thresholds of focal cerebral ischemia in awake monkeys. *J. Neurosurg.* **54**, 773-782.

Kaczmarek, L.K. (1986) The role of protein kinase C in the regulation of ion channels and neurotransmitter release. *Trends Neurosci.* **10**, 30-34.

Kadel, K.A., Heistad, D.D. & Faraci, F.M. (1990) Effects of endothelin on blood vessels of the brain and choroid plexus. *Brain Res.* **518**, 78-82.

Kader, A., Brisman, M.H., Maraire, N., Huh, J.-T. & Solomon, R.A. (1992) The effect of mild hypothermia on permanent focal ischemia in the rat. *Neurosurgery* **31**, 1056-1061.

Kagstrom, E., Smith, M.-L. & Siesjo, B.K. (1983) Recirculation in the rat brain following incomplete ischemia. *J. Cereb. Blood Flow Metabol.* **3**, 183-192.

Kamijyo, Y., Garcia, J.H. & Cooper, J. (1977) Temporary regional cerebral ischemia in the cat. A model of hemorrhagic and subcortical infarction. *J. Neuropath. Exp. Neurol.* **36**, 338-350.

Kanner, J., Harel, S. & Granit, R. (1992) Nitric oxide, an inhibitor of lipid oxidation by lipoxygenase, cyclooxygenase and hemoglobin. *Lipids* **27**, 46-49.

Kaplan B., Brint, S., Tanabe, J., Lacewicz, M., Wang, X.-J. & Pulsinelli, W. (1991) Temporal thresholds for neocortical infarction in rats subjected to reversible focal cerebral ischemia. *Stroke* **22**, 1032-1039.

Kataoka, Y., Koizumi, S., Kumakura, K., Kurihara, M., Niwa, M. & Ueki, S. (1989) Endothelin-1 triggered brain damage under hypoglycemia evidenced by real-time monitoring of dopamine release from rat striatal slices. *Neurosci. Lett.* **107**, 75-80.

Katusic, Z.S. (1991) Endothelium-independent contractions to N^{G}-monomethyl-L-arginine in canine basilar artery. *Stroke* **22**, 1399-1404.

Kebabian, J.W. & Calne, D.B. (1979) Multiple receptors for dopamine. *Nature* **277**, 93-96.

Kety, S.S. (1951) The theory and applications of the exchange of inert gas at the lungs and tissues. *Pharmacol. Rev.* **3**, 1-41.

Kety, S.S. & Schmidt, C.F. (1945) The determination of cerebral blood flow in man by the use of nitrous oxide in low concentrations. *Am. J. Physiol.* **143**, 53-66.

Kiedrowski, L., Manev, H., Costa, E. & Wroblewski, T. (1991) Inhibition of glutamate-induced cell death by sodium nitroprusside is not mediated by nitric oxide. *Neuropharmacol.* **30**, 1241-1243.

Kiedrowski, L., Costa, E. & Wroblewski, T. (1992a) Glutamate receptor agonists stimulate nitric oxide synthase in primary cultures of cerebellar granule cells. *J. Neurochem.* **58**, 335-341.

Kiedrowski, L., Costa, E. & Wroblewski, T. (1992b) Sodium nitroprusside inhibits N-methyl-D-aspartate-evoked calcium influx via a nitric oxide- and cGMP-independent mechanism. *Mol. Pharmacol.* **41**, 779-784.

Kiedrowski, L., Costa, E. & Wroblewski, T. (1992c) In vitro interaction between cerebellar astrocytes & granule cells: A putative role for nitric oxide. *Neurosci. Lett.* **135**, 59-61.

Kinouchi, H., Epstein, C.J., Mizui, T., Carlson, E., Chen, S.F. & Chan, P.H. (1991) Attenuation of focal cerebral ischemic injury in transgenic mice overexpressing CuZn superoxide dismutase. *Proc. Natl. Acad. Sci. USA* **88**, 11158-11162.

Kinuta, Y., Kimura, M., Itokawa, Y., Ishikawa, M. & Kikuchi, H. (1989) Changes in xanthine oxidase in ischemic rat brain. *J. Neurosurg.* **71**, 417-420.

Kirino, T.(1982) Delayed neuronal death in the gerbil hippocampus following ischemia. *Brain Res.* **239**, 57-69.

Kiwak, K.J., Coughlin, S.R. & Moskowitz, M.A. (1986) Arachidonic acid metabolism in brain blood vessels: implications for the pathogenesis and treatment of cerebrovascular diseases. In *Stroke: Pathophysiology, diagnosis and management*, ed. Barnett, H.J., Mohr, J.P., Stein, B.M. & Yatsu, F.M., pp 141-163, New York, Churchill Livingstone.

Kloog, Y., Bousso-Mittler, D., Bdolah, A. & Sokolovsky, M. (1989) Three apparent receptor subtypes for the endothelin/sarafotoxin family. *FEBS Lett.* **253**, 199-202.

Knowles, R.G., Palacios, M., Palmer, R.M.J. & Moncada, S. (1990) Nitric oxide synthase in the brain. In *Nitric oxide from L-arginine: a bioregulatory system*, ed. Moncada, S. & Higgs, E.A., pp 139-146, Amsterdam, Elsevier Science Publishers.

Kobatake, K., Sako, K., Izawa, M., Yamamoto, Y.L. & Hakim, A.M. (1984) Autoradiographic determination of brain pH following middle cerebral artery occlusion in the rat. *Stroke* **15**, 540-547.

Kochanek, P.M. & Hallenbeck, J.M. (1992) Polymorphonuclear leukocytes and monocytes/macrophages in the pathogenesis of cerebral ischemia and stroke. *Stroke* **23**, 1367-1379.

Koizumi, J.-I., Yoshida, Y., Nagasawa, T. & Ooneda, G. (1986) Experimental studies of ischemic brain edema. 1. A new experimental model of cerebral embolism in rats in which recirculation can be introduced in the ischemic area. *Jpn. J. Stroke* **8**, 1-8.

Koizumi, J.-I., Yoshida, Y., Nishigaya, K., Kanai, H. & Ooneda, G. (1989) Experimental studies of ischemic brain edema: effect of recirculation of the blood flow after ischemia on post-ischemic brain edema. *Jpn. J. Stroke* **11**, 11-17.

Kolleger, H., McBean, G.J. & Tipton, K.F. (1993) Reduction of striatal N-methyl-D-aspartate toxicity by inhibition of nitric oxide synthase. *Biochem. Pharmacol.* **45**, 260-264.

Konig, J.F.R. and Klippel, R.A. (1963) *The rat brain: a stereotaxic atlas of the forebrain and lower parts of the brain stem.* New York, Krieger.

Kontos, H.A. (1989) Oxygen radicals in cerebral ischemia. In *Cerebrovascular Diseases*, ed. Ginsberg, M.D. & Dietrich, W.D., pp 365-371, New York, Raven Press.

Kovach, A.G.B., Szabo, C., Benyo, Z., Csaki, C., Greenberg, J.H. & Reivich, M. (1992) Effects of N^G-nitro-L-arginine and L-arginine on regional cerebral blood flow in the cat. *J. Physiol.* **449**, 183-196.

Kozniewska, E., Oseka, M. & Stys, T. (1992) Effects of endothelium-derived nitric oxide on cerebral circulation during normoxia and hypoxia in the rat. *J. Cereb. Blood Flow Metabol.* **12**, 311-317.

Krause, G.S., DeGracia, D.J., Skjaerlund, J.M. & O'Neil, B.J. (1992) Assessment of free radical-induced damage in brain proteins after ischemia and reperfusion. *Resuscitation* **23**, 59-69.

Krejcy, K., Schwarzacher, S. & Raberger, R. (1993) Distribution and metabolism of N^G-nitro-L-arginine and N^G-nitro-L-arginine methyl ester in canine blood in vitro. *Naunyn-Schmiedeberg's Arch. Pharmacol.* **347**, 342-345.

Kukreja, R.C., Kontos, H.A., Hess, M.L & Ellis, E.F. (1986) PGH synthase and lipoxygenase generate superoxide in the presence of NADH or NADPH. *Circ. Res.* **59**, 612-619.

Kuroiwa, T., Ting, P., Martinez, H. & Klatzo, I. (1985) The biphasic opening of the blood-brain barrier to proteins following temporary middle cerebral artery occlusion. *Acta Neuropathol.* **68**, 122-129.

Kuroiwa, T., Shibutani, M.& Okeda, R. (1989) Nonhyperemic blood flow restoration and brain edema in experimental focal cerebral ischemia. *J. Neurosurg.* **70**, 73-80.

Kurumaji, A. & McCulloch, J. (1989) Effects of MK-801 upon local cerebral glucose utilisation in conscious rats and in rats anaesthetised with halothane. *J. Cereb. Blood Flow Metabol.* **9**, 786-794.

Ladoux, A. & Frelin, C. (1991) Endothelins inhibit adenylate cyclase in brain capillary endothelial cells. *Biochem. Biophys. Res. Comm.* **180**, 169-173.

Lafon-Cazal, M., Pietri, S., Culcasi, M. & Bockaert, J. (1993) NMDA-dependent superoxide production and neurotoxicity. *Nature* **364**, 535-537.

Laing, R.J., Jakubowski, J. & Laing, R.W. (1993) Middle cerebral artery occlusion without craniectomy in rats. Which model works best? *Stroke* **24**, 294-298.

Lamas, S., Marsden, P.A., Li, G.K., Tempst, P. & Michel, T. (1992) Endothelial nitric oxide synthase: Molecular cloning and characterization of a distinct constitutive enzyme isoform. *Proc. Natl. Acad. Sci. USA* **89**, 6348-6352.

Lambert, L.E., Whitten, J.P., Baron, B.M., Cheng, H.C., Doherty, N.S. & McDonald, I.A. (1991) Nitric oxide synthesis in the CNS, endothelium and macrophages differs in its sensitivity to inhibition by arginine analogues. *Life Sci.* **48**, 69-75.

Landolt, H., Bullock, R., Fujisawa, H., McCulloch, J. & Miller, S. (1993) Glutamate diffusion characteristics determine neurotoxicity in the rat brain: ^{14}C glutamate autoradiography. *J. Cereb. Blood Flow Metabol.* **13**, S1, S753.

Lassen, N.A. (1966) The luxury-perfusion syndrome and its possible relation to acute metabolic acidosis localized within the brain. *Lancet* **ii**, 1113-1115.

Lassen, N.A., Andersen, A.R., Friberg, L. & Paulson, O.B. (1988) The retention of Tc^{99m}-D,L-HMPAO in the human brain after intracarotid bolus injection: a kinetic analysis. *J. Cereb. Blood Flow Metabol.* **8**, S1, S13-S22.

Laurenza, A., McHugh Sutkowski, E. & Seamon, K.B.(1989) Forskolin: a specific stimulator of adenylyl cyclase or a diterpene with multiple sites of action? *Trends Pharmacol. Sci.* **10**, 442-447.

Lawrence, A.J. & Jarrott, B. (1993) Nitric oxide increases interstitial excitatory amino acid release in the rat dorsomedial medulla oblongata. *Neurosci. Lett.* **151**, 126-129.

Lear, J.L. (1988) Initial cerebral HM-PAO distribution compared to LCBF: use of a model which considers cerebral HM-PAO trapping kinetics. *J. Cereb. Blood Flow Metabol.* **8**, S1, S31-S37.

Lees, G.J. (1991) Inhibition of sodium-potassium-ATPase: a potentially ubiquitous mechanism contributing to central nervous system neuropathology. *Brain Res. Rev.* **16**, 283-300.

Lei, S.Z., Pan, Z.-H., Aggarwal, S.K., Chen, H.-S. V., Hartman, J., Sucher, N.J. & Lipton, S.A. (1992) Effect of nitric oxide production on the redox modulatory site of the NMDA receptor-channel complex. *Neuron* **8**, 1087-1099.

Lerman, A., Sandok, E.K., Hildebrand, F.L. & Burnett, J.C. (1992) Inhibition of endothelium-derived relaxing factor enhances endothelin-mediated vasoconstriction. *Circulation* **85**, 1894-1898.

Levine, S. & Marvin, K. (1960) Ischemic infarction and swelling in rat brain. *Arch. Pathol.* **69**, 76-85.

Lin, T.-N., He, Y.Y., Wu, G., Khan, M. & Hsu, C.Y. (1993) Effect of brain edema on infarct volume in a focal cerebral ischemia model in rats. *Stroke* **24**, 117-121.

Lin, W.-W., Lee, C.Y. & Chuang, D.-M. (1990) Endothelin-1 stimulates the release of preloaded [^{3}H]aspartate from cultured cerebellar granule cells. *Biochem. Biophys. Res. Comm.* **167**, 593-599.

Lin, Y. & Phillis, J.W. (1992) Deoxycoformycin and oxypurinol: protection against focal ischemic brain injury in the rat. *Brain Res.* **571**, 272-280.

Lindsay, S., Liu, T.-H., Xu, J., Marshall, P.A., Thompson, J.K., Parks, D.A., Freeman, B.A., Hsu, C.Y. & Beckman, J.S. (1991) Role of xanthine dehydrogenase and oxidase in focal cerebral ischemic injury to rat. *Am. J. Phys.* **261**, H2051-H2057.

Lipton, S.A., Choi, Y.-B., Pan, Z.-H., Lei, S.Z., Chen, H.-S. V., Sucher, N.J., Loscaizo, J., Singel, D.J. & Stamler, J.S. (1993) A redox-based mechanism for the neuroprotective and neurodestructive effects of nitric oxide and related nitroso-compounds. *Nature* **364**, 626-632.

Liu, T., McDonnell, P.C., Young, P.R., White, R.F., Siren, A.-L., Barone, F.C. & Feuerstein, G.Z. (1993) Interleukin-1ß mRNA expression increases in focal ischemic rat cortex. *Stroke* **24**, 183.

Liu, T.H., Beckman, J.S., Freeman, B.A., Hogan, E.L. & Hsu, C.Y. (1989) Polyethylene glycol-conjugated superoxide dismutase and catalase reduce ischemic brain injury. *Am. J. Phys.* **256**, H589-H593.

Lucas, D.R. & Newhouse, J.P. (1957) The toxic effect of sodium L-glutamate on the inner layers of the retina. *A.M.A. Arch. Ophthalmol.* **58**, 193.

Lunec, J. (1990) Free radicals: their involvement in disease processes. *Ann. Clin. Biochem.* **27**, 173-182.

Luscher, T.F., Yang, Z., Kiowski, W., Linder, L. & Dohi, Y. (1992) Endothelin-induced vasoconstriction and calcium antagonists. *J. Human Hypertension* **6**, S2, S3-S8.

Lustig, H.S., von Brauchitsch, K.L., Chan, J. & Greenberg, D.A. (1992a) Cyclic GMP modulators and excitotoxic injury in cerebral cortical cultures. *Brain Res.* **577**, 343-346.

Lustig, H.S., Chan, J. & Greenberg, D.A. (1992b) Comparative neurotoxic potential of glutamate, endothelins, and platelet-activating factor in cerebral cortical cultures. *Neurosci. Lett.* **139**, 15-18.

Lyrer, P., Landolt, H., Kabiersch, A., Langemann, H. & Kaser, H. (1991) Levels of low molecular weight scavengers in the rat brain during focal ischemia. *Brain Res.* **567**, 317-320.

McBurney, R.N., Daly, D., Fischer, J.B., Hu, L.-Y., Subbarao, K., Knapp, A.G., Kobayashi, K., Margolin, L., Reddy, N.L. & Goldin, S.M. (1992) New CNS-specific calcium antagonists. *J. Neurotrauma* **9**, S2, S531-S543.

McCord, J.M. (1985) Oxygen-derived free radicals in postischemic tissue injury. *N. Engl. J. Med.* **312**, 159-163.

McCulloch, J. & Edvinsson, L. (1984) Cerebrovascular smooth muscle reactivity; a critical appraisal of in vitro and in situ techniques. *J. Cereb. Blood Flow Metabol.* **4**, 129-139.

McCulloch, J., Uddman, R., Kingman, T.A. & Edvinsson, L. (1986) Calcitonin gene-related peptide: Functional role in cerebrovascular regulation. *Proc. Natl. Acad. Sci. USA* **83**, 5731-5735.

McCulloch, J., Bullock, R. & Teasdale, G.M.(1991) Excitatory amino acid antagonists: opportunities for the treatment of ischaemic brain damage in man. In *Excitatory amino acid antagonists*, ed.B.S. Meldrum, pp 287-326, Oxford, Blackwell Scientific Publications.

MacCumber, M.W., Ross,C.A. & Snyder, S.H. (1990) Endothelin in brain: receptors, mitogenesis, and biosynthesis in glia cells. *Proc. Natl. Acad. Sci. USA* **87**, 2359-2363.

MacDermott, A.B. & Dale, N. (1987) Receptors, ion channels and synaptic potentials underlying the integrative actions of excitatory amino acids. *Trends Neurosci.* **10**, 280-284.

McGonigle, P. & Molinoff, P.B. (1981) Quantitative aspects of drug-receptor interaction. In *Basic Neurochemistry*, ed. Siegel, G.J., Agranoff, B.W., Albers, R.W. & Molinoff, P.B., pp 183-201, New York, Raven Press.

Macrae, I.M. (1992) New models of focal cerebral ischaemia. *Br. J. Clin. Pharmacol.* **34**, 302-308.

Macrae, I.M., McAuley, M.A., Robinson, M.J., Reid, J.L. & McCulloch, J. (1991). Endothelin-1-induced hypertension: a consequence of medullary ischaemia? *J. Cardiovasc. Pharmacol.* **17**, S7, S496-S499.

Macrae, I.M., Robinson, M.J., Graham, D.I., Reid, J.L. & McCulloch, J. (1993) Endothelin-1 induced reductions in cerebral blood flow: dose dependency, time course and neuropathological consequences. *J. Cereb. Blood Flow Metabol.* **13**, 276-284.

Ma, X.-L., Lefer, A.M. & Zipkin, R.E. (1993) S-Nitroso-N-acetylpenicillamine is a potent inhibitor of neutrophil-endothelial interaction. *Endothelium* **1**, 31-39.

Mabe, H., Blomqvist, P. & Siesjo, B.K. (1983) Intracellular pH in the brain following transient ischemia. *J. Cereb. Blood Flow Metabol.* **3**, 109-114.

Malinski, T., Bailey, F., Zhang, Z.G. & Chopp, M. (1993) Nitric oxide measured by a porphyrinic microsensor in rat brain after transient middle cerebral artery occlusion. *J. Cereb. Blood Flow Metabol.* **13**, 355-358.

Manzoni, O., Prezeau, I., Marin, P., Deshager, S., Bockaert, J. & Fagni, L. (1992) Nitric oxide-induced blockade of NMDA receptors. *Neuron* **8**, 653-662.

Marin, P., Lafon-Cazal M. & Bockaert, J. (1992) A nitric oxide synthase activity selectively stimulated by NMDA receptors depends on protein kinase C activation in mouse striatal neurons. *Eur. J. Neurosci.* **4**, 425-432.

Martin de Aguilera, E., Irurzun, A., Vila, J.M., Aldasoro, M., Galeote, M.S. & Lluch, S. (1990) Role of endothelium and calcium channels in endothelin-induced contraction of human cerebral arteries. *Br. J. Pharmacol.* **99**, 439-440.

Martz, D., Beer, M. & Betz, A.L. (1990) Dimethylthiourea reduces ischemic brain edema without affecting cerebral blood flow. *J. Cereb. Blood Flow Metabol.* **10**, 352-357.

Martz, D., Rayos, G., Schielke, G.P. & Betz, A.L. (1989) Allopurinol and dimethylthiourea reduce brain infarction following middle cerebral artery occlusion in rats. *Stroke* **20**, 488-494.

Matsumiya, N., Koehler, R.C., Kirsch, J.R. & Traystman, R.J. (1991) Conjugated superoxide dismutase reduces extent of caudate injury after transient focal ischemia in cats. *Stroke* **22**, 1193-1200.

Matsumoto, T., Nakane, M., Pollock, J.S., Kuk, J.E. & Forstermann, U. (1993) A correlation between soluble brain nitric oxide synthase and NADPH-diaphorase activity is only seen after exposure of the tissue to fixative. *Neurosci. Lett.* **155**, 61-64.

Mayer, B., John, M. & Bohme, E. (1990) Purification of a Ca^{2+}/calmodulin-dependent nitric oxide synthase from porcine cerebellum. *FEBS Lett.* **277**, 215-219.

Mayer, B., Klatt, P.,Bohme, E. & Schmidt, K. (1992) Regulation of neuronal nitric oxide and cyclic GMP formation by Ca^{2+}. *J. Neurochem.* **59**, 2024-2029.

Meldrum, B. & Garthwaite, J. (1991) Excitatory amino acid neurotoxicity and neurodegenerative disease. *Trends Pharmacol. Sci.* **12**, 54-62.

Melloni, E. & Pontremoli, S. (1989) The calpains. *Trends Neurosci.* **12**, 438-444.

Memezawa, H., Minamisawa, H., Smith, M.-L. & Siesjo, B.K. (1992a) Ischemic penumbra in a model of reversible middle cerebral artery occlusion in the rat. *Exp. Brain Res.* **89**, 67-78.

Memezawa, H., Smith, M.-L. & Siesjo, B.K. (1992b) Penumbral tissues salvaged by reperfusion following middle cerebral artery occlusion in rats. *Stroke* **23**, 552-559.

Mendez, M.F., Adams, N.L. & Lewandowski, K.S. (1989) Neurobehavioral changes associated with caudate lesions. *Neurology* **39**, 349-354.

Michowiz, S.D., Melamed, E., Pikarsky, E. & Rappaport, Z.H. (1990) Effect of ischemia induced by middle cerebral artery occlusion on superoxide dismutase activity in rat brain. *Stroke* **21**, 1613-1617.

Mickel, H.S., Vaishnav, Y.N., Kempski, O., von Lubitz, D., Weiss, J.F. & Feuerstein, G. (1987) Breathing 100% oxygen after global brain ischemia in Mongolian gerbils results in increased lipid peroxidation and increased mortality. *Stroke* **18**, 426-430.

Miki, N., Kawabe, Y. & Kuriyama, K. (1977) Activation of cerebral guanylate cyclase by nitric oxide. *Biochem. Biophys. Res. Comm.* **75**, 851-856.

Mima, T., Yanagisawa, M., Shigeno, T., Saito, A., Goto, K., Takakura, K. & Masaki, T. (1989) Endothelin acts in feline and canine cerebral-arteries from the adventitial side. *Stroke* **20**, 11, 1553-1556.

Minami. M., Kuraishi, Y., Yabuuchi, K., Yamazaki, A. & Satoh, M. (1992) Induction of interleukin-1ß mRNA in rat brain after transient forebrain ischemia. *J. Neurochem.* **58**, 390-392.

Miyamoto, M., Murphy, T.H., Schnaar, R.L. & Coyle, J.T. (1989) Antioxidants protect against glutamate-induced cytotoxicity in a neuronal cell line. *J. Pharmacol. Exp. Ther.* **250**, 1132-1140.

Mizui, T., Kinouchi, H. & Chan, P.H. (1992) Depletion of brain glutathione by buthionine sulfoximine enhances cerebral ischemic injury in rats. *Am. J. Phys.* **262**, H313-H317.

Mohamed, A.A., Gotoh, O., Graham, D.I., Osborne, K.A., McCulloch, J., Mendelow, A.D., Teasdale, G.M. & Harper, A.M. (1986) Effect of pretreatment with the calcium antagonist, nimodipine, on local cerebral blood flow and histopathology after middle cerebral artery occlusion. *Ann. Neurol.* **18**, 705-711.

Mohr, J.P., Gautier, J.C., Hier, D.B. & Stein, R.W. (1986) Middle cerebral artery. In *Stroke: Pathophysiology, diagnosis and management*, ed. Barnett, H.J., Mohr, J.P., Stein, B.M. & Yatsu, F.M., pp 377-450, New York, Churchill Livingstone.

Monaghan, D.T., Bridges, R.J. & Cotman, C.W. (1989) The excitatory amino acid receptors: their classes, pharmacology, and distinct properties in the function of the central nervous system. *Annu. Rev. Pharmacol. Toxicol.* **29**, 365-402.

Moncada C., Lekieffre, D., Arvin, B. & Meldrum, B. (1992) Effect of NO synthase inhibition on NMDA- and ischaemia-induced hippocampal lesions. *NeuroReport* **3**, 530-533.

Moncada, S., Palmer, R.M.J. & Higgs, E.A. (1991) Nitric oxide: physiology, pathophysiology and pharmacology. *Pharmacol. Rev.* **43**, 109-142.

Monyer, H., Hartley, D.M. & Choi, D.W. (1990) 21-Aminosteroids attenuate excitotoxic neuronal injury in cortical cell cultures. *Neuron* **5**, 121-126.

Moore, P.K., al-Swayeh, O.A., Chong, N.W.S., Chong, R.A. & Gibson, A. (1990) L-N^G-Nitro arginine (L-NOARG), a novel, L-arginine-reversible inhibitor of endothelium-dependent vasodilatation in vitro. *Br. J. Pharmacol.* **99**, 408-412.

Moore, P.K., Babbedge, R.C., Wallace, P., Gaffen, Z.A. & Hart, S.L. (1993) 7-Nitro indazole, an inhibitor of nitric oxide synthase, exhibits anti-nociceptive activity in the mouse without increasing blood pressure. *Br. J. Pharmacol.* **108**, 296-297.

Moorhouse, P.C., Grootveld, M., Halliwell, B., Quinlan, J.G. & Gutteridge, J.M.C. (1987) Allopurinol and oxypurinol are hydroxyl radical scavengers. *FEBS Lett.* **213**, 23-28.

Morawetz, R.B., DeGirolami, U., Ojemann, R.G., Marcoux, F.W. & Crowell, R.M. (1978) Cerebral blood flow determined by hydrogen clearance during middle cerebral artery occlusion in unanesthetized monkeys. *Stroke* **9**, 143-149.

Mori, E., del Zoppo, G.J., Chambers, D., Copeland, B.R. & Arfors, K.E. (1992) Inhibition of polymorphonuclear leukocytes adherence suppresses no-reflow after focal cerebral ischemia in baboons. *Stroke* **23**, 712-718.

Morikawa, E., Ginsberg, M.D., Dietrich, W.D., Duncan, R.C., Kraydieh, S., Globus, M.-Y., T. & Busto, R. (1992a) The significance of brain temperature in focal cerebral ischemia: histopathological consequences of middle cerebral artery occlusion in the rat. *J. Cereb. Blood Flow Metabol.* **12**, 380-389.

Morikawa, E., Huang, Z. & Moskowitz, M.A. (1992b) L-Arginine decreases infarct size caused by middle cerebral arterial occlusion in SHR. *Am. J. Physiol.* **263**, H1632-H1635.

Morikawa, E., Rosenblatt, S. & Moskowitz, M.A. (1992c) L-Arginine dilates rat pial arterioles by nitric oxide-dependent mechanisms and increases blood flow during focal cerebral ischaemia. *Br. J. Pharmacol.* **107**, 905-907.

Morioka, T., Kalehua, A.N. & Street, W.J. (1993) Characterization of microglial reaction after middle cerebral artery occlusion in rat brain. *J. Comp. Neurol.* **327**, 123-132.

Morris, R.G.M. & Collingridge, G. (1993) Expanding the potential. *Nature* **364**, 104-105.

Moyer, D.J., Welsh, F.A. & Zager, E.L. (1992) Spontaneous cerebral hypothermia diminishes focal infarction in rat brain. *Stroke* **23**, 1812-1816.

Muldoon, S.M., Hart, J.L., Bowen, K.A. & Freas, W. (1988) Attenuation of endothelium mediated vasodilation by halothane. *Anesthesiol.* **68**, 31-37.

Murphy, S., Minor, R.L., Welk, G. & Harrison, D. (1990) Evidence for an astrocyte-derived vasorelaxing factor with properties similar to nitric oxide. *J. Neurochem.* **55**, 349-351.

Myers, P.R., Minor, R.L., Guerra, R., Bates, J.N. & Harrison, D.G. (1990) Vasorelaxant properties of the endothelium-derived relaxing factor more closely resemble S-nitrosocysteine than nitric oxide. *Nature* **345**, 161-163.

Nagafuji, T., Matsui, T., Koide, T. & Asano, T. (1992) Blockade of nitric oxide formation by N^{w}-nitro-L-arginine mitigates ischemic brain edema and subsequent cerebral infarction in rats. *Neurosci. Lett.* **147**, 159-162.

Nagasawa, H. & Kogure, K. (1989) Correlation between cerebral blood flow and histologic changes in a new rat model of middle cerebral artery occlusion. *Stroke* **20**, 1037-1043.

Nakane, M., Mitchell, J., Forstermann, U. & Murad, F. (1991) Phosphorylation by calcium calmodulin-dependent protein kinase II and protein kinase C modulates the activity of nitric oxide synthase. *Biochem. Biophys. Res. Comm.* **180**, 1396-1402.

Nathan, C. (1992) Nitric oxide as a secretory product of mammalian cells. *FASEB J.* **6**, 3051-3064.

Nedergaard, M. (1987) Neuronal injury in the infarct border: a neuropathological study in the rat. *Acta Neuropathol.* **73**, 267-274.

Nehls, D.G., Park, C.K., MacCormack, A.G. & McCulloch, J. (1990) The effects of N-methyl-D-aspartate receptor blockade with MK-801 upon the relationship between cerebral blood flow and glucose utilisation. *Brain Res.* **511**, 271-279.

Nellgard, B. & Wieloch, T. (1992) Postischemic blockade of AMPA but not NMDA receptors mitigates neuronal damage in the rat brain following transient severe cerebral ischemia. *J. Cereb. Blood Flow Metabol.* **12**, 2-11.

Nguyen, T., Brunson, D., Crespi, C.L., Penman, B.W., Wishnok, J.S. & Tannenbaum, S.R. (1992) DNA damage and mutation in human cells exposed to nitric oxide in vitro. *Proc. Natl. Acad. Sci. USA* **89**, 3030-3034.

Nicholls, D. & Attwell, D. (1990) The release and uptake of excitatory amino acids. *Trends Pharmacol. Sci.* **11**, 462-468.

Nikolov, R., Rami, A. & Krieglstein, J. (1993) Endothelin-1 exacerbates focal cerebral ischemia without exerting neurotoxic action in vitro. *Eur. J. Pharmacol.* **248**, 205-208.

Niwa, M., Kawaguchi, T., Fujimoto, M., Kataoka, Y. & Taniyama, K. (1991) Receptors for endothelin in the central nervous system. *J. Cardiovasc. Pharmacol.* **17**, S7, S137-S139.

Novelli, A., Reilly, J.A., Lysko, P.G. & Henneberry, R.C. (1988) Glutamate becomes neurotoxic via the N-methyl-D-aspartate receptor when intracellular energy levels are reduced. *Brain Res.* **451**, 205-212.

Nowicki, J.P., Duval, D., Poignet, H. & Scatton, B. (1991) Nitric oxide mediates neuronal death after focal cerebral ischaemia in the mouse. *Eur. J. Pharmacol.* **204**, 339-340.

Nozaki, K., Moskowitz, M.A., Maynard, K.I., Koketsu, N., Dawson, T.M., Bredt, D.S & Snyder, S.H. (1993) Possible origins and distribution of immunoreactive nitric oxide synthase-containing nerve fibers in cerebral arteries. *J. Cereb. Blood Flow Metabol.* **13**, 70-79.

O'Brien, M. & Waltz, A.G. (1973) Intracranial pressure gradients caused by experimental cerebral ischemia and edema. *Stroke* **4**, 694-698.

Ogura, K., Takayasu, M. & Dacey, R.G. (1991) Differential effects of intra- and extraluminal endothelin on cerebral arterioles. *Am. J. Physiol.* **261**, H531-H537.

Oh, S.M. & Betz, A.L. (1991) Interaction between free radicals and excitatory amino acids in the formation of ischemic brain edema in rats. *Stroke* **22**, 915-921.

Oliver, C.N., Starke-Reed, P.E., Stadtman, E.R., Liu, G.J., Carney, J.M. & Floyd, R.A. (1990) Oxidative damage to brain proteins, loss of glutamine synthetase activity, and production of free radicals during ischemia/reperfusion-induced injury to gerbil brain. *Proc. Natl. Acad. Sci. USA* **87**, 5144-5147.

Olney, J.W. (1978) Neurotoxicity of excitatory amino acids. In *Kainic Acid as a Tool in Neurobiology* , ed. McGeer, E.G., Olney, J.W. & McGeer, P.L., pp 95-121, New York, Raven Press.

Olney, J.W., Ho, O.L. & Rhee, V. (1971) Cytotoxic effects of acidic and sulphur containing amino acids on the infant mouse central nervous system. *Exp. Brain. Res.* **14**, 61-76.

Olsen, T.S. (1983) Should induced hypertension or hypotension ever be used in the treatment of stroke? *Acta Med. Scand.* **678**, 113-120.

Olsen, T.S. (1986) Regional cerebral blood flow after occlusion of the middle cerebral artery. *Acta Neurol. Scand.* **73**, 321-337.

Olsen, T.S. (1991) Outcome following occlusion of the middle cerebral artery. *Acta Neurol. Scand.* **83**, 254-258.

Olsen, T.S. & Lassen, N.A. (1984) A dynamic concept of middle cerebral artery occlusion and cerebral infarction in the acute state based on interpreting severe hyperemia as a sign of embolic migration. *Stroke* **15**, 458-468.

Onesti, S.T., Baker, C.J., Sun, P.P & Solomon, R.A. (1991) Transient hypothermia reduces focal ischemic brain injury in the rat. *Neurosurgery* **29**, 369-373.

Onodera, H. & Kogure, K.(1989) Mapping second messenger systems in the rat hippocampus after transient forebrain ischemia: in vitro [^{3}H]forskolin & [^{3}H]inositol 1,4,5-triphosphate binding. *Brain Res.* **487**, 343-349.

Onodera, H., Araki, T. & Kogure, K. (1989) Protein kinase C activity in the rat hippocampus after forebrain ischemia: autoradiographic analysis by [^{3}H]phorbol 12,13-dibutyrate. *Brain Res.* **481**, 1-7.

Osborne, K.A., Shigeno, T., Balarsky, A-M., Ford, I., McCulloch, J., Teasdale, G.M. & Graham, D.I. (1987) Quantitative assessment of early brain damage in a rat model of focal cerebral ischaemia. *J. Neurol. Neurosurg. Psychiatry* **50**, 402-410.

Palmer, R.M.J., Ferrige, A.G. & Moncada, S. (1987) Nitric oxide release accounts for the biological activity of endothelium-derived relaxing factor. *Nature* **327**, 524-526.

Palmer, R.M.J., Ashton, D.S. & Moncada, S. (1988) Vascular endothelial cells synthesize nitric oxide from L-arginine. *Nature* **333**, 664-666.

Palmer, R.M.J., Bridge, L., Foxwell, N.A. & Moncada, S. (1992) The role of nitric oxide in endothelial cell damage and its inhibition by glucocorticoids. *Br. J. Pharmacol.* **105**, 11-12.

Panetta, J.A., Phillips, M.L. & Clemens, J.A. (1989) Effects of various pharmacological treatments on brain damage in rats subjected to cerebral ischemia. *J. Cereb. Blood Flow Metabol.* **9**, S1, S635.

Pang, C.C.Y., Wang, Y.-X. & Abdelrahman A. (1992) Halothane attenuates pressor and hemodynamic effects of N^G-Nitro-L-arginine (L-NNA) in rats. *FASEB J.* **6**, A1298.

Park, C.K., Nehls, D.G., Graham, D.I., Teasdale, G.M. & McCulloch, J. (1988) The glutamate antagonist MK-801 reduces focal ischaemic brain damage in the rat. *Ann. Neurol.* **24**, 543-551.

Park, C.K., Nehls, D.G., Teasdale, G.M. & McCulloch, J. (1989) Effect of the NMDA antagonist MK-801 on local cerebral blood flow in focal cerebral ischaemia in the rat. *J. Cereb. Blood Flow Metabol.* **9**, 617-622.

Pasqualotto, B.A., Hope, B.T. & Vincent, S.R. (1991) Citrulline in the rat brain: immunohistochemistry and coexistence with NADPH-diaphorase. *Neurosci. Lett.* **128**, 155-160.

Patel, P.M., Drummond, J.C. & Cole, D.J. (1991a) Induced hypertension during restoration of flow after temporary middle cerebral artery occlusion in the rat: effect on neuronal injury and edema. *Surg. Neurol.* **36**, 195-201.

Patel, P.M., Drummond, J.C., Cole, D.J., Giamela, R. & Steinauer, J. (1991b) Delayed institution of hypertension during focal cerebral ischemia: effect on brain edema. *Acta Neuropathol.* **81**, 339-344.

Pellegrini-Giampetro, D.E., Cherici, G., Alesiani, M., Carla, V. & Moroni, F. (1988) Excitatory amino acid release from rat hippocampal slices as a consequence of free-radical formation. *J. Neurochem.* **51**, 1960-1963.

Pellegrini-Giampetro, D.E., Cherici, G., Alesiani, M., Carla, V. & Moroni, F. (1990) Excitatory amino acid release and free radical formation may cooperate in the genesis of ischemia-induced neuronal damage. *J. Neurosci.* **10**, 1035-1041.

Persson, L., Hardemark, H.-G., Bolander, H.G., Hillered, L. & Olsson, Y. (1989) Neurologic and neuropathologic outcome after middle cerebral artery occlusion in rats. *Stroke* **20**, 641-645.

Peterson, D.A., Peterson, D.C., Archer, S. & Weir, E.K. (1992) The non specificity of specific nitric oxide synthase inhibitors. *Biochem. Biphys. Res. Comm.* **187**, 797-801.

Petito, C.K., Chung, M.C., Verkhovsky, L.M. & Cooper, A.J.L. (1992) Brain glutamine synthetase increases following cerebral ischemia in the rat. *Brain Res.* **569**, 275-280.

Piani, D., Frei, K., Do, K.Q., Cuenod, M. & Fontana, A. (1991) Murine brain macrophages induce NMDA receptor mediated neurotoxicity in vitro by secreting glutamate. *Neurosci. Lett.* **133**, 159-162.

Poat, J.A., Cripps, H.E. & Iversen, L.L. (1988) Differences between high-affinity forskolin binding sites in dopamine-rich and other regions of rat brain. *Proc. Natl. Acad.Sci. USA* **85**, 3216-3220.

Pou, S., Pou, W.S., Bredt, D.S., Snyder, S.H. & Rosen, G.M. (1992) Generation of superoxide by purified brain nitric oxide synthase. *J. Biol. Chem.* **267**, 24173-24176.

Prado, R., Ginsberg, M.D., Dietrich,W.D., Watson,B.D. & Busto, R. (1988) Hyperglycaemia increases infarct size in collaterally perfused but not end-arterial vascular territories. *J. Cereb. Blood Flow Metabol.* **8**, 186-192.

Prado, R., Watson, B.D., Kuluz, J. & Dietrich, W.D. (1992) Endothelium-derived nitric oxide synthase inhibition. Effects on cerebral blood flow, pial artery diameter, and vascular morphology in rats. *Stroke* **23**, 1118-1124.

Pulsinelli, W.A. (1985) Metabolic and circulatory factors in ischemic brain injury. In *Cerebrovascular Survey Report 1985*, ed. McDowell, F.H. & Caplan, L.R., pp75-96.

Pulsinelli, W.A. & Brierley, J.B. (1979) A new model of bilateral hemispheric ischemia in the unanesthetized rat. *Stroke* **10**, 267-272.

Pulsinelli, W.A. & Duffy, T.E. (1983) Regional energy balance in rat brain after transient forebrain ischemia. *J. Neurochem.* **40**, 1500-1503.

Pulsinelli, W.A., Brierley, J.B. & Plum, F. (1982) Temporal profile of neuronal damage in a model of transient forebrain ischemia. *Ann. Neurol.* **11**, 491-498.

Radi, R., Beckman, J.S., Bush, K.M. & Freeman, B.A. (1991) Peroxynitrite-induced membrane lipid peroxidation: the cytotoxic potential of superoxide and nitric oxide. *Arch. Biochem. Biophys.* **288**, 481-487.

Radomski, M.W., Palmer, R.M.J. & Moncada, S. (1987) Comparative pharmacology of endothelium-derived relaxing factor, nitric oxide and prostacyclin in platelets. *Br. J. Pharmacol.* **92**, 181-187.

Radomski, M.W., Palmer, R.M.J. & Moncada, S. (1990a) Characterization of the L-arginine:nitric oxide pathway in human platelets. *Br. J. Pharmacol.* **101**, 325-328.

Radomski, M.W., Palmer, R.M.J. & Moncada, S. (1990b) Glucocorticoids inhibit the expression of an inducible, but not the constitutive, nitric oxide synthase in vascular endothelial cells. *Proc. Natl. Acad. Sci. USA* **87**, 10043-10047.

Rami, A. & Krieglstein, J. (1993) Protective effects of calpain inhibitors against neuronal damage caused by cytotoxic hypoxia in vitro and ischemia in vivo. *Brain Res.* **609**, 67-70.

Rappaport, Z.H., Young, W. & Flamm, E.S. (1987) Regional brain calcium changes in the rat middle cerebral artery occlusion model of ischemia. *Stroke* **18**, 760-764.

Rees, D.D., Palmer, R.M.J., Schulz, R., Hodson, H.F. & Moncada, S. (1990) Characterization of three inhibitors of endothelial nitric oxide synthase in vitro and in vivo. *Br. J. Pharmacol.* **101**, 746-752.

Regan, R.F., Renn, K.E. & Panter, S.S. (1993) NMDA neurotoxicity in murine cortical cell cultures is not attenuated by hemoglobin or inhibition of nitric oxide synthesis. *Neurosci. Lett.* **153**, 53-56.

Regidor, J., Edvinsson, L. & Divac, I. (1993) NOS neurones lie near branchings of cortical arteriolae. *NeuroReport* **4**, 112-114.

Rehncrona, S., Hauge, H.N. & Siesjo, B.K. (1989) Enhancement of iron-catalyzed free radical formation by acidosis in brain homogenates: difference in effect by lactic acid and CO_2. *J. Cereb. Blood Flow Metabol* **9**, 65-70.

Reiser, G. (1990) Endothelin and a Ca^{2+} ionophore raise cyclic GMP levels in a neuronal cell line via formation of nitric oxide. *Br. J. Pharmacol.* 101, 722-726.

Relton, J.K. & Rothwell, N.J. (1992) Interleukin-1 receptor antagonist inhibits ischaemic and excitotoxic neuronal damage in the rat. *Brain Res. Bull.* **29**, 243-246.

Rengasamy, A. & Johns, R.A. (1991) Characterization of endothelium-derived relaxing factor/nitric oxide synthase from bovine cerebellum and mechanism of modulation by high and low oxygen tensions. *J. Pharmacol. Exp. Ther.* **259**, 310-316.

Ridenour, T.R., Warner, D.S., Todd, M.M. & Baker, M.T. (1991) Effects of ketamine on outcome from temporary middle cerebral artery occlusion in the spontaneously hypertensive rat. *Brain Res.* **565**, 116-122.

Ridenour, T.R., Warner, D.S., Todd, M.M. & McAllister, A.C. (1992) Mild hypothermia reduces infarct size resulting from temporary but not permanent focal ischemia in rats. *Stroke* **23**, 733-738.

Rieke, G.K., Bowers, D.E. & Penn, P. (1981) Vascular supply pattern to rat caudatoputamen and globus pallidus: scanning electronmicroscopic study of vascular endocasts of stroke-prone vessels. *Stroke* **12**, 840-847.

Ringelstein, E.B., Biniek, R., Weiller, C., Ammeling, B., Nolte, P.N. & Thron, A. (1992) Type and extent of hemispheric brain infarctions and clinical outcome in early and delayed middle cerebral artery recanalization. *Neurology* **42**, 289-298.

Robinson, M.J. & McCulloch, J. (1990) Contractile responses to endothelin in feline cortical vessels in situ. *J. Cereb. Blood Flow Metabol.* **10**, 285-289.

Robinson, M.J., Macrae, I.M., Todd, M., Reid, J.L. & McCulloch, J. (1990) Reduction of local cerebral blood flow to pathological levels by endothelin-1 applied to the middle cerebral artery in the rat. *Neurosci. Lett.* **118**, 269-272.

Robinson, R.G., Shoemaker, W.J., Schlumpf, M., Valk, T. & Bloom, F.E. (1975) Experimental cerebral infarction in rat brain: effect on catecholamines and behavior. *Nature* **255**, 332-334.

Robinson, R.G. & Coyle, J.T. (1980) The differential effect of right versus left hemispheric cerebral infarction on catecholamines and behavior in the rat. *Brain Res.* **188**, 63-78.

Rogers, N.E. & Ignarro, L.J. (1992) Constitutive nitric oxide synthase from cerebellum is reversibly inhibited by nitric oxide formed from L-arginine. *Biochem. Biophys. Res. Comm.* **189**, 242-249.

Rosenblum, W.I. (1986) Endothelial dependent relaxation demonstrated in vivo in cerebral arterioles. *Stroke* **17**, 494-497.

Rosenblum, W.I. (1992) Endothelium-derived relaxing factor in brain blood vessels is not nitric oxide. *Stroke* **23**, 1527-1532.

Rosenblum, W.I., Nishimura, H. & Nelson, G.H. (1990) Endothelium-dependent L-arg- and L-NMMA-sensitive mechanisms regulate tone of brain microvessels. *Am. J. Physiol.* **259**, H1396-H1401.

Rosenblum, W.I., Nishimura, H. & Nelson, G.H. (1992) L-NMMA in brain microcirculation of mice is inhibited by blockade of cyclooxygenase and by superoxide dismutase. *Am. J. Physiol.* **262**, H1343-H1349.

Rothman, S. (1984) Synaptic release of excitatory amino acid neurotransmitter mediates anoxic neuronal death. *J. Neurosci.* **4**, 1884-1891.

Rothwell, N.J. (1991) Functions and mechanisms of interleukin-1 in the brain. *Trends Pharmacol. Sci.* **12**, 430-436.

Roussel, S., Pinard, E. & Seylaz, J. (1992a) Effect of MK-801 on focal brain infarction in normotensive and hypertensive rats. *Hypertension* **19**, 40-46.

Roussel, S., Pinard, E. & Seylaz, J. (1992b) The acute effects of MK-801 on cerebral blood flow and tissue partial pressures of oxygen and carbon dioxide in conscious and alpha-chloralose anaesthetized rats. *Neurosci.* **47**, 959-965.

Rubanyi, G.M. & Parker Botehlo, L.H. (1991) Endothelins. *FASEB J.* **5**, 2713-2720.

Rubanyi, G.M., Ho, E.H., Cantor, E.H., Lumma, W.C. & Parker Botehlo, L.H. (1991) Cytoprotective function of nitric oxide: inactivation of superoxide radicals produced by human leukocytes. *Biochem. Biophys. Res. Comm.* **181**, 1392-1397.

Saito, A., Shiba, R., Kimura, S., Yanagisawa, M., Goto, K. & Masaki, T. (1989) Vasoconstrictor response of large cerebral arteries of cats to endothelin, an endothelium-derived vasoactive peptide. *Eur. J. Pharmacol.* **162**, 353-358.

Saito, I., Segawa, H., Shiokawa, Y., Taniguchi, M. &Tsutumi, K. (1987) Middle cerebral artery occlusion: correlation of computed tomography and angiography with clinical outcome. *Stroke* **187**, 863-868.

Sakamoto, A., Ohnishi, S.T., Ohnishi, T. & Ogawa, R. (1991) Relationship between free radical production and lipid peroxidation during ischemia-reperfusion injury in the rat brain. *Brain Res.* **554**, 186-192.

Sakurada, O., Kennedy, C., Jehle, J., Brown, J.D., Carbin, G.L. & Sokoloff, L. (1978) Measurement of local cerebral blood flow with iodo[^{14}C]antipyrine. *Am. J. Physiol.* **234**, H59-H66.

Sakurai, T., Yanagisawa, M. & Masaki, T. (1992) Molecular characterization of endothelin receptors. *Trends Pharmacol. Sci.* **13**, 103-108.

Samson, W.K., Skala, K.D., Alexander, B.D. & Huang, F.L.S. (1990) Pituitary site of action of endothelin-selective-inhibition of prolactin-release in vitro. *Biochem. Biophys. Res. Comm.* **169**, 737-743.

Savasta, M., Dubois, A. & Scatton, B. (1986) Autoradiographic localization of D_1 receptors in the rat brain with [^{3}H]SCH23390. *Brain Res.* **375**, 291-301.

Sauter, A. & Rudin, M. (1986) Calcium antagonists reduce the extent of infarction in rat middle cerebral artery occlusion model as determined by quantitative magnetic resonance imaging. *Stroke* **17**, 1228-1234.

Schwarzacher, S. & Raberger, R. (1992) L-N^G-Nitro-Arginine methyl ester in the anaesthetized rabbit: venous vasomotion and plasma levels. *J. Vasc. Res.* **29**, 290-292.

Schmidley, J.W. (1990) Free radicals in central nervous system ischemia. *Stroke* **25**, 7-12.

Schoepp, D., Bockaert, J. & Sladeczek, F. (1990) Pharmacological and functional characteristics of metabotropic excitatory amino acid receptors. *Trends Pharmacol. Sci.* **11**, 508-515.

Schor, N.F. (1988) Inactivation of mammalian brain glutamine synthetase by oxygen radicals. *Brain Res.* **456**, 17-21.

Seamon, K. & Daly, J.W. (1981) Activation of adenylate cyclase by the diterpene forskolin does not require the guanine nucleotide regulatory protein. *J. Biol. Chem.* **256**, 9799-9801.

Sharkey, J., Ritchie, I.M. & Kelly, P.A.T. (1993) Perivascular microapplication of endothelin-1: a new model of focal cerebral ischemia in the rat. *J. Cereb. Blood Flow Metabol.* **13**, 865-871.

Sheardown, M.J., Nielsen, E.O., Hansen, A.J., Jacobsen, P. & Honore, T. (1990) 2,3-Dihydroxy-6-nitro-7-sulfamoxyl-benzo (F) quinoxaline: a neuroprotectant for cerebral ischemia. *Science* **247**, 571-574.

Shibuki, K. & Okada, D. (1991) Endogenous nitric oxide release required for long-term synaptic depression in the cerebellum. *Nature* **349**, 326-328.

Shiga, Y., Onodera, H., Kogure, K., Yamasaki, Y., Yashima, Y., Syozuhara, H. & Sendo, F. (1991) Neutrophil as a mediator of ischemic edema formation in the rat brain. *Neurosci. Lett.* **125**, 110-112.

Shigeno, T., Teasdale, G.M., McCulloch, J. & Graham, D.I. (1985) Recirculation model following MCA occlusion in rats. *J. Neurosurg.* **63**, 272-277.

Shigeno, T. & Mima, T. (1990) A new vasoconstrictor peptide, endothelin: profiles as vasoconstrictor and neuropeptide. *Cerebrovasc. & Brain Metabol. Rev.* **2**, 227-239.

Shinmi, O., Kimura, S., Sawamura, T., Sugita, Y., Yoshizawa, T., Uchiyama, Y., Yanagisawa, M., Goto, K., Masaki, T. & Kanazawa, I. (1989) Endothelin-3 is a novel neuropeptide: isolation and sequence determination of endothelin-1 and endothelin-3 in porcine brain. *Biochem. Biophys. Res. Comm.* **164**, 587-593.

Siesjo, B.K. (1981) Cell damage in the brain: a speculative synthesis. *J. Cereb. Blood Flow Metabol.* **1**, 155-185.

Siesjo, B.K. & Bengtsson, F. (1989) Calcium fluxes, calcium antagonists, and calcium-related pathology in brain ischemia, hypoglycemia, and spreading depression: a unifying hypothesis. *J.Cereb. Blood Flow Metabol.* **9**, 127-140.

Siesjo, B.K., Agardh, C.-D. & Bengtsson, F. (1989) Free radicals and brain damage. *Cerebrovasc. Brain Metabol. Rev.* **1**, 165-211.

Siesjo, B.K., Ekholm, A., Katsura, K., Memezawa, H., Ohta, S. & Smith, M.-L. (1990) The type of ischemia determines the pathophysiology of brain lesions and the therapeutic response to calcium channel blockade. In *Pharmacology of cerebral ischemia 1990*, ed. Krieglstein, J. & Oberpichler, H., pp 79-88, Stuttgart, Wissenschaftliche Verlagsgesellschaft mbH.

Simmons, M.L. & Murphy, S. (1993) Cytokines regulate L-arginine-dependent cyclic GMP production in rat glial cells. *Eur. J. Neurosci.* **5**, 825-831.

Simon, R. & Shiraishi, K. (1990) N-Methyl-D-aspartate antagonist reduces stroke size and regional glucose metabolism. *Ann. Neurol.* **27**, 606-611.

Simon, R., Swan, J., Griffiths, T. & Meldrum, B. (1984) Blockade of N-methyl-D-aspartate receptors may protect against ischemia in the brain. *Science* **226**, 850-852.

Smith, M.-L., Auer, R.N. & Siesjo, B.K. (1984) The density and distribution of ischemic brain injury in the rat following 2-10 min of forebrain ischemia. *Acta Neuropathol.* **64**, 319-332.

Sokoloff, L. (1981) Circulation and energy metabolism of the brain. In *Basic Neurochemistry*, ed. Siegel, G.J., Agranoff, B.W., Albers, R.W. & Molinoff, P.B., pp 565-590, New York, Raven Press.

Sokolovsky, M., Ambar, I. & Galron, R. (1992) A novel subtype of endothelin receptors. *J. Biol. Chem.* **267**, 20551-20554.

Southam, E. & Garthwaite, J. (1991) Comparative effects of some nitric oxide donors on cyclic GMP levels in rat cerebellar slices. *Neurosci. Lett.* **130**, 107-111.

Sperling, B. & Lassen, N.A. (1993) Hyperfixation of HMPAO in subacute ischemic stroke leading to spuriously high estimates of cerebral blood flow by SPECT. *Stroke* **24**, 193-194.

Stawski, G., Olse, U.B. & Grande, P. (1991) Cytotoxic effect of endothelin-1 during 'simulated' ischaemia in cultured rat myocytes. *Eur. J. Pharmacol.* **201**, 123-124.

Sudjarwo, S.A., Hori, M.N. & Karaki, H. (1992) Effect of endothelin-3 on cytosolic calcium level in vascular endothelium and on smooth muscle contraction. *Eur. J. Pharmacol.* **229**, 137-142.

Swan, J. & Meldrum, B. (1990) Protection by NMDA antagonists against selective cell loss following transient ischaemia. *J. Cereb. Blood Flow Metabol.* **10**, 343-351.

Symon, L. (1970) Regional vascular reactivity in the middle cerebral arterial distribution. An experimental study in baboons. *J. Neurosurg.* **33**, 532-541.

Szatkowski, M., Barbour, B. & Attwell, D. (1990) Non-vesicular release of glutamate from glial cells by reversed electrogenic glutamate uptake. *Nature* **348**, 443-446.

Takadera, T., Shimada, Y. & Mohri, T. (1992) Extracellular pH modulates N-methyl-D-aspartate receptor-mediated neurotoxicity and calcium accumulation in rat cortical cultures. *Brain Res.* **572**, 126-131.

Tamura, A., Asano, T. & Sano, K. (1980) Correlation between rCBF and histological changes following temporary middle cerebral artery occlusion. *Stroke* **11**, 487-493.

Tamura, A., Graham, D.I., McCulloch, J. & Teasdale, G.M. (1981a) Focal cerebral ischaemia in the rat: 1. Description of technique and early neuropathological consequences following middle cerebral artery occlusion. *J. Cereb. Blood Flow Metabol.* **1**, 53-60.

Tamura, A., Graham, D.I., McCulloch, J. & Teasdale, G.M. (1981b) Focal cerebral ischaemia in the rat: 2. Regional cerebral blood flow determined by [^{14}C]iodoantipyrine autoradiography following middle cerebral artery occlusion. *J. Cereb. Blood Flow Metabol.* **1**, 61-69.

Tanaka, K., Gotoh, F., Gomi, S., Takashima, S., Mihara, B. Shirai, T. Nogawa, S. & Nagata, E. (1991) Inhibition of nitric oxide synthesis induces a significant reduction in local cerebral blood flow in the rat. *Neurosci. Lett.* **127**, 129-132.

Toda, N. & Okamura, T. (1991) Role of nitric oxide in neurally induced cerebroarterial relaxation. *J. Pharmacol. Exp. Ther.* **258**, 1027-1032.

Todd, M.M. & Warner, D.S. (1992) A comfortable hypothesis reevaluated. Cerebral metabolic depression and brain protection during ischemia. *Anesthesiol.* **76**, 161-164.

Tominaga, T., Sato, S., Ohnishi, T. & Ohnishi, S.T. (1993) Potentiation of nitric oxide formation following bilateral carotid occlusion and focal cerebral ischemia in the rat: in vivo detection of the nitric oxide radical by electron paramagnetic resonance spin trapping. *Brain Res.* **614**, 342-346.

Toulmond, S., Vige, X., Fage, D. & Benavides, J. (1992) Local infusion of interleukin-6 attenuates the neurotoxic effects of NMDA on rat striatal cholinergic neurons. *Neurosci. Lett.* **144**, 49-52.

Trifiletti, R.R., Kader, A. & Solomon, R.A. (1992) Brain nitric oxide production in focal ischemia. *Soc. Neurosci. Abstr.* **18**, 1254.

Tyson, G.W., Teasdale, G.M., Graham, D.I. & McCulloch, J. (1982) Cerebrovascular permeability following MCA occlusion in the rat. The effect of halothane-induced hypotension. *J. Neurosurg.* **57**, 186-196.

Tyson, G.W., Teasdale, G.M., Graham, D.I. & McCulloch, J. (1984) Focal cerebral ischemia in the rat: topography of hemodynamic and histopathological changes. *Ann. Neurol.* **15**, 559-567.

Uematsu, D., Greenberg, J.H., Hickey, W.F. & Reivich (1989) Nimodipine attenuates both increase in cytosolic free calcium and histologic damage following focal cerebral-ischemia and reperfusion in cats. *Stroke* **20**, 1531-1537.

Uemura, Y., Miller, J.M., Matson, W.R. & Beal, M.F. (1991) Neurochemical analysis of focal ischemia in rats. *Stroke* **22**, 1548-1553.

Valenzuela, A. (1991) The biological significance of malondialdehyde determination in the assessment of tissue oxidative stress. *Life Sci.* **48**, 301-309.

Valtschanoff, J.G., Weinberg, R.J., Kharazia, V.N., Schmidt, H.H.H.W., Nakane, M. & Rustioni, A. (1993) Neurons in rat cerebral cortex that synthesize nitric oxide: NADPH diaphorase histochemistry, NOS immunocytochemistry, and colocalization with GABA. *Neurosci. Lett.* **157**, 157-161.

Vanella, A., Sorrenti, V., Castorina, C., Campisi, A., Di Giacomo, C., Russo, A. & Perez-Polo, J.R. (1992) Lipid peroxidation in rat cerebral cortex during post-ischemic reperfusion: effect of exogenous antioxidants and Ca^{++}-antagonist drugs. *Int. J. Devl. Neurosci.* **10**, 75-80.

Verity, M.A. (1992) Ca^{2+}-dependent processes as mediators of neurotoxicity. *Neurotoxicology* **13**, 139-148.

Vibulsresth, S., Dietrich, W.D., Busto, R. & Ginsberg, M.D. (1987) Failure of nimodipine to prevent ischemic neuronal damage in rats. *Stroke* **18**, 210-216.

Vila, J.M., De Aguilera, E.M., Martinez, M.C., Rodriguez, M.D., Irurzun, A., Lluch, S. (1989) Endothelin action on goat cerebral arteries. *J. Pharm. Pharmacol.* **42**, 370-372.

Villacara, A., Spatz, M., Dodson, R.F., Corn, C. & Bembry, J. (1989) Effect of arachidonic acid on cultured cerebromicrovascular endothelium: permeability, lipid peroxidation and membrane "fluidity". *Acta Neuropathol.* **78**, 310-316.

Vincent, S.R. & Kimura, H. (1992) Histochemical mapping of nitric oxide synthase in the rat brain. *Neurosci.* **46**, 755-784.

Wallace, M.C. (1991) ^{3}H-Forskolin binding: an early outcome measure following experimental focal cerebral ischemia. *J. Cereb. Blood Flow Metabol.* **11**, S2, S546.

Wallenstein, S., Zucker, C.L. & Fleiss, J.L. (1980) Some statistical methods useful in circulation research. *Circ. Res.* **47**, 1-9.

Wallis, R.A., Panizzon, K. & Wasterlain, C.G. (1992) Inhibition of nitric oxide synthase protects against hypoxic neuronal injury. *NeuroReport* **3**, 645-648.

Wang, Y.-X., Zhou,T., Chua, T.C. & Pang, C.C.Y. (1991) Effects of inhalation and intravenous anaesthetic agents on pressor response to N^{G}-nitro-L-arginine. *Eur. J. Pharmacol.* **198**, 1831.

Wardlaw, J.M. & Warlow, C.P. (1992) Thrombolysis in acute ischemic stroke: does it work? *Stroke* **23**, 1826-1839.

Warner, D.S., Todd, M.M., Ludwig, P., McFarlane, C. & McAllister, A. (1993) Volatile anaesthetics reduce focal ischemic brain damage in the rat. *J. Cereb. Blood Flow Metabol.***13**, S1, S684.

Watson, B.D., Busto, R., Goldberg, W.J., Santiso, M., Yoshida, S. & Ginsberg, M.D.(1984) Lipid peroxidation in vivo induced by reversible global ischemia in rat brain. *J. Neurochem.* **42**, 268-274.

Watson, B.D., Dietrich, W.D., Busto, R., Wachtel, M.S. & Ginsberg, M.D.(1985) Induction of reproducible brain infarction by photochemically initiated thrombosis. *Ann. Neurol.* **17**, 497-504.

Watson, B.D., Prado, R., Dietrich, W.D., Busto, R., Scheinberg, P. & Ginsberg, M.D.(1987) Mitigation of evolving cortical infarction in rats by recombinant tissue plasminogen activator following photochemically induced thrombosis. In *Cerebrovascular diseases. Fifteenth research (Princeton) conference*, ed. Powers, W.J. & Raichle, M.E., pp 317-330, New York, Raven Press.

Watson, B.D. & Ginsberg, M.D.(1989) Ischemic injury in the brain. Role of oxygen radical-mediated processes. *Ann. N.Y. Acad. Sci.* **559**, 269-281.

Wei, E.P., Kukreja, R. & Kontos, H.A. (1992) Effects in cats of inhibition of nitric oxide synthesis on cerebral vasodilation and endothelium-derived relaxing factor from acetylcholine. *Stroke* **23**, 1623-1629.

Weissmann, G., Smolen, J.E. & Korchak, H.M. (1980) Release of inflammatory mediators from stimulated neutrophils. *N. Engl. J. Med.* **303**, 27-34.

Welch, K.M.A. & Barkley, G.L. (1986) Biochemistry and pharmacology of cerebral ischemia. In *Stroke: Pathophysiology, diagnosis and management*, ed. Barnett, H.J., Mohr, J.P., Stein, B.M. & Yatsu, F.M., pp 75-90, New York, Churchill Livingstone.

Westergaard, N., Beart, P.M. & Schousboe, A. (1993) Transport of L-[^{3}H]arginine in cultured neurons: characteristics and inhibition by nitric oxide synthase inhibitors. *J. Neurochem.* **61**, 364-367.

White, B.C., Tribhuwan, R.C., Vander Laan, D.J., DeGracia, D.J., Krause, G.S. & Grossman, L.I. (1992) Brain mitochondrial DNA is not damaged by prolonged cardiac arrest or reperfusion. *J. Neurochem.* **58**, 1716-1722.

Wilkinson, J.L. (1986) *Neuroanatomy for medical students*. London, Wright.

Willette, R.N., Sauermelch, C., Ezekiel, M., Feuerstein, G. & Ohlstein, E.H. (1990) Effect of endothelin on cortical microvascular perfusion in rats. *Stroke* **21**, 451-458.

Willette, R.N., Ohlstein, E., Pullen, M., Sauermelch, C.F., Cohen, A. & Nambi, P. (1992) Transient forebrain ischemia alters acutely endothelin receptor density and immunoreactivity in gerbil brain. *Life Sci.* **52**, 35-40.

Williams, J.L., Shea, M., Furlan, A.J., Little, J.R.& Jones, S.C. (1991) Importance of freezing time when iodoantipyrine is used for measurement of cerebral blood flow. *Am. J. Physiol.* **261**, H252-H256.

Willis, C.L., Brazell, C. & Foster, A.C. (1991) Plasma and CSF levels of dizocilpine (MK-801) required for neuroprotection in the quinolinate-injected rat striatum. *Eur. J. Pharmacol.* **196**, 285-290.

Willmore, L.J. & Rubin, J.J. (1982) Formation of malonaldehyde and focal brain edema induced by subpial injection of $FeCl_2$ into rat isocortex. *Brain Res.* **246**, 113-119.

Wong, M.C.W. & Haley, E.C. (1990) Calcium antagonists: stroke therapy coming of age. *Stroke* **21**, 494-501.

Wood, P.L., Emmett, M.R., Rao, T.S., Cler, J., Mick, S.& Iyengar, S. (1990) Inhibition of nitric oxide synthase blocks N-methyl-D-aspartate-, quisqualate-, kainate-, harmaline-, and pentylenetetrazole-dependent increases in cerebellar cyclic GMP in vivo. *J. Neurochem.* **55**, 346-348.

Xie, Q., Cho, H., Calaycay, J., Mumford, R.A., Swiderek, K.M., Lee, T.D., Ding, A., Troso, T. & Nathan, C. (1992) Cloning and characterisation of inducible nitric oxide synthase from mouse macrophages. *Science* **256**, 225-228.

Xue, D., Huang, Z.G., Gertler, S.Z. & Buchan, A.M. (1992a) Blockade of nitric oxide synthetase by nitro-arginine failed to protect the brain against transient focal ischemia in two rat MCA models. *Soc. Neurosci. Abstr.* **18**, 1254.

Xue, D., Huang, Z.G., Smith, K.E. & Buchan, A.M. (1992b) Immediate or delayed mild hypothermia prevents focal cerebral infarction. *Brain Res.* **587**, 66-72.

Yamamoto, M., Shima, T., Uozumi, T., Sogabe, T., Yamada, K. & Kawasaki, T. (1983) A possible role of lipid peroxidation in cellular damages caused by cerebral ischemia and the protective effect of alpha-tocopherol administration. *Stroke* **14**, 977-982.

Yamamoto, S., Golanov, E.V., Berger, S.B. & Reis, D.J. (1992) Inhibition of nitric oxide synthesis increases focal ischaemic infarction in rat. *J. Cereb. Blood Flow Metab.* **12**, 717-726.

Yamasaki, Y., Suzuki, T., Yamaya, H., Matsuura, N., Onodera, H. & Kogure, K. (1992) Possible involvement of interleukin-1 in ischemic brain edema formation. *Neurosci. Lett.* **142**, 45-47.

Yamashita, K., Kataoka, Y., Niwa, M., Shigematsu, K., Himeno, A., Koizumi, S. & Taniyama, K. (1993) Increased production of endothelins in the hippocampus of stroke-prone spontaneously hypertensive rats following transient forebrain ischemia: histochemical evidence. *Cell. Molecul. Neurobiol.* **13**, 15-23.

Yamori, Y., Horie, R., Handa, H., Sato, M. & Fukase, M. (1976) Pathogenetic similarity of strokes in stroke-prone spontaneously hypertensive rats and humans. *Stroke* **7**, 46-53.

Yanagisawa, M., Kurihara, H., Kimura, S., Tomobe, Y., Kobayashi, M., Mitsui, Y., Yazaki, Y., Goto, K. & Masaki, T. (1988) A novel potent vasoconstrictor peptide produced by vascular endothelial cells. *Nature* **332**, 411-415.

Yang, G.Y., Weinstein, P.R., Chen, S.F., Babuna, O.A., Simon, R.P. & Chan, P.H. (1991) N-Methyl-D-aspartate antagonist, MK-801, reduces reperfusion injury after focal cerebral ischemia in rats. *J. Cereb. Blood Flow Metabol.* **11**, S2, S288.

Yang, G.Y., Chen, S.F., Kinouchi, H., Chan, P.H. & Weinstein, P.R. (1992) Edema, cation content and ATPase activity after middle cerebral artery occlusion in rats. *Stroke* **23**, 1331-1336.

Yao, J., Keri, J.E., Taffs, R.W. & Colton, C. (1992) Characterization of interleukin-1 production by microglia in culture. *Brain Res.* **591**, 88-93.

Yatsu, F.M. (1982) Acute medical therapy of strokes. *Stroke* **13**, 524-526.

Yip, P.K., He, Y.Y., Hsu, C.Y., Garg, N., Marangos, P. & E.L. Hogan (1991) Effect of plasma glucose on infarct size in focal cerebral ischemia-reperfusion. *Neurology* **41**, 899-905.

Yoshida, K., Burton, G.F., McKinney, J.S., Young, H. & Ellis, E.F. (1992) Brain and tissue distribution of polyethylene glycol-conjugated superoxide dismutase in rats. *Stroke* **23**, 865-869.

Yoshida, S., Inoh, S., Asano, T., Sano, K., Kubota, M., Shimazaki, H. & Ueta, N. (1980) Effect of transient ischemia on free fatty acids and phospholipids in the gerbil brain. *J. Neurosurg.* **53**, 323-331.

Yoshimoto, S., Ishizaki, Y., Kurihara, H., Sasaki, T., Yoshizumi, M., Yanagisawa, M., Yazaki, Y., Masaki, T., Takakura, K. & Murota, S.-I. (1990) Cerebral microvessel endothelium is producing endothelin. *Brain Res.* **508**, 283-285.

Yoshimoto, S., Ishizaki, Y., Sasaki, T. & Murota, S.-I. (1991) Effect of carbon dioxide and oxygen on endothelin production by cultured porcine cerebral endothelial cells. *Stroke* **22**, 378-383.

Yoshimoto, S., Ishizaki, Y., Mori, A., Sasaki, T., Takakura, K. & Murota, S.-I. (1991) The role of cerebral microvessel endothelium in regulation of cerebral blood flow through production of endothelin-1. *J. Cardiovasc. Pharmacol.* **17**, S7, S260-S263.

Yue, T.-L., Gu, J.-L., Lysko, P.G., Cheng, H.-Y., Barone, F.C. & Feuerstein, G. (1992) Neuroprotective effects of phenyl-t-butyl-nitrone in gerbil global brain ischemia and in cultured rat cerebellar neurones. *Brain Res.* **574**, 193-197.

Zea Longa, E., Weinstein, P.R., Carlson, S. & Cummins, R. (1989) Reversible middle cerebral artery occlusion without craniectomy in rats. *Stroke* **20**, 84-91.

Zhang, F. & Iadecola, C. (1993) Nitroprusside improves blood flow and reduces brain damage after focal ischemia. *Neuroreport* **4**, 559-562.

Zhang, J., Benveniste, J. & Piantadosi, C.A. (1993) Inhibition of nitric oxide synthase increases extracellular cerebral glutamate concentration after global ischemia. *Neurosci. Lett.* **157**, 179-182.

Zhang, R.-L., Chopp, M., Chen, H., Garcia, J.H. & Zhang, Z.G. (1993) Postischemic (1 hour) hypothermia significantly reduces ischemic cell damage in rats subjected to 2 hours of middle cerebral artery occlusion. *Stroke* **24**, 1235-1240.

Zini, I., Tomasi, A., Grimaldi, R., Vannini, V. & Agnati, L.F. (1992) Detection of free radicals during brain ischemia and reperfusion by spin trapping and microdialysis. *Neurosci. Lett.* **138**, 279-282.

Ziv, I., Fleminger, G., Djaldetti, R., Achiron, A., Melamed, E. & Sokolovsky, M. (1992) Increased plasma endothelin-1 in acute stroke. *Stroke* **23**, 1014-1016.

PUBLICATIONS

Dawson, D.A., Robinson, M.J., Macrae, I.M., Reid, J.L. & McCulloch, J. (1992) Autoradiographic evaluation of forskolin and D_1 dopamine receptor binding in a rat model of focal cerebral ischaemia. *Brain Res.* **577**, 210-217.

Dawson, D.A., Kusumoto, K., Graham, D.I., McCulloch, J. & Macrae, I.M. (1992) Inhibition of nitric oxide synthesis does not reduce infarct volume in a rat model of focal cerebral ischaemia. *Neurosci. Lett.* **142**, 151-154.

Dawson, D.A., McCulloch, J. & Macrae, I.M. (1993) Cerebrovascular effects of N^G-nitro-L-arginine methylester are conserved under halothane anaesthesia. *Eur. J. Pharmacol.* **249**, 7-11.

Fujisawa, H., Dawson, D., Browne, S.E., Mackay, K.B., Bullock, R. & McCulloch, J. (1993) Pharmacological modification of glutamate neurotoxicity in vivo. *Brain Res.* **629**, 73-78.

Macrae, I.M., Dawson, D.A., Norrie, J.D. & McCulloch, J. (1993) Inhibition of nitric oxide synthesis: effects on cerebral blood flow and glucose utilisation in the rat. *J. Cereb. Blood Flow Metabol.* **13**, 985-922.

Ross, B., Dawson, D., Dewar, D., Macrae, M., Knowler, J. & McCulloch, J. (1993) Effects of post mortem delay on high affinity forskolin binding sites and adenylate cyclase activity in rat and human striatum and cerebral cortex. *Brain Res.* **629**, 225-230.

ABSTRACTS

Dawson, D.A., Robinson, M.J., Macrae, I.M., Reid, J.L. & McCulloch, J. (1991) Reductions in forskolin and D_1 dopamine receptor binding following focal cerebral ischaemia in the rat. *Br. J. Pharmacol.* **104**, 262P.

Dawson, D.A., Graham, D.I., McCulloch, J. & Macrae, I.M. (1993) Evolution of ischaemic damage in a new model of focal cerebral ischaemia in the rat. *J. Cereb. Blood Flow Metabol.* **13**, S1, S461.

Dawson, D.A., McCulloch, J., Graham, D.I. & Macrae, I.M. (1993) Recovery from anaesthesia improves outcome following transient but not permanent focal cerebral ischaemia in the rat. *Soc. Neurosci. Abstr* **18**, 1654.

Macrae, I.M., Dawson, D.A., Reid, J.L. & McCulloch, J. (1991) Effect of nitric oxide synthetase inhibition on cerebral blood flow (CBF) in the conscious rat. *Soc. Neurosci. Abstr.***17**, 475.

Macrae, I.M., Dawson, D.A., Mackay, K.B., Graham, D.I. & McCulloch, J. (1993) Comparison of infarct size and degree of swelling in permanent and reversible acute focal cerebral ischaemia. *J. Cereb. Blood Flow Metabol.* **13**, S1, S94.